Tran-SET

Transportation Consortium of South-Central States

Solving Emerging Transportation Resiliency, Sustainability, and Economic Challenges through the Use of Innovative Materials and Construction Methods: From Research to Implementation

Impacts of Moisture on Asphalt Properties

Project No. 17BASU03

Lead University: Arkansas State University

Preserving Existing Transportation Systems

Final Report

October 2018

Disclaimer

The contents of this report reflect the views of the authors, who are responsible for the facts and the accuracy of the information presented herein. This document is disseminated in the interest of information exchange. The report is funded, partially or entirely, by a grant from the U.S. Department of Transportation's University Transportation Centers Program. However, the U.S. Government assumes no liability for the contents or use thereof.

Acknowledgments

The authors gratefully acknowledge the funding support, which is provided by the United States Department of Transportation (USDOT) through Transportation Consortium of South Central States (Tran-SET). The authors are also thankful to the Arkansas Department of Transportation (ARDOT), and suppliers of the materials for their technical support throughout this study. The authors also appreciate all members of the Project Review Panel (PRC) for providing inputs throughout the duration of this project. Furthermore, the authors would like to thank the industry partner, Ergon Inc., for providing matching funds for this study.

TECHNICAL DOCUMENTATION PAGE

1. **Project No.**	**2. Government Accession No.**	**3. Recipient's Catalog No.**
17BASU03		

4. Title and Subtitle	**5. Report Date**
Impacts of Moisture on Asphalt Properties	Oct. 2018
	6. Performing Organization Code
7. Author(s)	**8. Performing Organization Report No.**
PI: Dr. Zahid Hossain https://orcid.org/0000-0003-3395-564X GRA: Sumon Roy https://orcid.org/0000-0001-6183-6619	
9. Performing Organization Name and Address	**10. Work Unit No. (TRAIS)**
Transportation Consortium of South-Central States (Tran-SET) University Transportation Center for Region 6 3319 Patrick F. Taylor Hall, Louisiana State University, Baton Rouge, LA 70803	**11. Contract or Grant No.** 69A3551747106
12. Sponsoring Agency Name and Address	**13. Type of Report and Period Covered**
United States of America Department of Transportation Research and Innovative Technology Administration	Final Research Report May 2017 – May 2018
	14. Sponsoring Agency Code

15. Supplementary Notes

Report uploaded and accessible at: Tran-SET's website (http://transet.lsu.edu/).

16. Abstract

Stripping related moisture damage has been recognized as one of the major pavement distresses since the early 1990s. The main objective of this study is to establish an effective test protocol to quantify moisture susceptibility of asphalt pavements. To this end, selective test methods (Texas Boiling test, Tensile Strength Ratio, Retained Stability, and Hamburg Wheel Test), and procedures based on surface chemistries and molecular-level mechanistic properties have been investigated in this study. Firstly, a comprehensive list of literature related to moisture damage in asphalts was reviewed. Based on the literature review, a detailed project plan and test matrix were developed. Binder samples originated from two different crude sources were collected. The moisture resistance related tests such as static contact angle measurements and Texas Boiling tests were conducted. Besides, asphalt binders' nanomechanical properties using an Atomic Force Microscopy (AFM) and surface chemistries using a static contact were evaluated in the laboratory. Based on limited test data and analysis, it is concluded that there does not exist any single test method that all agencies are comfortable and equipped to follow in their daily work as each technique has some merits and demerits. However, the Texas Boiling test is found to be the simplest method that requires minimal time and resources. On the other hand, surface chemistry and atomic force microscope-based techniques are becoming popular among researchers and pavement professionals. Findings of this study are expected to help ARDOT in selecting an appropriate moisture resistance test method that is simple, reliable, and easy to implement in their routine work.

17. Key Words	**18. Distribution Statement**
Asphalts, Pavements, Moisture damage, Morphology, Micromechanical properties	No restrictions.

19. Security Classif. (of this report)	**20. Security Classif. (of this page)**	**21. No. of Pages**	**22. Price**
Unclassified	Unclassified	130	

Form DOT F 1700.7 (8-72) **Reproduction of completed page authorized.**

SI* (MODERN METRIC) CONVERSION FACTORS

APPROXIMATE CONVERSIONS TO SI UNITS

Symbol	When You Know	Multiply By	To Find	Symbol
		LENGTH		
in	inches	25.4	millimeters	mm
ft	feet	0.305	meters	m
yd	yards	0.914	meters	m
mi	miles	1.61	kilometers	km
		AREA		
in^2	square inches	645.2	square millimeters	mm^2
ft^2	square feet	0.093	square meters	m^2
yd^2	square yard	0.836	square meters	m^2
ac	acres	0.405	hectares	ha
mi^2	square miles	2.59	square kilometers	km^2
		VOLUME		
fl oz	fluid ounces	29.57	milliliters	mL
gal	gallons	3.785	liters	L
ft^3	cubic feet	0.028	cubic meters	m^3
yd^3	cubic yards	0.765	cubic meters	m^3
		NOTE: volumes greater than 1000 L shall be shown in m^3		
		MASS		
oz	ounces	28.35	grams	g
lb	pounds	0.454	kilograms	kg
T	short tons (2000 lb)	0.907	megagrams (or "metric ton")	Mg (or "t")
		TEMPERATURE (exact degrees)		
^oF	Fahrenheit	5 (F-32)/9 or (F-32)/1.8	Celsius	^oC
		ILLUMINATION		
fc	foot-candles	10.76	lux	lx
fl	foot-Lamberts	3.426	$candela/m^2$	cd/m^2
		FORCE and PRESSURE or STRESS		
lbf	poundforce	4.45	newtons	N
lbf/in^2	poundforce per square inch	6.89	kilopascals	kPa

APPROXIMATE CONVERSIONS FROM SI UNITS

Symbol	When You Know	Multiply By	To Find	Symbol
		LENGTH		
mm	millimeters	0.039	inches	in
m	meters	3.28	feet	ft
m	meters	1.09	yards	yd
km	kilometers	0.621	miles	mi
		AREA		
mm^2	square millimeters	0.0016	square inches	in^2
m^2	square meters	10.764	square feet	ft^2
m^2	square meters	1.195	square yards	yd^2
ha	hectares	2.47	acres	ac
km^2	square kilometers	0.386	square miles	mi^2
		VOLUME		
mL	milliliters	0.034	fluid ounces	fl oz
L	liters	0.264	gallons	gal
m^3	cubic meters	35.314	cubic feet	ft^3
m^3	cubic meters	1.307	cubic yards	yd^3
		MASS		
g	grams	0.035	ounces	oz
kg	kilograms	2.202	pounds	lb
Mg (or "t")	megagrams (or "metric ton")	1.103	short tons (2000 lb)	T
		TEMPERATURE (exact degrees)		
^oC	Celsius	1.8C+32	Fahrenheit	^oF
		ILLUMINATION		
lx	lux	0.0929	foot-candles	fc
cd/m^2	$candela/m^2$	0.2919	foot-Lamberts	fl
		FORCE and PRESSURE or STRESS		
N	newtons	0.225	poundforce	lbf
kPa	kilopascals	0.145	poundforce per square inch	lbf/in^2

TABLE OF CONTENTS

LIST OF FIGURES

LIST OF TABLES

ACRONYMS, ABBREVIATIONS, AND SYMBOLS

AAS	Arkansas Academy of Science
AASHTO	American Association of State Highway and Transportation Officials
AAPT	Association of Asphalt Paving Technologies
AC	Asphalt Concrete
AFM	Atomic Force Microscopy
APA	Asphalt Pavement Analyzer
ARDOT	Arkansas Department of Transportation
ASTM	American Society for Testing and Materials
ASU	Arkansas State University
BBR	Bending Beam Rheometer
DSR	Dynamic Shear Rheometer
Caltrans	California Department of Transportation
CR	Compatibility Ratio
CTM	California Test Method
DGAC	Dense Graded Asphalt Concrete
DMT	Derjaguin, Muller, and Toropov
DOT	Department of Transportation
ECS	Environmental Conditioning System
ERSA	Evaluation of Rutting and Stripping of Asphalt
FTIR	Fourier Transform Infrared spectroscopy
GLWT	Georgia Loaded Wheel Tester
HCA	Heat Cast Approach
HMA	Hot Mix Asphalt
HWT	Hamburg Wheel Test
HWTD	Hamburg Wheel-Tracking Device
HWTT	Hamburg Wheel Tracking Test
ISSA	International Slurry Surfacing Association

ITS	Indirect Tensile Strength
LAA	Liquid Anti-stripping Agents
MB	Methylene Blue
MBV	Methylene Blue Adsorption Value
MMMC	Martin Marietta Mill Creek
M_R	Modulus Ratio
NAT	Net Adsorption Test
NCHRP	National Cooperative Highway Research Program
NMR	Nuclear Magnetic Resonance
OCA	Optical Contact Analyzer
OCG	van Oss, Chaudhury, and Good
PAV	Pressure Aging Vessel
PFQNM™	Peak-Force Quantitative Nanomechanical Mapping
PG	Performance Grade
PPA	Polyphosphoric Acid
R &W	Riedel and Weber
WOC	Work of Cohesion
RAC-G	Gap Graded Rubber Modified Asphalt Concrete
RNS	Research Needs Statements
RTFO	Rolling Thin Film Oven
RV	Rotational Viscosity
S1	Source 1
S2	Source 2
SARA	Saturates, Aromatics, Resins, and Asphaltenes
SBS	Styrene-Butadiene-Styrene
SD	Sessile Drop
SFE	Surface Free Energy
SFE	Surface Free Energy
SHRP	Strategic Highway Research Program

S-value	Creep Stiffness
Tran-SET	Transportation Consortium of South-Central States
TRB	Transportation Research Board
TSR	Tensile Strength Ratio
TTI	Texas Transportation Institute
WP	Wilhelmy Plate
WRI	Western Research Institute
%	Percent
ΔG_{dry}	Adhesion Energy under the Dry Condition
eV	Unit of Dissipation Energy
G*	Complex Shear Modulus
Hz	Unit of Frequency used in DSR Test
mJ/m^2	Unit of Cohesion Energy
m-value	Slope of the Stiffness Curve
Na_2CO_3	Sodium Carbonate
Pa.s	Unit of Viscosity used in RV tests
rpm	Rotation per Minute
W^a	Interfacial Bond Strength
Γ^-	A Mono-Polar Basic Component
Γ^+	A Mono-Polar Acidic Component
Γ^{AB}	Acid-base component of total SFE, which is geometric mean of Γ^- and
Γ^{LW}	An apolar or Lifshitz-Van Der Waals Component
Γ^{total}	Total Surface Free Energy
δ	Phase Angle
ΔG_{wet}	Adhesion Energy under the Wet Condition

EXECUTIVE SUMMARY

Moisture damage in asphalt pavements is one of the major distresses to state Departments of Transportation (DOTs) and transportation agencies in the U.S. The main purpose of this study is to find a simple and cost-effective test method to predict the moisture damage of asphalt mixtures. In-house performance data of asphalts and pertinent information available in the public domain have been analyzed to make meaningful conclusions and recommendations. In this regard, selected mechanistic-empirical approaches such as Texas Boiling test, Tensile Strength Ratio, and Hamburg Wheel-Tracking Test, and surface sciences and atomic force microscope-based test methods and analyses have been considered. Based on the findings of an extensive literature review, a detailed project plan consisting of several tasks and a test matrix was developed and executed.

To execute the test plan, asphalt binder samples were collected from two different crude sources (the Arabian and the Canadian). These crude sources were decontaminated, refined, and processed at the industry partner's facility to obtain desired Performance Grade (PG) binders. Both base binders were PG 64-22, and they were further modified with different additives to prepare PG 70-22 and PG 76-22 binders. The additives used in the modification process included styrene-butadiene-styrene (SBS), polyphosphoric acid (PPA), and liquid anti-stripping agent (LAA). These custom binders were then transported in the Liquid Binders Laboratory at Arkansas State University for further testing. In the first part of the test plan, Superpave tests were conducted to estimate various performance properties of the asphalt binders. Later, the moisture resistance related tests such as Surface Free Energy (SFE) analysis, Texas Boiling tests, Hamburg wheel-tracking device (HWTD), and Tensile Strength Ratio (TSR) tests were done to evaluate the moisture susceptibility of the asphalt mixture samples. In addition, an Atomic Force Microscopy (AFM) was used to investigate the effects of moisture on the properties of the asphalt binders at the molecular level. Using the AFM, morphology, and other nanomechanical properties of the binders were also analyzed. At the end of the test plan, chemical analyses including SARA (Saturates Aromatics Resins and Asphaltenes) and Fourier Transformation Infrared (FTIR) tests were performed. The SARA analysis was done to determine the percentages of certain families of chemical constituents in the tested asphalt binders, and the FTIR analysis was conducted to identify the changes in any specific functional group in asphalt binders due to modifications.

The gathered test results from various test methods and procedures were analyzed and compared to find any trends. Based on limited test data and analysis, it is concluded that there is no single test method that all agencies are comfortable and equipped to follow in their routine work as each technique has some merits and demerits. However, Texas Boiling test is found to be the simplest that requires minimal time and resources. Some agencies prefer to use HWTD or TSR for testing asphalt mixture samples. On the other hand, surface chemistry and atomic force microscope-based techniques are becoming popular among researchers and pavement professionals in recent years. Findings of this study are expected to help the Arkansas DOT (ARDOT) in selecting an appropriate moisture resistance test method that is simple, reliable, and easy to implement in their routine work.

IMPLEMENTATION STATEMENT

Toward meeting the implementation goals of this project, the team has participated in the ARDOT-sponsored Technical Research Council (TRC) conferences held in May 2018. The authors presented the findings in the form of a poster in the TRC conference attended by ARDOT engineers, contractors, suppliers, and industry representatives. The team will be preparing an Implementation Report at the end of the implementation phase of this project and it will be shared with ARDOT. Furthermore, results have been disseminated through journal publications, conference and symposium papers, posters and presentations along with an ongoing Master's thesis. The followings are the major publications/presentations based on the outcomes of the project: Hossain, Z. (2018). "Evaluating Performance of Asphalt Pavements in Arkansas," presented (oral) at the 2018 TRB Annual Conference, held in January 2018 in Washington, D.C.

- Hossain, Z., Rashid, F. and Roy, S. (2018). "Multiscale Evaluation of Rejuvenated Asphalt Binders with a High RAP Content," presented (Poster) and Compendium Paper at the 2018 TRB Annual Conference held in Washington, D.C. in January 2018.
- Alam, S., and Hossain, Z. (2018). "Changes in chemical fingerprints of asphalt binders due to aging and chemical modification," accepted for publication and Presentation in the 2018 GeoChina, to be held in July 2018 in China.
- Roy, S. (2018). "Evaluation of Moisture Susceptibility of Asphalt Binders Using Atomic Force Microscopy (AFM)," Master's Thesis Prospectus, Department of Civil Engineering, Arkansas State University, Jonesboro, Arkansas.
- Hossain, Z., Rashid, F., and Roy, S. (2018). "Microscopic examination of rejuvenated binders with high reclaimed asphalts," manuscript submitted (JMI-2018-0008) for publication at the Journal of Microscopy.
- Roy, S., and Hossain, Z. (2018). "Evaluation of Effects of Moisture on Asphalt Pavements", An Extended Abstract has been submitted at 2018 Tran-SET conference, held in April 2018 in New Orleans, LA.
- Roy, S., and Hossain, Z. (2018). "Use of atomic-level dissipated energy to predict effects of moisture on asphalt pavements," A manuscript has been submitted for presentation and publication at the 2019 TRB Annual Meeting, will be held on January 13-17, 2019 in Washington, D.C.

Future Plans and Activities:

- The research team will disseminate the findings in the form of papers and posters in the regional conferences such as 2019 Tran-SET Conference and 2018 Oklahoma Research Day.
- Findings of this study will be reported in the form of a graduate (MS) thesis.
- The PI will share the outcomes of this research in conferences and technical meetings such as 2019 Transportation Research Board (TRB) Annual Meeting.

1. INTRODUCTION

Stripping-related moisture damage is considered as a major distress of asphalt pavements and plays an important role in pavement design and construction. Besides, the performance and durability of the pavements are seriously affected due to the moisture-induced damage. As a result, moisture damage is now accepted as one of the prime concerns to the pavement professionals and other pertinent transportation agencies in designing and constructing asphalt pavements. However, moisture damage in asphalt concrete (AC) due to stripping is a complex phenomenon, which can result from adhesive failure (failure of the bond between the asphalt binder and the aggregate), cohesive failure (failure within binder itself), or a combination of both adhesive and cohesive failures. The main goal of this study is to find an effective test method to quantify the moisture sensitivity and to evaluate the effects of moisture on the properties of asphalt binders. At present, the Texas Boiling Test (ASTM D3625), Tensile Strength Ratio (TSR) (AASHTO T 283), and Hamburg Wheel-Tracking Test (HWTT) (AASHTO T 324) methods are the most popular forms of moisture sensitivity tests of asphalt mixtures to the transportation agencies. On the other hand, the Arkansas Department of Transportation (ARDOT) is the only state agency that still uses the Retained Stability test (AASHTO T 245), which is based on the Marshall technique. The Retained Stability test is old and has been discarded by other states agencies as it fails to correlate with the field performance. The conventional mechanistic-empirical approaches also have some limitations to estimate the moisture resistance accurately as they lack scientific rigors. To quantify the moisture damage precisely, the mineral aggregates and asphalt binder interaction along with the physical test results will have to be taken into consideration. Furthermore, the mechanism of moisture damage is necessary to be identified properly prior to establishing a cost-effective, reliable, and simple test procedure. Also, the properties of the asphalt binder, aggregate, asphalt aggregate mixtures, and the interactions of the asphalt-aggregate system must be determined at the macro, micro, and nano levels. The developed tests must be calibrated on the basis of local parameters before the final implementations. Moreover, suitable field correlations must be established through the laboratory tests, which will be helpful to predict the moisture damage potential more precisely. Furthermore, chemical analysis and mechanical properties of the materials can provide a great insight to better understand the stripping phenomena in asphalt mixtures.

Considering these shortcomings, this study aims to find a simple but meaningful test method to estimate the moisture damage potentials of asphalt pavements. Findings of this study are expected to help ARDOT and other pertinent agencies to reduce the moisture-induced damage by applying the most effective moisture resistance test method and suitable pavement materials.

1.1. Literature Review

Moisture damage is one of the major pavement distress types in the United States (US) since the 1990s. According to Santucci *(1)*, "Moisture damage is caused by a loss of adhesion, commonly referred to as "stripping" of the asphalt film from the aggregate surface or a loss of cohesion within the asphalt binder itself, resulting in a reduction in asphalt mix stiffness." Moisture damage negatively affects the performance and serviceability of the asphalt pavements considerably by accelerating the formation of potholes or promoting declamations between pavement layers, presented in Figure 1. Additionally, moisture-induced damage can result in

other yearly asphalt pavement distresses such as rutting, cracking, and raveling, shown in Figure 2.

(a) Pothole **(b) Declamation**

Figure 1. Moisture-induced pavement distresses *(1).*

(a) Rutting **(b) Fatigue Cracking**

Figure 2. Early asphalt pavement failures due to moisture damage *(1).*

1.1.1. Factors Influencing Moisture Damage

The two major causes of moisture damage are i) the loss of adhesion between the binder or the mastic (including fine aggregates) and the aggregates and ii) the loss of cohesion in the mastic due to the presence of moisture *(1-3).* Table 1 represents the moisture damage based on adhesive or cohesive failure. Factors that promote moisture-induced damage in asphalt pavements are summarized by a group of researchers *(4,5).* Physical properties of the aggregate (e.g., shape, surface texture, porosity, and gradation) and of the binder (e.g., viscosity) play a major role in causing moisture damage *(1).* Chemical properties of aggregates and asphalt also have a significant contribution to water action in asphalt pavements. In addition, surface chemistry of the aggregate and asphalt is also responsible for causing moisture damage. Moreover, poor construction practices that trap moisture in pavement layers is also important.

Table 1. Moisture damage mechanism associated with adhesive or cohesive failure *(2)*.

Mechanism	Adhesion	Cohesion
Detachment	**x**	
Displacement/Film Rupture	**x**	
Spontaneous Emulsification		**x**
Pore Pressure	**x**	**x**
Hydraulic Scour	**x**	
pH Instability	**x**	
Environmental Factors	**x**	**x**

1.1.2. Mechanisms of Moisture Damage

A comprehensive understanding of the chemical and mechanical mechanisms for the causes of damage is needed to take effective measures to prevent moisture damage (6). Several mechanisms, shown in Table 1, have been proposed to describe moisture damage in asphalt pavements, which includes detachment, displacement, film rupture, spontaneous emulsification, pore pressure, hydraulic scour, pH instability, and environmental factors (1,7-12). It is noted that these mechanisms are responsible for adhesive failure individually or together in bituminous mixtures. A brief description of each of the above mechanisms of stripping is stated below.

Detachment: Detachment is the separation of an asphalt film from an aggregate surface by a thin layer of water with no obvious break in the asphalt film *(1,4)*. The asphalt film can be peeled cleanly from the aggregate, where stripping is caused by detachment, resulting from a complete loss of adhesion *(1)*. The theory of interracial energy provides the fundamental explanations of the detachment mechanism. This popular theory considers adhesion as a thermodynamic phenomenon related to the surface energies of the materials involved, i.e., asphalt and mineral aggregates. The surface tension of water is much lower than that of asphalt. The wettability of aggregate increases as the surface tension (or free surface energy) of the adhesive decreases *(4)*. Thus, the presence of water decreases the free surface energy between asphalt and aggregate interface system, which is more than that of asphalt to form a thermodynamically stable condition of minimum surface energy *(4)*. The interfacial energy theory underscores the effect of the polarity of the molecules present at the aggregate-asphalt. Asphalt is composed primarily of high molecular weight hydrocarbons that exhibits little polar activity. Conversely, most aggregates have electrically charged surfaces. Therefore, the bond that develops mainly due to relatively weak dispersion forces between asphalt and an aggregate *(6)*. Conversely, water molecules are highly polar and are attracted to aggregates by much stronger orientation forces *(6)*.

Displacement: Displacement is caused by a break in the asphalt film due to the penetration of water to the aggregate *(1,4,7,8)*. The break can be initiated because of the incomplete coating of the aggregate initially or by film rupture. Multiple researchers mentioned that displacement can result from pinholes in the asphalt film, which can be formed immediately after coating a dusty aggregate *(1,4,6,7)*. In another study *(8)*, the chemical reaction theory of adhesion was used to explain stripping by displacement.

Spontaneous Emulsification: In spontaneous emulsification, water and asphalt combine to form an inverted emulsion, which leads to stripping *(9).* The formation of such emulsions is aggravated by the presence of emulsifiers such as mineral clays or asphalt additives *(1,7-9).* It is observed that the rate of emulsification depends on the nature of the asphalt and the presence of additives *(9).*

Pore Pressure: Pore pressure is developed in the entrapped water in the asphalt mix. Stresses due to repeated traffic load applications may induce high excess pore pressures, resulting in stripping of the asphalt film from the aggregate *(1,4).*

Hydraulic Scouring: Hydraulic scouring occurs at surface courses of the pavement. Stripping due to this mechanism results from the action of vehicle tires on a saturated pavement surface. It has been shown that the diffusion of water vapor through asphalt itself is considerable and that asphalt mastics can retain a significant amount of water *(9).* This causes compression (water is pressed down into the pavement in front of the tire) and tension cycle (immediately sucked away from the pavement behind the tire) that contributes to the stripping of the asphalt film from the aggregate *(1).*

pH Instability: pH instability (shifts in pH) of the contact water can affect chemical bonds and hence influence adhesion between asphalt and aggregate *(11).* It may also affect the value of the contact angle and the wetting characteristics of the asphalt-aggregate interface.

Environmental Factors: Environmental factors (such as temperature, air, and water) play a major role in pavement durability *(12).* Pavement distress may be induced due to primarily traffic loading in mild climates where good quality asphalts and aggregates are available. However, early pavement failure may result from using poor materials in combination with severe weather such as freeze-thaw conditions, excessive rainfall, severe aging of the asphalt, etc. Little and Jones *(2)* described these mechanisms in detail and presented them at the 2003 National Seminar on Moisture Sensitivity of Asphalt Pavements.

Extensive research was done on the asphalt-stripping mechanism at the University of Idaho *(13,14).* Authors reported that due to water in the subgrade or subbase, the air voids in asphalt concrete may become saturated with water even from the condensation of vapor. Subsequently, a temperature rise can cause expansion of the water trapped in the mixture voids and results in significant void pressure when the voids are saturated. It was noticed that void water pressure may develop to 20 psi under the differential thermal expansion of the compacted asphalt mixture and may exceed the adhesive strength at the binder-aggregate surface. As a result, water may flow out through the void spaces under the pressure developed by the temperature rise and, due to the relative pressure developed, if asphalt concrete is permeable. Otherwise, the tensile stress may break adhesion bonds and the water may flow around the aggregates, which results stripping. This stripping-damage is an internal phenomenon and cannot be seen on the exterior sides of the specimens unless it is opened for visual examination.

In another study, Tarrer *(10)* reported that adhesive bonding between the binder and aggregate resulted from the physical and chemical interaction between the two component materials along with the non-uniform and opposite charge distributions on their surfaces. The binder-aggregate adhesive bond is also affected by aggregate mineralogy and its surface charge, and adsorbed cations on the aggregate surface, with clay particles degrading the adhesive bond. Howson et

al. *(15)* also focused on calculating adhesive bond strengths from measured surface energies of the component materials in both wet and dry conditions for selecting suitable binder-aggregate combinations with higher resistance to moisture damage. However, it is reported that the functional groups existed in the binder form the most durable, tenacious, and moisture-resistant bonds with the aggregates, which are not necessarily strongly adsorbed on dry aggregates *(16).* Santucci *(1)* provided an excellent technology transfer update on minimizing moisture damage. A technical overview of the mechanisms of moisture damage is given by a research team *(16,17).*

1.1.3. Previous Research on Moisture Sensitivity Tests

Extensive research has been conducted to find out the root causes of moisture-induced failure, interpret its failure mechanisms, and provide effective solutions to mitigate moisture damage in asphalt pavements for many years. In regard to moisture damage, Hubbard (18) reported the following observations: (1) higher viscosity of asphalt binder provides better adhesion but lower wettability of aggregate, ii) higher surface tension gives greater wettability for a solid, iii) aggregates with smoother surface texture easily get wetted, but one rougher surfaces get wetted they show higher adhesion, iv) once wetted porous aggregates shows better adhesion because of mechanical interlocking, and v) polarity of aggregates is the most significant property, which is affected by adhesion. In another research, Hveem (19) reported that four engineering properties (water resistance, consistency, durability, and setting rate) might be determined for selection the quality of asphalt binder in the construction of pavement.

Hallberg *(20)* demonstrated that the required internal water pressure causing an asphaltic mixture to have adhesive or interracial tension failure (stripping) is inversely proportional to the diameter of the pores. Andersland and Goetz *(21)* introduced a sonic test for evaluation of the stripping resistance of compacted asphalt mixes. Thelan *(22)* investigated the surface free energy of aggregates and asphalt to interpret the moisture damage. The author reported that the rate at which stripping occurs depends upon the surface energy of the materials in the mixes. Rice *(23)* also studied the relationship between aggregate properties and moisture sensitivity to asphalt mixes. This researcher identified several important properties such as surface texture, surface coatings, particle size and surface area to evaluate the moisture damage. The immersion-compression test, introduced by Goode *(24),* is the first moisture sensitivity test on compacted asphalt mixes.

In the 1960s, Skog and Zube *(25)* proposed four new test methods that can be used by the California Division of Highways that measure the effects of water on the bituminous pavement. One of their proposed tests was performed on the loose mixture for measuring the degree of striping quantitative; the other three tests are conducted on compacted specimens and yield methods for measuring the change in physical properties in the presence of moisture vapor or free water exposure. These studies illustrate that the consistency of the bituminous binder plays a significant role in preventing failures from water action. Mack *(26)* demonstrated the pumping action by which tires cause movement of water in a wet pavement. He also stated that these forces are far greater than thermodynamic ones and gave primary importance to the resulting loosening and perhaps emulsification of the binder. However, Schulze and Geipel *(27)* reported no deleterious effects of salt on the asphalt mixtures they tested. In another research, it is revealed that excessive pore pressure buildup causes stripping and subsequent failure in some mixtures *(28).*

In the 1970s, several researchers attempted to develop test protocols to predict the moisture sensitivity of asphalt mixtures *(29-31)*. These researchers focused on the simulation of field conditions in the laboratory to characterize the asphalt mixes. Schmidt and Graf *(29)* used the resilient modulus test to find effects of cycling load on the stiffness of asphalt mixes in moist conditions. Findings of these studies demonstrated that the damage due to cohesive failure had impacts on the performance of asphalt pavements. Jimenez *(30)* stated that all stripping failures are associated with the presence of water. The author also mentioned that the stresses that caused failure of the asphalt film were presumed due to the water pressure and erosion caused by traffic or thermal load or a combination of both on wet pavements. Lottman et al. *(31)* reported that there was a possibility of having a disintegrated pavement layer caused by moisture damage. A follow up study by Lottman (*32,33*) evaluated detrimental effects of water and freeze-thaw cycling on asphalt mixes. In that study the author used vacuum saturation followed by freezing and hot water bath condition. The Lottman's laboratory test protocol, which measures the retained strength of compacted or cores asphalt samples subjected to defined exposure conditions, which was later modified and standardized as AASHTO T 283.

In the early 1980s, Tunnicliff and Root *(34,35)* developed a new version of the Lottman test procedure through an extensive evaluation of antistripping additives. Around the same time, the Texas freeze-thaw pedestal test and the Texas boiling test were introduced to evaluate moisture sensitivity of asphalt mixes *(36,37)*. The boiling test was developed based on a conducted work in departments of transportation in Louisiana, Texas, and Virginia. This test is very similar to the test used by Saville and Axon *(38)*. On the other hand, the freeze-thaw pedestal test was a modification of the procedure introduced earlier by Plancher et al. *(39)* at the Western Research Institute. Ensley et al. *(40)* conducted research for the measurement of the bonding energy of asphalt-aggregate systems. This research work was extended on moisture sensitivity with the pedestal test by Graf *(41)*.

Stripping-related damage to asphalt pavements has drawn a major concern to all transportation agencies for many years, with special attention focused on this topic in several national and international conferences, e.g., American Society for Testing and Material (ASTM) Symposium on "Water Damage of Asphalt Pavements: Its Effect and Prevention" in Williamsburg, Virginia in 1984; the Moisture Damage Symposium in Laramie Wyoming in 2002; the Moisture Sensitivity of Asphalt Pavements: A National Seminar in San Diego, California in, 2003; and the International Workshops on Moisture Induced Damage of Asphaltic Mixes in The Netherlands in 2005, and in College Station, Texas in 2007. A wide range of research also conducted on similar issues by a group of researchers *(8,28,42-44)*.

To identify the root causes of moisture damage and to develop better test methods for predicting moisture damage in the mix design process, the Strategic Highway Research Program (SHRP) conducted several research projects during 1987 through 1993. The program funded research for the development of performance-based asphalt specifications to directly relate laboratory analysis with field performance. An environmental conditioning system (ECS) was developed to evaluate moisture damage of asphalt mixes by Al-Swailmi and Terrel *(45,46)*. The interactions between Asphalt and aggregate were investigated by Curtis et al. *(47)* based on adhesion and absorption properties. The researchers concluded that the interactions of the asphalt-aggregate system are dominated by aggregate chemistry with asphalt playing a minimal role. At the same

time, the Hamburg wheel-tracking device (HWTD) was introduced in the United States *(47)* and was evaluated by several states, mainly Colorado, Texas, and Utah, to predict moisture damage *(48-51).*

To develop new reliable test procedures for the determination of moisture sensitivity, researchers at the Western Research Institute (WRI) have conducted extensive research on asphalt chemistry and its relationship to moisture damage. The WRI research concluded that displacement of polars from aggregate by water differs based on asphalt source. At present, the WRI team is working on developing a rapid centrifugation method to simulate displacement of polars by water. The tested hypothesis is: asphalt-aggregate mixtures that form insoluble calcium salts of asphalt components have a very minimal effect on moisture damage. On the other hand, the determination of the adhesion of asphalt-aggregate systems based on the concept of surface energy has reemerged *(52).* However, these recent research developments play an important role in determining the compatible and moisture-resistant asphalt-aggregate mixtures, without addressing the effect of the interaction between traffic and water on moisture damage. Therefore, a new test procedure on compacted samples, with a proper simulation of environment/traffic factors regarding moisture damage, is being investigated under the National Cooperative Highway Research Program (NCHRP) Project 9-34 *(52).*

A national seminar on Moisture Sensitivity of Asphalt Pavements was initiated by the California Department of Transportation (Caltrans) in San Diego, California in 2003. This seminar was designed to better understand how to deal with moisture sensitivity issues that had developed in northern parts of the state in the early 1990s. The seminar was aimed at examining moisture-related distress in asphalt pavements through a series of focused papers followed by breakout workshop sessions. The development of a roadmap was one of the major outcomes of the seminar. The roadmap comprised of summarizing best practices for the various topics covered in the seminar and an identifying the gaps in knowledge and research necessities related to moisture damage of asphalt pavements.

Caltrans also conducted a statewide field investigation and laboratory testing to determine the severity and major factors associated with moisture damage *(53).* The field investigation surveyed the condition of 194 pavement sections that includes dense graded asphalt concrete (DGAC) (now known as HMA), and gap graded rubber modified asphalt concrete (RAC-G) (now known as R-HMA) located in California. Based on the test results, it was evident that about 10 percent of the pavement sections showed moderate to severe moisture damage, which recommended that the evaluation of moisture damage must be considered in assessing the performance of asphalt pavements in California. On the other hand, the effect of variables (such as air void content and binder content) on moisture damage was determined by the laboratory testing, and dynamic loading test procedures were also developed for evaluating moisture sensitivity. Also, the effectiveness of the HWTD and the long-term effectiveness of hydrated lime and liquid anti-strip additives were evaluated. The outcomes of the laboratory tests are: i) if void contents $\leq$ 7.0 percent, dense-graded HMA sections showed little or no moisture damage, but medium or severe moisture damage was observed for void content higher than 7.0 percent, ii) a few R-HMA sections with high air void contents (>7%) showed severe stripping, iii) R-HMA sections did not show an advantage in resisting moisture damage over dense-graded HMA, iv) well designed and maintained adequate pavement drainage systems may reduce the moisture

damage, and v) HWTD was found to be an effective predictor with a reasonable correlation with field performance. Based on both laboratory and field data, it was observed that hydrated lime and liquid anti-strip agents increased the moisture resistance of asphalt mixes.

1.1.4. Moisture Sensitivity Tests

The tests developed to estimate the moisture sensitivity of asphalt mixes can be grouped into three general categories *(1)*: i) tests on asphalt mix components and component compatibility, ii) tests on the loose mix, and iii) tests on the compacted mix. The descriptions of these tests are given below.

Components and Compatibility Tests: The most common tests used on asphalt mix components to determine the potential for moisture damage include the sand equivalent test, the plasticity index, the cleanness value, and the methylene blue test.

Sand Equivalent Test: This test determines the relative amount of clay material in the fine aggregate of a mix. This test is conducted in accordance with California Test Method **(**CTM) Test No. 217 *(54).*

Plasticity Index: This test provides an indication of the plastic nature of fine aggregate. This test is conducted in accordance with CTM Test No. 217 *(54).*

Cleanness Value: This test measures clay-like particles clinging to coarse aggregate. This test is conducted in accordance with CTM Test No. 227 *(54).*

Methylene Blue Test: This test was developed in France and recommended by the International Slurry Seal Association (ISSA) *(55)* to quantify the amount of harmful clays in fine aggregates. The test method titled "Determination of Methylene Blue Adsorption Value (MBV) of Mineral Aggregate Fillers and Fines" was contained in Technical Bulletin 145 of ISSA. This test is not a direct measurement of stripping since no asphalt is used. In this test, methylene blue (MB) is dissolved in distilled water with a known concentration. The filler finer than 75 microns with known weight is also uniformly stirred and dispersed in a separate beaker. While stirring, 0.5 mL of MB solution is added to each solution with a burette one at a time. One drop of the solution is removed using a stirring rod after adding each drop of MB and placed on filter paper. The test is continued until a light blue halo is formed around the drop. The amount of harmful clay is determined based on the absorption of MB by clay, with larger amounts of harmful clays indicating greater absorption. Kandhal et al. *(56)* reported that larger MB values correspond to lower tensile strength ratios from AASHTO T 283.

Net Adsorption Test (NAT): The test is used to measure the affinity and compatibility of an asphalt-aggregate pair and the sensitivity of the combination to water *(47).* In the early 1990s, this test was developed under SHRP and documented in SHRP Report A-341 *(47).* The test comprises two steps: firstly, asphalt is adsorbed onto aggregate from a toluene solution, the amount of asphalt remaining in solution is measured, and the amount of asphalt adsorbed to the aggregate is calculated, and secondly, water is introduced into the system, asphalt is desorbed from the aggregate surface, afterward, the asphalt present in the solution is measured, and the amount remaining on the aggregate surface is then calculated. The amount of asphalt remaining on the surface after desorption is termed net adsorption. The NAT offers a direct means of comparing the affinity of different asphalt-aggregate pairs. However, SHRP Report A-341

provides mixed conclusions in terms of the correlation between NAT results and moisture sensitivity results from indirect tension tests on compacted specimens. Scholz et al. *(57)* reported that there is little or no correlation to wheel-tracking tests on the mixes.

Tests on Loose Mix

Film Stripping Test: This is a modified version of the test procedure of AASHTO T 182 (Coating and Stripping of Bitumen-Aggregate Mixtures, shown in Figure 3). In this test (CTM Test No. 302) *(54)*, a 60-gm mass of aggregate coated with asphalt is placed in an oven for 15-18 h at 60 °C. Then, the sample is cooled to room temperature and placed in a jar fulfilled with about 175 mL of distilled water. The jar is capped securely and placed in the testing apparatus, with a rotation of about 35 rpm for 15 mins. The sample is then removed, and the percentage of stripping is estimated using fluorescent light. Finally, the results are reported in terms of the percent total aggregate surface stripped.

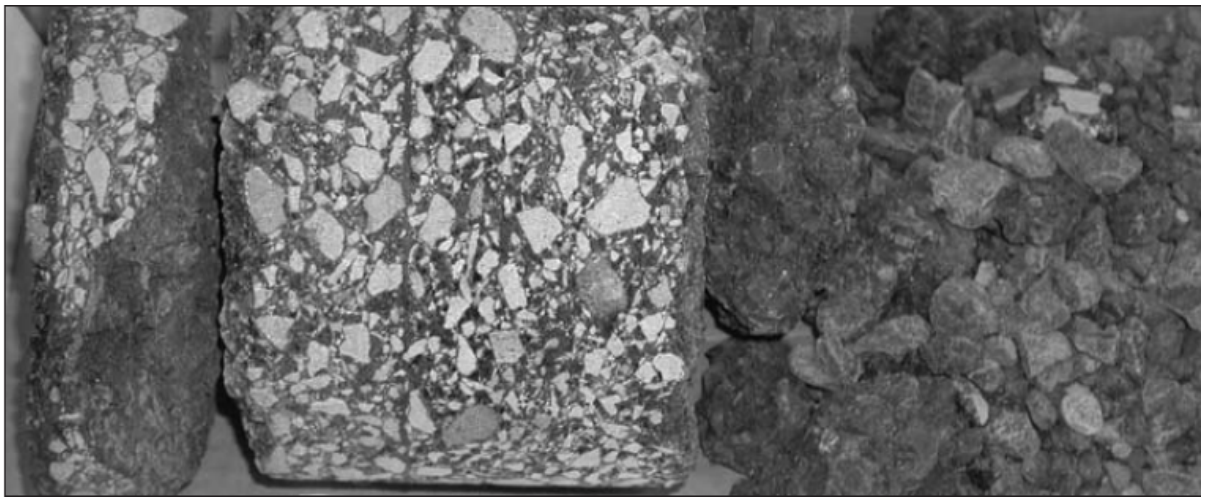

Figure 3. Stripping in asphalt treated base layer due to moisture *(1)*.

Static Immersion Test: This test was described originally under ASTM Standard Practice D1664, but it is now under AASHTO T 182 standard method *(58)*. In this test, the asphalt-aggregate mixture is cured for 2 hours (hrs.) at 60 °C and cooled to room temperature. Later, the mixture is placed in a glass jar and fulfilled with 600 mL of distilled water. The jar is then capped and placed in a water bath at 25 °C and left undisturbed for 16-18 hrs. Based on the established criteria, the amount of stripping is estimated visually. The total visible area of the aggregate is estimated as either less than or greater than 95%, which is a major limitation of the test. Based on the test results, it is revealed that the amount of stripping increased when samples are placed at 60 °C bath rather than 25 °C for 18 hrs.

Dynamic Immersion Test: This test is used to accelerate the stripping effect compared with the static immersion test. However, this test has not been standardized and is not widely used. In this test, the preparation of samples of asphalt-aggregate mixtures is done using the similar way of the static immersion test, with an additional agitation of 4 hrs. The degree of stripping increases as the period of agitation increases. However, both static and dynamic immersion tests fail to address the pore pressure effect and traffic action, which is applicable for all tests on loose mixtures.

Chemical Immersion Test: The determination of the adhesion between bitumen and stone aggregate by means of boiling asphalt-coated aggregate successively in distilled water is covered by this test method *(59).* In this test, increasing concentrations of sodium carbonate (Na_2CO_3) are used, numbered 0 to 9 and referred to as the Riedel and Weber (R&W) number where zero refers to distilled water, 1 implies 0.41 gm of sodium carbonate in 1 L of water, and 9 refers to the highest concentration, which is 106 gm of Na_2CO_3 in 1 L of water. For every doubling of concentration between 1 and 9, the R&W number is increased by one. The stripping value is defined as the number of the concentration at which the bitumen strips to such a degree that it is no longer a film but only droplets. A mass of 100 gm of the test sample of the asphalt-aggregate mixture is dried in an oven at 110 °C. The aggregates are mixed with the binder at high temperature and then cooled to room temperature. Solutions of sodium carbonate at different concentrations are prepared using distilled water. Then, approximately 50 mL of distilled water is heated up to boiling in a 200-mL glass beaker. Later, 10 gm of the prepared aggregate-binder mix is placed into the boiling water. The water is drained after 1 minute (min) of boiling, and the sample is placed on filter paper. After drying, the sample is examined for stripping. The stripping value of the aggregate is the R&W number of the lowest concentration at which stripping occurs. Generally, a stripping value of 10 is given to the aggregate, if the sample does not strip at number 9. However, the procedure is repeated, starting with the weakest concentration of sodium carbonate if no stripping is observed.

Surface Reaction Test: To quantify the level of stripping for loose asphalt-aggregate mixtures, several test procedures were developed at different times. One of the procedures was developed by Ford et al. *(60)*, which is known as the surface reaction test. The principle of this test is that calcareous or siliceous minerals will react with a suitable reagent and generate a gas as part of the chemical reaction products. This generated gas will create a certain pressure in a sealed container that can be considered proportional to the mineral surface area exposed to the reagent. Usually, an acid is used as the reagent. The test is conducted on the asphalt-aggregate mixture after subjecting to the stripping effects of water. Different exposed surface areas of aggregate particles result in different levels of stripping. Higher gas pressure is generated due to the larger exposed surface area. This test is simple and reproducible, which takes less than 10 mins to perform. On the other hand, the use of highly corrosive and toxic acids is required for the test.

Texas Boiling Test: Kennedy et al. (37) developed this test procedure as part of an extensive experimental study. In this test method, the asphalt-aggregate mixture is added to boiling water. Afterward, the water must be brought back to boiling temperature after this addition. The mixture is then allowed to cool after 10 mins, while the stripped asphalt is skimmed away. Later, the wet mixture is placed on a paper towel after draining the water out and allowed to dry. Finally, the degree of stripping estimated using visual inspection. This procedure is standardized as ASTM D3625 (Effect of Water on Bituminous-Coated Aggregate Using Boiling Water). This test procedure is less time consuming for evaluating the moisture damage of an asphalt-aggregate mixture. The test may be used for quick evaluation of various asphalt-aggregate combinations as a relative measure of the bond quality and stripping resistance. However, the mechanical properties of the mix and the effects of traffic action are not included in this test.

Pneumatic Pull-Off Test: This test provides a quick and reproducible means of evaluating moisture sensitivity of asphalt binders. The tensile and bonding strength of the asphalt binder,

measured by the experimental procedure applied to a glass plate as a function of time while exposed to water. Asphalt binder that contains 1.0% by weight of glass beads, is applied to a porous disk, which is then pressed onto a glass plate. The glass beads are used to control the thickness of the asphalt film have no effect on the results. The pressure required for debonding the conditioned specimen is measured with a pneumatic adhesion tester at 25 °C. Typically, the pulling rate is about 66 kPa/s, and the asphalt film thickness is around 200 microns. The test showed that soak time is an important factor, as expected. This means that the mixture that is susceptible to debonding, shows higher stripping damage due to longer exposure to water. Youtcheff and Aurilio *(61)* reported that the viscosity building structure provided by Asphaltenes is disrupted by the presence of water, and the resistance to moisture damage of the binder is dependent on the properties of the maltenes.

Surface Free Energy (SFE) Test: In recent years, numerous researchers used the fundamental science-based techniques to measure the moisture sensitivity in asphalt pavements. Hence, extensive research was performed to investigate the relationship between SFE and moisture damage potential *(62-66).* It can be noted that a majority of the research on SFE of asphalt-aggregate systems has been conducted at Texas A&M University *(67-70).*

The concept of SFE is based on the principle that the cohesive bonding within asphalt and the adhesive bonding between asphalt and aggregate are related to the SFE of the asphalt and aggregate. The SFE of asphalt can be determined by using a Wilhelmy plate (WP) test, Sessile Drop (SD), and Atomic Force Microscopy (AFM). The SD *(71)* and universal sorption device (USD) test methods were developed by some researchers at Texas A&M University, which are useful for measuring the SFE of the aggregates. The WP test measures the dynamic contact angle between asphalt and a liquid solvent to determine the SFE.

Rolling Bottle Test: This test was developed by Isacsson and Jorgensen *(72)* in Sweden. In this test, aggregate chips are coated with binder and covered with water in glass jars. Then, the jars are rotated so that the contents are agitated. Afterward, the coating of the stones is periodically estimated visually.

Tests on Compacted Mixtures

Moisture Vapor Susceptibility: This procedure was developed by the Caltrans (CTM Test No. 307) *(54)* and has been used in California. Two specimens are prepared and compacted using the kneading compactor, as for mix design testing, except that they are prepared in stainless steel molds. The compacted surface of each specimen is covered with an aluminum seal cap, and a silicone sealant is applied around the edges to prevent the escape of moisture vapor. An assembly with a felt pad, seal cap, and strip wick is prepared to make water vapor available to the specimen by placing the free ends of the strip wick in water. After the assembly is left in an oven at 60 °C with the assembly suspended over water for 75 hrs, the specimen is removed and tested immediately in the Hveem stabilometer. A minimum Hveem stabilometer value is required, which is less than that required for the dry specimens used for mix design.

Immersion-Compression Test: Goode *(24)* introduced this test procedure (Effect of Water on Compressive Strength of Compacted Bituminous Mixtures) for evaluating the moisture sensitivity, originally published as ASTM D1075-49 (AASHTO T 165-55). Among all tests,

this is the first one to be used to measure the moisture damage in asphalt mixes. However, several revisions were made to the procedure in 1996.

Marshall Immersion Test: The conditioning phase of this test is identical to the one used for the immersion-compression test *(74)*. However, Marshall Stability is used as a strength parameter rather than compressive strength.

Texas Freeze-Thaw Pedestal Test: This test was proposed by Kennedy et al. *(36)* as a modification of the water susceptibility test procedure proposed by Plancher et al. *(39)* at the Western Research Institute. The test evaluates the compatibility between the asphalt binder and aggregate and the corresponding adhesiveness. The test is aimed to use a uniform-sized aggregate to reduce the effect of mechanical properties of the mix. It suggests the preparation of hot mix using a fine fraction of aggregate, passing the No. 20 (0.85-mm) and retained on the No. 35 (0.50-mm) sieve and asphalt at 150 °C. The hot mix is prepared by keeping the mix in the oven for 2 hrs at 150 °C and stirred to ensure uniformity of temperature every hour. Afterward, the mix is removed from the oven and cooled to room temperature, reheated to 150 °C, and compacted with a load of about 28 kN for 15 mins to form a briquette 41 mm in diameter by 19 mm in height. Later, the briquette is cured for 3 days at room temperature and placed on a pedestal in a covered jar of distilled water. It is then subjected to thermal cycling at -12 °C for 15 hrs followed by 9 hrs at 49 °C. The briquette surface is checked for cracks after each cycle. The number of cycles required to induce cracking is a measure of water susceptibility (typically 10 freeze-thaw cycles). Figure 4 shows a typical compacted specimen in a water jar during the Freeze-Thaw Pedestal Test.

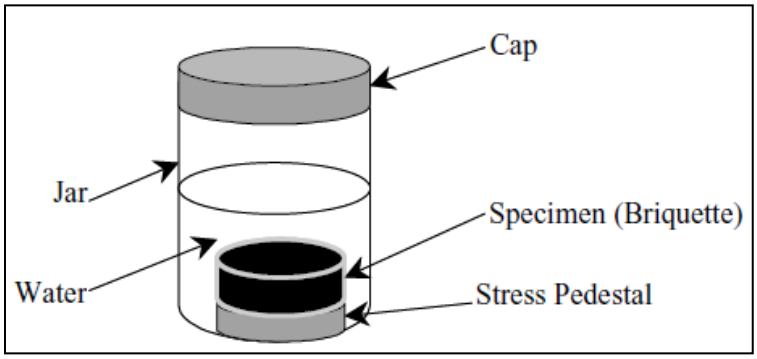

Figure 4. Compacted specimen in a water jar ready for thermal cycling during freeze-thaw pedestal test.

Pedestal test specimens are prepared using uniform-sized aggregate particles coated with 5% asphalt. This formulation reduces aggregate particle interactions in the mixture matrix, and the thin asphalt coating between aggregate particles produces a highly permeable test specimen that allows penetration of water into the interstices found between aggregate particles. Therefore, moisture-induced damage in the specimen can easily arise either from bond failure at the asphalt-aggregate interface region (stripping) or from the fracture of the thin asphalt-cement films bonding aggregate particles (cohesive failure) by the formation of ice crystals.

Original Lottman Indirect Tension Test: The original Lottman procedure was developed by Lottman at the University of Idaho in the late 1970s *(32)*. The procedure requires a total of two groups of specimens (dry and conditioned). The specimens are 4 in. in diameter and about 2.5 in. thick. A vacuum saturation is applied for conditioning in which the specimens are subjected

to 26 in. of mercury vacuum for 30 mins followed by 30 mins at atmospheric pressure. Then, these specimens are frozen at 0°F for 15 hrs followed by 24 hrs in a 140 °F (60 °C) water bath. This is considered accelerated freeze-thaw conditioning. Lottman *(32)* proposed thermal cyclic conditioning as an alternative. For each cycle, after 4 hrs of freeze at 0 °F, the temperature is changed to 140 °F (60 °C) and maintained for 4 hrs before being changed back to 0 °F. Therefore, a complete thermal cycle lasts 8 hrs. The specimens are subjected to 18 thermal cycles in this type. Lottman stated that thermal cycling was somewhat more severe than the accelerated freeze-thaw conditioning with a water bath. Indirect tensile equipment is used to test both conditioned and dry specimens for measuring tensile resilient modulus and tensile strength. The loading rate is 0.065 in./min for testing at 55 °F or 0.150 in./min for testing at 73 °F. The severity of moisture sensitivity is judged based on the ratio of test values for conditioned and dry specimens.

Modified Lottman Indirect Tension Test Procedure: The AASHTO Standard Method of Test T 283 *(58)*, "Resistance of Compacted Bituminous Mixture to Moisture Induced Damage," is one of the most commonly used procedures for determining HMA moisture susceptibility. This test is similar to the original Lottman with a few exceptions. One of the modifications was that the vacuum saturation is continued until a saturation level between 70% and 80% is achieved, compared with the original Lottman procedure that required a set time of 30 mins. The other changes were made in the test temperature and loading rate for the strength test. The modified procedure requires a rate of 2 in./min (5 cm/min) at 25 °C rather than 0.065 in./min (16 mm/min) at 13 °C. A higher rate of loading and a higher temperature were selected to allow testing of specimens with a Marshall Stability tester, available in most asphalt laboratories. The higher temperature also eliminates the need for a cooling system.

Briefly, the test includes curing loose mixtures for 16 hrs at 60 °C, followed by a 2-hr aging period at 135 °C. At least six specimens are prepared and compacted. The compacted specimens should have air void contents between 6.5% and 7.5%. Half of the compacted specimens are conditioned through a freeze (optional) cycle followed by a water bath. Firstly, a vacuum is applied to partially saturate specimens to a level between 55% and 80%. Vacuum-saturated samples are kept in a -18 °C freezer for 16 hrs and then placed in a 60 °C water bath for 24 hrs. After this period the specimens are considered conditioned. The other three samples remain unconditioned. All the samples are brought to a constant temperature, and the indirect tensile strength is measured on both dry (unconditioned) and conditioned specimens, as shown in Figure 5.

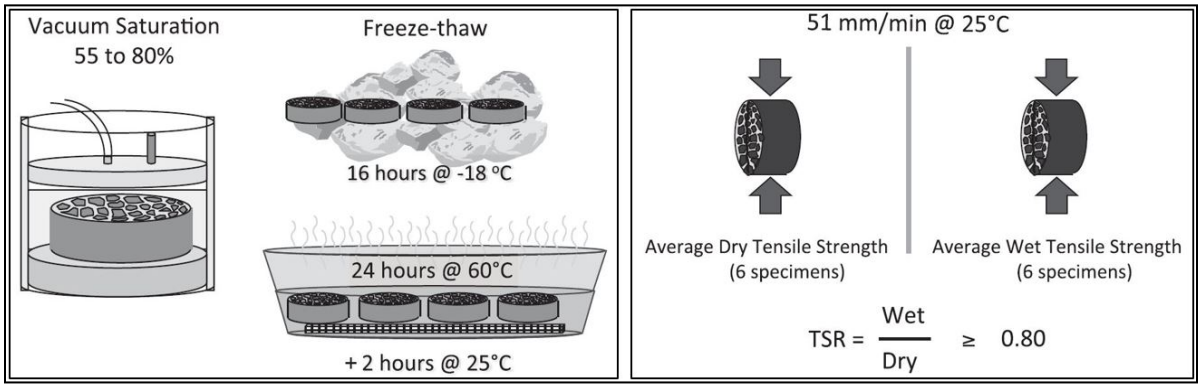

Figure 5. Test sequence for modified Lottman indirect tension test *(58)*.

State highway agencies use this test method because of its reproducibility and its ability to quantify moisture-induced damage with a certain confidence level *(75).* However, all agencies report the mixed success of results with the outcome of this method. Although several research projects have been conducted to identify the limitations of this method and provided some suggestion to update this method, the test remains empirical and provides ambiguous results to predict moisture damage potential.

The Superpave system adopted AASHTO T 283 test procedure as required for determining of moisture sensitivity. Afterward, state highway agencies followed this adoption and made this test as the most widely used procedure for determining the moisture damage. Later, Epps et al. *(76)* investigated the validity and suitability of this test extensively under NCHRP Project 9-13. The project titled "Evaluation of Water Sensitivity Tests" was done and recommended several changes to AASHTO T 283 for its better use in the Superpave system. The researchers examined the effect of various factors on the test results such as different compaction types, the diameter of the specimen, the degree of saturation, and the freeze-thaw cycle, etc. In this investigation, the researchers used five aggregates (two considered good performers and rest three considered to have low to moderate resistance to moisture damage), and specific binder to each mix that includes PG 58-28, PG 64-22, PG 64-28, and PG 70-22.

Tunnicliff-Root Test Procedure: The test method, "Standard Test Method for Effect of Moisture on Asphalt Concrete Paving Mixtures," as designated as ASTM D4867 is comparable with AASHTO T 283, which is known as Tunnicliff-Root Test Procedure *(35).* The freeze cycle is optional in both methods. However, the ASTM D4867 procedure eliminates the curing of the loose mixture in a 60 °C oven for 16 hrs.

Hamburg Wheel-Tracking Test: The Hamburg Wheel-Tracking Device (HWTD) Test (AASHTO T 324) was developed in Germany to evaluate rutting and stripping potential by rolling a steel wheel across the surface of an asphalt concrete specimen that is immersed in hot water *(77).* The wheel rolls back and forth on the submerged specimen. Recently, some agencies use the HWTD to evaluate moisture damage potential of asphalt mixtures due to good repeatability and correlation with field performance *(78,79).* The specimens are submerged in hot water and subjected to 50 passes of a steel wheel per minute, shown in Figure 6. Typically, each sample is loaded for a maximum of 20,000 passes or until 0.8in (20mm) of deformation occurs at a temperature of 45 ^{o}C (113 ^{o}F) or 50 ^{o}C (122 ^{o}F). Some states use this test with some modification based on their own specification. For example, a rut depth of less than 0.5in (12.5mm) after 20,000 passes is required by the Texas Department of Transportation (TxDOT) when a PG 76 binder or higher grade is used. The results from the test provide four phases (post-compaction consolidation, creep slope, stripping slope, and stripping inflection point) of mix behavior, presented in Figure 7. The post-compaction consolidation is the deformation measured at 1,000 passes, considering that the mixture wheel is densified within the first 1,000-wheel passes. The creep slope is the number of repetitions or wheel passes to create a rut depth of 1 mm due to viscous flow. The stripping slope is the number of passes needed to create a 1 mm impression from stripping. The stripping inflection point is the number of passes at the intersection of the creep slope and the stripping slope. This test measures the moisture damage resistance of the HMA and is assumed to be the initiation of stripping *(48).*

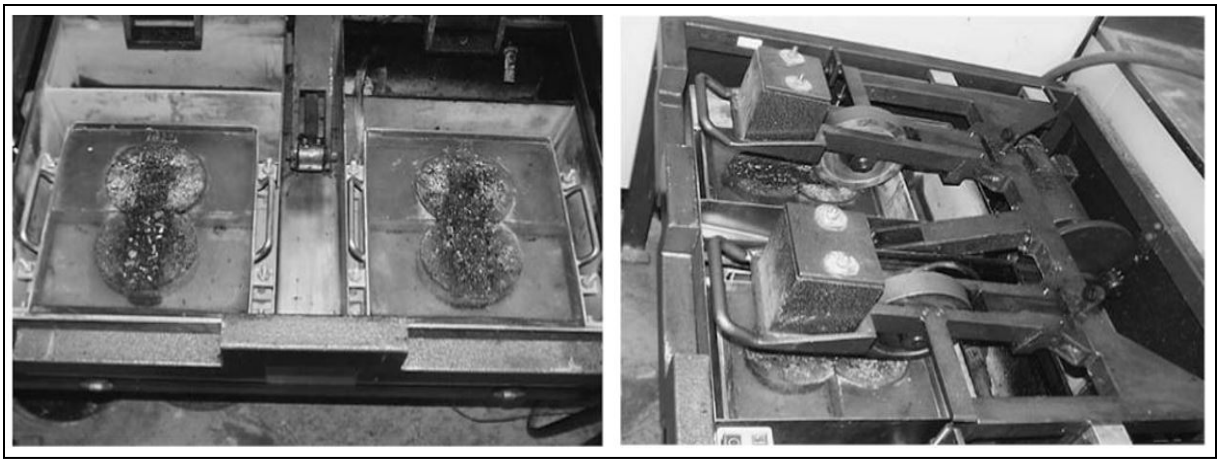

Figure 6. Submerged specimens in the HWTD (left) and HWTD Testing (right) *(80).*

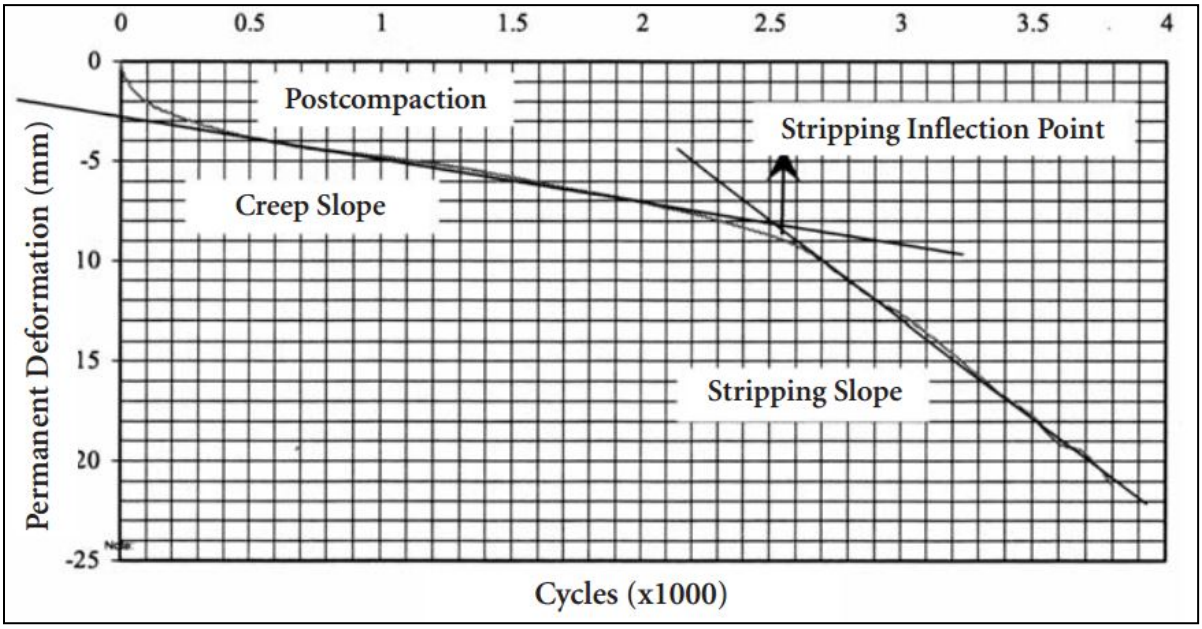

Figure 7. Typical results from HWTT device.

Environmental Conditioning System (ECS) with Modulus: The Environmental Conditioning System (ECS) was developed during the SHRP to more realistically simulate field conditions using repeated hydraulic loading and repeated load cycles *(46).* This ECS system was utilized with a retained resilient modulus ratio (ECS-M_R ratio) with and without multiple moisture conditioning cycles (vacuum saturation, hot water, and optional freeze cycle) (AASHTO TP34) *(46).* This non-destructive test parameter was measured after each moisture-conditioning cycle. The specifications require a minimum retained resilient modulus of 70% of conditioned specimens to unconditioned specimens. Several modifications to the original ECS conditioning parameters and M_R measurement protocols have been made to provide a better correlation between test results and field performance *(51, 81).*

Asphalt Pavement Analyzer: The Asphalt Pavement Analyzer (APA) is a modification of the Georgia Loaded Wheel Tester (GLWT), shown in Figure 8. The APA was first manufactured by Pavement Technology, Inc. in 1996, and used to evaluate the rutting, fatigue, and moisture resistance of HMA mixtures *(82).*

Figure 8. Asphalt pavement analyzer *(82).*

The APA follows a similar rut-testing procedure like GLWT and allows for a maximum rut depth. A wheel is loaded onto a pressurized linear hose and tracked back and forth over a testing sample to induce rutting. The test criterion is the ratio of conditioned rut depth to unconditioned rut depth where the values greater than 1 suggest the mixture is susceptible to moisture damage *(82).* It is reported that the APA testing of saturated mixtures can be used to predict moisture sensitivity by simulating the repeated hydraulic loading that pavements undergo desirable testing efficiency *(83).*

Aschenbrener *(84)* conducted a survey and reported that most agencies use several retained strength tests on compacted mixtures (Lottman, modified Lottman, Tunnicliff-Root, or immersion-compression) to evaluate moisture damage potential of asphalt pavements, shown in Table 2. Kiggundu and Roberts *(42)* investigated the success rate of predicting moisture damage in the field and reported the limitations of the most popular test method (AASHTO T 283), presented in Table 3.

Most recently, Caro and Rivera *(85)* conducted a comprehensive survey on moisture damage among all DOTs where 39% of the states participated in the survey. The purpose of this study was to identify the current state of knowledge in moisture damage in asphalt mixtures to define a new Research Needs Statements (RNS). One of the major findings of this survey is that approximately 60% of the participated states consider the moisture damage as a major issue for affecting the durability of flexible pavements. These authors found that sixteen states use modified Lottman (AASHTO T 283) test method, one state uses Hamburg Wheel-Tracking Test,

one state follows various specifications, and three states do not use any test method or specification for controlling or preventing moisture damage, shown in Figure 9. They also investigated that 160 papers were published in the pavement engineering related journal in the last 10 years, in which moisture damage of asphalt pavements was the main research issue. After reviewing the literature, they classified the scale of the study on moisture damage into several categories, as shown in Figure 10. These researchers also mentioned that DOT uses various additives or antistripping agents, for example, nine states use liquid antistripping agents while hydrated lime is used by six agencies. However, some DOTs use other types of additives and/or follow the contractor's recommendations for controlling the moisture damage potential.

Table 2. Agencies using different moisture sensitivity tests after SHRP *(4)*.

Name of Test Methods	Number of Agencies using the Method
Boiling Water (ASTM D 3625)	0
Static Immersion (AASHTO T 182)	0
Lottman (NCHRP 246)	3
Tunnicliff-Root (ASTM D 4867)	6
Modified Lottman (AASHTO T 283)	30
Immersion-compression (AASHTO T 165)	5
Hamburg Wheel-Tracking	2

Table 3. Success rates of the moisture sensitivity test methods *(42)*.

Test Methods	Minimum Test Criteria	% Success
Modified Lottman (AASHTO T 283)	TSR = 70%	67
	TSR = 80%	76
Tunnicliff-Root	TSR = 70%	60
	TSR = 80%	67
	TSR = 70% - 80%	67
10-min Boil Test	Retained Coated, 85% - 90%	58
Immersion-compression (AASHTO T 165)	Retained Strength, 75%	47

Note: TSR = Tensile Strength Ratio

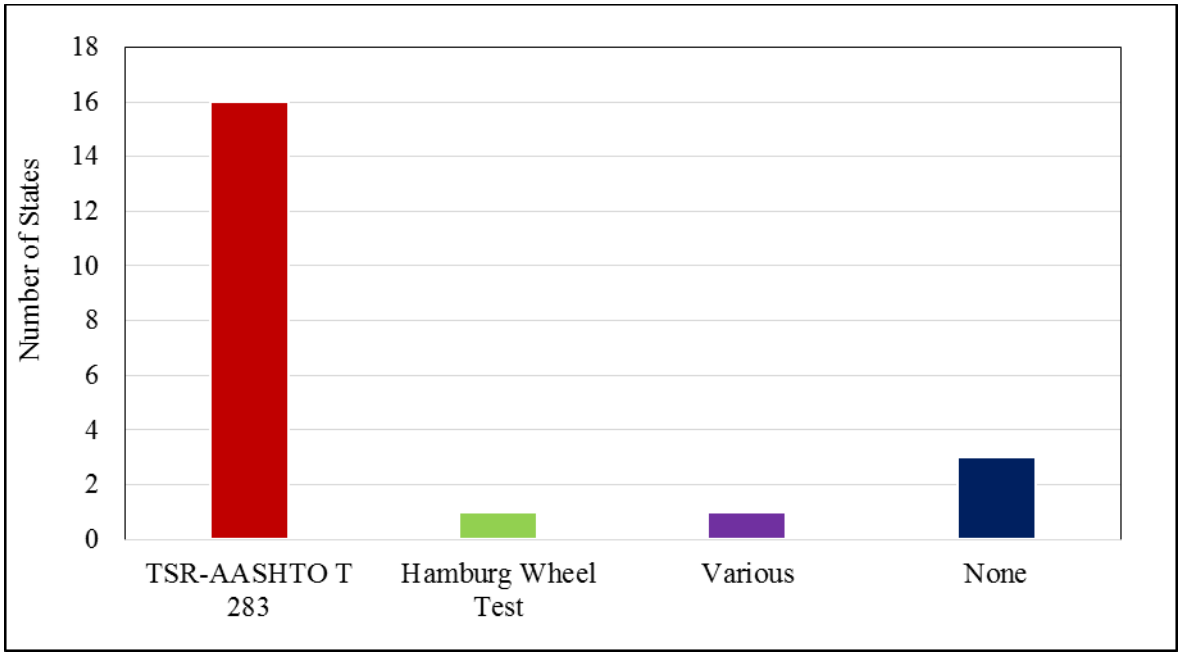

Figure 9. DOT survey on moisture damage (85).

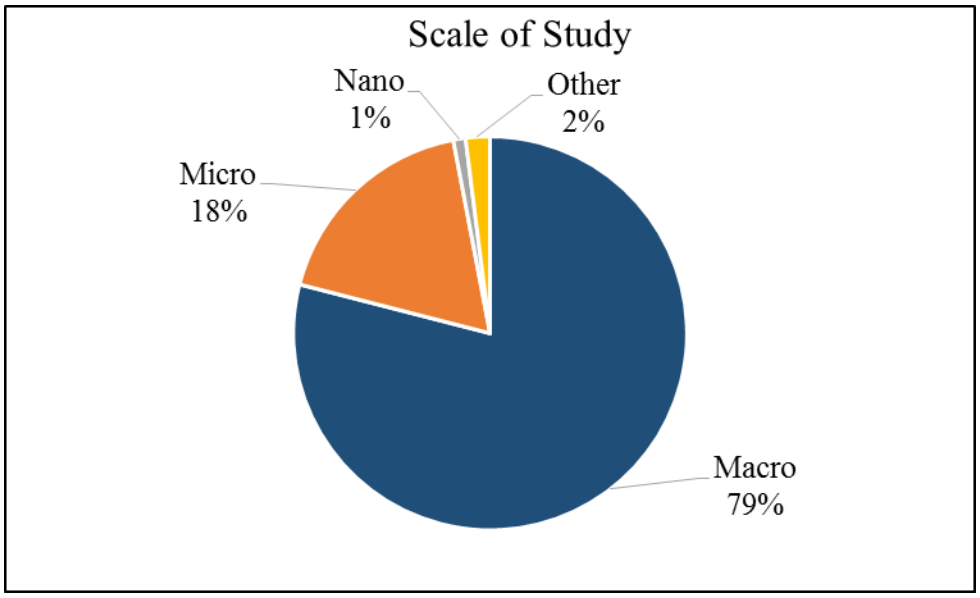

Figure 10. Scale of study on moisture damage in last 10 years *(85)*.

It can be noted that the conventional moisture sensitivity tests are performed at the macro level, which is unable to provide an atomic-level understanding of the moisture damage phenomenon and its mechanisms. Prior to developing an effective test method, a comprehensive knowledge of the moisture damage at both macro and micro-level is necessary. Recently, the researchers are interested to use nanotechnology to gain a comprehensive knowledge of the moisture damage mechanisms and its effects on the asphalt binder's properties at the nanoscale.

AFM is one of the emerging advanced technologies that is capable of scanning and capturing the topography images of the sample surface of a selected area that contains the morphological

information at the nanometer scale *(86).* In an earlier study, Leober et al. *(87)* also reported that a new direct observation of the asphalts and binders at the nano level is possible using AFM. The AFM can be used to investigate the surface morphology and the micromechanical properties such as DMT (Derjaguin, Muller, and Toropov) modulus, adhesion, deformation, and energy dissipation of the asphalt binders by several researchers *(88-94).* These researchers described three distinct phases such as Catana or dispersed phase, Peri-phase or interstitial phase, and Para-phase or matrix to characterize the morphological clusters, which were also used in this study. Moreover, the AFM technology was used to investigate the moisture damage of asphalt binder and mixture samples in *(95, 96).* Yao et al. *(95)* used AFM to capture force-displacement curves at nine sites on the topographic images of the binders. They quantified the nanomechanical properties using NanoScope Analysis 1.50 and characterized two types of moisture damage (adhesive and cohesive failures) of asphalt binders based on adhesion force and modulus values. In this study, moisture effects on morphological and nanoscopic properties of asphalt binder are investigated through Peak-Force Quantitative Nanomechanical Mapping (PFQNM) techniques of AFM (Dimension icon, Bruker) and NanoScope Analyses 1.5.

1.2. Findings from Literature Review

Moisture damage in asphalt pavements is a major concern to all DOTs and all other transportation agencies in the world. Stripping related damage in pavements is a complex phenomenon, which is largely dependent on the physical and mechanical properties of asphalt and aggregate or related to the interaction of asphalt-aggregate systems. A considerable number of tests on moisture sensitivity have been developed by researchers, DOTs, and agencies over the past 70 years. Some of these tests are developed based on the properties of loose mixtures of asphalt and aggregate, while some tests were conducted on the compacted mixture. Many researchers consider the effect of water action and traffic loads during the measurement of moisture sensitivity. On the other hand, some researchers account the permanent deformation (rutting) of the compacted mix under the combined action of water and traffic loads. Besides, multiple researchers and industries use surface free energy to quantify the moisture damage.

In conclusion, after conducting a comprehensive literature review, the summary of the moisture damage tests along with their corresponding references are presented in Table 4. Furthermore, based on the importance, effectiveness, and suitability of their adaptation to evaluate the moisture damage potentials in asphalt pavements, previous studies (*84-85*) ranked the commonly used moisture resistance tests, as shown in Table 5. From Table 5 it is seen that a ranking point of less than 4 means “poor,” whereas a ranking value from 4 to 6 denotes “good.” If the ranking value varies between 7 and 8, the tests are classified as “very good.” Moreover, the ranking points between 9 and 10 are considered “excellent.”

Table 4. Summary of moisture sensitivity tests.

Components and Compatibility Test	References
Sand Equivalent	CTM, Test No. 217 *(54)*
Plasticity Index	CTM, Test No. 204 *(54)*
Cleanness Value	CTM, Test No. 227 *(54)*
Methylene Blue	Technical Bulletin 145, ISSA *(55)*

Components and Compatibility Test	References
Net Adsorption	SHRP-A-341 *(47)*
Tests on Loose Mix	
Film Stripping	CTM, Test No. 302 *(54)*
Static Immersion	AASHTO T 182 *(47)*
Dynamic Immersion	---
Chemical Immersion	Road Research Laboratory, England *(59)*
Surface Reaction	Ford et al. (1974) *(60)*
Boiling	D3625 Tex 530-C (Kennedy et al. 1984) *(37)*
Pneumatic Pull-Off	Youtcheff and Aurilio (1997) *(61)*
Surface Energy	Cheng et al. (2002) *(68);* Thelen (1958) *(70)*
Rolling Bottle	Isacsson and Jorgensen (1987) *(72)*
Quick Bottle	Maupin (1980) *(73)*
Tests on Compacted Mix Specimens	
Moisture Vapor Susceptibility	CTM, Test No. 307 *(54)*
Immersion-Compression	AASHTO T 165 *(58)*
Marshall Immersion	Stuart (1986) *(74)*
Freeze-Thaw Pedestal	Kennedy et al. (1984) *(36)*
Original Lottman Indirect Tension	Lottman (1982) *(32)*
Modified Lottman Indirect Tension	AASHTO T 283 *(58)*
Tunnicliff-Root	ASTM D4867 (Tunnicliff and Root 1984) *(35)*
Hamburg Wheel-Tracking	Tex-242-F, Texas DOT (37)
ECS with Resilient Modulus	SHRP-A-403 *(46)*
Asphalt Pavement Analyzer	---

Table 5. Ranking of moisture sensitivity tests based on literature review.

Test Methods	Ranking (Out of 10 points) (*84-85*)
Modified Lottman (AASHTO T 283)	10 (Excellent)
Hamburg Wheel Tracking (AASHTO T 324)	10 (Excellent)
Tunnicliff-Root (ASTM D 4867)	08 (Very Good)
Immersion-compression (AASHTO T 165)	08 (Very Good)
Surface Free Energy	07 (Very Good)
Boiling Water (ASTM D 3625)	07 (Very Good)

Test Methods	**Ranking (Out of 10 points) (*84-85*)**
Chemical Analysis	06 (Good)
Atomic Force Microscope Test	05 (Good)
Static Immersion (AASHTO T 182)	03 (Poor)
Other	02 (Poor)

2. OBJECTIVE

The key objective of this project is to recommend an effective test protocol to quantify moisture susceptibility of asphalt mixtures considering the surface chemistries and molecular level properties as well as aggregate-binder compatibility. Specific objectives of this study are to:

1. Measure the stripping resistance of aggregate-binder systems using surface chemistries and atomic level material properties,
2. Quantify the moisture damage of asphalt mixture samples using conventional mechanistic-empirical test procedures,
3. Find the most effective test method to evaluate moisture susceptibility based on materials' surface chemistries, mechanistic and field performance data.

3. SCOPE

The scope of this project is limited to reviewing existing literature, conducting laboratory study on asphalt binder samples and analyzing test results of limited asphalt mixture samples. Moreover, ARDOT TRC 1501 project was a matching fund for this study; thus, moisture damage related test data of TRC 1501 project was analyzed in this study. Specifically, the following steps were followed to achieve the overall goal of the project:

- Find the state-of-practice for predicting moisture resistance of asphalt concrete mixtures' binders modified with different additives.
- Perform routine performance (Superpave) tests of selected ARDOT-certified asphalt binders modified with different additives. The Superpave tests included Dynamic Shear Rheometer (DSR) per AASHTO T 315, Rotational Viscosity (RV) per AASHTO T 316, Rolling Thin Film Oven (RTFO) per AASHTO T 240, Pressure Aging Vessel (PAV) per AASHTO R 28, and Bending Beam Rheometer (BBR) per AASHTO T 313.
- Predict moisture resistance of selected aggregate-binder systems by following the surface science approaches and develop a compatibility database.
- Perform Atomic Force Microscope (AFM) tests on unaged binders on both dry and wet-conditioned samples to observe the moisture effects on the properties of asphalt binders at the atomic level. Conduct selective chemical tests (SARA and FTIR) of the selected asphalt binders to investigate relationship striping and chemical fingerprints, if any.
- Analyzing experimental data of commonly used moisture resistance mixture tests such as Texas Boling, Hamburg Wheel Test Device (HWTD), and Tensile Strength Ratio (TSR).
- Find the most effective stripping test by analyzing existing and new test data.

4. METHODOLOGY

To fulfill the goals of this project, a high-level project flow diagram (Figure 11) was developed. It shows the critical steps and associated tasks for the successful completion of the project.

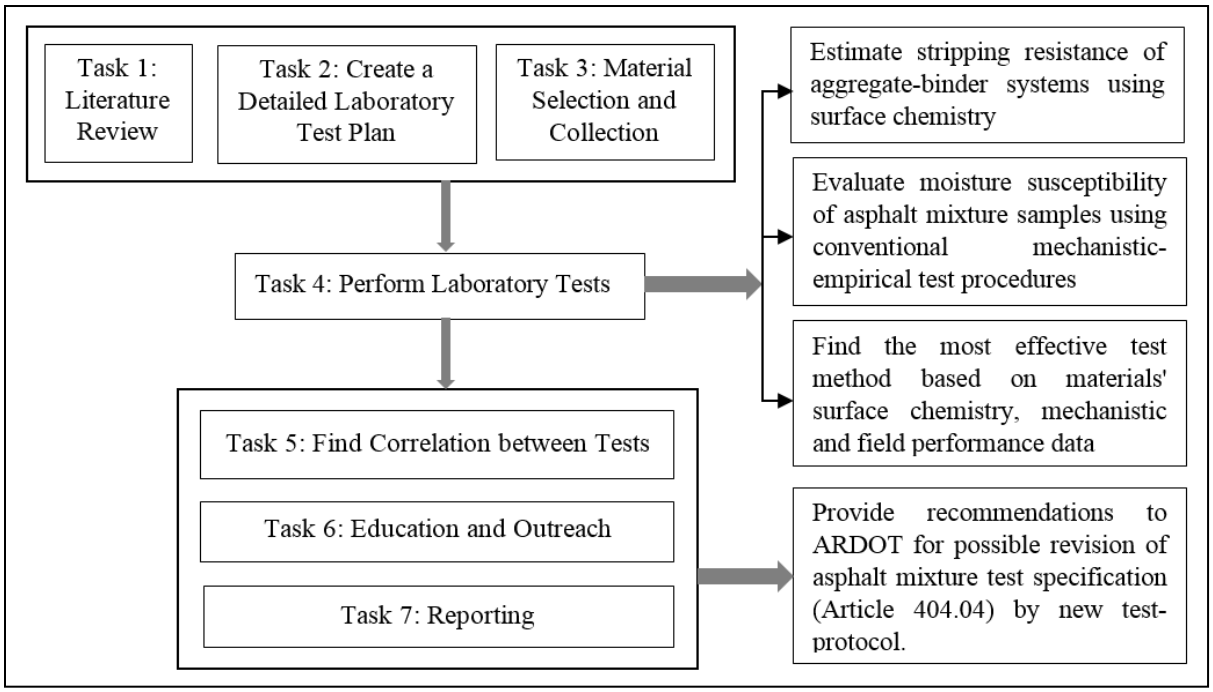

Figure 11. High-level project flow diagram showing research objectives and critical tasks.

4.1. Materials

Both unmodified and modified asphalt binders were collected, and they included Performance Grade (PG) PG 64-22, SBS-modified PG 70-22, PPA-modified PG 70-22, and SBS plus PPA modified PG 76-22 binders. These binders are collected from two different sources. The first asphalt binder was a Canadian crude source (S1), and it was supplied by Ergon Asphalt and Emulsions, Inc. Memphis, TN. The second binder was an Arabian crude source, which was a combination of "sweet and sour crudes (S2)," and it was supplied by Marathon Petroleum Corporation, Catlettsburg, KY. Details of sample modifications and nomenclatures are shown in Table 6. Furthermore, three different liquid anti-stripping agents (LAAs) (ADhere HP Plus, Permatac Plus, and Evotherm) were also used to further modify the PG binders, as shown in Table 7.

Table 6. Details of sample nomenclature used in this study.

Modification	Crude Source	Refinery Name	Additive	Marketed PG	Nomenclature
PG 64-22	Canadian	S1	-	PG 64-22	S1B1
PG 64-22	Canadian	S1	0.5% PPA	PG 70-22	S1B3
PG 64-22	Canadian	S1	2% SBS	PG 70-22	S1B7
PG 64-22	Canadian	S1	2% SBS, 0.5% PPA	PG 76-22	S1B8
PG 64-22	Arabian	S2	-	PG 64-22	S2B1
PG 64-22	Arabian	S2	0.75% PPA	PG 70-22	S2B3
PG 64-22	Arabian	S2	2% SBS	PG 70-22	S2B7
PG 64-22	Arabian	S2	2% SBS, 0.75% PPA	PG 76-22	S2B8

Table 7. Nomenclatures of LAA modified binders used in this study.

Base Binder	Type of LAA	Nomenclature
S1B1	PermaTac Plus	S1B1+PermaTac
S1B1	Adhere HP Plus	S1B1+Adhere
S1B1	Evotherm M1	S1B1+Evotherm
S2B1	PermaTac Plus	S2B1+PermaTac
S2B1	Adhere HP Plus	S2B1+Adhere
S2B1	Evotherm M1	S2B1+Evotherm

Two different aggregates, namely, Sandstone and Gravel, both from APAC Central (Preston Quarry at Van Buren) Arkhola, Arkansas were used to find out their compatibilities with different asphalt binders. Plant asphalt mixes prepared with these aggregates were collected for selected laboratory tests. Historically, Sandstone has been reported to be highly susceptible to stripping, and it has been a major concern for the ARDOT. The other aggregate (gravel) is also susceptible to stripping but to a lesser extent than Sandstone. These aggregates were collected by the Co-PI of a recently completed project (TRC 1501), funded by the ARDOT. They were processed, and mixture samples were tested at the University of Arkansas Laboratory at Fayetteville. However, stripping resistance of mixtures was not the primary focus of TRC 1501.

4.2. Laboratory Tests

SBS-, PPA- and LAA-modified asphalt binders were tested in the laboratories. The following tests were performed in the laboratory to achieve the goals of the projects.

4.2.1. Performance (Superpave) Tests

To evaluate rheological properties of the collected binder samples, Superpave tests including Rotational Viscometer (AASHTO T 316), Dynamic Shear Rheometer (AASHTO T 315), Rolling Thin-Film Oven (RTFO) (AASHTO T 240), Pressure-Aging Vessel (PAV) (AASHTO R 28), and Bending Beam Rheometer (BBR) (AASHTO T 313) were conducted. These tests are briefly discussed below.

Rotational Viscosity (RV) Test: The viscosity of the asphalt binder is the measure of the workability, pumpability, and mixability of the asphalt binders. The RV test was performed in

accordance with AASHTO T 316. Figure 12 shows a DV-II+ Pro rotational viscometer (RV) from Brookfield Engineering Inc. in which the test was performed. The RV test is performed to measure the viscosity of asphalt binders at higher temperatures. In this study, the RV test was done from 135 °C to 180 °C at a 15 °C interval. Firstly, the asphalt binder sample is heated until fluid and 10 gm of asphalt binder is poured into the sample chamber. The temperature is set to the desired temperature by using a temperature controller and it is kept for 30 mins to bring it to the set temperature. At that temperature, the asphalt binder sits for 10 mins to ensure the stability of the test temperature. After that, the motor is turned on and 3 separate readings are taken at 1 min interval. The spindle rotates at a constant speed of 20 rpm and the amount of torque required maintaining a constant speed (20 rpm) of the cylindrical spindle indicates the viscosity of the binder. The Superpave specification for unaged asphalt binder is that the viscosity of the binder should be ≤ 3 Pa.s at 135 °C.

Figure 12. RV test device.

Dynamic Shear Rheometer (DSR) Test: The DSR test is performed to characterize the viscous and elastic behavior of asphalt binder at high and intermediate service temperatures. The DSR measures the complex shear modulus (G*) and phase angle (δ) of asphalt binders at desired temperatures and frequency of loading. The G* is the measure of the total resistance of the binder to deformation when repeatedly sheared whereas, the δ is the measure of elasticity of the binder. The lower the values of δ, the more elastic the binder is, whereas a higher value indicates viscous binder. In this study, an Anton Paar MCR 302 DSR machine was used as shown in Figure 13. In the DSR test, a thin binder sample is sandwiched between two circular plates where the lower plate is fixed, and the upper plate oscillates back and forth at a certain frequency, creating a shearing action. According to AASHTO T 315, the test frequency is 10 radians per second (1.59

Hz). The test is performed according to AASHTO T 315 in different aging conditions, namely, unaged, RTFO-aged and PAV-aged, of the binders. For unaged and RTFO-aged binders, the primary measurement according to the Superpave specification is the rutting parameter, which is calculated by taking the ratio of G* and sinδ (i.e., G*/sinδ). On the other hand, the DSR test for PAV-aged binders calculates fatigue factor at intermediate temperatures by multiplying G* and sinδ (i.e., G*.sinδ).

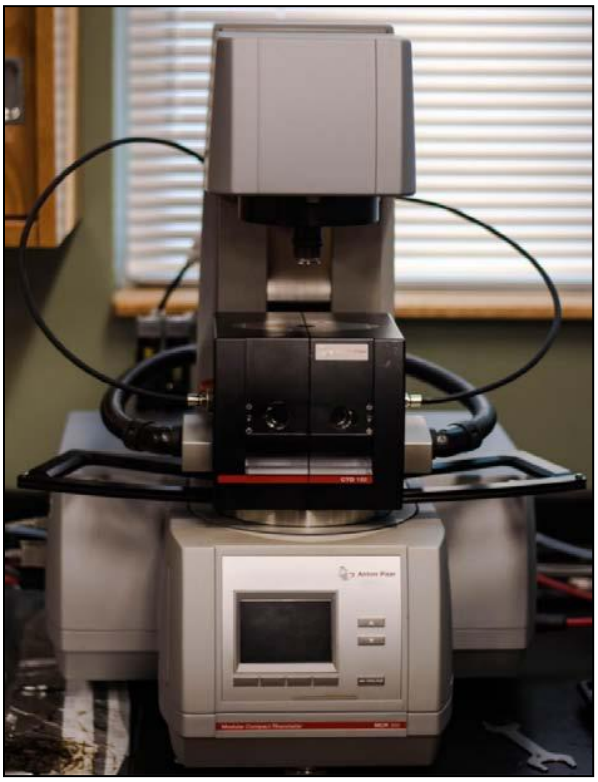

Figure 13. Dynamic shear rheometer.

The Superpave specifications with respect to the DSR test results for unaged, RTFO-aged and PAV-aged binders are shown in Table 8.

Table 8. Superpave specification for rutting and fatigue factor.

Material	Value	Test Temperature (oC)	Specification
Unaged binder	G*/sinδ	High Service	≥ 1.0 kPa (0.145 psi)
RTFO-aged binder	G*/sinδ	High Service	≥ 2.2 kPa (0.319 psi)
PAV-aged binder	G*.sinδ	Intermediate Service	≤ 5000 kPa (725 psi)

Bending Beam Rheometer (BBR) Test: The BBR test is performed to measure low-temperature stiffness and stress relaxation properties of asphalt binders. These parameters indicate asphalt binders' resistance to low-temperature cracking. Apart from that BBR test also provides the low service temperature of the PG grading. From the BBR test creep stiffness and the slope of the master stiffness curve referred to as "m-value" at 60 seconds (s) is measured. The test is performed in accordance with AASHTO T 313. A typical BBR device is shown in Figure 14. The Superpave specifications for BBR test are shown in Table 9.

Figure 14. Bending beam rheometer (BBR).

Table 9. Superpave specification for BBR test.

Parameter	Test Temperature (°C)	Specification
"m-value" at 60 second	Low Service Temperature +10 °C	≥ 0.300
Stiffness at 60 seconds	Low Service Temperature +10 °C	≤ 300 MPa

For the test, degassed PAV-aged binders are used to prepare a 0.246 x 0.492 x 5.000 inch (6.25 x 12.5 x 127 mm) solid asphalt beam. This beam is loaded at its midpoint in a simply supported set-up where the two supports are 4.02 inches (102 mm) apart and the load is 0.22 lb (100 g). The beam deflection is measured at 8, 15, 30, 60, 120 and 240 seconds. A stiffness master curve is plotted for these points. From the curve, slopes are drawn at 8, 15, 30, 60, 120 and 240 seconds to calculate the "m" values. The test is performed at a 10 °C higher than the expected the low service temperature. To simulate the low service temperature, the time-temperature superposition principle is used.

Rolling Thin Film Oven (RTFO): The RTFO oven simulates short-term aging of asphalt binders for using in DSR test as well as for PAV-aging. The RTFO oven uses high temperature and air pressure to simulate the aging phenomenon happens to asphalt binders during the heating and storage inside of a mixing plant. Figure 15 shows an RTFO oven used for this study. The RTFO-aging of asphalt binders is done according to AASHTO T 240. At first, 35 gm asphalt binder is poured into cleaned and preheated RTFO glass bottles. The glass bottles are then placed into the RTFO sample rack which rotates at a speed of 15 rpm. The test temperature is 163 °C and the aging time is 85 mins. During the test, 244 in^3/min (4 L/min) air flows into each sample bottles.

Figure 15. Rolling thin film oven (RTFO).

Pressure Aging Vessel (PAV): The PAV simulates long-term aging of asphalt binders (7 to 10 years). The PAV aging is done in accordance with AASHTO R 28. Figure 16 shows the PAV device used for this study. The aging process is conducted at various temperatures namely, 90 °C, 100 °C, and 110 °C depending on the climatic condition. For this study, a temperature of 100 °C for aging was selected. Moreover, the aging process takes 20 hrs. The required air pressure for PAV aging is 300 psi (2.07 MPa). The PAV-residues are used for DSR tests for measuring the fatigue factor and BBR test to measure the low-temperature cracking properties of asphalt binder. However, before using the PAV residues for any test, it is recommended to degas the sample in a vacuum degassing oven. Figure 17 shows a vacuum degassing oven used in this study. The degassing process is done at a temperature of 170 °C for a period of 30 mins.

Figure 16. Pressure aging vessel (PAV).

Figure 17. Vacuum degassing oven.

4.2.2. Texas Boiling Test

Texas Boiling Test is a simple and quick method for evaluating the moisture damage of the asphalt mixture samples. It has been utilized by different highway agencies. In this test method, a fraction of aggregates or all aggregates used to use used in preparing the asphalt mixture are tested for moisture resistance. For an individual aggregate mixture, the following aggregates could be used: i) passing 3/8 inch retained on No. 4, ii) passing No. 4 retained on No. 10, iii) passing No. 10 retaining on No. 40, and iv) passing No. 40 retaining on No. 80. To evaluate the total aggregate mixture, the sample should have the same gradation as proposed for the construction work. However, the aggregates greater than 7/8 inch are normally discarded for this test.

The Texas boiling test includes heating the mixture inside a glass beaker with boiling water. At first, a 1000 ml beaker is filled with 500 ml of distilled water and heated to boiling temperature. Afterward, the mixture that is kept at room temperature is added to the boiling water. As the temperature of water decreases, heat is applied to the glass beaker at a rate so that the water re-boils within two to three minutes. The water needs to be maintained at a medium boil for ten minutes and stirred with a glass rod at three-minute intervals. The stripped asphalt should be skimmed away by the paper towel to prevent recoating of the aggregate again. Later, the mixture is let to cool inside the beaker to a room temperature before the final observation. Then the water is drained out from the beaker and the wet mixture is emptied on a paper towel and allowed to dry. The final data should be taken at least half an hour after the aforementioned process. Figure 18 shows guidelines given by the Texas Transportation Institute (TTI) for determining what percentage of asphalt is remaining on the surface of the aggregates, which was followed in this study.

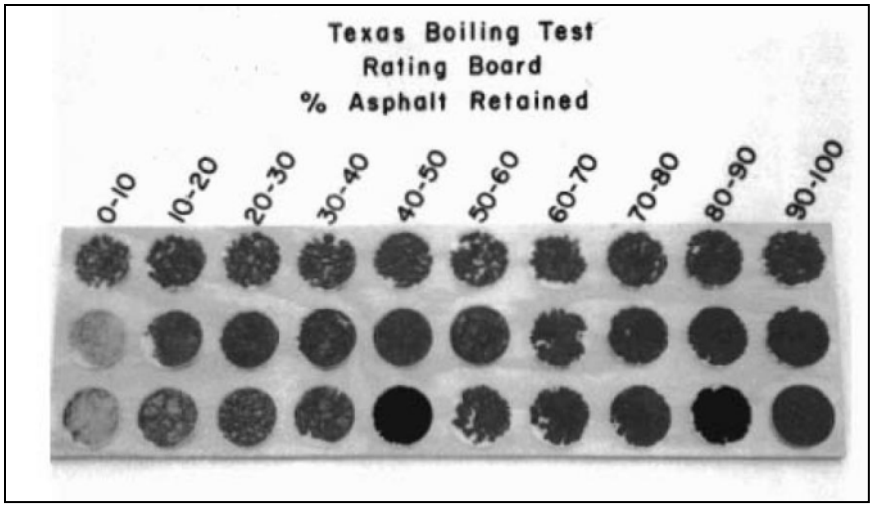

Figure 18. Rating board for Texas Boiling Test *(36)*.

Hamburg Wheel Testing Device (HWTD): The HWTD is used for evaluating the rutting and moisture-susceptibility of HMA. It determines the susceptibility of premature failure of HMA caused by weakness in the aggregate structure, inadequate binder stiffness, or moisture damage. From this test, the rut depth and the number of passes to failure are measured. A slightly modified version of the HWTD test was adopted in the TRC 1501 project (97), and it was referred as ERSA (Evaluation of Rutting and Stripping of Asphalt) test.

To perform the ERSA test, a laboratory-compacted specimen of HMA, which can be sat-cut slab specimen or a core from a compacted pavement, is needed. The thickness of the cylindrical specimen can be from 38 mm (1.5 in.) to 100 mm (4 in.) and the diameter of 150 mm (6 in.). Two samples are needed for each test, shown in Figure 19. The specimen should be submerged in a water bath of 40 ^{o}C to 50 ^{o}C. The ERSA Tracking machine has a moving wheel of 203.2 mm (8 in.) and 47 mm (1.85 in.) wide steel which goes along the specimen. It is noted that ERSA test is identical to the HWTD based on its specification. The wheel has a load of 158 lbs., and it should make 52 passes across the specimen per minute with a maximum speed of 0.305 m/s. Since ARDOT specifications for surface courses require a maximum rut depth of 8.0 mm at 8,000 cycles for an APA style wheel tracking tests, the TRC 1501 study considered the maximum cycle of 8,000 and a maximum rut depth of 8.0 mm in the ERSA test.

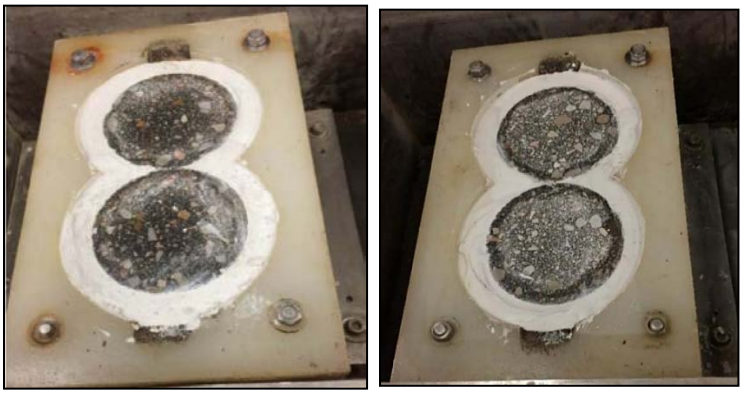

Figure 19. ERSA test samples *(97)*.

4.2.3. Tensile Strength Ratio (TSR)

The TSR test (AASHTO T 283) is used to evaluate the effects of saturation and accelerated water conditioning with a freeze-thaw cycle in the compacted asphalt mixtures. It compares the split tensile strength of unconditioned samples to samples partially saturated with water to assess the potential for moisture damage in an asphalt mixture. As part of the TRC 1501 project *(97),* TSR tests were performed by compacting asphalt mixture specimen with an air voids content of 6% to 8%. Generally, six replicates were used. Three specimens were tested in the dry condition and the rest ones after saturation and moisture condition with the freeze-thaw cycles. The specimens were tested for Indirect Tensile Strength (ITS) by loading the specimen at a constant rate and measuring the force required to fad the specimen. The TSR was calculated by comparing the ITS value of the conditioned and dry samples.

4.2.4. Surface Free Energy (SFE) Analysis

In recent years, SFE analysis has been conducted by many researchers including the research team of the current project to evaluate the moisture damage potential of a mix by calculating the surface properties of aggregates and asphalt binders separately. The principle behind using the concept of surface free energy is that the cohesive bonding within asphalt and the adhesive bonding between the asphalt and aggregate are related to the surface free energy of the asphalt and aggregate individually. Various methods such as WP method, the SD method, and Universal Sorption Device are used by researchers. The SD method was used in this research because of its usage simplicity and availability of the testing tool to the research team.

Researchers at Texas Transportation Institute (TTI) introduced a parameter, called as compatibility ratio (CR), which is the ratio of adhesion energy in dry condition to the adhesion energy in the presence of moisture between aggregates and asphalt binders. A higher CR value indicates a binder with low moisture susceptibility, whereas a lower value indicates a highly moisture susceptible mixture. Figure 20 shows an Optical Contact Analyzer (OCA) device used in this study to determine the wetting ability of any reference solvent on a solid surface. An OCA 15 device from Future Digital Scientific was used to measure contact angles of asphalt binders and aggregates with three reference solvents: Water, Ethylene glycol, and Formamide. Contact angles measured from the OCA tests were used to estimate the SFE by using the van Oss, Chaudhury, and Good (OCG) approach *(98).* The acid-basic component (γ^{AB}) is the geometric mean of γ^{+} and γ^{-}, and the total SFE (γ^{total}) can be written as the sum of γ^{LW} and γ^{AB}. The interfacial bond strength (W^{a}) between a liquid (I) and a solid (s) is estimated by using the Young-Dupre's equation.

Figure 20. Optical Contact analyzer (OCA) device.

4.2.5. Atomic Force Microscopy (AFM) Test

An AFM (Dimension Icon from Bruker) has been used to investigate the surface morphology and the mechanical properties of the asphalt binders at the atomic level. In this study, the effects of moisture on the properties of the asphalt binders were analyzed for both dry and wet-conditioned samples at the nanoscale using the Peak-Force Quantitative Nanomechanical Mapping (PFQNM™) mode of the AFM.

For the preparation of the asphalt samples, the heat cast approach (HCA) was followed in this study as it provided a natural surface of the asphalt. In the HCA approach, a small amount of asphalt binder was placed on a 2in. x 3in. (50mm x 75mm) glass plate which is then placed in an oven at 160 °C for about 15 mins. Generally, a uniform and smooth surface of the asphalt binders is developed on the glass plate during this time of heating. However, it is noticed that this heating time is extended up to 20 mins while using stiff binders. The samples prepared in this way were considered as "Dry Specimens," which were stored in a humidity-controlled desiccator and tested after three days. For preparing the "Wet-conditioned Specimens," dry specimens were removed from the desiccator after 1 hr. assuming that microstructures are stabilized within this time. Later, the following steps were followed to make the wet conditioned samples: i) prepared specimens were placed in Aluminum cans and fulfilled with deionized water with a minimum of one-inch depth of water above the specimens; ii) aluminum cans were placed in the vacuum container; iii) a vacuum of 20-25 in. Hg partial pressure (67-84 kPa absolute pressure) was applied for 10 mins using a vacuum oven; iv) vacuum is stopped after 10 mins and specimens were left submerged in water for a rest period of another 10 mins; v) the specimens

were then placed in a zip-lock bag, and 10ml deionized water was added; vi) afterward, the specimens were placed all the samples in the freezer at -18 ^{o}C ± 3 ^{o}C for 24 hrs ± 1 hr.; vii) later, the specimens were removed from the freezer, and placed in a water bath for 24 hrs ±1 hours at 60 ^{o}C ±1 ^{o}C; viii) later, the specimens were placed in a water bath for 2 hrs ± 10 mins at 25 ^{o}C ± 0.5 ^{o}C maintaining a water depth of 1in. above the specimens, ix) the specimens were then removed from the water bath and dabbed the excess water off from the surface of the specimens using paper towels; x) the specimens were placed in the oven for 16 hours at 25 ^{o}C ± 1 ^{o}C to ensure the absence of water on the surface of the asphalt binders. Prepared samples were then tested using the AFM. Figure 21 shows major steps involving the sample (dry and wet-conditioned) preparation to scan using the AFM. Besides, Figure 22 shows the working principles of the PFQNM™ mode of the AFM.

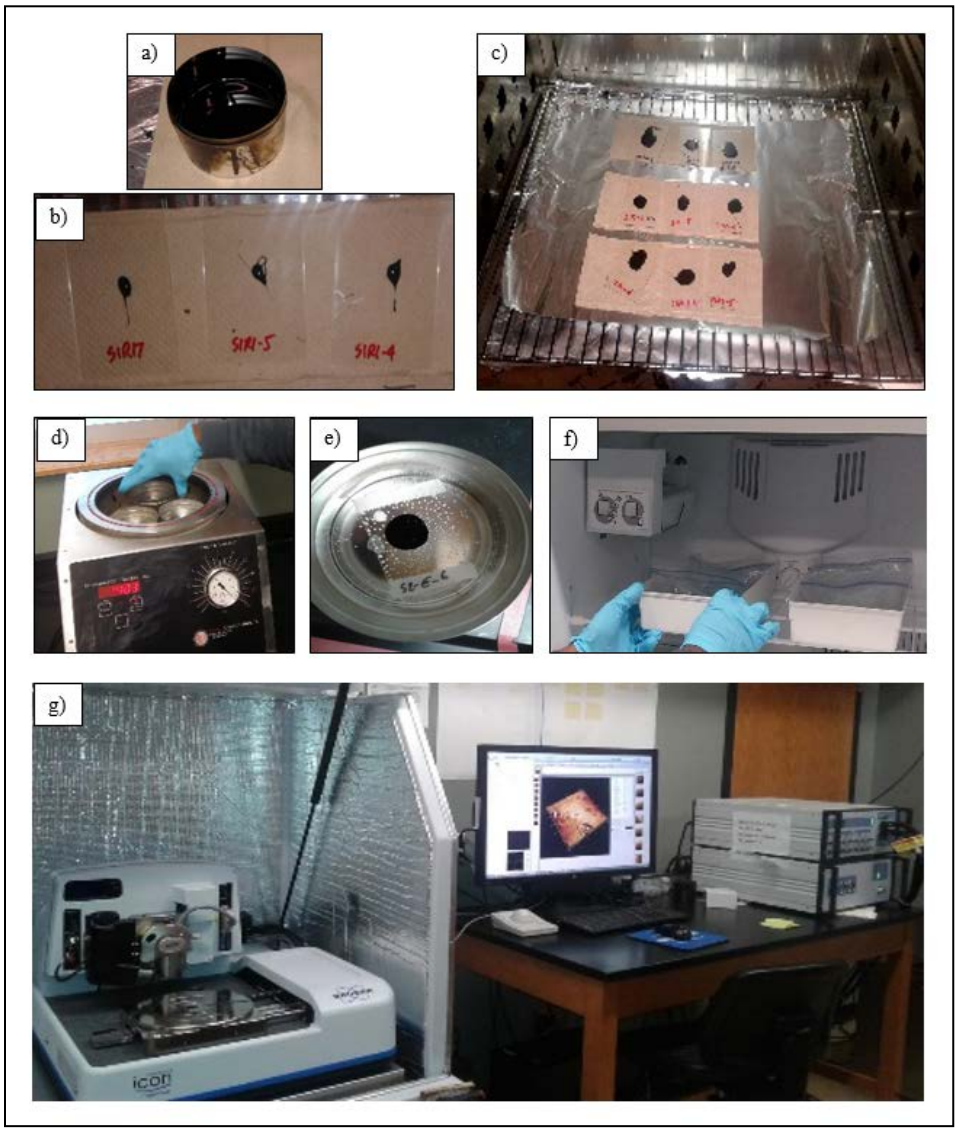

Figure 21. a)-c) Dry sample, d)-f) Wet-conditioned samples, and g) AFM system.

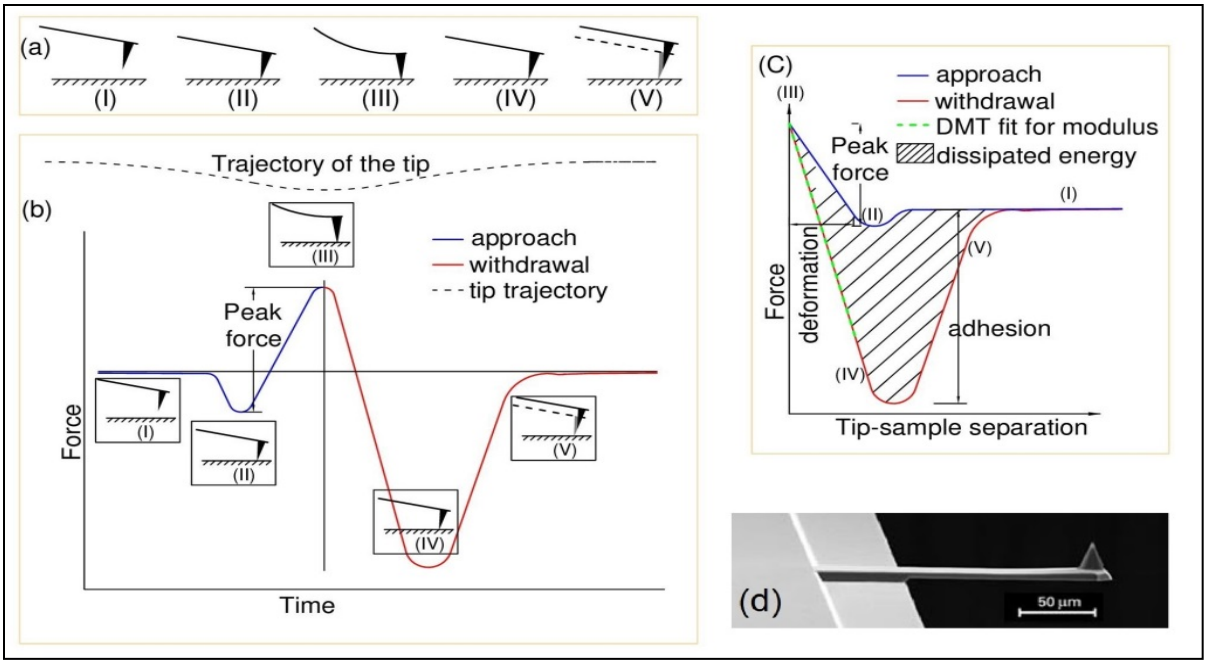

Figure 22: Working principles of PFQNM™ mode, (a) Traversing cycle of AFM tip: approach and withdrawal, (b) PeakForce tapping with tip trajectory, (c) Force-distance curve, and (d) A typical AFM probe.

In this study, the following scan parameters were used: scan size of 10 µm x 10 µm, a scan rate of 0.500 Hz, samples/lines of 512. For each test, three replicates were tested, and average values were taken to compare the test results. After conducting AFM scans, the surface morphology and mechanical properties of asphalt binder are quantified using NanoScope Analyses 1.5 software.

4.2.6. Saturates Aromatics Resins and Asphaltenes (SARA) Analysis

The SARA analysis was conducted for determining the percentages of certain families of chemical constituents in the tested asphalt binders, as shown in Figure 23. The improvement in rheological properties happens through certain alteration of chemical constituents, which lead to a change in the percentages of chemical constituent fractions. The SARA analysis was performed in accordance with "ASTM D 4124-09: Standard Test Method of Separating Asphalt into Four Fractions." The test specimen is put into reflux with n-Heptane for at least 3 hours. This reflux operation causes the solid fraction (Asphaltenes) to precipitate. The n-Heptane dissolves the other three fractions except for the Asphaltenes. The other three fractions are typically termed as the maltenes. Maltenes is loaded onto a chromatographic column containing activated alumina (pH 9-10) of particle size 50-200 µm and allowed to elute under gravity. Maltenes come out in a sequence as saturates, aromatics and resins. The four fractions are reported as percentage fractions of the original binder sample taken. The test was conducted on the base and modified asphalt binder samples to observe any changes in the chemical composition.

Figure 23. SARA analysis of asphalt binders using column chromatography.

4.2.7. Fourier Transform Infrared Spectroscopy (FTIR)

FTIR analysis is a common and quick technique to identify the functional groups present in asphalt binders. It is commonly used in the asphalt industry to identify the presence of any specific functional group in asphalt binders. FTIR test was conducted on both the base and modified binder samples. A Thermo Nicolet 8700 spectrometer was used in conducting FTIR tests. A Nuclear Magnetic Resonance (NMR) spectrometer was used to verify the separated SARA fractions of asphalt binders through 1H and C-13 NMR spectra.

In FTIR test, the most challenging task is the preparation of the sample as it could result in an erroneous result due to improper preparation of the sample *(99)*. In this study, disposable Real Crystal IR cards were used for preparing the samples, as shown in Figure 24. The IR cards contained a KBr substrate. Asphalt binder was heated at 163 °C to make sufficiently fluid. A tiny speck of asphalt binder was dropped right outside the aperture and dragged over the KBr substrate. This way the sample was completely coated on the KBr plate. The aperture of the hole in the plate was 15 mm. A KBr beam splitter from a spectrum range of 350 to 7400 cm^{-1} was used in this study. The samples were run over 50 scans at 4 cm^{-1} resolution for 30 seconds. The test was executed at a relative humidity under 5%. Prior to starting the test, a blank card was scanned first. The data analysis was done using OMNIC 6.2 software, which provides the absorbance and wavenumber data for a sample. The data was plotted with the help of the MS Excel tool.

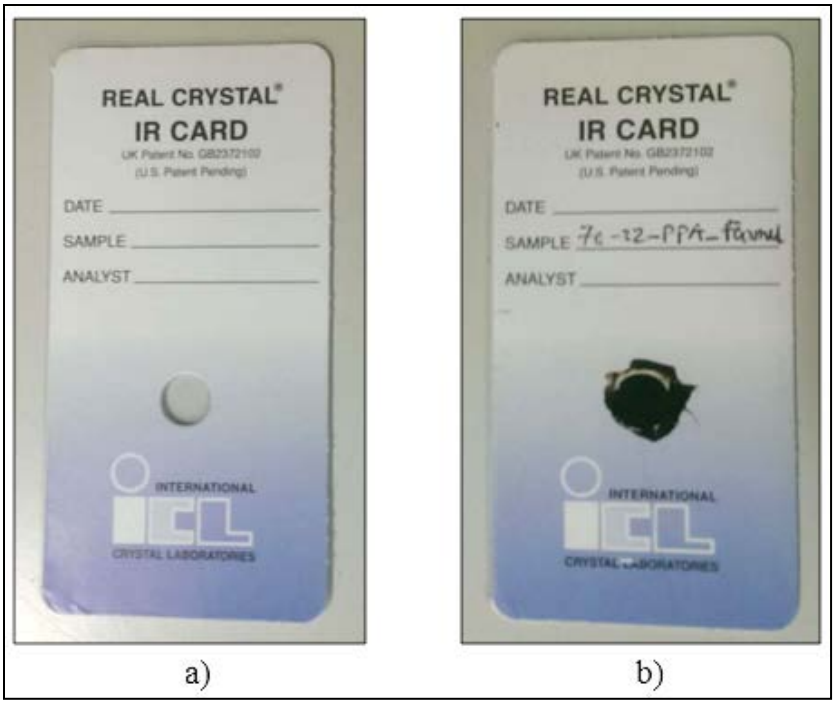

Figure 24. a) An empty IR card and b) A sample ready for FTIR test.

5. FINDINGS

5.1. Binder Performance (Superpave) Tests

5.1.1. Rotational Viscosity (RV) Tests

The RV test data showed that the binders from S2 had significantly lower viscosity values compared to their corresponding binders from S1, as presented in Table 10. Thus, S1 binders were relatively softer than S2 around mixing and compaction temperatures. It is also observed that the base binder (PG 64-22) from both sources showed the lowest viscosity among all binders used in this study.

Table 10. Rotational viscosity (mPa.s) Data of S1 and S2 binder samples.

Binder Type	Sample Source	Viscosity at 135 °C	Viscosity at 150 °C	Viscosity at 165 °C	Viscosity at 180 °C
S1B1	S1	504.17	254.17	145.83	75.00
S1B3	S1	704.17	345.83	183.33	100.00
S1B7	S1	1271.00	595.67	312.50	175.00
S1B8	S1	1929.33	870.67	450.00	262.50
S2B1	S2	445.83	208.33	112.50	62.50
S2B3	S2	645.83	295.83	145.83	75.00
S2B7	S2	1271.00	554.17	279.17	162.5
S2B8	S2	1767.00	758.33	350.00	187.50

The mixing and compaction temperatures for all asphalt binder samples from S1 and S2 were calculated using RV test data in accordance with the Asphalt Institute (AI). According to AI, these temperatures should be determined where the viscosity-temperature line crosses the viscosity ranges of 170 ± 20 mPa.s (mixing temperature range) and 280 ± 30 mPa.s (compaction temperature range). The method described in ASTM D2493 titled as “Standard Viscosity-Temperature Charts for Asphalts” was used to draw the viscosity-temperature line. Table 11 shows the mixing and compaction temperatures of all the binders used in this study. All other related graphs are assembled in the Appendix A. From Table 11, it is observed that the mixing and compaction temperatures of S1B7 or S2B7 binder (SBS-modified PG 70-22 binder) are considerably higher than those of S1B3 or B2B3 (PPA-modified PG 70-22 binder). Therefore, based on the energy consumption perspective, it can be said that PPA-modified binders exhibit more favorable results than the SBS-modified binders.

Table 11. Mixing and compaction temperatures of PPA and SBS modified binders.

Binder Type	High Mixing Temperature (°C)	Low Mixing Temperature (°C)	High Compaction Temperature (°C)	Low Compaction Temperature (°C)
S1B1	165	158	150	145
S1B3	170	164	157	152
S1B7	183	177	171	165
S1B8	191	186	180	175
S2B1	158	152	146	142
S2B3	164	159	154	149
S2B7	182	176	168	162
S2B8	185	180	173	168

5.1.2. Dynamic Shear Rheometer (DSR) Tests

In this study, DSR tests were performed in three aging conditions, namely, unaged, RTFO-aged and PAV-aged for the characterization of the viscoelastic behavior of asphalt binders at high and intermediate service temperatures. DSR test results of unaged and RTFO-aged asphalt binders from S1 and S2 are shown in Figures 25 through 28. The rest of the pertinent tables and graphs are presented in Appendix B. Based on the results as presented in these figures, it is shown that all tested binders met the corresponding Superpave rutting factor (G*/sinδ) criteria at their high PG temperatures (G*/sinδ should be at least 1.00 kPa for unaged binders and 2.20 kPa for RTFO-aged binders). The Superpave acceptance criterion is shown with the horizontal lines in these figures. It is observed that PPA-modified unaged and RTFO-aged binders showed increased rutting factor (G*/sinδ) compared to the unmodified binders. Furthermore, SBS-modified binders indicated the higher rutting resistance than the corresponding PPA-modified PG 70-22 binders.

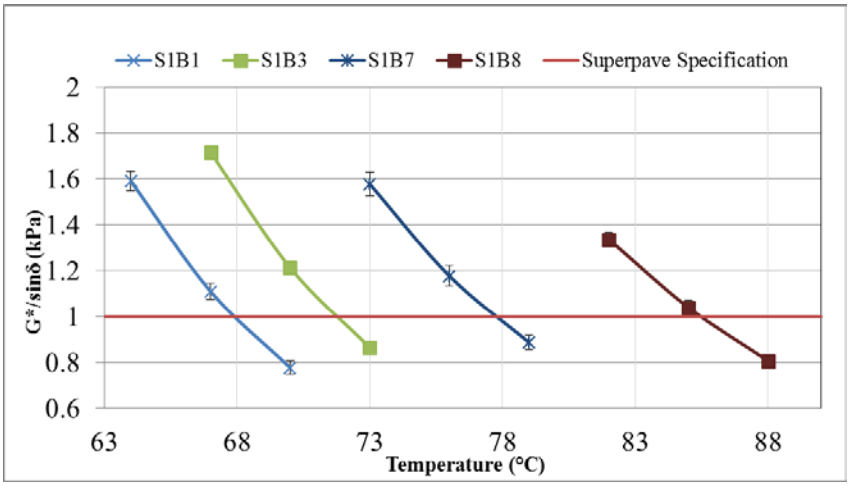

Figure 25. DSR test results of unaged binders from S1.

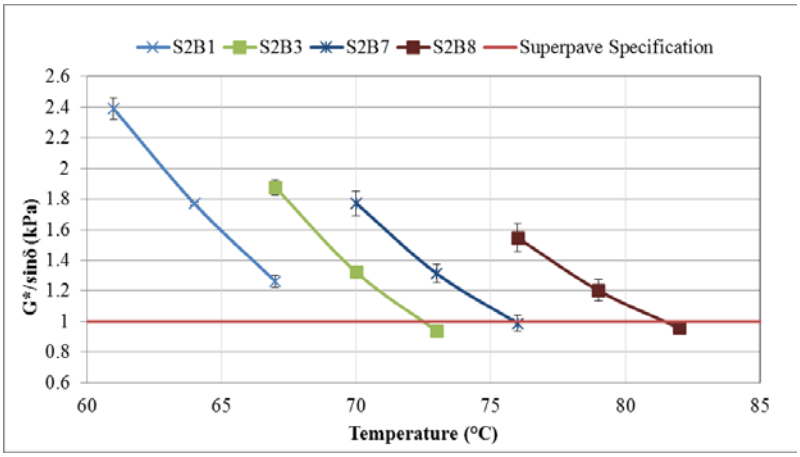

Figure 26. DSR test results of unaged binders from S2.

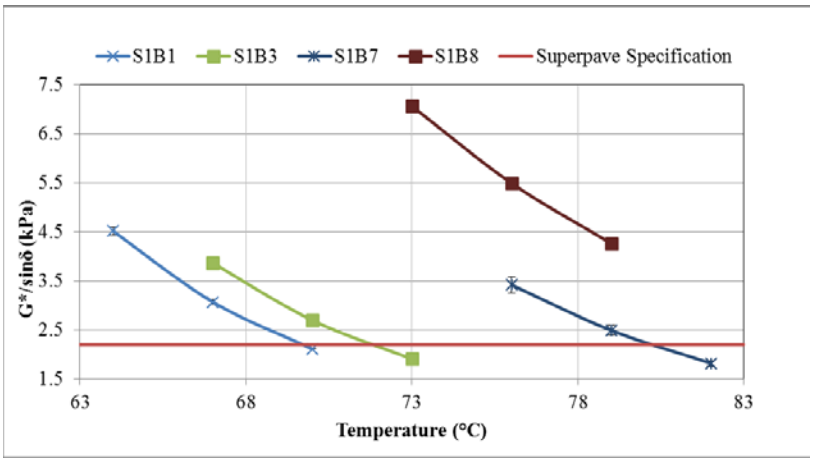

Figure 27. DSR test results of RTFO-aged binders from S1.

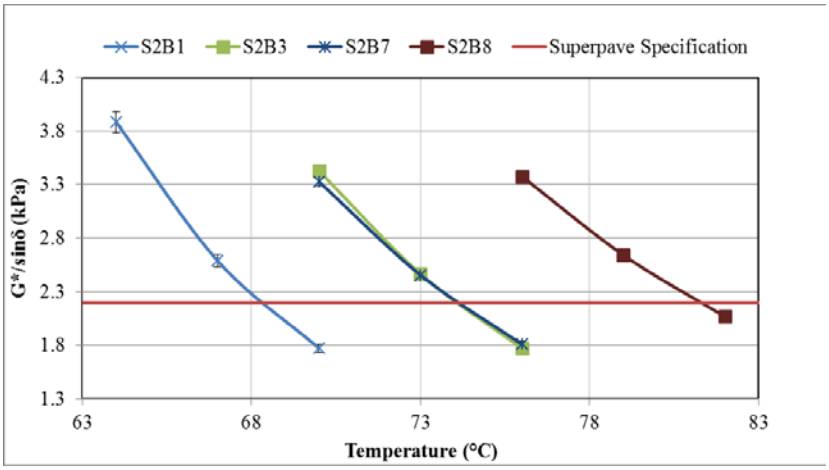

Figure 28. DSR test results of RTFO-aged binders from S2.

The effects of LAA on the rutting resistance of PPA-modified binders of S1 and S2 in both unaged and RTFO-aged conditions are shown in Figures 29 through 32. As seen in these figures, it is obvious that LAAs used in this study were not compatible as they failed to meet the Superpave rutting criteria for both unaged and RTFO-aging conditions and Adhere HP Plus was the least compatible among them. Therefore, it is recommended to avoid these LAAs when PPA is used as a modifier.

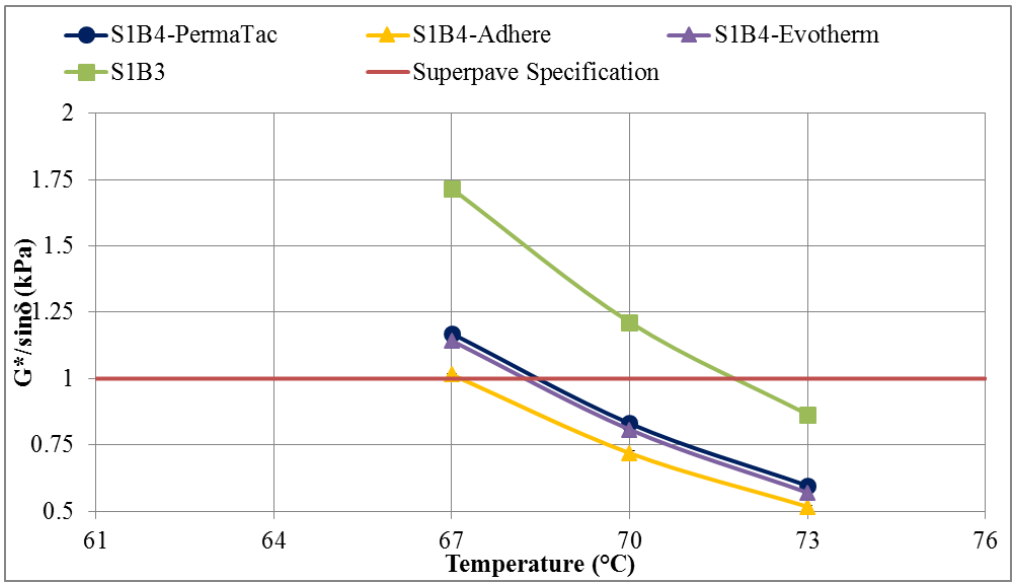

Figure 29. DSR test results of unaged PPA+LAA modified binders from S1.

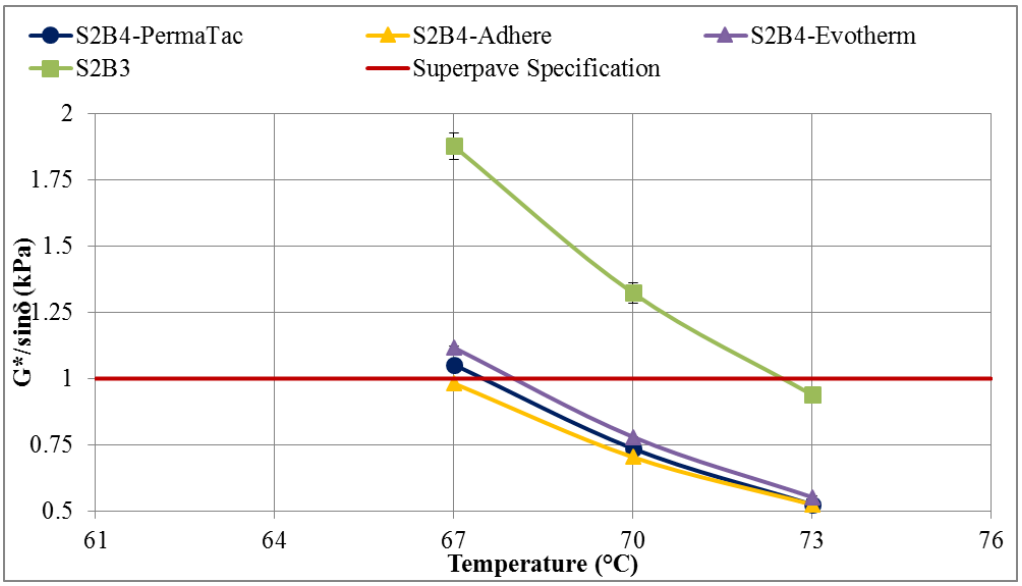

Figure 30. DSR test results of unaged PPA+LAA modified binders from S2.

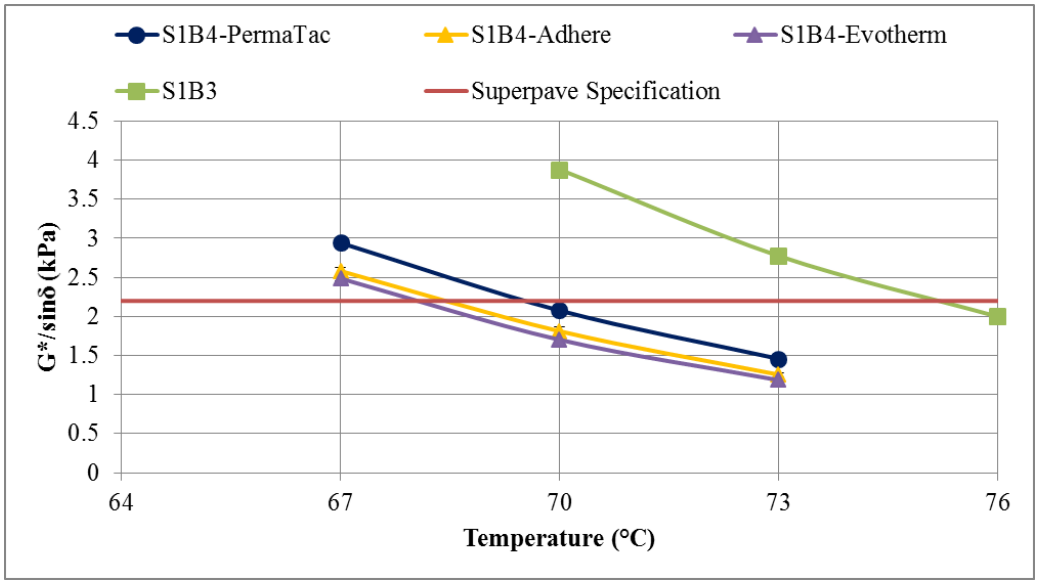

Figure 31. DSR test results of RTFO-aged PPA+LAA asphalt binders from S1.

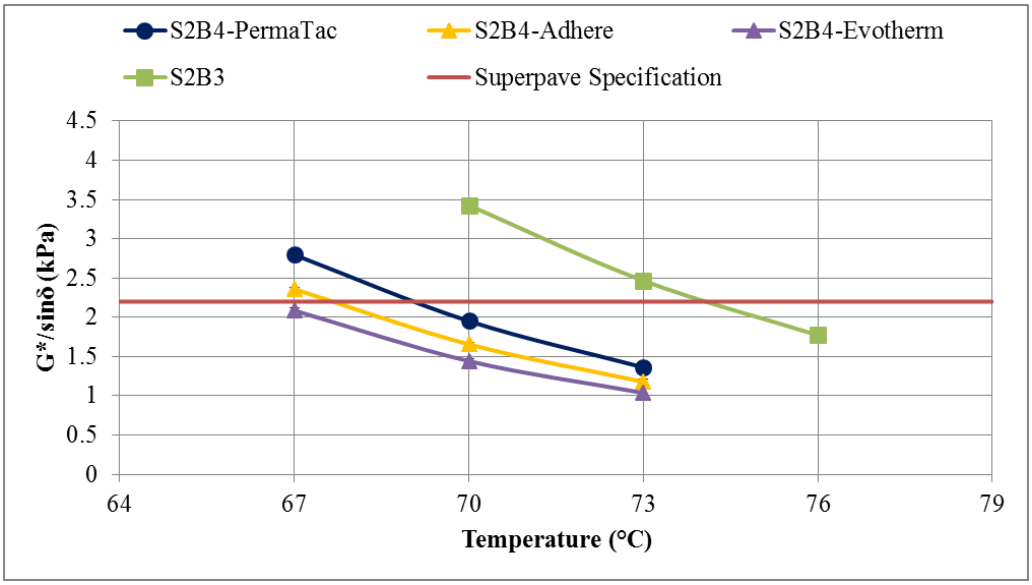

Figure 32. DSR test results of RTFO-aged PPA+LAA asphalt binders from S2.

DSR test results on PAV-aged binders show fatigue characteristics of tested asphalt binders from S1 and S2 (Figures 33 through 34). As per the Superpave specifications, the G*×sinδ value of a PAV-aged binder at the intermediate temperature should not be more than 5000 kPa. The horizontal lines in these figures represent the Superpave maximum limit for fatigue resistance of binders. The test results reveal that all tested binder samples met the Superpave fatigue criterion. The results also indicate that PPA-modified binders (S1B3 or S2B3) are more fatigue resistant than the corresponding SBS-modified binders (S1B7 or S2B7).

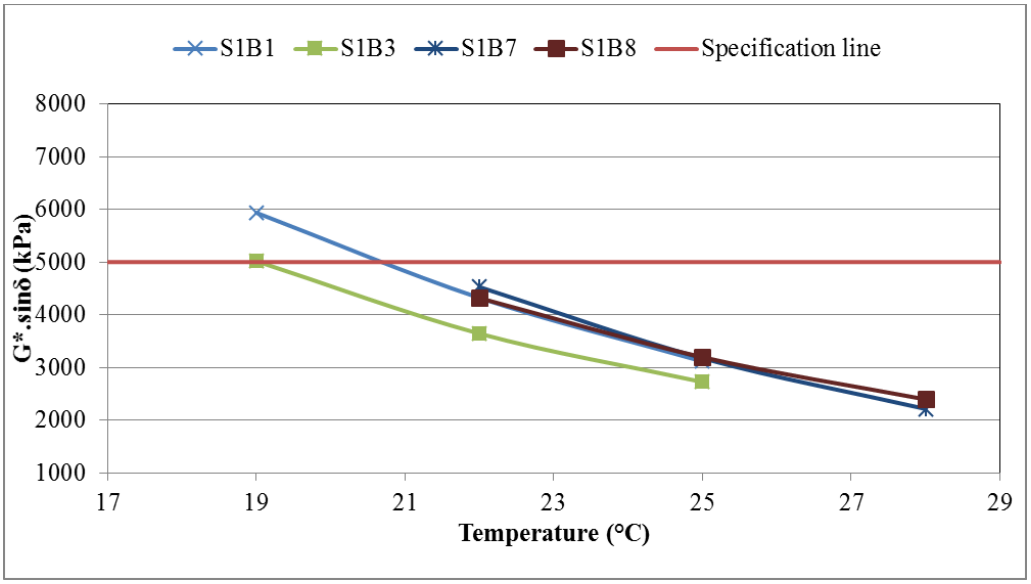

Figure 33. DSR test results of PAV-aged asphalt binders from S1.

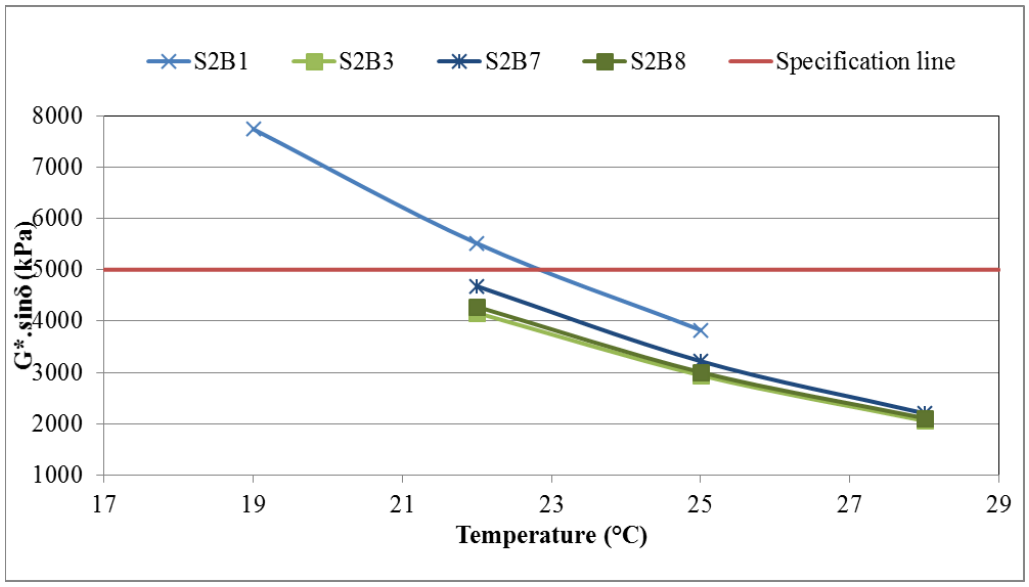

Figure 34. DSR test results of PAV-aged asphalt binders from S2.

Figures 35 and 36 show DSR test results of LAAs in PPA-modified PG 70-22 binders of S1 and S2. As seen from these figures, the addition of LAAs increased G*×sinδ values in several cases for both sources (S1 and S2) but did not cause them to fail the Superpave specification limit for fatigue. For S1 binders, ADhere HP Plus showed the better results whereas it slightly crossed the maximum of the Superpave specification for S2 binders. Thus, the outcomes show the necessity for selecting a suitable LAA for PPA-modified asphalt binders.

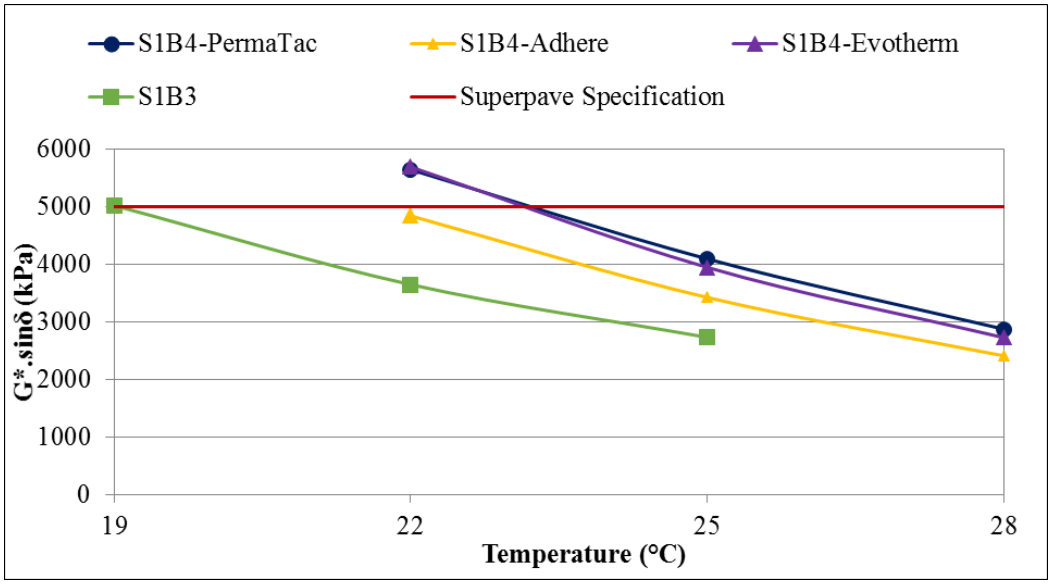

Figure 35. DSR test results of PAV-aged PPA+LAA binders from S1.

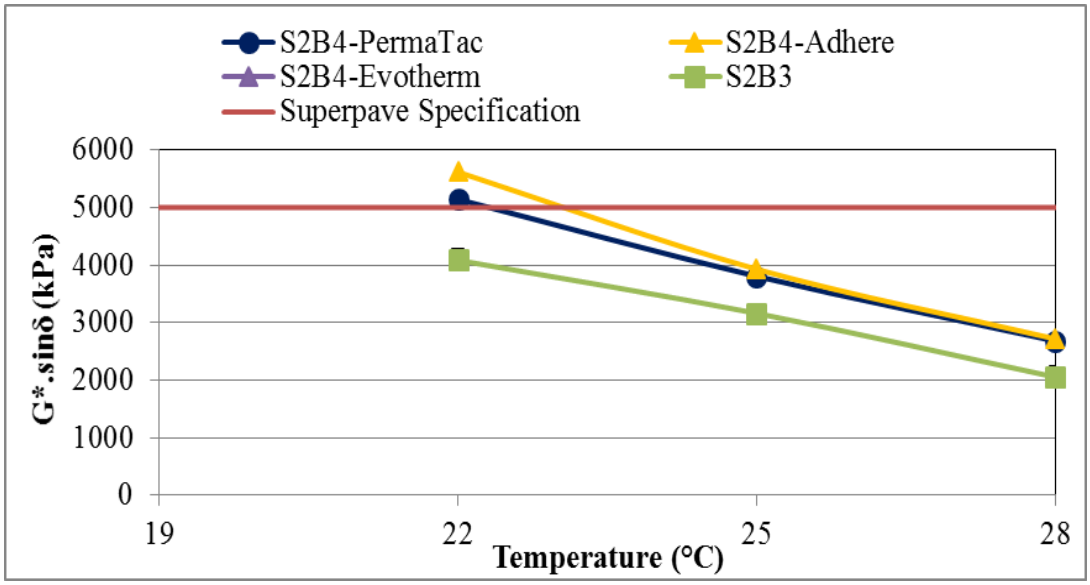

Figure 36. DSR test results of PAV-aged PPA+LAA binders from S2.

5.1.3. Bending Beam Rheometer (BBR) Tests

BBR tests were performed to measure low-temperature stiffness and stress relaxation properties of asphalt binders. From the BBR test results, S-value (creep stiffness) and m-value (the slope of the stiffness curve) were measured at 60 s. According to the recommendations under the Superpave test specifications, all BBR tests were conducted at 10°C higher than the low PG temperatures of the binders in this study. For example, BBR tests for PG 70-22 binders were conducted at -12 °C. As per the Superpave specifications requirements, binder's S-value should be not more than 300 MPa, and m-value should be at least 0.300.

Figures 37 and 38 show the S-values of tested binder samples from S1 and S2. As seen from these figures, all binders met the Superpave criterion for S-value. It is observed that the lowest S-value for all binders from S1 is found for S1B8 (PPA+SBS modified PG 76-22 binder) when then test temperature was -12 °C. For S2 binders, the lowest creep stiffness was observed for S2B7 (SSB-modified PG 70-22 binder). Moreover, Appendix C represents some of the BBR test data of the asphalt binders tested in this study.

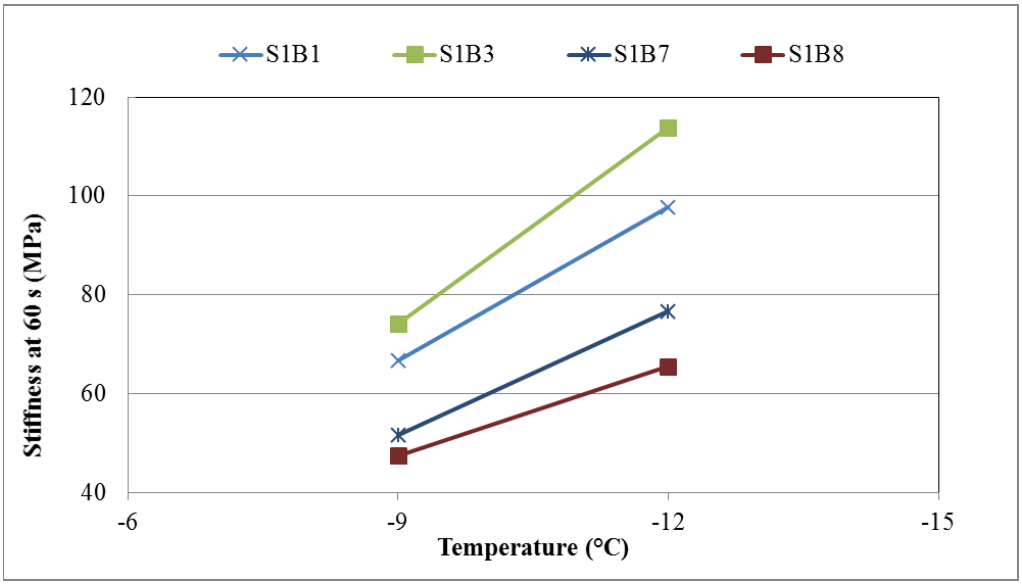

Figure 37. Creep stiffness of the asphalt binders from S1.

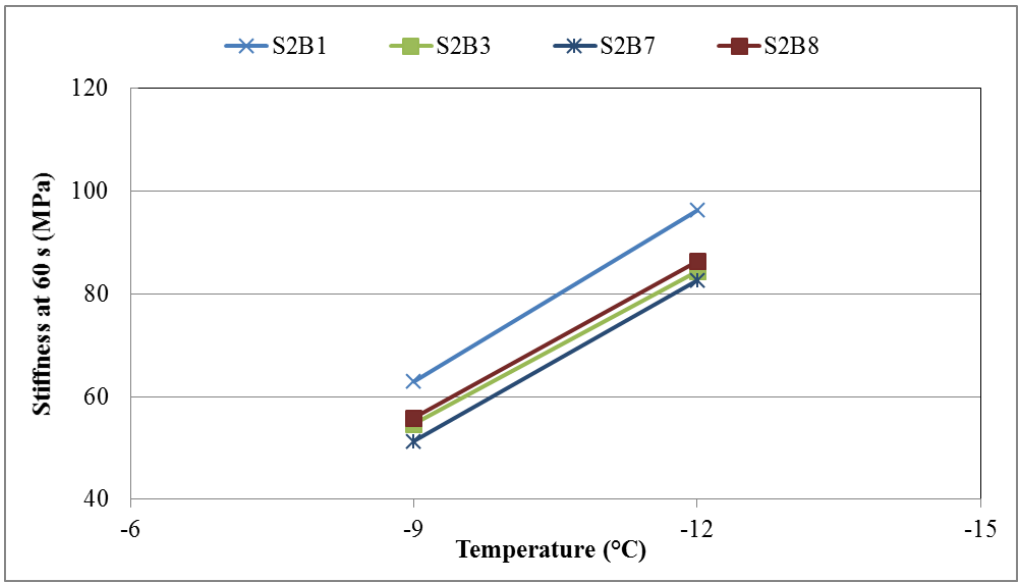

Figure 38. Creep stiffness of asphalt binders from S2.

Figures 39 and 40 show m-values of all tested binder samples from S1 and S2. From these figures, it is noted that all binder samples met the Superpave criterion for m-value at their low PG temperature (-22 °C). It is observed that the highest m-value among all S1 binders was found

to be 0.4 for both S1B7 and S1B8 when the testing temperature was -12 °C. It is also found that their m-values at any particular test temperature (-9 °C or -12 °C) are the same and overlapped with each other, shown in Figure 39 and 40. However, among all S2 binders, the highest "m" value was observed for S2B8 (PPA+SBS-modified binder), which is found to be 0.42 at the testing temperature of -12 °C. At this testing temperature, it is also found that the same "m" value was observed for S2B3 and S2B7 of S2 binders.

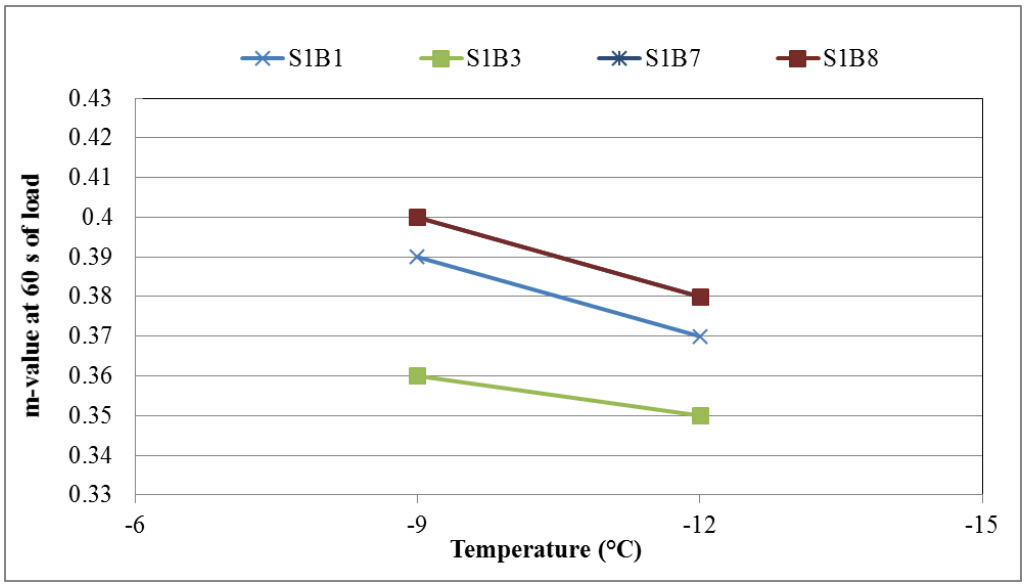

Figure 39. "m-values" of asphalt binders from S1.

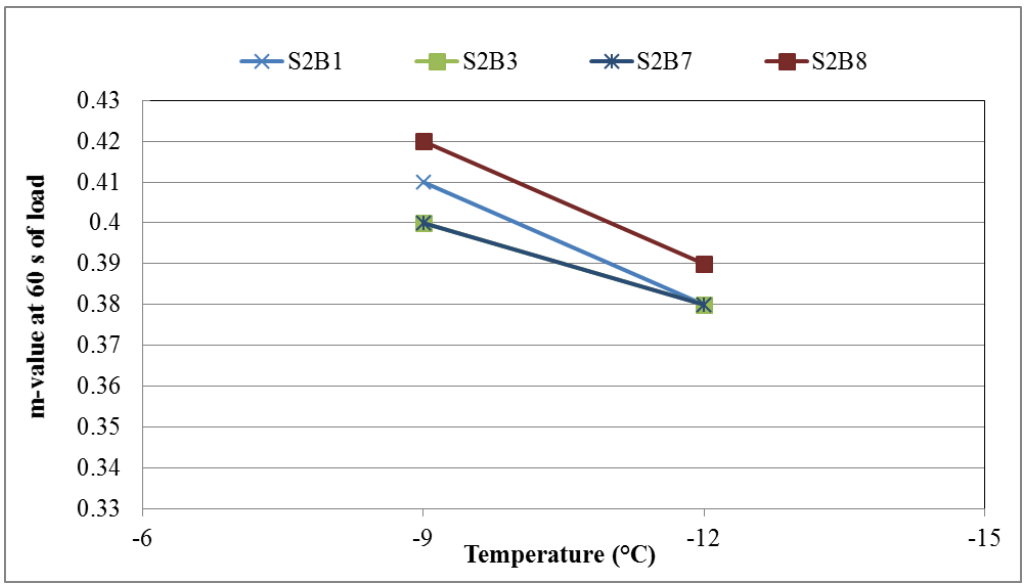

Figure 40. "m-values" of asphalt binders from S2.

5.2. Mixture Performance Tests

5.2.1. Texas Boiling Tests

As mentioned earlier, the Texas Boiling test is widely used for measuring the moisture damage of an asphalt mix for its simple procedure that takes very little time compared to the other test methods. The stripping of asphalt binders is measured by visual observation according to the TTI guidelines. Figure 41 shows the summary of the boiling test used in this study.

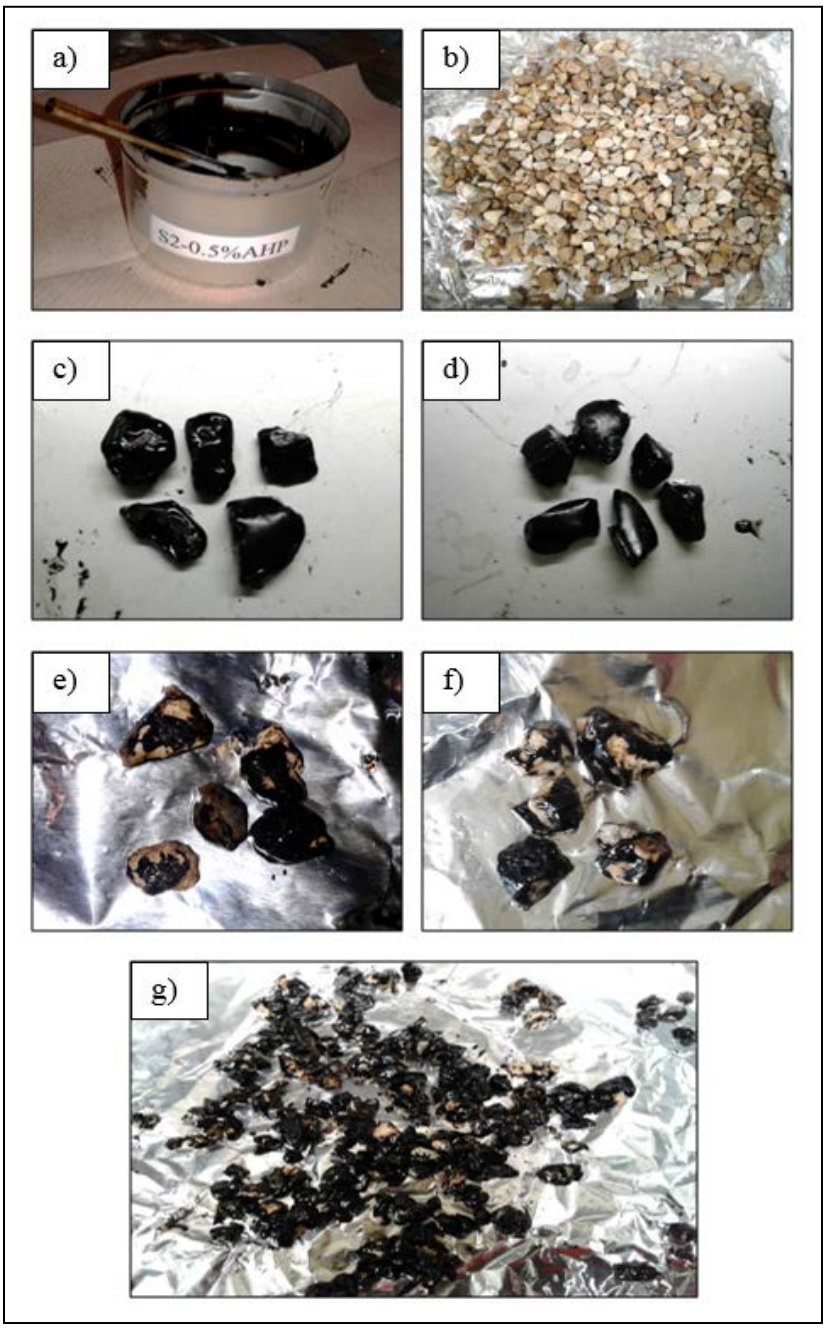

Figure 41. Sample a) Hot-liquid binder, b) Aggregates, c)-d) Sample mixture preparation, and e)-g) Samples after the Texas Boiling Test.

In this test, moisture susceptibility of the asphalt mixes was determined based on the percentage of the asphalt retention, which is shown in Table 12 and Figure 42. It is noted that PG 64-22 binders (S1B1 and S2B1) for both sources showed a lower percentage of asphalt retention after the boiling test compared to any other binder used in this study. On the other hand, the higher asphalt retention rates were found for S1B8 and S2B8 (PPA+SBS-modified binders) from S1 and S2, which is also higher than the PPA-modified binder's values. Another interesting finding is that the PPA-modified binder from S1 exhibited less stripping resistance than the PPA-modified binder from S2. It is also found that LAAs did not improve the moisture resistance of the binders from S1 and S2. However, among all LAAs, Permatac Plus slightly increased the percentage of asphalt retention, which is 60% for both sources and equal to the value of S1B3 binders (PPA-modified PG 70-22 binder).

Table 12. Summary of the Texas Boiling Tests results.

Asphalt Binder Sample	Percentage of Asphalt Retained (%)
S1B1	50
S1B3	60
S1B7	70
S1B8	80
S2B1	55
S2B3	65
S2B7	70
S2B8	80
S1B1+ Permatac	60
S2B1+ Permatac	60
S1B1+ Adhere	55
S2B1+ Adhere	60
S1B1+ Evotherm	50
S2B1+ Evotherm	50

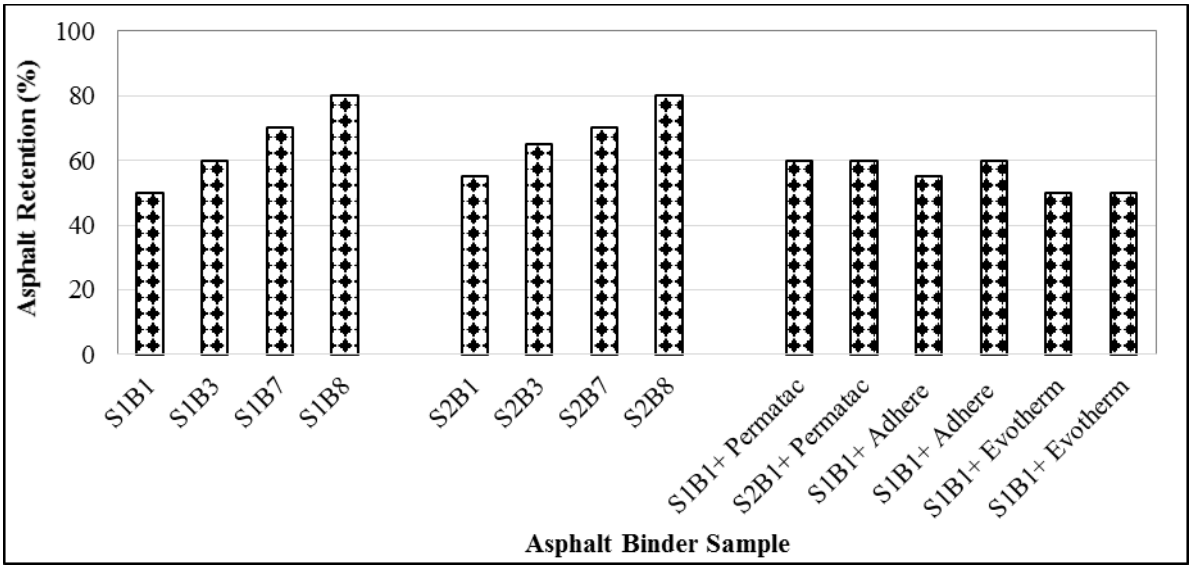

Figure 42. Asphalt retained (%) from Texas Boiling Tests.

5.2.2. Evaluation of Rutting and Stripping of Asphalt (ERSA) Tests

The ERSA test was performed to determine the susceptibility of premature failure of HMA caused by weakness in the aggregate structure, inadequate binder stiffness, or moisture damage. The ERSA test was done for three mixtures, namely, SB1, S1B3, and S1B7. The aggregates were from Van Buren and are known to be moisture susceptible. The summary of ERSA test results is shown in Figure 43.

Figure 43 shows that the numbers of cycles required for 8.0 mm rut depth were 6,686 (13,372 passes) in case of S1B1. After 8,000 cycles (16,000 passes), the rut depth was 10.26 mm. The rut depths for PPA-modified PG 70-22 (S1B3) mixture and SBS-modified PG 70-22 (S1B7) mixture at 8000 cycles (16,000 passes) were found to be 1.48 mm and 2.7 mm, respectively. Based on the test results it is noted that the number of passes to reach a rut depth of 8 mm were more than 16,000 for these mixtures (S1B3 and S1B7). Therefore, this finding validated that the addition of either PPA or SBS to the binders improved the rutting resistance of the mixture over 100%.

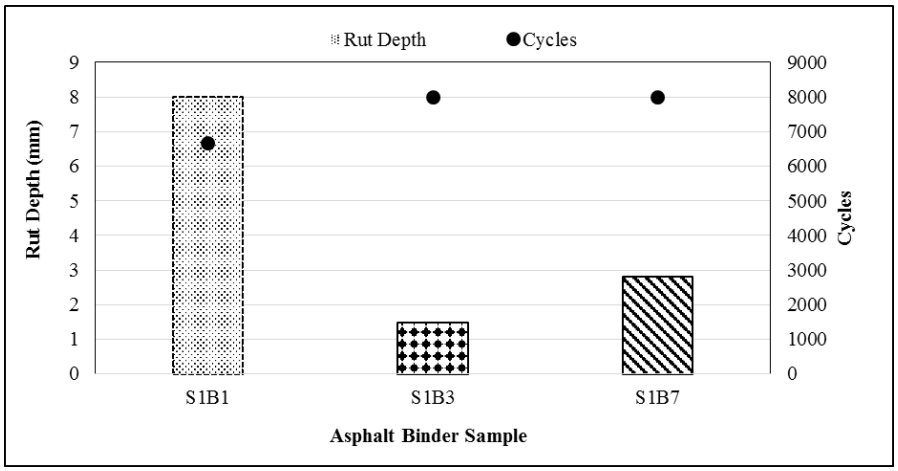

Figure 43: Summary of ERSA tests results *(97)*.

5.2.3. Tensile Strength Ratio (TSR) Tests

The summary of the TSR results of the tested mixture samples is shown in Table 13 and Figure 44. It is seen that the SBS-modified (S1B7) mixture revealed higher tensile strength under both wet and dry conditions between the two PG 70-22 mixtures, and the resulting TSR is 1.18. It is also noted that S1B1 binder showed the lowest values in both conditions, and the TSR was 0.92. Moreover, the tensile strength results of LAA-modified mixtures did not show any improvement from the results of PPA-modified mixtures, which correlates with the data obtained from the SFE analysis of the corresponding asphalt binders that is discussed later.

Table 13. Summary of TSR test results.

Asphalt Binder Sample	Dry Tensile Strength (psi)	Wet Tensile Strength (psi)	TSR
S1B1	17.15	15.70	0.92
S1B3	18.12	21.88	1.21
S1B7	19.58	23.12	1.18

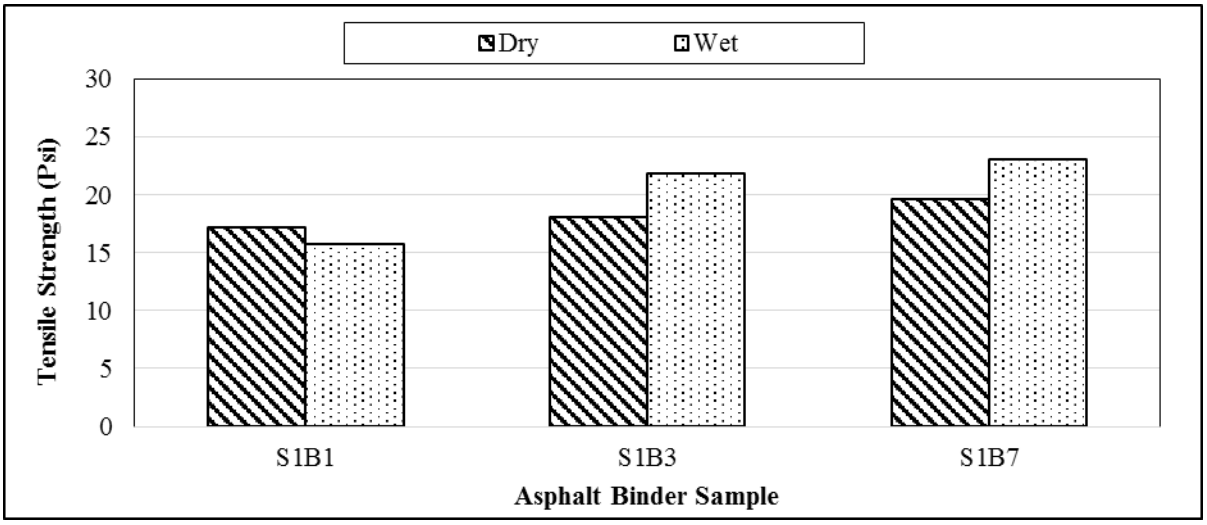

Figure 44. Summary of the TSR test results *(97)*.

5.3. Binder's Surface Science-Based Tests

5.3.1. Surface Free Energy (SFE) Analysis

The SFE tests were performed on unaged binders at a room temperature. Firstly, the static contact angles of the asphalt binders and aggregate samples were measured using three probe liquids (water, ethylene glycol, and formamide) of known SFE components. For this study, four aggregates were chosen for the SFE analysis. Among all aggregates, two of these aggregates were sandstone (Preston Sandstone) and gravel (Preston Gravel) from Arkansas, and SFE values of two other aggregates (Snyder Granite and Martin Marietta Mill Creek (MMMC) Granite) were chosen from literature for comparison. From the contact angles of asphalt binders and aggregate samples, the SFE components, namely, a mono-polar acidic component (Γ^+), a mono-polar basic component (Γ^-), and an apolar or Lifshitz-van der Waals component (Γ^{LW}) were calculated. Figures 45 and 46 show the contact angles of the asphalt binder samples coated on thin glass

slides. It is found that water made the highest contact angles with the asphalt binder samples among three probe liquids, as expected. It is also observed that the samples from the former had higher contact angles than those from the latter between the binders from S1 and S2, which was expected as the binders from S2 were stiffer than those of S1 at a room temperature.

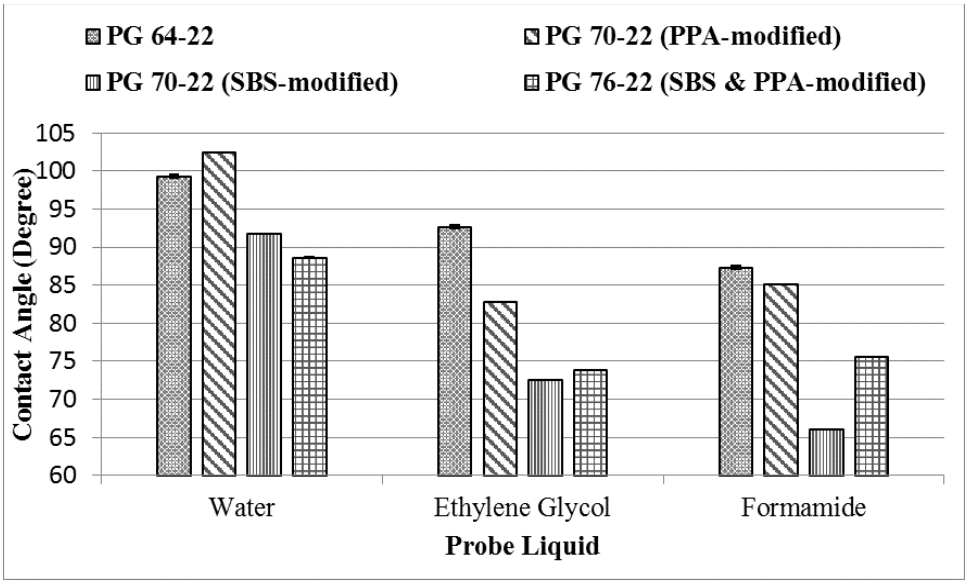

Figure 45. Contact angles of Asphalt sample binders from S1.

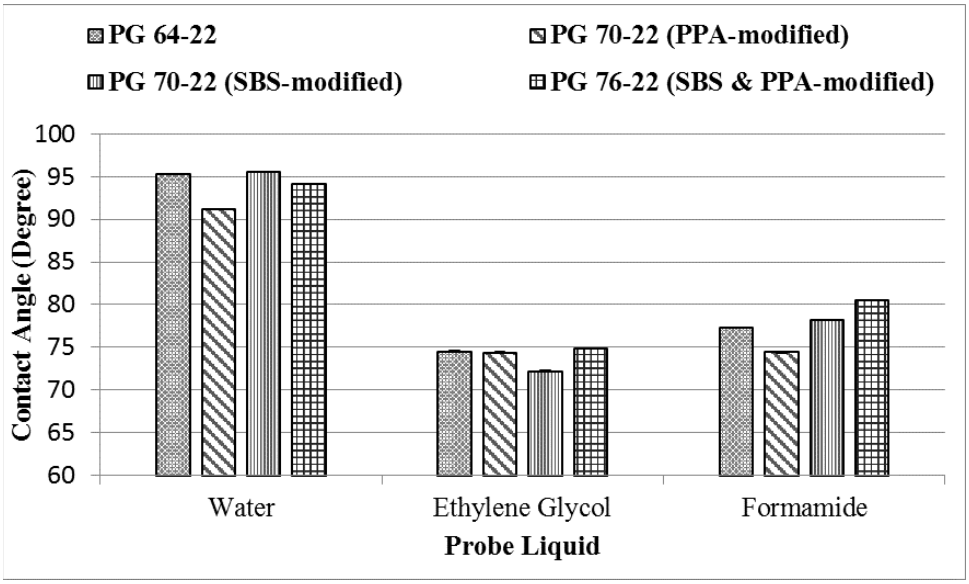

Figure 46. Contact angles of asphalt samplebBinders from S2.

Table 14 shows the SFE parameters along with work of cohesion (WOC) values for asphalt binders from S1 and S2. Here, Γ^{ab} is the acid-base component of the SFE, and it is the geometric average of Γ^{+} and Γ^{-}. It is found that the WOC is applicable for asphalt binders, and it is twice of Γ^{total}, which is the sum of Γ^{ab} and Γ^{LW}. If the WOC of an asphalt binder becomes higher, the more energy is needed to break its cohesive bonds. The SFE values of aggregates are irrelevant while estimating the asphalt binder's WOC. For S1 binders, the highest WOC was observed from

S1B8 (PPA+SBS-modified binder). However, none of the PPA-modified binders had higher cohesion energy compared to their base binders (PG 64-22 aka S1B1). It is found that all binders modified by PPA alone showed less cohesion energy than S1B1 for S1. Based on the compassion between the PPA-modified (S1B3) and SBS-modified (S1B7) binders, S1B7 had higher cohesion energy than S1B3. For S2 binders, S2B3 had an increased WOC compared to S2B1 and S2B7 binder.

Table 14. SFE parameters (mJ/m^2) and cohesion energy (mJ/m^2) of asphalt binders.

Probe Liquid/ Test Sample	γ^+	γ^-	γ^{LW}	γ^{ab}	γ^{total}	W^{CL}
Water	25.50	25.50	21.80	-	72.80	N/A
Ethylene Glycol	1.92	47.00	29.00	-	48.00	N/A
Formamide	2.28	39.60	39.00	-	58.00	N/A
Snyder Granite	0.10	8.43	35.15	1.87	37.03	N/A
MMMC Granite	0.42	36.98	35.84	7.89	43.73	N/A
Preston Gravel	20.93	14.95	13.75	35.37	49.12	N/A
Preston Sandstone	20.76	14.76	13.56	35.00	48.56	N/A
S1B1	12.61	2.56	0.94	11.36	12.30	24.60
S1B3	12.50	2.31	0.43	10.74	11.17	22.34
S1B7	12.92	3.34	2.90	13.13	16.03	32.06
S1B8	13.23	4.00	3.55	14.54	18.09	36.18
S2B1	12.70	2.63	2.15	11.55	13.70	27.40
S2B3	13.02	3.44	3.01	13.38	16.39	32.78
S2B7	12.67	2.83	2.44	11.97	14.41	28.82
S2B8	12.67	2.83	2.44	11.97	14.41	28.82

Table 15 shows the variation of adhesion energy under the dry condition (ΔG_{dry}). The work of adhesion is defined as the amount of energy necessary to separate two materials at their interface. From Table 15, it is noted that MMMC granite showed higher ΔG_{dry} values than the others, irrespective of the binder types. In the dry condition, SBS- and PPA-modified PG 76-22 binder (S1B8) from S1 showed the highest ΔG_{dry} value among all tested aggregates. However, PPA-modified PG 70-22 binder (S2B3) showed the highest ΔG_{dry} for S2. It is also found that the ΔG_{dry} values between Preston gravel and Preston sandstone did not show noticeable differences, but they were notably lower than those of MMMC granite.

The SFE analysis also shows that an increase in the PPA amount did not increase the ΔG_{dry} value for Preston's gravel or sandstone. It is found the better adhesive bonds exist between aggregates and binder under the dry condition in case of higher ΔG_{dry}. However, it is the

opposite in the case of the adhesion energy under the wet condition (ΔG_{wet}) as values presented in Table 16 are negative.

Table 15. Work of adhesion (mJ/m^2) for asphalt-aggregate system in dry condition.

Binder Sample	Aggregates: Preston Gravel	Aggregates: Preston Sandstone	Aggregates: Snyder Granite	Aggregates: Granite MMMC
S1B1	34.7	34.4	32.1	54.8
S1B3	32.2	32.0	28.3	50.9
S1B7	40.4	40.2	41.1	64.1
S1B8	42.1	41.8	43.5	66.8
S2B1	38.4	38.2	38.1	60.9
S2B3	40.8	40.5	41.5	64.7
S2B7	39.1	38.9	39.2	62.0
S2B8	39.1	38.9	39.2	62.0

The ΔG_{wet} is a measure of adhesion energy under the wet condition and the negative values suggest the de-bonding potential of asphalt binders and aggregates in the presence of water. Table 16 shows that the ΔG_{wet} of the binders were slightly decreased (as values are negative) for PPA-modified binders from S1. This finding indicates that the addition of PPA would make the binder more moisture susceptible. However, S2 binders showed a different trend with the addition of PPA. For instance, S2B3 binder (0.75% PPA) had slightly higher ΔG_{wet} values compared to the base binder (S2B1) (from -12.9 mJ/m^2 to -12.1 mJ/m^2) that indicates an increased resistance to stripping.

Table 16. Work of adhesion (mJ/m^2) for asphalt-aggregate system in wet condition.

Binder Sample	Aggregates: Preston Gravel	Aggregates: Preston Sandstone	Aggregates: Snyder Granite	Aggregates: Granite MMMC
S1B1	13.9	14.3	29.8	17.5
S1B3	14.6	15.1	29.8	17.4
S1B7	12.2	12.5	29.3	17.5
S1B8	11.6	11.9	27.9	16.6
S2B1	12.9	13.3	30.8	18.7
S2B3	12.1	12.4	29.0	17.4
S2B7	12.7	13.1	30.4	18.4
S2B8	12.7	13.1	30.4	18.4

However, the combination of adhesion energy values under both dry and wet conditions rather than only dry or wet condition would have to be considered in determining the compatibility between aggregates and binders and a get a better understanding of their stripping resistance. The term “compatibility ratio,” introduced by the TTI was used in this study. The “compatibility ratio” of an asphalt binder and the aggregate system indicates the potentiality of moisture resistance of the binder with the aggregate. A higher compatibility ratio (CR) means the binder and aggregate system is less vulnerable to moisture damage. CR is the ratio of ΔG_{dry} and $-\Delta G_{wet}$. It is noted that the CR increases if the ΔG_{dry} increases and/or ΔG_{wet}

decreases, and vice versa. As suggested by the TTI researchers, the qualitative description of compatibility is shown in Table 17. As seen from this table, a CR value of less than 0.5 is considered "very poor," whereas CR values of more than 0.5 signify good compatibility between binder and aggregates. If the CR value is greater than 1.5 the compatibility is rated as "very good" and it is graded as an "A." The range of CR between 0.5 and 1.5 means "good" and graded as "B" whereas and CR values between 0.5 and 0.75 means "poor" and graded as "C." Furthermore, CR values less than 0.5 means "very poor" compatibility and graded as "D."

Table 17. Qualitative description of compatibility ratio.

Compatibility Ratio Range	Grading
Greater Than 1.5	A (Very Good)
0.75 – 1.5	B (Good)
0.5 – 0.75	C(Poor)
Less Than 0.5	D (Very Poor)

Figures 47 and 48 show the compatibility analysis data of all tested asphalt binder samples from S1 and S2, respectively. As seen from these figures, it is noted that the CR values of the binder aggregate systems ranged from "B" to "A." It is found that the two aggregates (Preston's gravel and sandstone) collected from Arkhola, AR showed similar CR values for S1. A similar pattern is also observed for the binder from S2. On the other hand, MMMC granite showed the highest CR values whereas Snyder granite showed the lowest values. Besides, S2B3 (PPA-modified PG 70-22) showed higher CR values than either S2B8 (PPA+SBS modified PG 76-22) or S2B7 (SBS-modified PG 70-22) for S2.

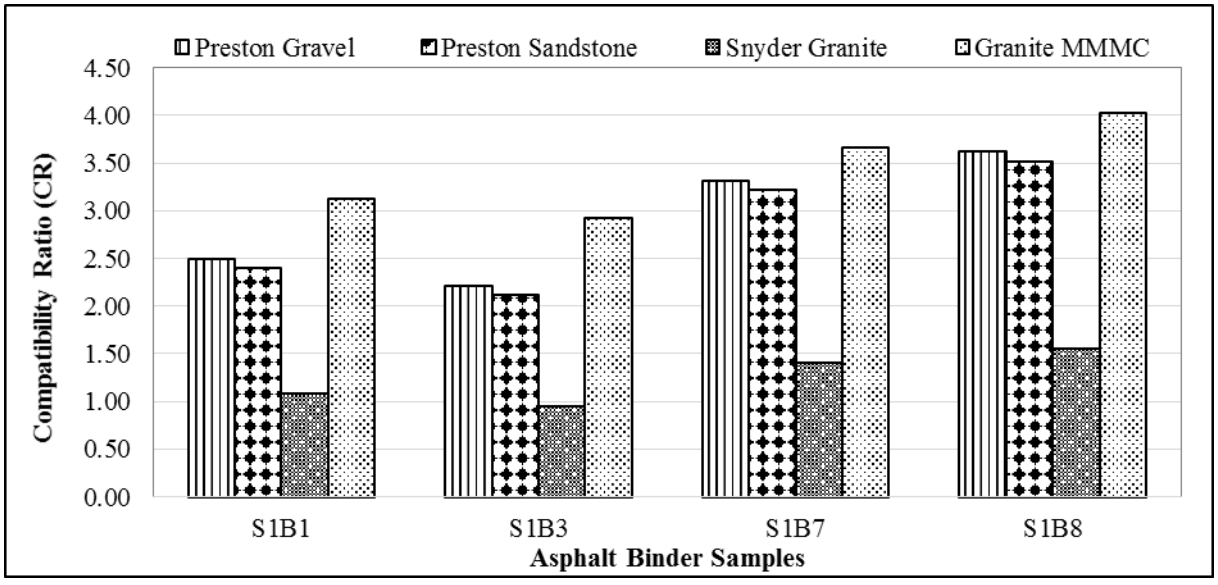

Figure 47. Compatibility ratio of asphalt binders from S1.

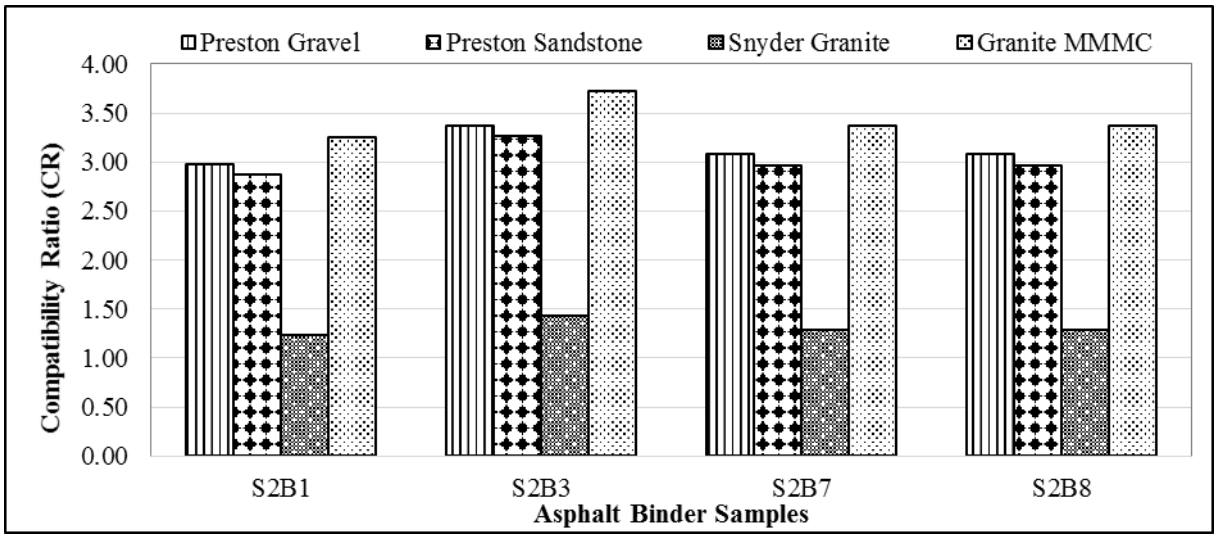

Figure 48. Compatibility ratio of asphalt binders from S2.

Table 18 shows the CR values of PPA+LAA modified binders of S1 and S2. As seen from this table, it is found that the CR values are in the compatibility category of "B" or "A." However, for S1, the CR value reduced significantly when AD-Here HP Plus was used as the LAA. This indicated to a hypothesis that if a "C" category of binder aggregate system was modified with AD-Here HP Plus, its CR would degrade to "D." It is also found that MMMC granite was found to have the same or increased CR values with all LAAs. However, for S2, MMMC granite was found to have the increased CR values with PermaTac Plus and AD-Here HP Plus. Therefore, these outcomes reiterate the necessity for a careful selection of LAA when PPA is used as a modifier.

Table 18. Compatibility ratio of PPA+LAA modified binders.

Binder Type	Preston Gravel	Preston Sandstone	Snyder Granite	Granite MMMC
S1B4-Permatac	1.70	1.64	0.87	3.18
S1B4-Adhere	2.19	2.12	1.12	4.15
S1B4-Evotherm	2.18	2.11	1.11	4.10
S1B3	2.21	2.12	0.95	2.93
S2B4-Permatac	2.23	2.15	1.14	4.20
S2B4-Adhere	2.36	2.28	1.21	4.43
S2B4-Evotherm	1.67	1.61	0.85	3.05
S2B3	3.37	3.27	1.43	3.72

5.3.2. Atomic Force Microscopy (AFM) Tests

Figure 49 shows the typical AFM maps of the morphology (surface roughness) of PG 64-22 S1 binders for dry (left) and wet-conditioned (right) samples and rest of the maps are added in Appendix D. From the AFM tests results, it is noted that three distinct phases such as Dispersed (Catena), Interstitial (Peri), and Matrix (Perpetua) were observed in dry condition. The summary of the roughness values is presented in Table 19. As seen from Table 19, in most of the asphalt

binders, “bee” like structures were significantly changed in size, decreased in numbers, sometimes also dispersed after wet conditioning the samples. It also found that the overall average surface roughness values were reduced over 50% for both S1 and S2 binders. However, in case of control binder (S2B1) and PPA-modified binder (S2B3) from S2, the surface roughness values were slightly increased as expected. It is also found that among all asphalt binders the S1B7 and S2B7 binders (SBS-modified) showed a noticeable reduction of the surface roughness in the wet samples. Also, the addition of LAAs, presented in Table 20, show lower roughness values for all binders (S1 and S2) in wet samples compared to their corresponding values in the dry samples. Moreover, the comparisons of the surface morphology among all tested binders are shown in Figures 50 and 51.

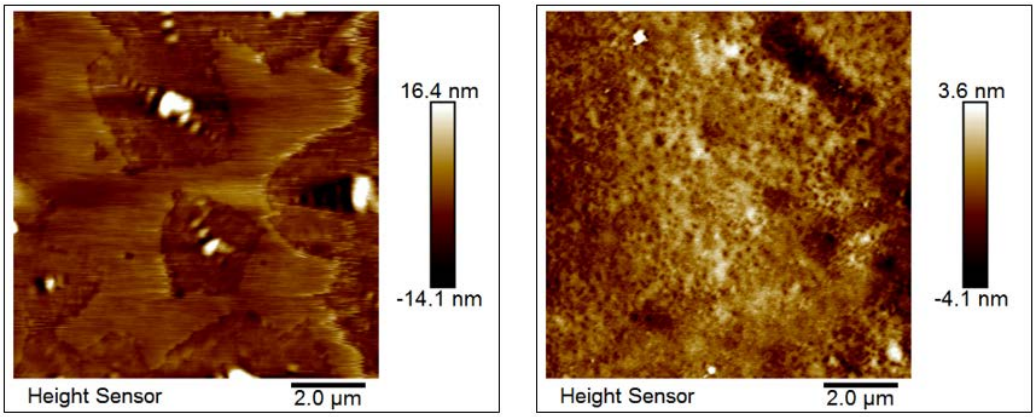

a) b)

Figure 49. Sample AFM maps of PG 64-22 (control) binder from S1: Morphology a) Dry and b) Wet-conditioned sample.

Table 19. Summary of surface roughness (nm) of asphalt binders of S1 and S2.

Binder Type	Sample Condition	Average Value	Dispersed and Interstitial Phase	Matrix Phase
S1B1	Dry	5.45	1.72-10.3	0.67-2.05
S1B1	Wet	1.57	0.817-4.98	0.478-1.91
S1B3	Dry	3.98	1.69-12.8	0.562-4.24
S1B3	Wet	2.14	1.01-3.62	0.592-1.85
S1B7	Dry	4.47	1.65-11.8	0.727-2.36
S1B7	Wet	2.24	0.549-4.35	0.382-2.11
S1B8	Dry	4.60	2.78-12.4	0.685-1.89
S1B8	Wet	1.66	1.00-8.44	0.392-3.91
S2B1	Dry	1.99	0.726-4.5	0.284-0.952
S2B1	Wet	2.08	0.937-4.75	0.436-2.15
S2B3	Dry	5.21	2.97-8.22	1.56-5
S2B3	Wet	6.09	3.51-10.21	0.856-3.45
S2B7	Dry	4.90	1.41-10.6	0.386-1.46
S2B7	Wet	2.11	1.00-5.78	0.277-1.25
S2B8	Dry	4.27	2.00-8.05	0.329-0.914
S2B8	Wet	3.13	1.99-7.49	1.25-2.52

Table 20. Summary of surface roughness (nm) of LAA-modified S1 and S2 binders.

Binder Type	Sample Condition	Average Value	Dispersed and Interstitial Phase	Matrix Phase
S1B1+Adhere	Dry	4.33	1.35-13.5	0.316-0.955
S1B1+Adhere	Wet	2.35	0.938-3.84	0.316-1.11
S1B1+Permatac	Dry	4.34	1.89-10.6	0.449-1.42
S1B1+Permatac	Wet	3.17	1.18-8	0.419-1.23
S1B1+Evotherm	Dry	4.24	1.05-12.1	0.351-1.08
S1B1+Evotherm	Wet	3.02	1.20-7.45	0.398-0.864
S2B1+Adhere	Dry	3.32	1.08-12.1	0.285-0.596
S2B1+Adhere	Wet	2.75	1.08-7.39	0.294-0.903
S2B1+Permatac	Dry	3.29	1.01-9.75	0.298-1.16
S2B1+Permatac	Wet	2.23	0.635-3.85	0.308-0.654
S2B1+Evotherm	Dry	3.88	1.02-13.3	0.343-0.675
S2B1+Evotherm	Wet	1.53	0.558-2.42	0.304-0.78

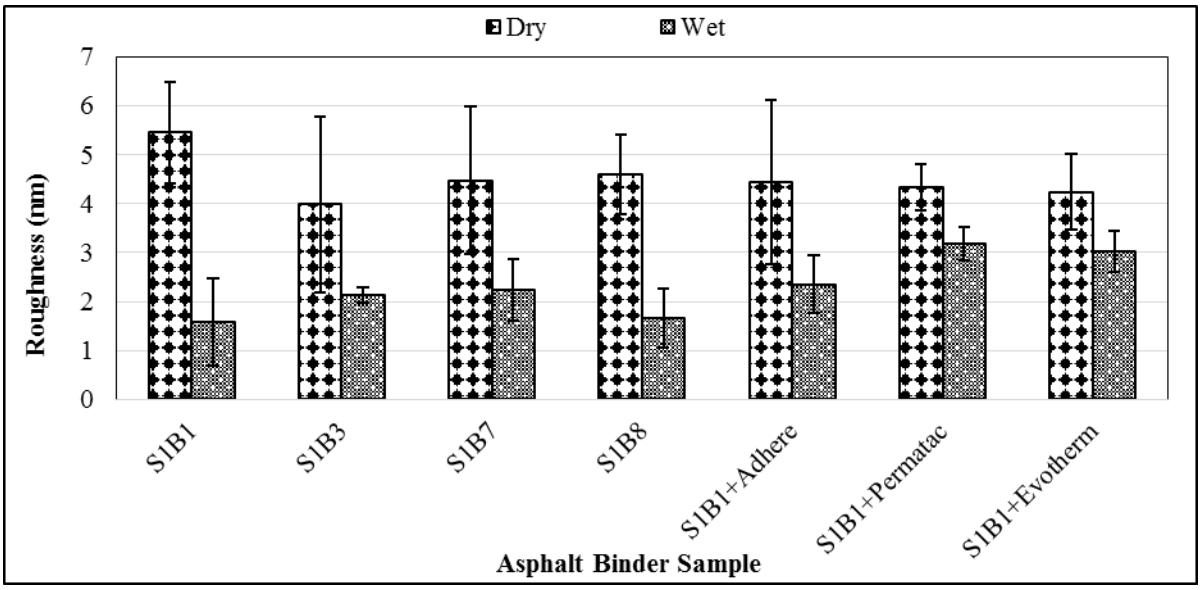

Figure 50. Comparison of surface roughness (nm) of all asphalt binders of S1.

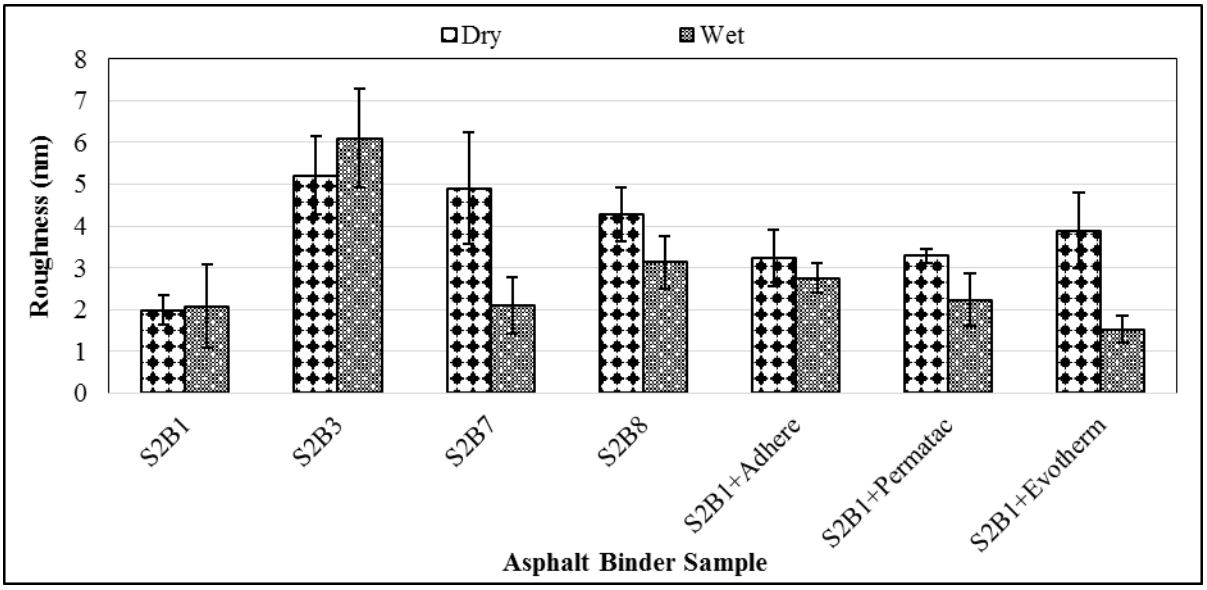

Figure 51. Comparison of surface roughness (nm) of all asphalt binders of S2.

Figure 52 shows the typical AFM maps of the modulus of SBS-modified PG 70-22 binders from S1 for dry (left) and wet-conditioned (right) samples and rest of the maps are added in Appendix D. Table 21 shows the summary of the modulus values for all the tested asphalt binders from S1 and S2.

AFM results showed that all S1 binders had lower modulus values in the wet conditioned sample compared to S2 binders. The comparison of the modulus values among all tested binders are shown in Figures 53 and 54. It is also found that the modulus value was only reduced for S2B3 binder (PPA-modified PG 70-22) of S2, which is varied from 963 MPa to 491 MPa. AFM results also show that PG 64-22 binder had a higher DMT modulus value (from 43 MPa to 175 MPa),

whereas PPA-and SBS-modified binder had minimal effect (from 173 MPa to 189 MPa) among all S2 binders. Based on the AFM analysis, it can be reported that binders that modified with the combination of PPA and SBS for both sources (S1 and S2) had better moisture resistance among all asphalt binders. The LAAs modified binders, presented in Table 22, showed decreased modulus in both dry and wet samples and for all cases, the higher values were observed in the dry samples except for the Adhere HP Plus of S1 binders.

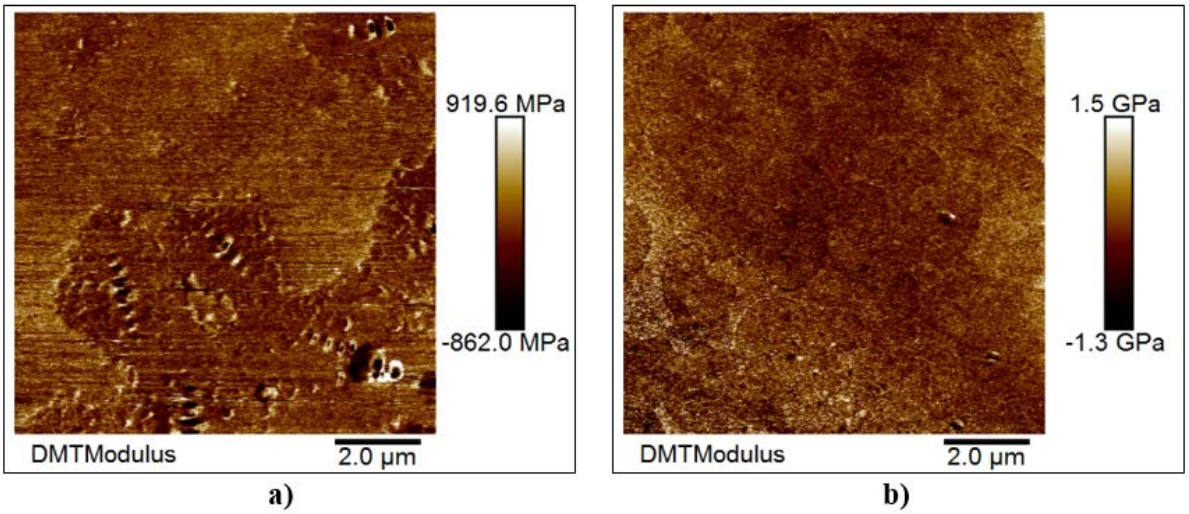

Figure 52. Sample AFM maps of PG 70-22 (SBS-modified) binder from S1: Modulus a) Dry and b) Wet-conditioned sample.

Figure 55 shows the sample AFM maps of the adhesion of SBS-modified PG 70-22 binders from S2 for dry (left) and wet-conditioned (right) samples and rest of the maps are added in Appendix D. Table 23 shows the summary of the adhesion force (nN) values for all the tested asphalt binders from S1 and S2. Furthermore, the comparison of the adhesion force among all tested binders is shown in Figures 56 and 57.

Table 21. Summary of DMT modulus (MPa) of asphalt binders from S1 and S2.

Binder Type	Sample Condition	Average Value	Dispersed and Interstitial Phase	Matrix Phase
S1B1	Dry	536.33	250-842	78.9-324
S1B1	Wet	271.73	55.6-630	53.1-339
S1B3	Dry	462.00	120-1334	55.7-278
S1B3	Wet	198.33	69.5-546	56.9-122
S1B7	Dry	489.67	188-2028	128-723
S1B7	Wet	306.27	64.7-532	44.3-353
S1B8	Dry	141.63	35.7-342	19.7-132
S1B8	Wet	75.93	52.7-133	45.5-81
S2B1	Dry	43.30	30-114	25.8-50.7
S2B1	Wet	174.95	42.9-345	39.6-225
S2B3	Dry	962.67	747-1173	444-965
S2B3	Wet	490.67	195-814	74.2-494
S2B7	Dry	590.67	264-1085	244-473
S2B7	Wet	652.33	303-2005	231-563
S2B8	Dry	173.33	111-359	62.1-130
S2B8	Wet	189.00	95.1-406	63.7-197

Table 22. Summary of DMT modulus (MPa) of LAA-modified binders from S1 and S2.

Binder Type	Sample Condition	Average Value	Dispersed and Interstitial Phase	Matrix Phase
S1B1+Adhere	Dry	60.80	29.8-123	26.4-49.6
S1B1+Adhere	Wet	144.97	38.4-359	27.9-165
S1B1+Permatac	Dry	85.77	34.5-183	24-66.8
S1B1+Permatac	Wet	41.50	20.2-81.5	18.1-39.2
S1B1+Evotherm	Dry	99.40	36.9-281	31.9-101
S1B1+Evotherm	Wet	53.03	33.6-76.3	23-62.9
S2B1+Adhere	Dry	131.33	96.3-323	79.3-120
S2B1+Adhere	Wet	56.50	36.63-129	26.2-46.2
S2B1+Permatac	Dry	180.43	61-537	50.3-235
S2B1+Permatac	Wet	146.07	61.3-560	19.2-160
S2B1+Evotherm	Dry	146.00	90-372	76-103
S2B1+Evotherm	Wet	56.40	36.1-107	25.4-51.5

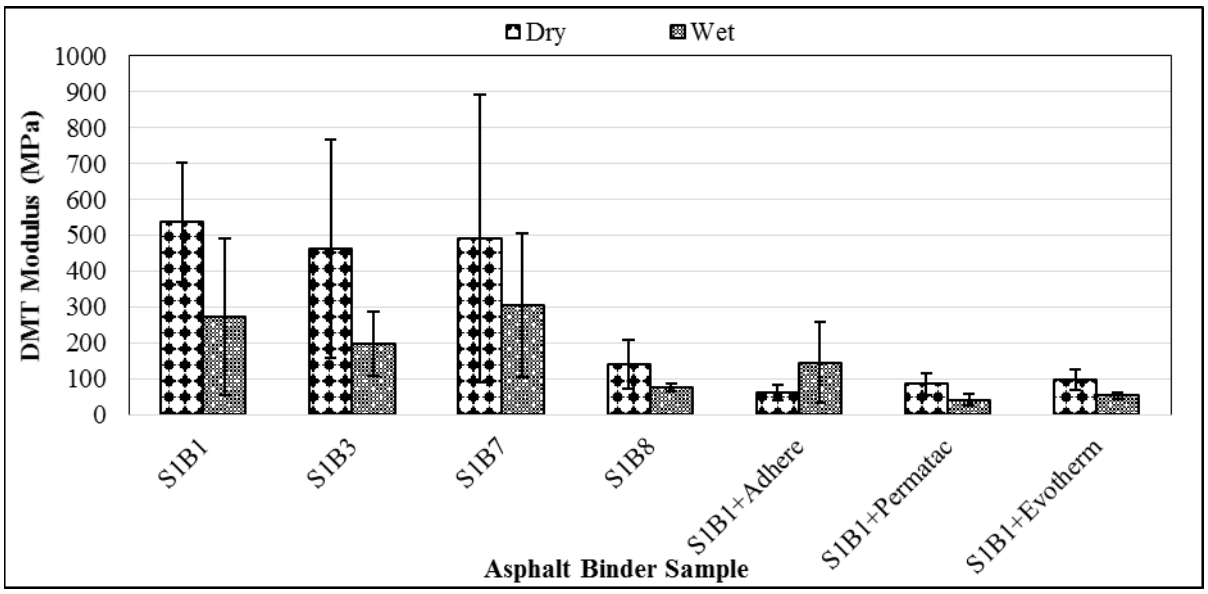

Figure 53. Comparison of DMT modulus (MPa) values of all asphalt binders of S1.

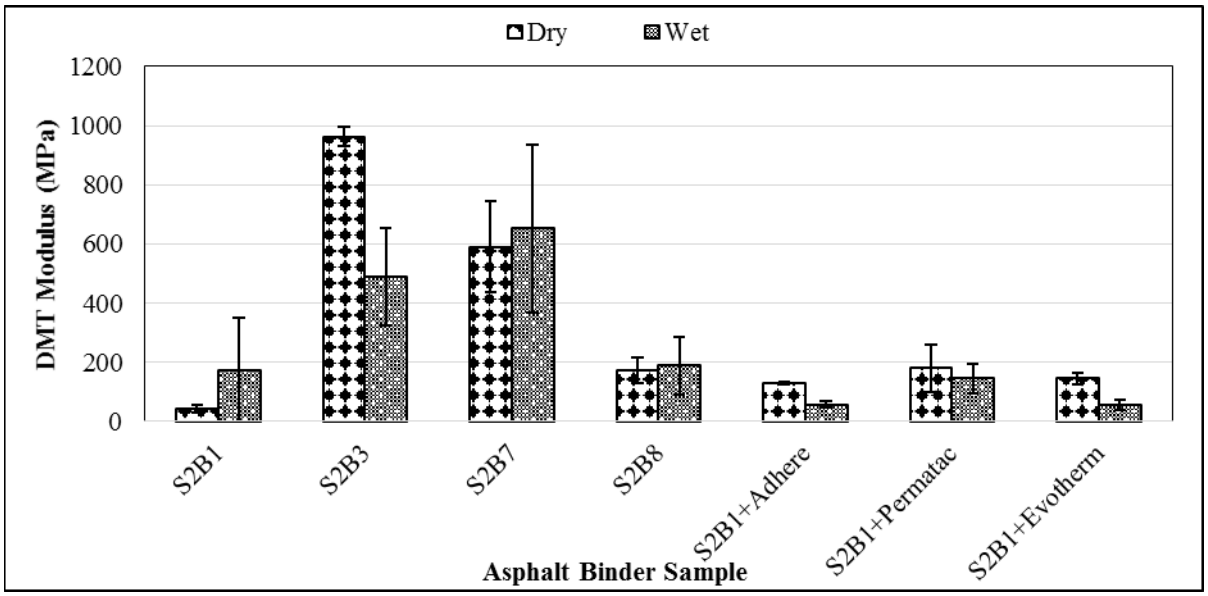

Figure 54. Comparison of DMT modulus (MPa) values of all asphalt binders of S2.

Based on the AFM results, it is found that the average adhesion values were reduced in all S1 binders due to the action of water, and the PG 76-22 binder, which was modified with PPA and SBS, showed the lowest reduction (31 nN to 7 nN). A similar decreasing trend was also observed in the case of S2 binders. On the other hand, S2B7 binder (SBS-modified PG 70-22) showed a lower decreasing rate that ranges from 13 nN to 11.50 nN. Therefore, the AFM test results concluded that SBS-modified binders from both sources (S1 and S2) showed better resistance to moisture damage. Furthermore, the effects of LAAs were also presented in Table 24. As seen

from this table, for all LAA-modified binders, the adhesion values were found to be lower although S1B1 modified with Adhere HP Plus showed a higher value, which is more than twice in the wet-conditioned sample than the dry sample.

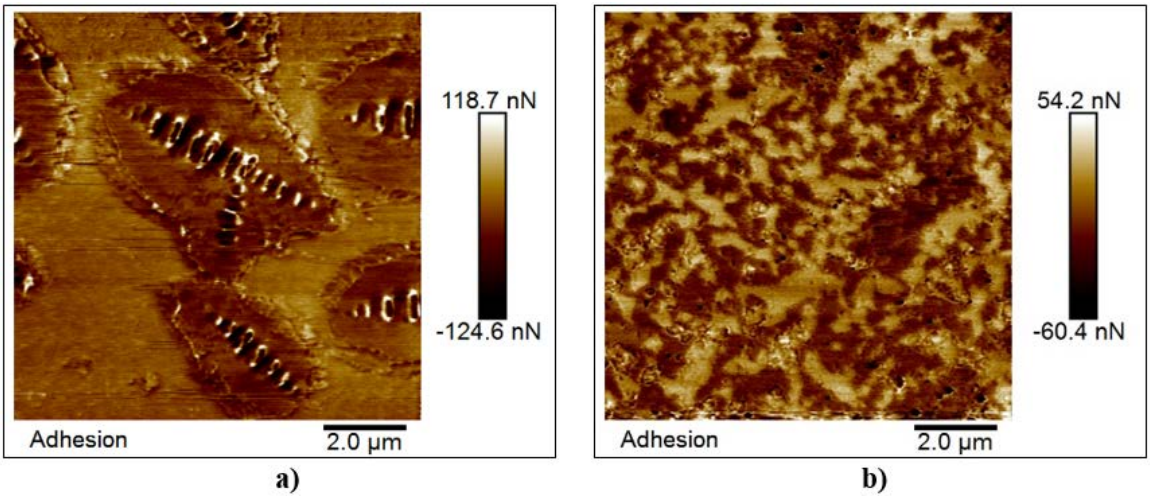

Figure 55. Sample AFM maps of PG 70-22 (SBS-modified) binder from S2: Adhesion a) Dry and b) Wet-conditioned sample.

In Figure 58, typical AFM maps of the deformation (nm) of SBS-modified PG 70-22 binders from S2 for dry (left) and wet-conditioned (right) samples are shown while the rest of the AFM maps are added in Appendix D. The summary of the deformation values for all the tested asphalt binders from S1 and S2 are presented in Table 25. Also, the comparison of the deformation values among all tested binders is shown in Figures 59 and 60.

Table 23: Summary of Average Adhesion Force (nN) of Binders from S1 and S2.

Binder Type	Sample Condition	Average Value	Dispersed and Interstitial Phase	Matrix Phase
S1B1	Dry	84.67	18-172	13-94
S1B1	Wet	20.16	4.29-51.8	2.1-19.4
S1B3	Dry	113.33	50.2-199	12.1-125
S1B3	Wet	53.53	17.7-112	7.46-42.2
S1B7	Dry	16.10	7.45-24	2.82-14.5
S1B7	Wet	8.55	3.06-10.8	1.67-4.55
S1B8	Dry	30.67	16.9-79	4.24-14.3
S1B8	Wet	6.95	2.36-19.7	1.65-8.65
S2B1	Dry	4.61	2.12-15.7	1.33-4.73
S2B1	Wet	10.19	2.69-28.6	2.22-10
S2B3	Dry	220.67	160-278	113-209
S2B3	Wet	130.33	73.5-190	33.5-122
S2B7	Dry	12.67	2.84-16.2	1.46-8.11
S2B7	Wet	11.48	3.18-19.7	1.67-7.93
S2B8	Dry	24.33	12.2-38.5	2.86-10.5
S2B8	Wet	32.83	14.2-84.4	4.96-36.3

Table 24. Summary of adhesion force (nN) of LAA-modified S1 and S2 binders.

Binder Type	Sample Condition	Average Value	Dispersed and Interstitial Phase	Matrix Phase
S1B1+Adhere	Dry	13.13	2.37-35.1	1.94-5.46
S1B1+Adhere	Wet	27.40	6.58-60.9	2.5-32
S1B1+Permatac	Dry	16.47	6.78-31.7	2.59-6.29
S1B1+Permatac	Wet	13.45	3.84-29.8	2.11-10.9
S1B1+Evotherm	Dry	11.46	4.03-53.5	2.13-6.28
S1B1+Evotherm	Wet	7.81	2.29-15.4	1.83-5.45
S2B1+Adhere	Dry	12.62	2.92-46.9	2.5-3.43
S2B1+Adhere	Wet	7.98	3.41-29.5	1.87-5.62
S2B1+Permatac	Dry	24.10	5.48-63.1	1.95-33.9
S2B1+Permatac	Wet	12.56	2.92-33.5	1.32-8.83
S2B1+Evotherm	Dry	18.67	6.55-68.6	2.57-6.67
S2B1+Evotherm	Wet	12.60	3.21-36.2	1.97-8.54

From the AFM tests results, it is noticed that deformation values were found to lower in the case of all S1 binders. However, higher values were found for S1B3 binder (PPA-modified PG 70-22) among all binders in the case of S1. On the other hand, all S2 binders showed a higher deformation value in the wet conditioned samples than their corresponding dry samples even though S2B1 binder showed very close value. Also, S2B3 binder (PPA-modified PG 70-22) showed a higher deformation value after the water immersion of the sample compared to other binders from S2. The effects of LAA-modified binders are also shown in Table 26. From this table, it is found that among all LAAs, Adhere HP Plus increased the deformation values for both sources. However, both Permatac and Evotherm decreased the deformation values for S1 binders but increased the values in the case of S2 binders.

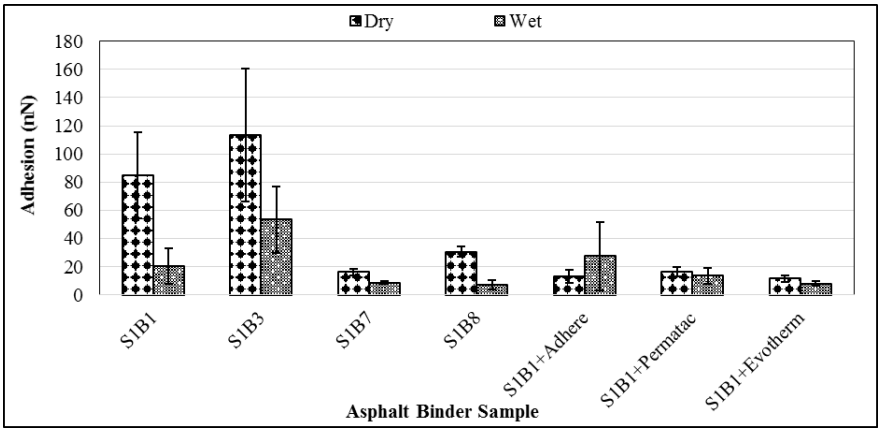

Figure 56. Comparison of adhesion force (nN) values of all asphalt binders of S1.

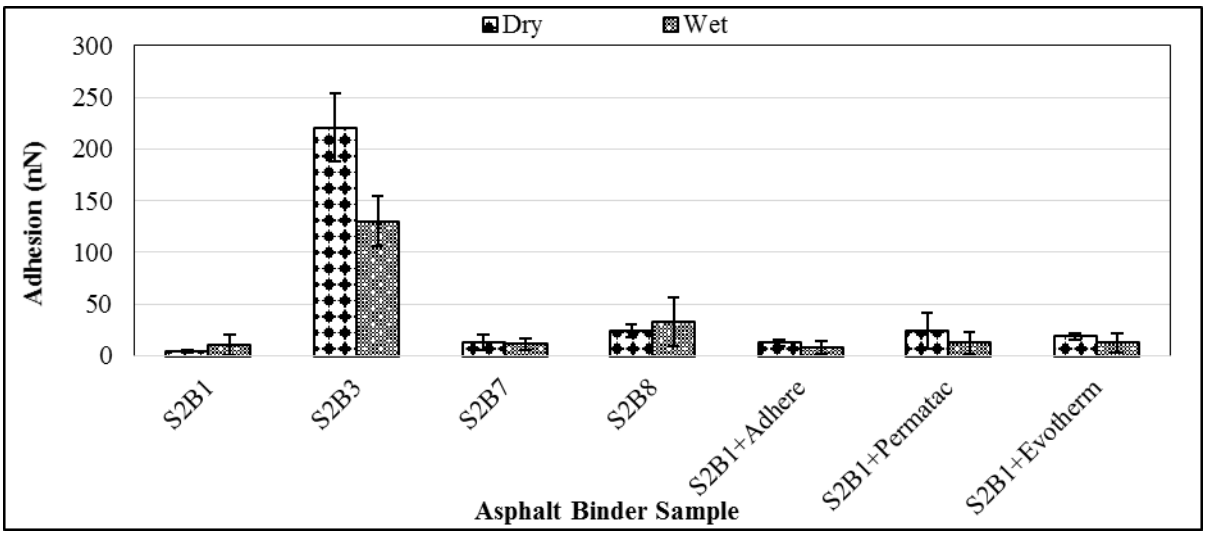

Figure 57. Comparison of adhesion force (nN) values of all asphalt binders of S2.

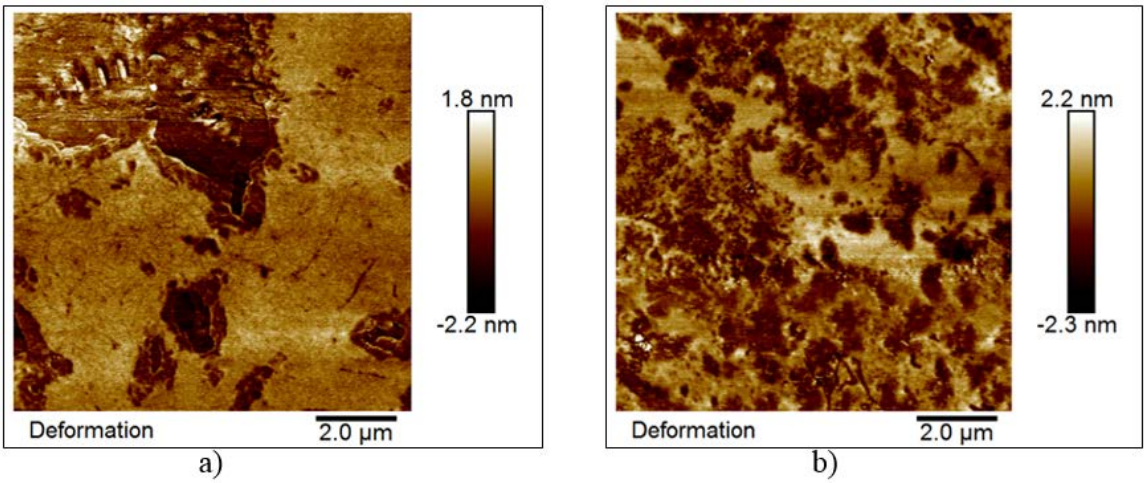

Figure 58. AFM maps of PG 70-22 (SBS-modified) binder from S2: Deformation a) Dry and b) Wet-conditioned sample.

Table 25. Summary of deformation (nm) values of binders from S1 and S2.

Binder Type	Sample Condition	Average Value	Dispersed and Interstitial Phase	Matrix Phase
S1B1	Dry	1.73	0.521-3.1	0.274-1.33
S1B1	Wet	0.43	0.127-1.02	0.116-0.565
S1B3	Dry	2.25	1.13-3.89	0.598-1.75
S1B3	Wet	1.33	0.56-3.5	0.667-1.01
S1B7	Dry	1.04	0.369-1.48	0.21-1.25
S1B7	Wet	0.57	0.237-1.19	0.101-0.498

Binder Type	Sample Condition	Average Value	Dispersed and Interstitial Phase	Matrix Phase
S1B8	Dry	2.12	1.08-3.04	0.443-1.56
S1B8	Wet	0.79	0.219-1.20	0.169-0.785
S2B1	Dry	0.32	0.206-0.699	0.145-0.307
S2B1	Wet	0.31	0.187-0.461	0.195-0.294
S2B3	Dry	2.71	1.44-4.58	1.01-2.67
S2B3	Wet	4.34	2.48-6.33	0.755-3.08
S2B7	Dry	0.68	0.378-1.13	0.20-0.374
S2B7	Wet	0.73	0.396-0.926	0.101-0.490
S2B8	Dry	0.64	0.285-1.21	0.144-0.395
S2B8	Wet	1.48	1.07-2.14	0.462-1.17

Table 26. Summary of deformation (nm) of LAA-modified S1 and S2 binders.

Binder Type	Sample Condition	Average Value	Dispersed and Interstitial Phase	Matrix Phase
S1B1+Adhere	Dry	0.86	0.273-1.88	0.252-0.744
S1B1+Adhere	Wet	1.44	0.468-3.44	0.176-0.795
S1B1+Permatac	Dry	1.41	0.502-2.2	0.231-1.41
S1B1+Permatac	Wet	0.97	0.522-2.08	0.323-0.694
S1B1+Evotherm	Dry	1.45	0.5-2.17	0.332-0.985
S1B1+Evotherm	Wet	0.99	0.501-1.75	0.339-0.738
S2B1+Adhere	Dry	0.22	0.142-0.513	0.14-0.152
S2B1+Adhere	Wet	0.44	0.348-1.12	0.155-0.313
S2B1+Permatac	Dry	0.53	0.117-1.77	0.1-1.19
S2B1+Permatac	Wet	0.65	0.318-1.17	0.163-0.351
S2B1+Evotherm	Dry	0.44	0.281-0.956	0.148-0.363
S2B1+Evotherm	Wet	0.47	0.204-0.844	0.16-0.24

Figure 61 shows the typical AFM maps of the dissipation of PPA+SBS-modified PG 76-22 binders from S2 for dry (left) and wet-conditioned (right) samples, and the rest of the AFM maps are added in Appendix D. Table 27 shows the summary of the dissipation values for all the tested

asphalt binders from S1 and S2. Moreover, Figures 62 and 63 show the comparison of the dissipation values of all tested binders in this study.

The AFM results show that dissipation values were decreased in the case of all binders from S1. However, all binders except for S2B3 binder showed higher dissipation values in the wet samples for S2. This could be the influence of PPA in the presence of water, which is responsible for the dispersion of smaller asphaltenes in the asphalt binder *(100).* Comparing all results, it is found that PPA-modified PG 70-22 binders from both sources had the lower dissipation values due to the moisture effects. The effects of LAAs are also shown in Table 28. It is seen that for all Evotherm-modified binders, the dissipation energy values reduced for both sources. The other two LAAs (Permatac and Adhere HP Plus) increased the dissipation energy values for S1 binders but decreased the values in the case of S2 binders.

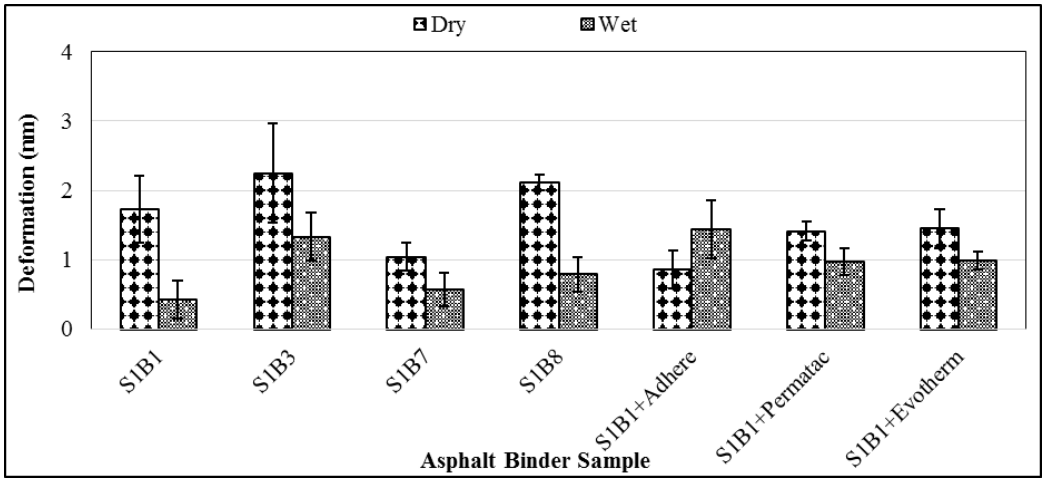

Figure 59. Comparison of deformation (nm) values of all asphalt binders of S1.

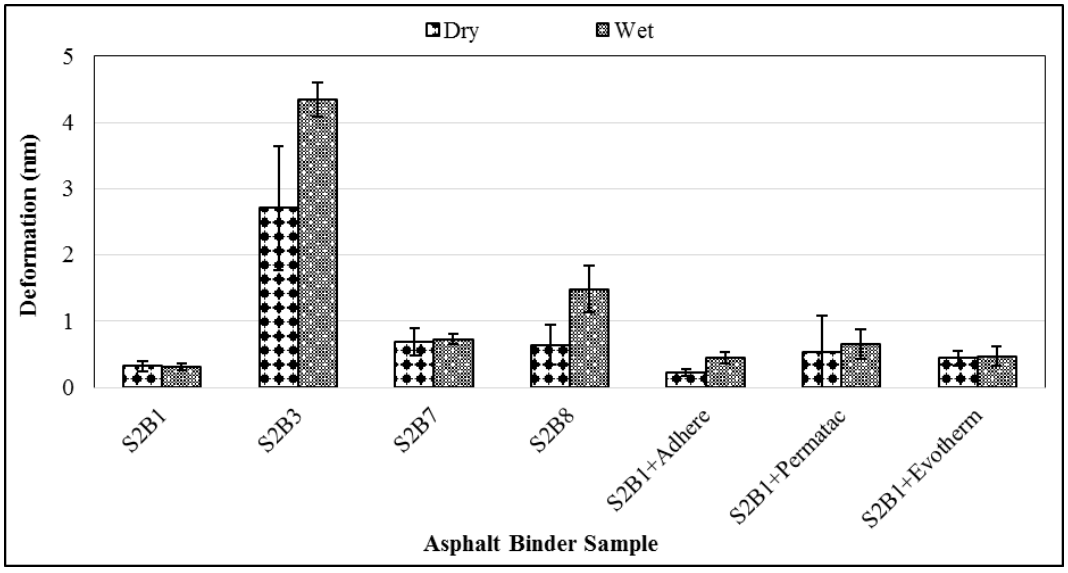

Figure 60. Comparison of deformation (nm) values of all asphalt binders of S2.

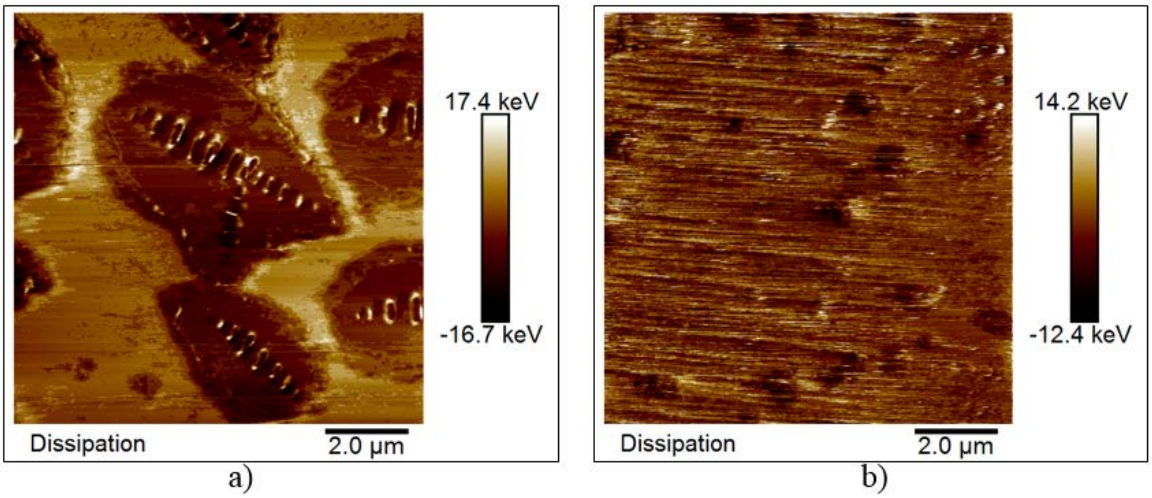

Figure 61. AFM maps of PG 76-22 (PPA+SBS-modified) binder from S2: Dissipation a) Dry and b) Wet-conditioned sample.

Table 27. Summary of dissipation energy (eV) values of binders from S1 and S2.

Binder Type	Sample Condition	Average Value	Dispersed and Interstitial Phase	Matrix Phase
S1B1	Dry	13996.67	3228-28655	2242-12333
S1B1	Wet	3208.33	1052-9552	369-2105
S1B3	Dry	22689.00	6512-44779	2644-11160
S1B3	Wet	8981.33	3112-20093	1871-4816
S1B7	Dry	3247.67	1072-4039	333-2264
S1B7	Wet	2075.33	917-3135	62.4-950
S1B8	Dry	6904.33	3516-14402	1446-4760
S1B8	Wet	2265.67	1575-4129	99.5-2250
S2B1	Dry	1527.67	1375-2644	527-1611
S2B1	Wet	1859.00	1237-2417	1032-1619
S2B3	Dry	45829.00	30100-61753	19777-43058
S2B3	Wet	26876.00	21131-37623	6873-20415
S2B7	Dry	1726.33	972-3710	36.2-996
S2B7	Wet	2011.33	1114-2979	69.2-461
S2B8	Dry	3854.67	1483-2866	46-1695
S2B8	Wet	5434.67	2061-9905	1311-6304

Table 28. Summary of dissipation energy (eV) of LAA-modified S1 and S2 binders.

Binder Type	Sample Condition	Average Value	Dispersed and Interstitial Phase	Matrix Phase
S1B1+Adhere	Dry	4219.67	1817-8196	1498-2203
S1B1+Adhere	Wet	6962.00	2147-14898	1265-6283
S1B1+Permatac	Dry	3986.33	2422-6625	1768-2740
S1B1+Permatac	Wet	15099.33	2256-8973	1378-2917
S1B1+Evotherm	Dry	4917.00	2184-7423	1004-3528
S1B1+Evotherm	Wet	3240.67	1457-3584	645-2463
S2B1+Adhere	Dry	2413.33	1562-8465	127-1271
S2B1+Adhere	Wet	2154.33	1243-4937	104-1484
S2B1+Permatac	Dry	4540.67	1686-23901	113-4870
S2B1+Permatac	Wet	3325.67	1391-8011	306-1932
S2B1+Evotherm	Dry	2959.00	1059-9923	473-1908
S2B1+Evotherm	Wet	2605.33	1256-5365	339-1718

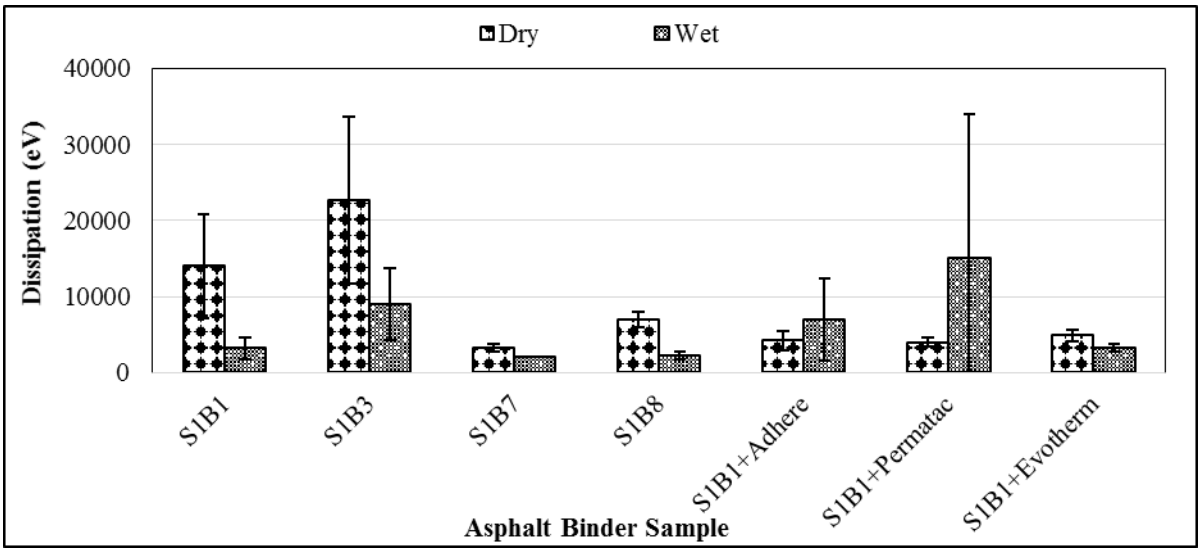

Figure 62. Comparison of dissipation energy (eV) values of all asphalt binders of S1.

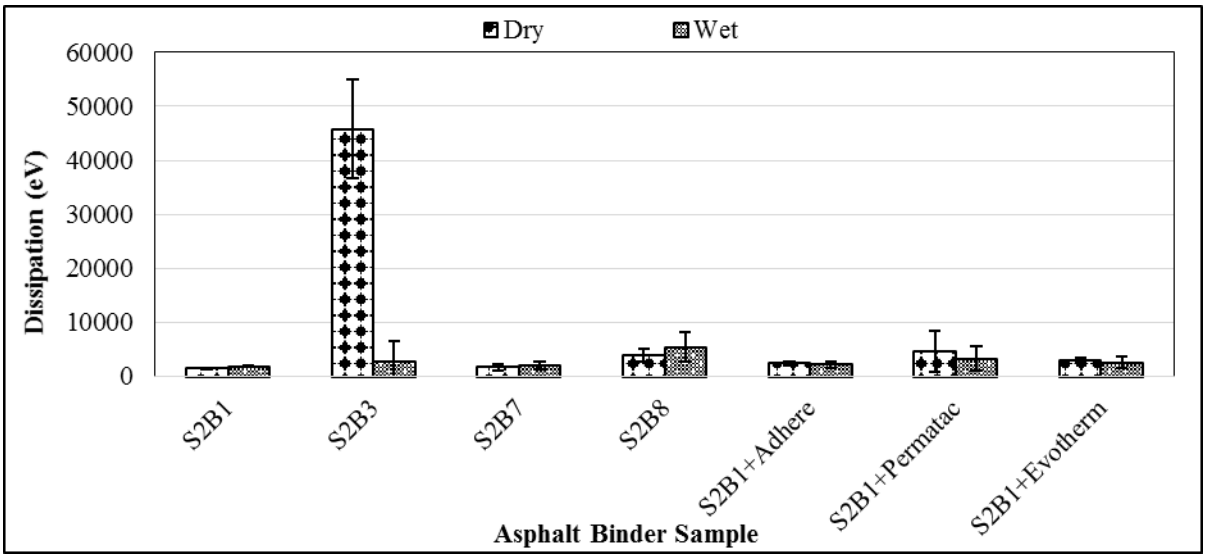

Figure 63. Comparison of dissipation energy (eV) values of all asphalt binders of S2.

5.4. Binder Chemical Tests

5.4.1. Saturates Aromatics Resins and Asphaltenes (SARA) Analysis

The results of the chromatographic separation of both sets of binders were analyzed and the data is presented in Table 29 and in Figures 64 and 65. The results show that the asphalt binder samples from S1 (the Canadian crude source) had a high Asphaltenes content (15%) compared to those (12.8%) from S2 (the Arabian crude source). It is noted that the Asphaltenes content increased and Resins content decreased with the addition of PPA, which made the binder stiffer than the base binder. These findings agree with the results of the rheological data discussed earlier section in this report.

Table 29. SARA analysis of asphalt binders.

Binder Type	Asphaltenes (%)	Resins (%)	Aromatics (%)	Saturates (%)
S1B1	15	21.6	59.1	4.3
S1B3	17.8	14.8	58.1	9.3
S1B7	17.5	24.2	53	5.3
S1B8	20.7	22	53	4.4
S2B1	12.8	14.3	68.1	4.8
S2B3	15.7	14.6	63.4	6.3
S2B7	15.1	15.7	62.7	6.5
S2B8	16.2	13.1	62.3	8.3

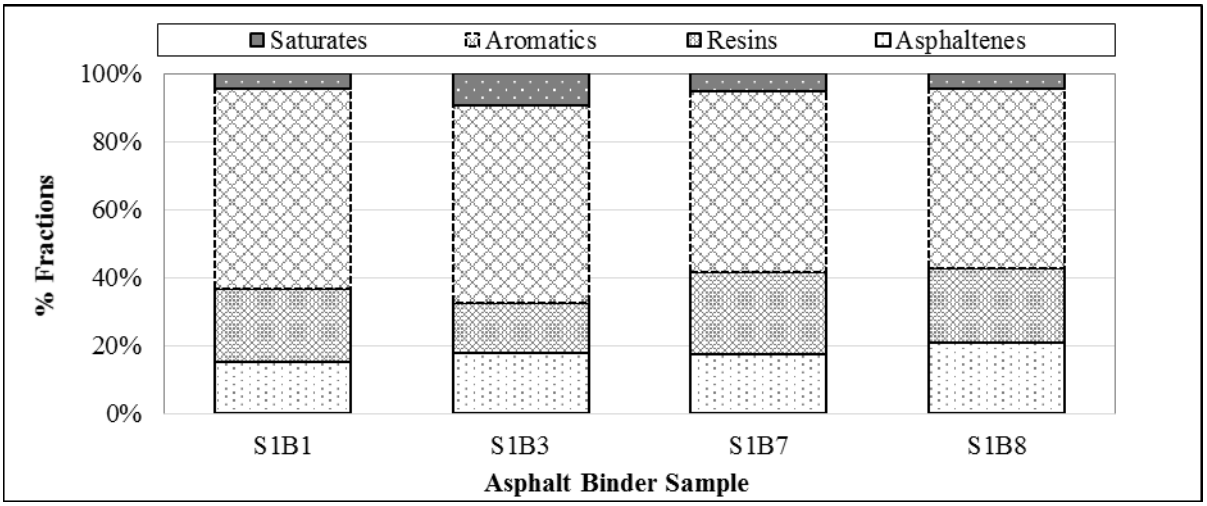

Figure 64. SARA fractions of asphalt binders from S1.

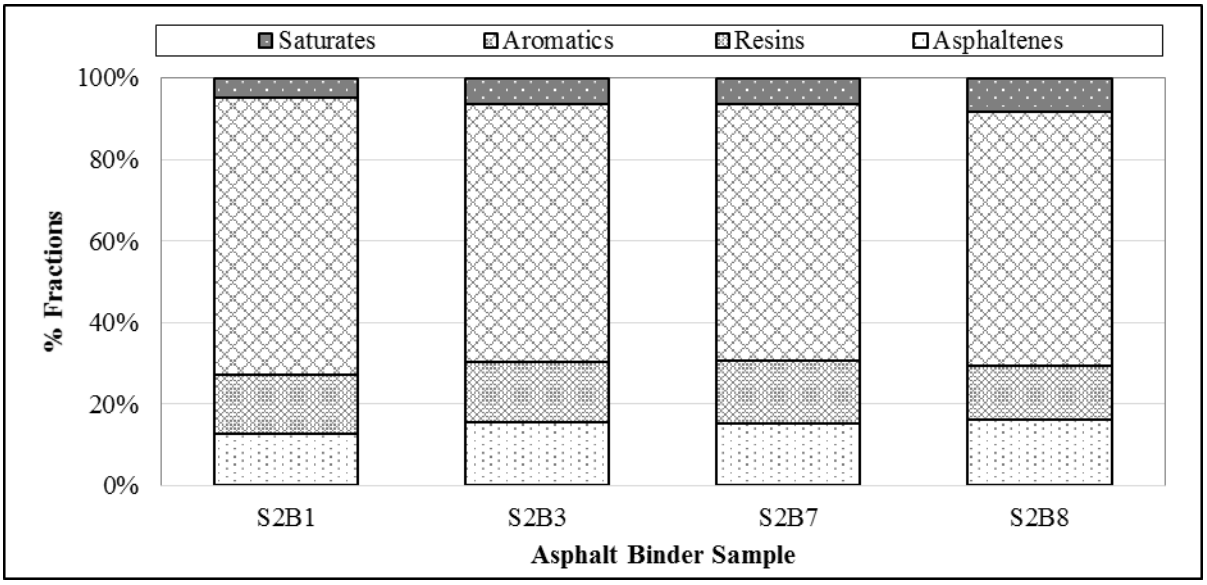

Figure 65. SARA fractions of asphalt binders from S2.

5.4.2. Fourier Transform Infrared Spectroscopy (FTIR) Analysis

FTIR analysis was performed to observe any differences in the peaks due to the addition of SBS and PPA in asphalt binders. Figure 66 shows the FTIR analysis for S1B1 and S1B2, and Figures 67 and 68 show the FTIR spectrum for SBS-modified (S2B7) and PPA-and SBS-modified (S2B8) binders from S2. The rest of the FTIR spectra of the tested binders are shown in Appendix E. From the FTIR analysis, it is found that the polymer modified samples show peaks at 965cm^{-1}, which indicated to SB and SBS. The ratio of the SB and SBS peak versus the asphalt peak is then used to determine the polymer content of the asphalt. Moreover, an NMR was used to verify the separated SARA fractions of asphalt binders, which are assembled in Appendix F.

Table 30 shows the absorbance and area analysis for S2B7 (2% SBS) and S2B8 (2% SBS and 0.75% PPA). From this table, it is found that the absorbance ratios of S2B7 and S2B8 are 0.35 and 0.10, respectively, which indicate a corresponding polymer content of 5%, and 1.85%.

However, the SBS content in these binders was 2%. Based on the area analysis, the area ratios of S2B7 and S2B8 are 0.25 and 0.13, respectively, indicating the corresponding polymer contents of 3.5% and 2%. Thus, the area analysis appears to be a better approach than the absorbance analysis to predict the polymer content.

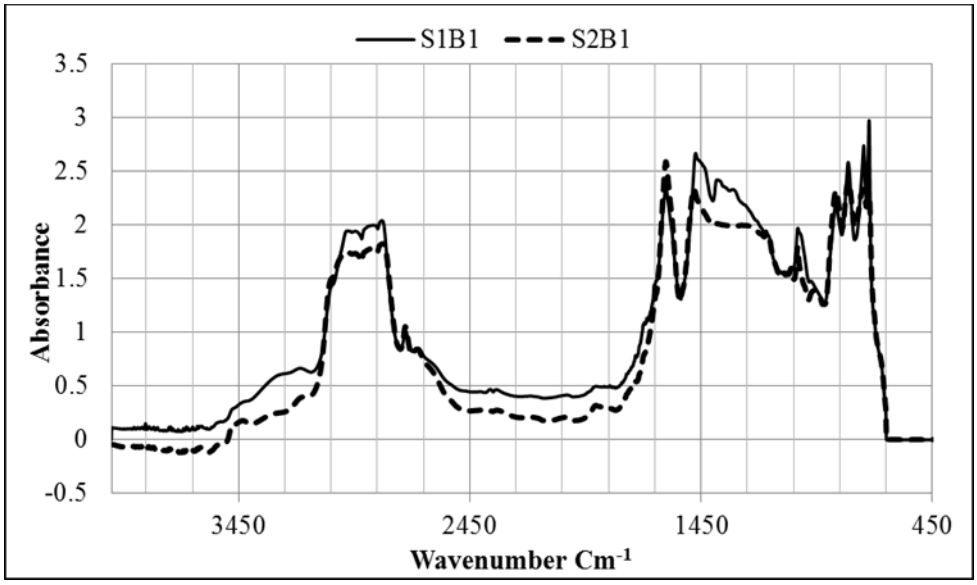

Figure 66. FTIR spectrum of PG 64-22 binders from S1 and S2.

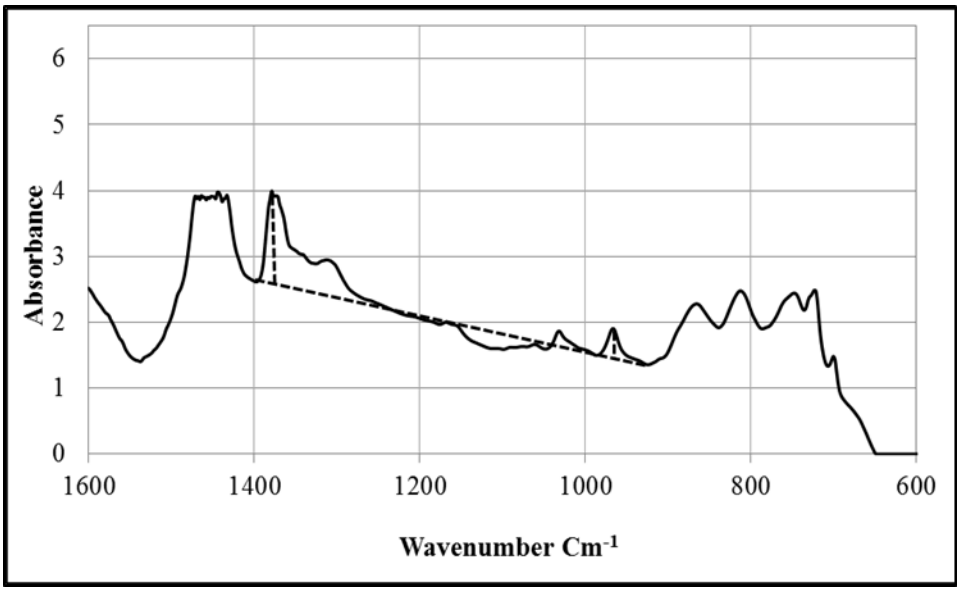

Figure 67. Polymer content analysis of S2B7.

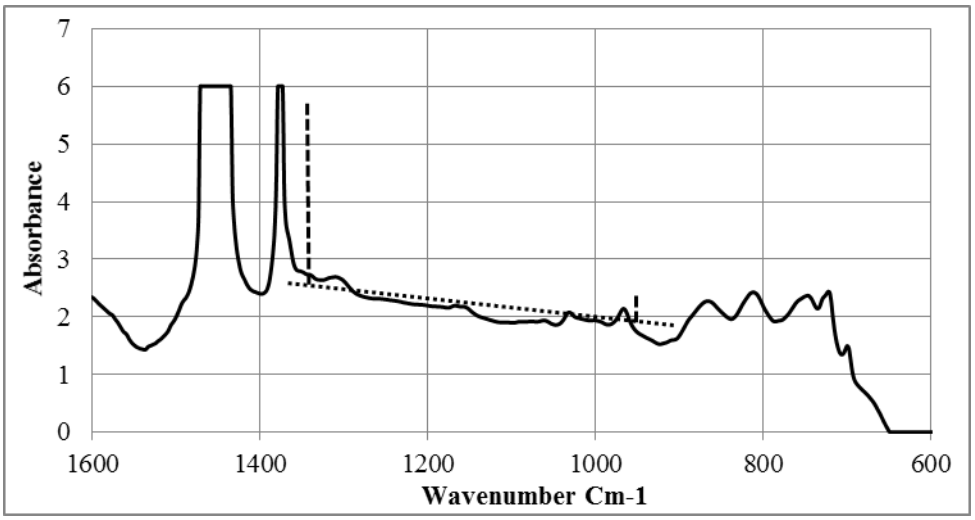

Figure 68. Polymer content analysis of S2B8.

Table 30. Absorbance and area analysis of S2B7 and S2B8.

Binder Sample	Absorbance at Peak 966	Area at Peak 966	Absorbance at Peak 1375	Area at Peak 1375	Absorbance Ratio	Area Ratio
S2B7	0.428	8.463	1.237	34.432	0.35	0.25
S2B8	0.382	6.552	3.526	51.334	0.10	0.13

5.5. Correlations Among Test Results

5.5.1. Relative Moisture Resistance Ranking

Table 31 summarizes a subset (e.g., samples considered in all test methods) of moisture sensitivity test results analyzed in the current study. As seen in Table 31, three binder samples, namely, PG 64-22 (Control), PPA-modified PG 70-22, and SBS-modified PG 70-22 are used to compare the results of the selected test methods. The moisture resistance ranking (RR) of the performed tests, shown in Table 32, are estimated based on the normalized resistance (NR) of the corresponding asphalt binder samples. To obtain NR values, test results of S1B1, S1B3, and, S1B7 samples are divided by their corresponding values of S1B1 for each moisture damage test. For example, in the case of TSR test results, the NR values for S1B7 binder sample is found to be 1.290, which is calculated by dividing 1.181 with 0.915. Thus, the NR-values are determined and later the RR values are given for each test. The smallest RR value represents the numerical value of 1, 3 for the largest, and 2 for all others. For instance, the ranking of the S1B1, S1B3, and, S1B7 binders for TSR test are 1, 3, and 2, respectively, as shown in Table 32.

Table 31. Summary of the moisture sensitivity test results.

Binder Type	TSR (Ratio = Wet/Dry)	HWTD (No. of wheel passes)	Texas Boiling (% Asphalt Retained)	Preston Gravel, SFE (CR values)	Preston Sandstone, SFE (CR values)	Asphaltenes, SARA (%)	Re-sins, SARA (%)	Adhesion, AFM (Ratio = Wet/Dry)	Dissipation, AFM (Ratio = Wet/Dry
S1B1	0.915	6686	50	2.496	2.406	15	21.6	0.238	0.229
S1B3	1.208	8000	60	2.205	2.119	17.8	14.8	0.472	0.396
S1B7	1.181	8000	70	3.311	3.216	17.5	24.2	0.531	0.639

Figure 69 shows the comparison of the NR-values of the moisture sensitivity tests of the binder samples. It is evident that the two mixture tests, namely, TSR and HWTD, show a similar pattern with the SARA analysis while considering the percentage of the Asphaltenes fraction. On the other hand, the Texas boiling test results show a similar trend with the AFM test results. Moreover, similarities are also observed between the SFE tests (for Preston Gravel and Sandstone) and the percentage of the Resins fraction from SARA analysis. Thus, it can be said there exist some correlations among the results of different test methods. However, all test methods do not give a single trend.

Table 32. Ranking of the moisture sensitivity tests.

Binder Type	TSR (Ratio = Wet/Dry)	HWTD (No. of wheel passes)	Texas Boiling (% Asphalt Retained)	Preston Gravel, SFE (CR values)	Preston Sandstone, SFE (CR values)	Asphaltenes, SARA (%)	Re-sins, SARA (%)	Adhesion, AFM (Ratio = Wet/Dry)	Dissipation, AFM (Ratio = Wet/Dry
S1B1, NR	1	1	1	1	1	1	1	1	1
S1B1, RR	(1)	(1)	(1)	(2)	(2)	(1)	(2)	(1)	(1)
S1B3, NR	1.31	1.19	1.20	0.88	0.88	1.18	0.68	1.98	1.72
S1B3, RR	(3)	(3)	(2)	(1)	(1)	(3)	(1)	(2)	(2)
S1B7, NR	1.29	1.19	1.40	1.32	1.33	1.16	1.12	2.22	2.78
S1B7, RR	(2)	(2)	(3)	(3)	(3)	(2)	(3)	(3)	(3)

Note: NR: Normalized Resistance and RR: Moisture Resistance Ranking.

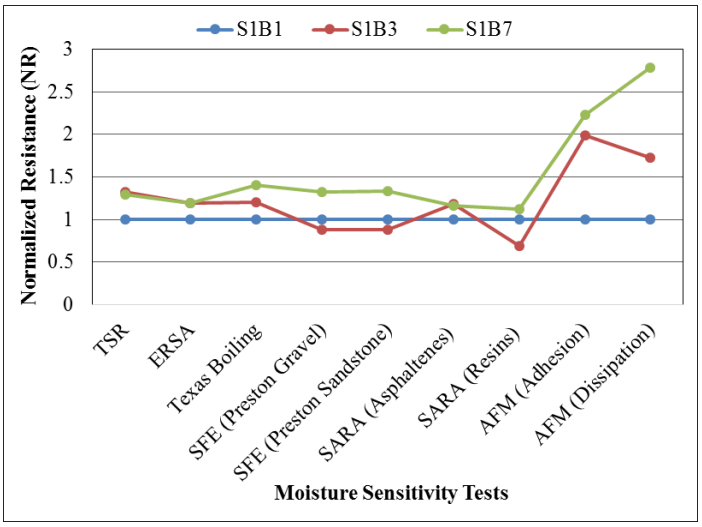

Figure 69. Comparison of the NR-values of the moisture sensitivity tests of the binder samples.

Based on the R-values presented in Figure 70 and simplicity of the test method, the Texas Boiling test can be followed by transportation agencies for qualitative measurements of moisture damage of the asphalt mixtures because of its simple test procedures and fewer time requirements to perform the test. Even though the Texas Boiling test does not warrant a mix design and asphalt mix, it still mimics the mix by coating aggregates with asphalt binder. On the other hand, SFE analysis can be included in determining the moisture susceptibility of the asphalt binders as it considers the binder-aggregate compatibility. Another advantage of the SFE method is that it does not require to do mix designs or prepare asphalt mixes, which save a significant amount of sample preparation time and efforts. Further, SFE test can be done at any stage of the asphalt binder and aggregate characterization task. Two other test methods (TSR and HWTD) are solely on the asphalt mixtures, and either of these tests is conducted at the very last stage of asphalt mix design when it is too late to make significant adjustments. Additionally, the AFM test also is an effective tool to quantify the moisture damage resistance of the binders to moisture for its quantitative and quantitative measurements in the molecular level, and it is recommended for research projects as transportation agencies are still not equipped with the testing device and test operators.

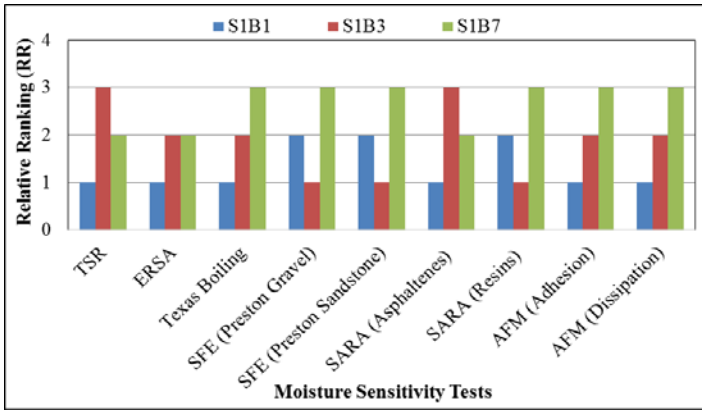

Figure 70. Comparison of the RR-values of the moisture sensitivity tests.

6. CONCLUSIONS

The purpose of this study is to investigate the moisture effects on the properties of the asphalt binders. To achieve the goal of this study, selected macro and micro-level moisture sensitivity tests were performed in the laboratory. Besides, the conventional test methods, some fundamental science-based advanced tests were also included in the test plan. Asphalt binder samples used for this study were collected from two different sources (S1 and S2). The tested binders included unmodified PG 64-22, modified PG 70-22 and PG 76-22. The additives used in the modified binders were polyphosphoric acid (PPA), styrene-butadiene-styrene (SBS), and a combination of PPA and SBS. Three types of liquid anti-stripping agents (LAAs) were also used to observe their effects in the tested binders. To fulfill the objectives of this project, a variety of laboratory tests were performed, and tests data were analyzed to find the simplest and most effective test method. Based on the findings of this study, the following conclusions can be drawn:

- The Hamburg Wheel-Tracking (HWT) device is commonly used by transportation agencies to estimate rutting and moisture resistance of asphalt mixes.
- Among all tests performed in this project, the Texas boiling test is simple, quick and easy to perform for measuring the moisture susceptibility of the asphalt binder qualitatively. The Texas boiling test is very cost-effective that requires less labor to obtain the test results.
- The atomic force microscope (AFM) tool is also effective to predict the moisture damage of the asphalt binders at the atomic scale. However, the sample preparation and calibration processes of an AFM are relatively complex and time consuming. Further, the AFM tool involves a very high initial and maintenance cost.
- The optical contact angle (OCA) tool is also capable of determining the asphalt binder's moisture resistance through the measurements of cohesion and adhesion energies of aggregate-binder systems.
- No strong correlation has been found between chemical components and moisture resistance of asphalt. However, the asphaltene content appears to be a good indicator of moisture resistance.

7. RECOMMENDATIONS

The following recommendations can be made:

1. Based on the findings of this study, it is recommended that ARDOT may include Texas Boiling test along with the current test method to evaluate the effects of moisture of the asphalt mixture. Therefore, necessary changes and relevant revision should be made in the asphalt mixture test specification section (Article 404.04 Quality Control of Asphalt Mixtures.
2. The AFM technology can provide a wide range of data in terms of qualitative and quantitative measurements of morphological as well as mechanical properties of the asphalt binders. Therefore, the AFM can be a useful tool in investigating the changes in the microstructure of the asphalt binders that occurred due to the moisture damage.
3. Additionally, SARA analysis may also be used to predict the moisture damage of the asphalt binders. The percentage of the asphaltene fraction measured from SARA analysis helps to estimate the moisture susceptibility of the binders.
4. In this project, no WMA additives were tested with PPA-modified binders. However, the effects of different WMA additives need to be tested on the performance of PPA-modified asphalt binders to ensure the performance of the base, SBS and PPA-modified binders with WMA.
5. In this study, only three LAAs (mostly ARDOT certified ones) were tested for determining the effect with the base, PPA, and SBS-modified binders. However, the effects of other LAAs will be tested with SBS and PPA-modified binders.
6. This study was limited to perform the ERSA tests for only three types of the mixtures from S1 binders, namely, SB1, S1B3, and S1B7. To observe the effects of PPA plus SBS, S1B8 binder may include under this test. In addition, this will be performed for the asphalt binders from S2 for the comparison among the test results.
7. In this project, no RAP or RAS was used to modify asphalt binders. As a result, the performance of SBS and PPA modified binders with RAP was unknown. So, the effects of PPA on RAP and RAS need to be tested.
8. For this research, other commonly used mixture tests such as Uniaxial Dynamic Modulus, Evaluation of Rutting and Stripping of Asphalt Test can also be investigated to assess their viability in measuring moisture resistance of asphalt mixes.

REFERENCES

1. Santucci, L. “Minimizing Moisture Damage in Asphalt Pavements.” Pavement Technology Update, University of California Pavement Research Center, Transfer Program, Vol. 2, No. 2, 2010, pp. 1-12.

2. Little, D.N. and Jones D.R. “Chemical and Mechanical Processes of Moisture Damage in Hot-Mix Asphalt Pavements.” Topic 2, National Seminar on Moisture Sensitivity of Asphalt Pavements, TRB Miscellaneous Report, ISBN 0-309-09450-X, Feb. 2003, pp. 37-70.

3. Zollinger, C.J. “Application of Surface Energy Measurements to Evaluate Moisture Susceptibility of Asphalt and Aggregates.” Master’s Thesis, Texas A & M University, 2005.

4. Hicks, R.G., Santucci, L. and Aschenbrener, T. “Introduction and Seminar Objectives.” Topic 1, National Seminar on Moisture Sensitivity of Asphalt Pavements, TRB Miscellaneous Report ISBN 0-309-09450-X, Feb., 2003.

5. Lu, Q. “Investigation of Conditions for Moisture Damage in Asphalt Concrete and Appropriate Laboratory Test Methods.” Proposal for doctoral thesis, Department of Civil and Environmental Engineering, University of California, Berkeley, 2003.

6. Scherocman, J.A., Proctor, J.J., and Morris, W.J. “Prevention of Moisture Damage in Asphalt Concrete Pavement.” Journal of the Canadian Technical Asphalt Association, Vol. 30, 1985, pp. 102-121.

7. Sebaaly, P.E., Elie, H., Dallas, L., Sivakulan, S., Thileepan, S., and Kamilla, V. “Evaluating the Impact of Lime on Pavement Performance.” University of Nevada, Reno, 2010.

8. Taylor, M.A., and Khosla, N.P. “Stripping of Asphalt Pavements: State of the Art.” In Transportation Research Record 911. Transportation Research Board, National Research Council, Washington, D.C., 1983, pp. 150-158.

9. Fromm, H.J. “The Mechanisms of Asphalt Stripping from Aggregate Surfaces.” Association of Asphalt Paving Technologists, Vol. 43, 1974.

10. Tarrer, A.R. and Wagh, V. “The Effect of the Physical and Chemical Characteristics of the Aggregate on Bonding.” SHRP-A-403, Strategic Highway Research Program, National Research Council, 1991.

11. Scott, J.A.N. “Adhesion and Disbonding Mechanisms of Asphalt Used in Highway Construction and Maintenance.” Proceedings, Association of Asphalt Paving Technologists, Vol. 47, 1978.

12. Terrel, R.L., and Shute, J.W. Summary Report on Water Sensitivity. SHRP-A/IR-89-003. Strategic Highway Research Program, National Research Council, 1991.

13. Lottman, R.P. (1971). “The Moisture Mechanism That Causes Asphalt Stripping in Asphalt Pavement Mixtures,” University of Idaho, Moscow, Idaho, Final Report Research Project R-47, Feb.1971.

14. Lottman, R.P. “Debonding Within Water-Saturated Asphalt Concrete Due to Cyclic Effects.” American Chemical Society, Vol. 16, No. 1, 1977.

15. Howson, J.E., Masad, E.A., Bhasin, A., Branco, V.C., Arambula, E., Lytton, R.L., and Little, D.N. Application of Surface Energy Measurements to Evaluate Moisture Susceptibility of Asphalt and Aggregates. Report No. 0-4524-S. Texas Transportation Institute, College Station, TX, 2006.

16. Caro, S., Masad, E., Bhasin, A., and Little, D. “Moisture Susceptibility of Asphalt Mixtures, Part l: Mechanisms.” International Journal of Pavement Engineering, Vol. 9, No. 2, 2008a, pp. 81-98.

17. Caro, S., Masad, E., Bhasin, A., Little, and D. “Moisture Susceptibility of Asphalt Mixtures, Part 2: Characterization and Modeling." International Journal of Pavement Engineering, Vol. 9, No. 2, 2008b, pp. 99-114.

18. Hubbard, P. “Adhesion of Asphalt to Aggregate in Presence of Water.” Proceedings, Highway Research Board, Vol. 18, Part 1, 1938.

19. Hveem, F. “Quality Tests for Asphalt: A Progress Report.” Proceedings, Association of Asphalt Paving Technologists, Vol. 15, 1943.

20. Hallberg, S. “The Adhesion of Bituminous Binders and Aggregates in the Presence of Water.” Statens Vaginstitut, Stockholm, Meddeland, Vol. 78, 1950.

21. Andersland, O.B. and Goetz, W.L. “Sonic Test for Evaluation of Stripping Resistance in Compacted Bituminous Mixtures.” Proceedings, Association of Asphalt Paving Technologists, Vol. 25, 1956.

22. Thelan, E. “Surface Energy and Adhesion Properties in Asphalt-Aggregate Systems.” Bulletin 192, Highway Research Board, National Research Council, 1958.

23. Rice, J.M. “Relationship of Aggregate Characteristics to the Effect of Water on Bituminous Paving Mixtures.” Symposium on Effect of Water on Bituminous Paving Mixtures, ASTM STP 240, 1958.

24. Goode, F.F. “Use of Immersion Compression Test in Evaluating and Designing Bituminous Paving Mixtures.” ASTM STP 252, 1959.

25. Skog, J. and Zube, E. “New Test Methods for Studying the Effect of Water Action on Bituminous Mixtures.” Proceedings, Association of Asphalt Paving Technologists, Vol. 32, 1963.

26. Mack, C. “Physical Chemistry of Bituminous Materials.” Interscience Publishers, New York Vol. 1, Chap. 2, 1964.

27. Schulze, K. and Geipel, H. “Effect of Street Salting on the Adhesion of Bituminous Binders and Gravel under the Influence of Water and Frost.” Bitumen, Teere, Asphaltene, Peche, Vol. 19, No. 12, 1968.

28. Majidzadeh, K., and Brovold, F.N. State of the Art: Effect of Water on Bitumen-Aggregate Mixtures. Special Report No. 98. Highway Research Board, Washington, D.C., 1968.

29. Schmidt, R.J. and Graf, P.E. “The Effect of Water on the Resilient Modulus of Asphalt Treated Mixes.” Proceedings, Association of Asphalt Paving Technologists, Vol. 41, 1972.

30. Jimenez, R.A. “Testing for Debonding of Asphalt from Aggregates.” Transportation Research Record No. 515. In Transportation Research Board, National Research Council, Washington, D.C., 1974.

31. Lottman, R.P. Chen, R.P., Kumar, K.S., and Wolf, L.W. “A Laboratory Test System for Prediction of Asphalt Concrete Moisture Damage.” In Transportation Research Record No. 515. Transportation Research Board, National Research Council, Washington, D.C., 1974.

32. Lottman, R.P. Predicting Moisture-Induced Damage to Asphaltic Concrete. NCHRP Report No. 192. Transportation Research Board, National Research Council, Washington, D.C., 1978.

33. Lottman, R.P. Predicting Moisture-Induced Damage to Asphaltic Concrete: Field Evaluation. NCHRP Report No. 246. Transportation Research Board, National Research Council, Washington, D.C. 1982.

34. Tunnicliff, D.G. and Root, R.E. “Antistripping Additives in Asphalt Concrete: State-of-the-Art.” Proceedings, Association of Asphalt Paving Technologists, Vol. 51, 1982.

35. Tunnicliff, D.G. and Root, R.E. Use of Antistripping Additives in Asphaltic Concrete Mixtures: Laboratory Phase. NCHRP Report No. 274. Transportation Research Board, National Research Council, 1984.

36. Kennedy, T.W., Roberts, F.L., and Lee, K.W. “Evaluation of Moisture Susceptibility of Asphalt Mixtures Using the Freeze-Thaw Pedestal Test.” Proceedings, Association of Asphalt Paving Technologists, Vol. 51, 1982.

37. Kennedy, T.W., Roberts, F.L., and Lee, K.W. “Evaluating Moisture Susceptibility of Asphalt Mixtures Using the Texas Boiling Test.” In Transportation Research Record 968. Transportation Research Board, National Research Council, Washington, D.C., 1984.

38. Saville, V. and Axon, E. “Adhesion of Asphaltic Binders to Mineral Aggregates.” Proceedings of the Technical Sessions, Association of Asphalt Paving Technologists, Dec.1937, pp. 87-101.

39. Plancher, H., Miyake, G., Venable, R.L., and Petersen, J.C. “A Simple Laboratory Test to Indicate the Susceptibility of Asphalt-Aggregate Mixtures to Moisture Damage during Repeated Freeze-Thaw Cycling.” Proceedings of the Canadian Technical Asphalt Association, Nov., Vol. 25, 1980.

40. Ensley, E.K., Petersen, J.C., and Robertson, R.E. “Asphalt-Aggregate Bonding Energy Measurements by Microcalorimetric Methods.” Thermochimica Acta, Vol. 77, 1984.

Graf, P.E. “Factors Affecting Moisture Susceptibility of Asphalt Concrete Mixes.” Proceedings, Association of Asphalt Paving Technologists, Vol. 55, 1986.

41. Kiggundu, B.M., and Roberts, F.L. Stripping in HMA Mixtures: State-of-the-Art and Critical Review of Test Methods. NCAT Report No. 88-2, National Center for Asphalt Technology (NCAT), Auburn, AL, 1988.

42. Stuart, K. D. Moisture Damage in Asphalt Mixture-A State of the Art Report. Report No. FHWA-RD-90-019, Federal Highway Administration, Mclean, VA, Aug. 1990, pp 125.

43. Hicks, R.G. "NCHRP Synthesis of Highway Practice 175: Moisture Damage in Asphalt Concrete." In Transportation Research Board, National Research Council, Washington, D.C., 1991.

44. Al-Swailmi, S. and Terrel, R.L. "Evaluation of Water Damage of Asphalt Concrete Mixtures Using the Environmental Conditioning System (ECS)." Journal of the Association of Asphalt Paving Technologists, Vol. 61, 1992.

45. Al-Swailmi, S. and Terrel, R.L. Water Sensitivity of Asphalt-Aggregate Mixtures: Test Selection. SHRP-A-403. Strategic Highway Research Program, National Research Council, 1994.

46. Curtis, C.W., Ensley, K., and Epps, J.A. Fundamental Properties of Asphalt-Aggregate Interactions Including Adhesion and Absorption. SHRP-A-341. Strategic Highway Research Program, National Research Council, 1993.

47. Aschenbrener, T. and Currier, G. "Influence of Testing Variables on the Results from the Hamburg Wheel-Tracking Device." Report No. CDOT-DTD-R-93-22, Colorado Department of Transportation (CDOT), Denver, CO, 1993.

48. Aschenbrener, T. "Evaluation of Hamburg Wheel Tracking Device to Predict Moisture Damage in Hot Mix Asphalt." In Transportation Research Record 1492. Transportation Research Board, National Research Council, Washington, D.C., 1995.

49. Rand, D.A. "Field Observations and Validation, Designed Tests and Forensic Analysis." Moisture Damage Symposium, 39th Annual Petersen Asphalt Research Conference, 2002.

50. Aschenbrener, T., McGennis, R.B., and Terrel, R.L. "Comparison of Several Moisture Susceptibility Tests to Pavements of Known Field Performance." Journal of the Association of Asphalt Paving Technologists, Vol. 64, 1995, pp. 163-208.

51. Solaimanian, M., Harvey, J., Tahmoressi, M., and Tandon, V. "Test Methods to Predict Moisture Sensitivity of Hot-Mix Asphalt Pavements." Topic 3, National Seminar on Moisture Sensitivity of Asphalt Pavements, Transportation Research Board, National Research Council, Washington, D.C., 2003, pp 77-110.

52. Lu, Q., Harvey, J.T., and Monismith, C.L. "Investigation of Conditions for Moisture Damage in Asphalt Concrete and Appropriate Laboratory Test Methods: Summary Version." Draft Research Report: UCPRC-SR-2005-01, University of California Pavement Research Center, Aug. 2007.

53. California Department of Transportation, California Test Methods, Materials, Engineering and Testing Services, http://www.dot.ca.gov/hq/esc/ctms. Accessed October 31, 2017.

54. International Slurry Surfacing Association. “Design Technical Bulletin 145.” 2007.

55. Kandhal, P.S., Lynn, C.Y., and Parker, F. “Tests for plastic fines in aggregates related to stripping in asphalt paving mixtures.” NCAT Report No. 98-03, National Center for Asphalt Technology, Auburn University, Alabama, Mar. 1998.

56. Scholz, T.V., Terrel, R.L., Al-Joaib, A., and Bea, J. Water Sensitivity: Binder Validation. SHRP-A-402. Strategic Highway Research Program, National Research Council, Washington, D.C., 1994.

57. American Association of State Highway and Transportation Officials (AASHTO). “Standard Specifications for Transportation Materials and Methods of Sampling and Testing.” 1990.

58. Road Research Laboratory, Standard Method TMHI, 1986. http://www.scribd.com/doc/35705372/tmh1. Accessed October 31, 2017.

59. Ford, M.C. Jr., Manke, P.G., and O’Bannon, C.E. “Quantitative Evaluation of Stripping by the Surface Reaction Test.” In Transportation Research Record 515. Transportation Research Board, National Research Council, Washington, D.C., 1974.

60. Youtcheff, J. and Aurilio, V. “Pneumatic Pull-Off Test.” Proceedings, Canadian Technical Asphalt Association, 1997.

61. Kim, Y.R., Little, D., and Lytton, R. “Effect of moisture damage on material properties and fatigue resistance of asphalt mixtures.” In Transportation Research Record 1891. Transportation Research Board, National Research Council, Washington, D.C., 2004. pp. 48-54.

62. Bhasin, A., and Little, D.N. “Characterizing surface properties of aggregates used in hot mix asphalt.” Technical Report No. ICAR-505-2, Texas Transportation Institute, College Station, TX, 2006.

63. Howson, J.E., Masad, E.A., Bhasin, A., Branco, V.C., Arambula, E., Lytton, R.L., and Little, D. System for the Evaluation of Moisture Damage Using Fundamental Material Properties. Report No. FHWA/TX-0710-4524-1. Texas Transportation Institute, College Station, TX, 2007.

64. Xiao, F., Jordan, J., and Amirkhanian, S. N. “Laboratory Investigation of Moisture Damage in Warm-Mix Asphalt Containing Moist Aggregate.” In Transportation Research Record 2126. Transportation Research Board, National Research Council, Washington, D.C., 2009, pp. 115-124.

65. Wasiuddin, N., Saltibus, N., and Mohammad, L. “Novel Moisture-Conditioning Method for Adhesive Failure of Hot- and Warm-Mix Asphalt Binders.” In Transportation Research Record 2208. Transportation Research Board, National Research Council, Washington, D.C., 2011, pp. 108-117.

66. Elphingstone, G.M. “Adhesion and cohesion in asphalt-aggregate systems.” Ph.D. Dissertation, Texas A & M University, College Station, TX, 1997.

67. Cheng, D. “Surface free energy of asphalt-aggregate systems and performance analysis of asphalt concrete based on surface free energy.” Ph.D. Dissertation, Texas A & M University, College Station, TX, 2002.

68. Cheng, D., Little, D.N., Lytton, R.L., and Holtse, J.C. “Use of Surface Free Energy Properties of Asphalt-Aggregate System to Predict Damage Potential.” Presentation, Annual Meeting of the Association of Asphalt Paving Technologists, Mar. 2002.

69. Thelen, E. “Surface Energy and Adhesion Properties in Asphalt-Aggregate Systems.” Bulletin 192, HRB, National Research Council, 1958, pp. 63-74.

70. Koc, M, and Rifat Bulut, R. “Assessment of a Sessile Drop Device and a New Testing Approach Measuring Contact Angles on Aggregates and Asphalt Binders.” Journal of Materials in Civil Engineering, Vol. 26, Issue 3, 2014, pp 391-398.

71. Isacsson, W., and Jorgensen, T. “Laboratory Methods for Determination of the Water Susceptibility of Bituminous Pavements.” VIT report, Swedish Road, and Traffic Research Institute, No. 324A, 1987.

72. Maupin, G.W. “Detection of Antistripping Additives with Quick Bottle Test.” Final Report, Virginia Highway, and Transportation Research Council, Charlottesville, Oct. 1980.

73. Stuart, K.D. Evaluation of Procedures Used to Predict Moisture Damage in Asphalt Mixtures. FHWA/RD-86/091. Draft Report, 1986.

74. Solaimanian, M., and Kennedy, T.W. The precision of the Moisture Susceptibility Test Method TEX-531-C: Research Report. Report No. FHWA/TX-03/4909-1. Center for Transportation Research, Austin, TX, 2002.

75. Epps, J.A., Sebally, P.E., Penaranda, J., McCain, M.B., and Hand, A.J. “Compactability of Test for Moisture-Induced Damage with Superpave Volumetric Mix Design.” NCHRP Report No. 444. In Transportation Research Board, National Research Council, Washington, D.C., 2000.

76. Texas Department of Transportation. “Test Procedure Tex-242-F,” www.txdot.gov/business/contractors_consultants/test_procedures/default.htm. Accessed October 31, 2017.

77. Epps, M.A., Rand, D., Weitzel, D., Tedford, D., Sebaaly, P.E, Lane, L., Bressette, T., and Maupin, G.W. “Field Experiences" Moisture Sensitivity of Asphalt Pavements: A National Seminar.” San Diego, California, Proceedings, Feb. 2003, pp. 229-260.

78. Izzo, R.P., and Tahmoressi, M. “Use of the Hamburg Wheel-Tracking Device for Evaluating Moisture Susceptibility of Hot-Mix Asphalt.” In Transportation Research Record 1681, Transportation Research Board, National Research Council, Washington, D.C., 1999. pp. 76-86.

79. Solaimanian, M., Bonaquist, R.F., and Tandon, V. “Improved Conditioning and Testing for HMA Moisture Susceptibility.” NCHRP Report No. 589. In Transportation Research Board, National Research Council, Washington, D.C., 2007.

80. Alam, M.M., Vemuri, N., Tandon, V., Nazarian, S., and Picornell, M. “A Test Method for Identifying Moisture Susceptible Asphalt Concrete Mixes.” Report No. TX-98-1455-2F, Center for Highway Materials Research, El Paso, TX, 1998, pp. 92.

81. Kandhal P.S., Cooley, L.A. “Accelerated Laboratory Rutting Tests: Evaluation of the Asphalt Pavement Analyzer.” National Cooperative Highway Research Program, NCHRP Report No. 508. In Transportation Research Board, National Research Council, Washington, D.C., 2003.

82. Bausano, J., Kvasnak, A., and Williams, R.C. “Development of Simple Performance Tests Using Laboratory Test Procedures to illustrate the Effects of Moisture Damage on Hot Mix Asphalt.” Report No. RC-1521, Michigan Technological University, Houghton, MI, 2006, pp. 366.

83. Aschenbrener, T. “Results of Survey on Moisture Damage of Hot-Mix Asphalt Pavements.” Appendix, Topic 1, National Seminar on Moisture Sensitivity of Asphalt Pavements, Transportation Research Board (TRB) Miscellaneous Report ISBN 0-309-09450-X, Feb. 2003.

84. Caro, S. and Riveria, C. “Moisture damage RNS: facing new challenges.” AFK40 Annual Meeting, Surface Requirements of Asphalt Mixtures, Transportation Research Board Los Andes University, Colombia, Jan. 2017.

85. Hung, A.M., and Fini, E.H. “AFM study of asphalt binder ‘‘bee” structures: origin, mechanical fracture, topological evolution, and experimental artifacts.” Journal of Royal Society of Chemistry Advances, Vol. 5, No. 117, 2015, pp. 96972-96982.

86. Loeber, L., Sutton, O., Morel, J., Valleton, J.-M., and Muller, G. “New direct observations of asphalts and asphalt binders by scanning electron microscopy and atomic force microscopy.” Journal of Microscopy, Vol. 182, NO. 1, 1996, pp. 32-39.

87. Masson, J.F., Leblond, V., and Margeson, J. “Bitumen morphologies by phase-detection atomic force microscopy.” Journal of Microscopy, Vol. 221, 2006, pp. 17-29.

88. Dourado, E.R., Simao, R.A., and Leite, L.F.M. “Mechanical properties of asphalt binders evaluated by atomic force microscopy.” Journal of Microscopy, Vol. 245, No. 2, 2012, pp. 119-128.

89. Fischer, H., Stadler, H., and Erina, N. “Quantitative temperature-depending mapping of mechanical properties of bitumen at the nanoscale using the AFM operated with PeakForce TappingTM mode.” Journal of Microscopy, Vol. 250, No. 3, 2013, pp. 210-217.

90. Nahar, S.N., Schmets, A.J.M., Schitter, G., and Scarpas, A. “Quantitative nanomechanical property mapping of bitumen micro-phases by peak-force atomic force microscopy.” 12th ISAP Conference on 30 Asphalt Pavements, Raleigh, N.C., 2014.

91. Hossain, Z., Rashid, F., Mahmud, I., and Rahaman, M. “Morphological and Nanomechanical Characterization of Industrial and Agricultural Waste-Modified Asphalt Binders.” International Journal of Geomechanics, Vol. 17, No. 3, 2016.

92. Rashid, A.F., and Hossain, Z. “Morphological and nanomechanical analyses of ground tire rubber-modified asphalts.” Innovative Infrastructure Solutions, Vol. 1, No. 1, 2016, pp. 36.

93. Rashid, F., Hossain, Z., and Bhasin, A. “Nanomechanistic properties of reclaimed asphalt pavement modified asphalt binders using an atomic force microscope.” International Journal of Pavement Engineering, 2017, pp. 1-9.

94. Yao, Z., Zhu, H., Gong, M., Yang, J., Xu, G., and Zhong, Y. “Characterization of asphalt materials’ moisture susceptibility using multiple methods.” Journal of Construction and Building Materials, Vol. 155, No. 30, Nov. 2017, pp. 286-295.

95. Tarefder, R.A. and Arifuzzaman, M. “A study of moisture damage in plastomeric polymer modified asphalt binder using functionalized AFM tips.” Journal of Systemics, Cybernetics, and Informatics, Vol. 9, No. 5, 2011, pp. 1-12.

96. Hossain, Z., Braham, A., and Baumgardner, G. (2017). “Effects of Poluphosphoric Acid on Performance of Asphalts,” Final Report of TRC 1501 project, submitted to the Arkansas Department of Transportation, Little Rock, Arkansas, 2017.

97. Van Oss, C.J., Chaudhury, M.K., and Good, R.J. “Interfacial Lifshitz-van der Waals and Polar Interactions in Macroscopic Systems.” Chemical Reviews, Vol. 88, No. 6, 1998, pp. 941-972.

98. Nasrazadani, S. “Review of Applications of Fourier Transform Infrared Spectrophotometry (FTIR) in Characterization of Construction Materials.” Geo-Frontiers Congress, Dallas, Texas, United State, 2011.

99. Baumgardner, G. L., Masson, J-F., Hardee, J. R., Menapace, A. M., and Williams, A. G. “Polyphosphoric Acid Modified Asphalt: Proposed Mechanisms.” Proceedings of Association of Asphalt Paving Technologists, Vol. 74, 2005, pp. 283-305.

APPENDIX

APPENDIX-A: ROTATIONAL VISCOSITY (RV) TEST DATA

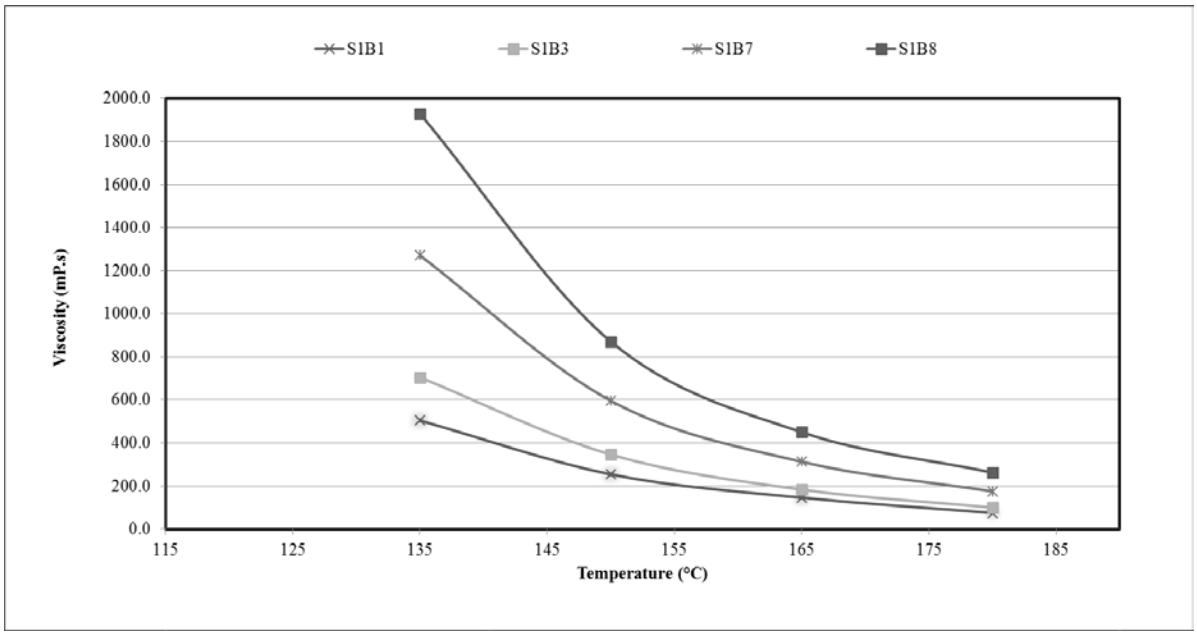

Figure 71. Viscosity (mP.s) vs. temperature (°C) curves of asphalt binders from S1.

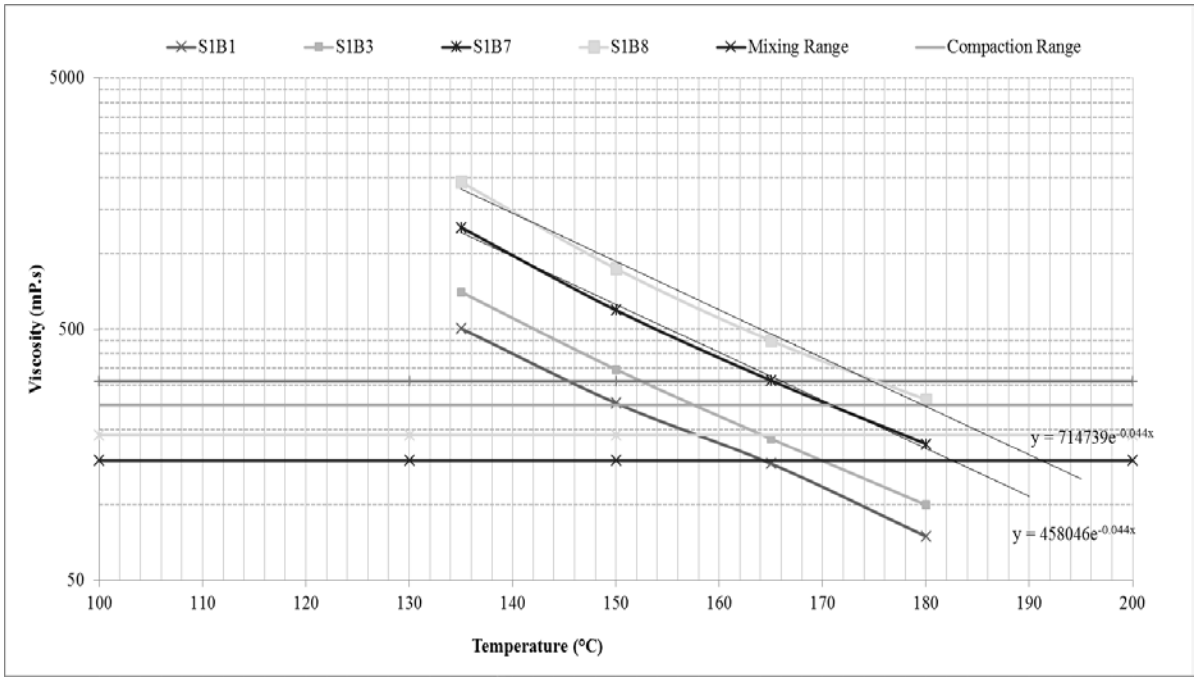

Figure 72. Determination of mixing and compaction temperatures of asphalt binders from S1.

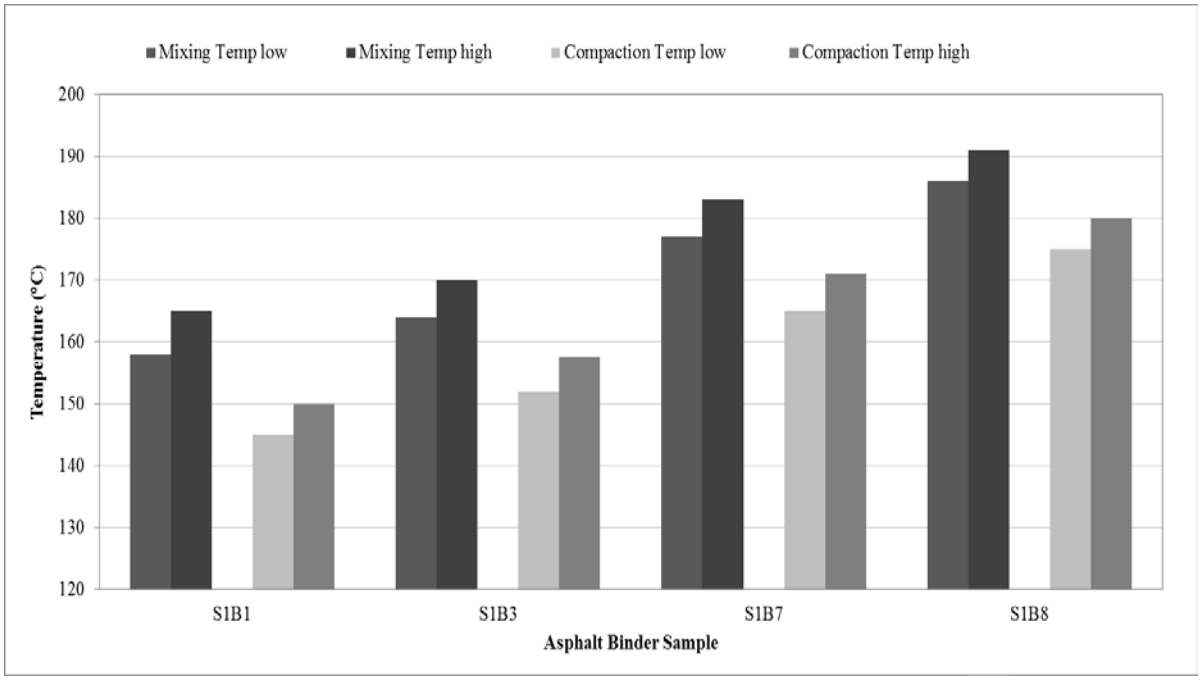

Figure 73. Mixing and compaction temperatures of asphalt binders from S1.

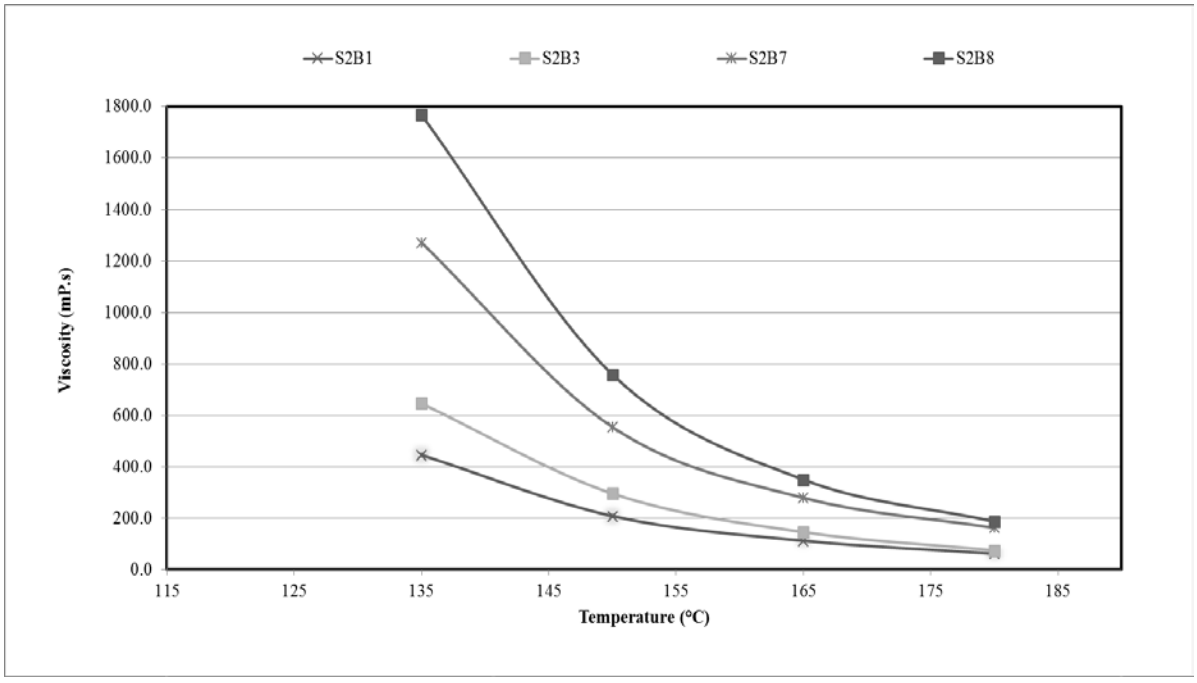

Figure 74. Viscosity (mP.s) vs. temperature (°C) curves of asphalt binders from S2.

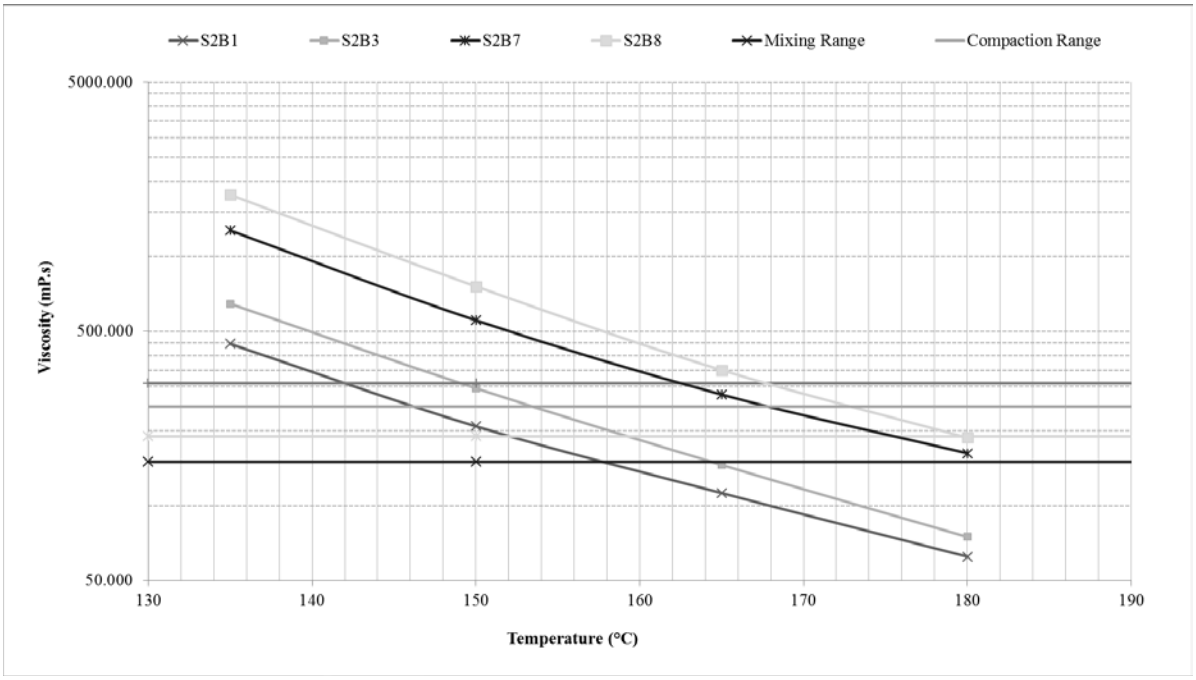

Figure 75. Determination of mixing and compaction temperatures of asphalt binders from S2.

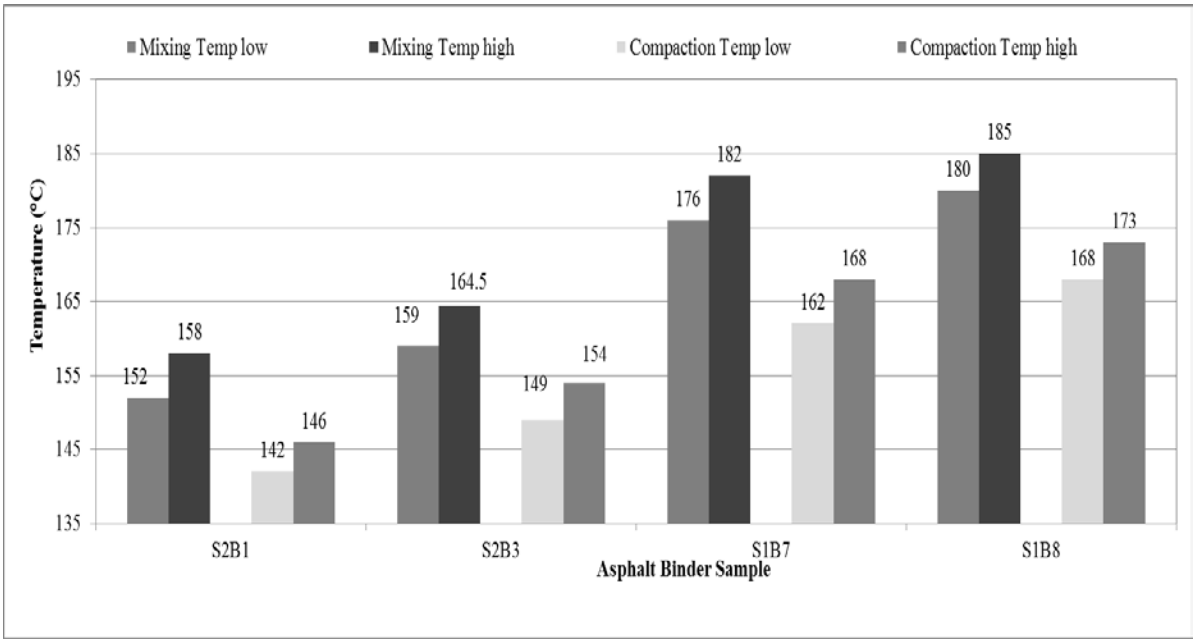

Figure 76. Mixing and compaction temperatures of asphalt binders from S2.

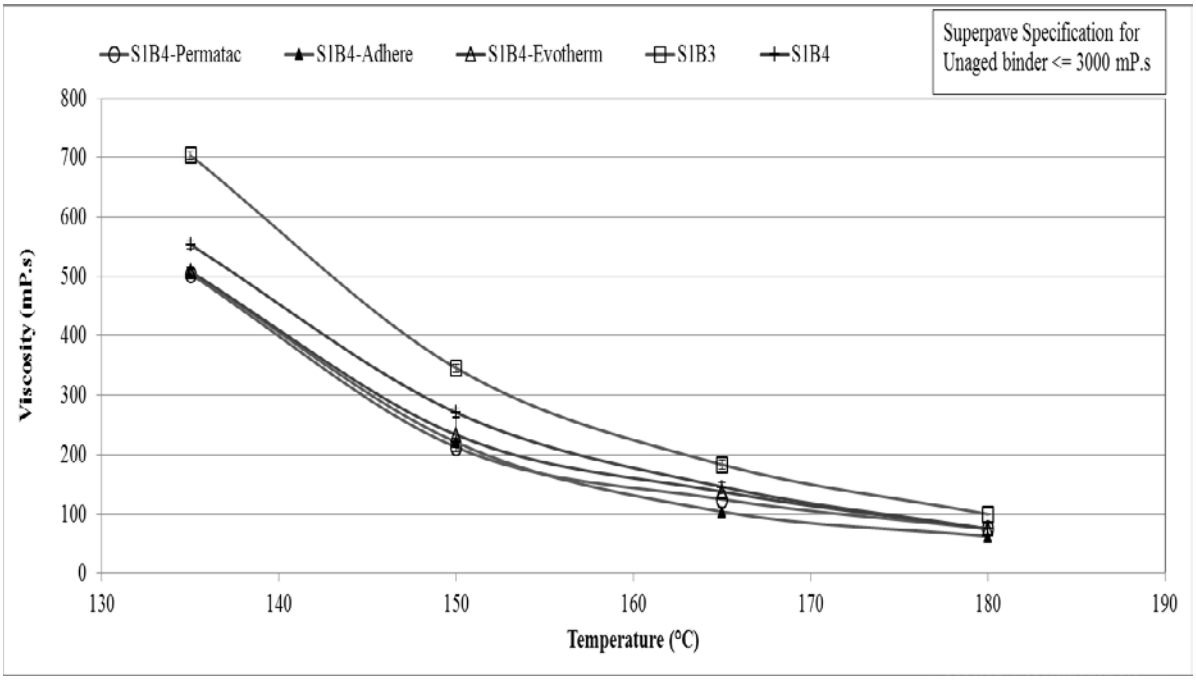

Figure 77. Viscosity (mP.s) vs. temperature (°C) curves of LAA-modified asphalt binders from S1.

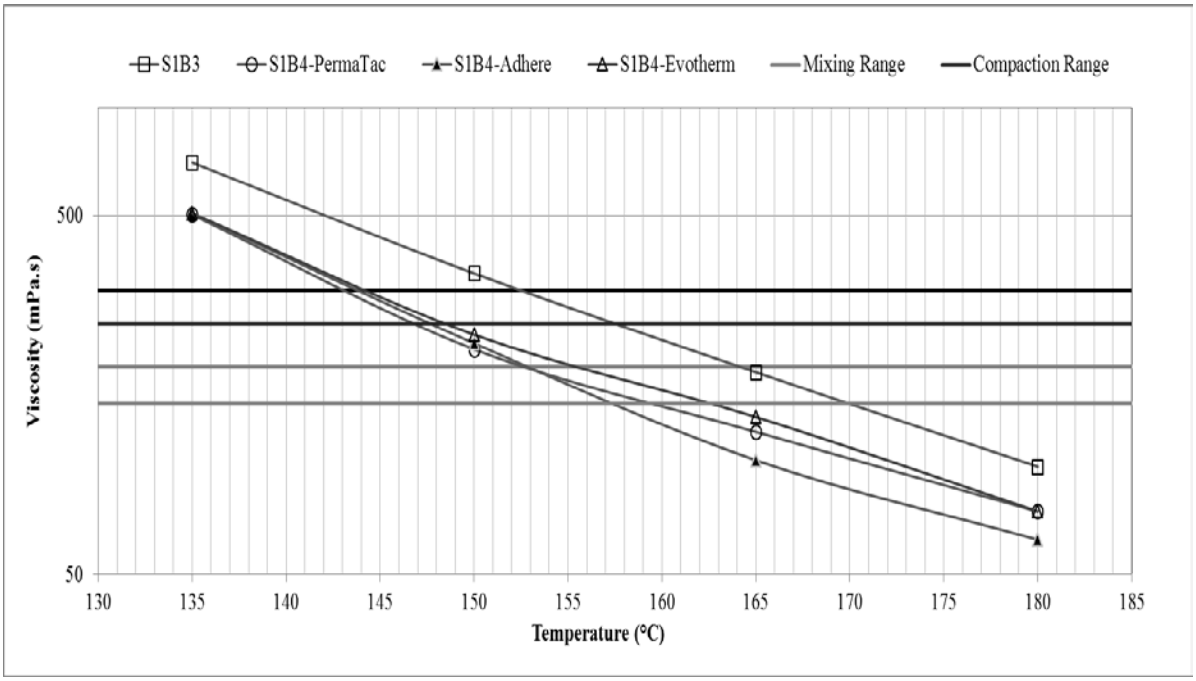

Figure 78. Determination of mixing and compaction temperatures of LAA-modified asphalt binders from S1.

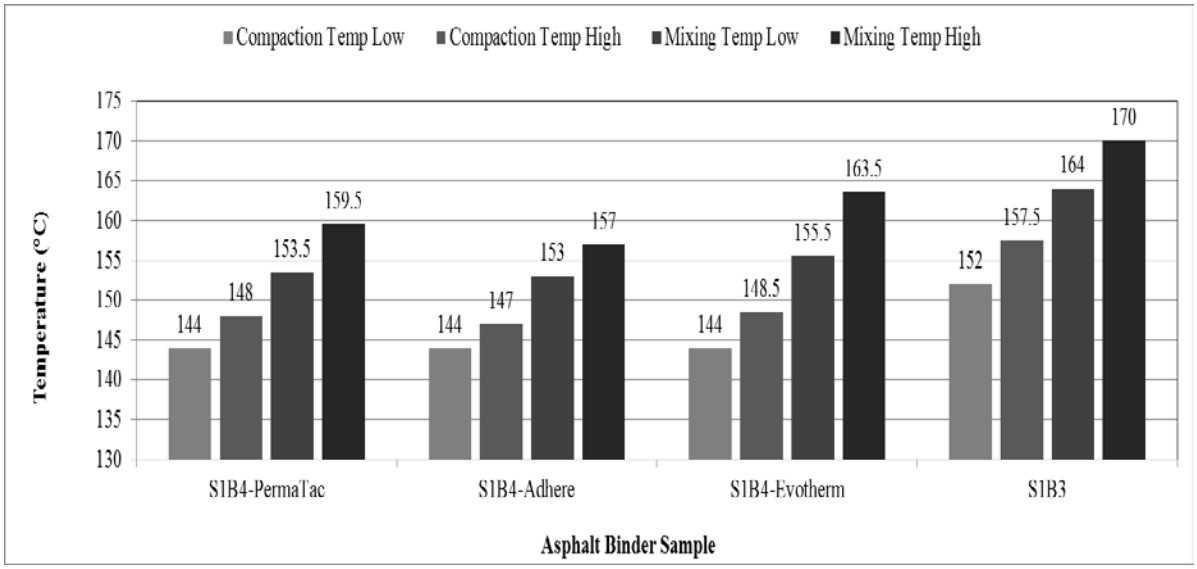

Figure 79. Mixing and compaction temperatures of LAA-modified asphalt binders from S1.

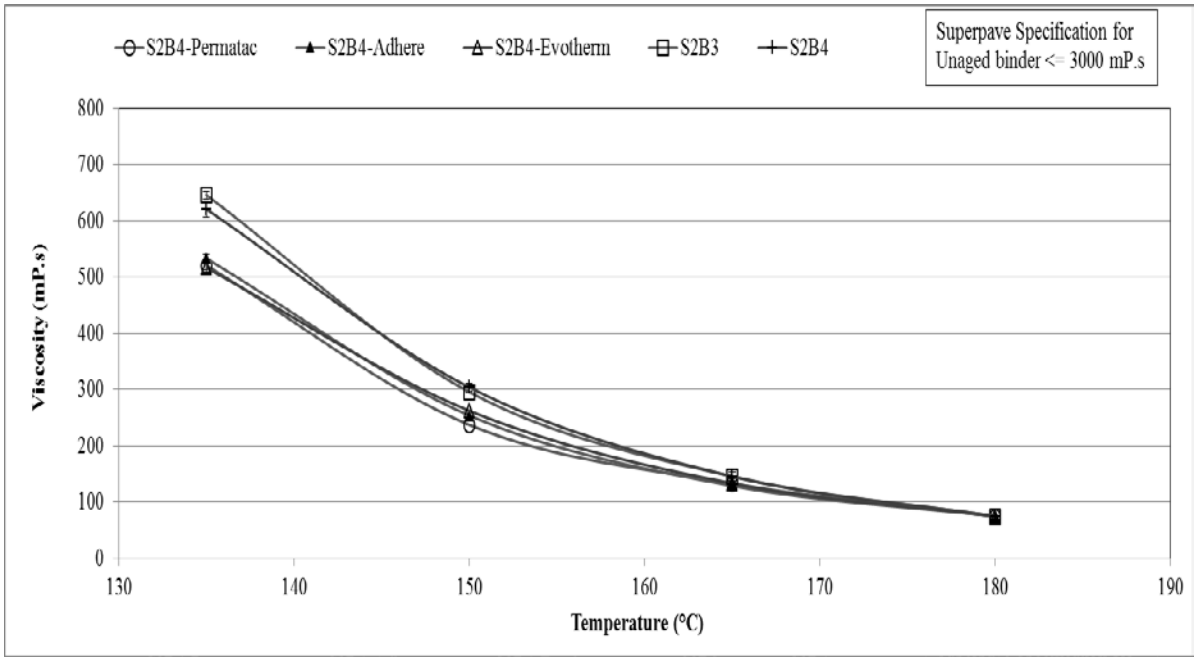

Figure 80. Viscosity (mP.s) vs. temperature (°C) curves of LAA-modified asphalt binders from S2.

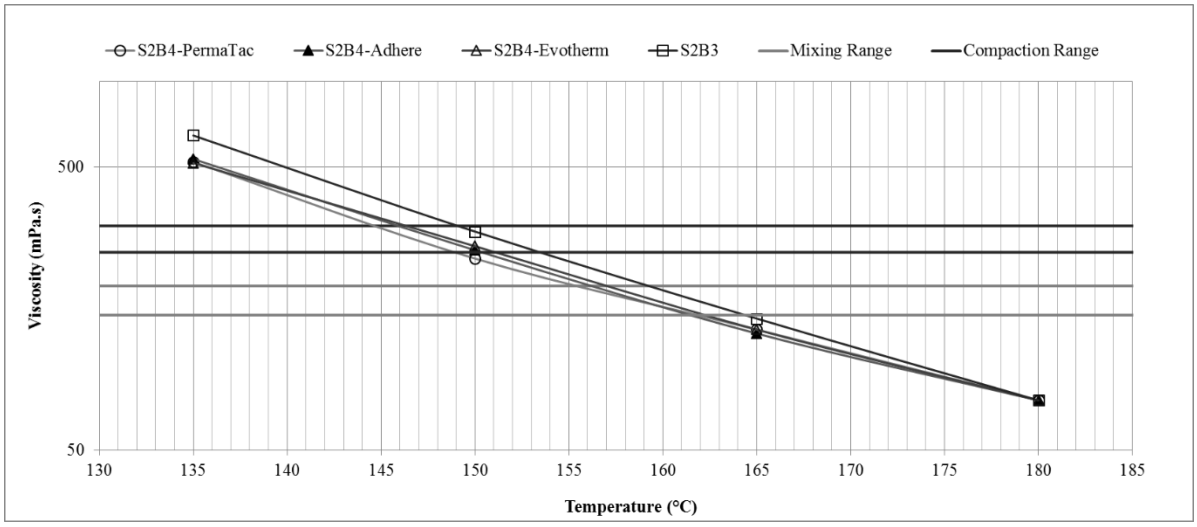

Figure 81. Determination of mixing and compaction temperatures of LAA-modified asphalt binders from S2.

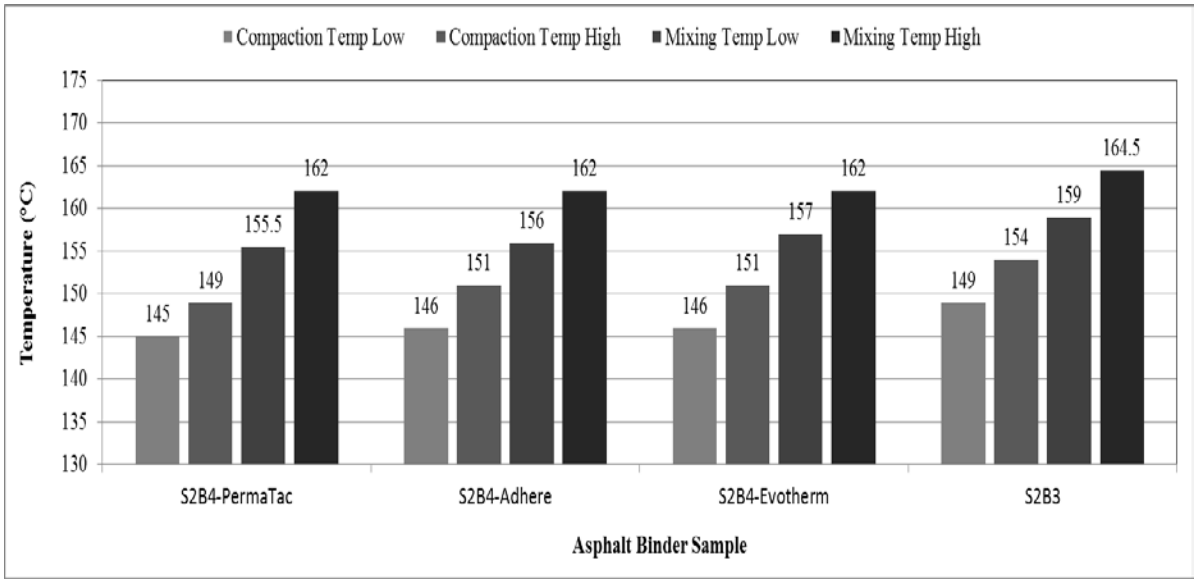

Figure 82. Mixing and compaction temperatures of LAA-modified asphalt binders from S2.

APPENDIX-B: DYNAMIC SHEAR RHEOMETER (DSR) TEST DATA

Table 33. Summary of DSR test results of unaged asphalt binders from S1.

Temperature (°C)	G*/sin δ (kPa), S1B1	G*/sin δ (kPa), S1B1	G*/sin δ (kPa), S1B3	G*/sin δ (kPa), S1B3	G*/sin δ (kPa), S1B7	G*/sin δ (kPa), S1B7	G*/sin δ (kPa), S1B8	G*/sin δ (kPa), S1B8
64	1.59	0.0436	-	-	-	-	-	-
67	1.11	0.03605	1.717	0.0208	-	-	-	-
70	0.778	0.0292	1.213	0.0152	-	-	-	-
73	-	-	0.865	0.0098	1.577	0.051	-	-
76	-	-	-	-	1.177	0.045	-	-
79	-	-	-	-	0.887	0.031	-	-
82	-	-	-	-	-	-	1.337	0.03
85	-	-	-	-	-	-	1.04	0.03
88	-	-	-	-	-	-	0.808	0.02

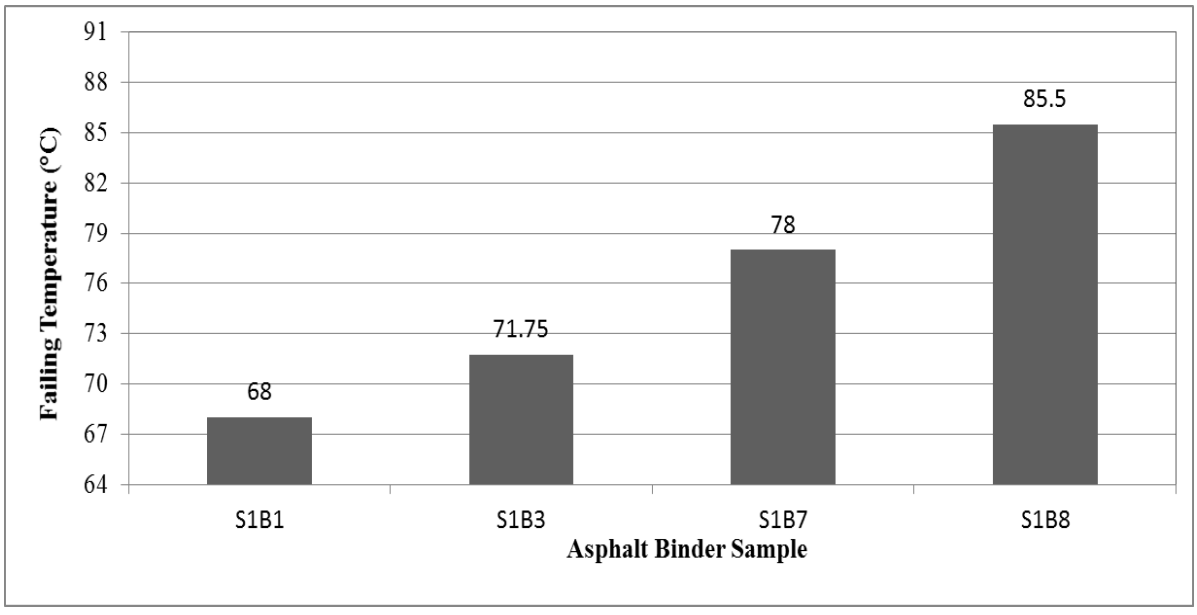

Figure 83. Failure temperature (°C) from DSR test of unaged asphalt binders from S1.

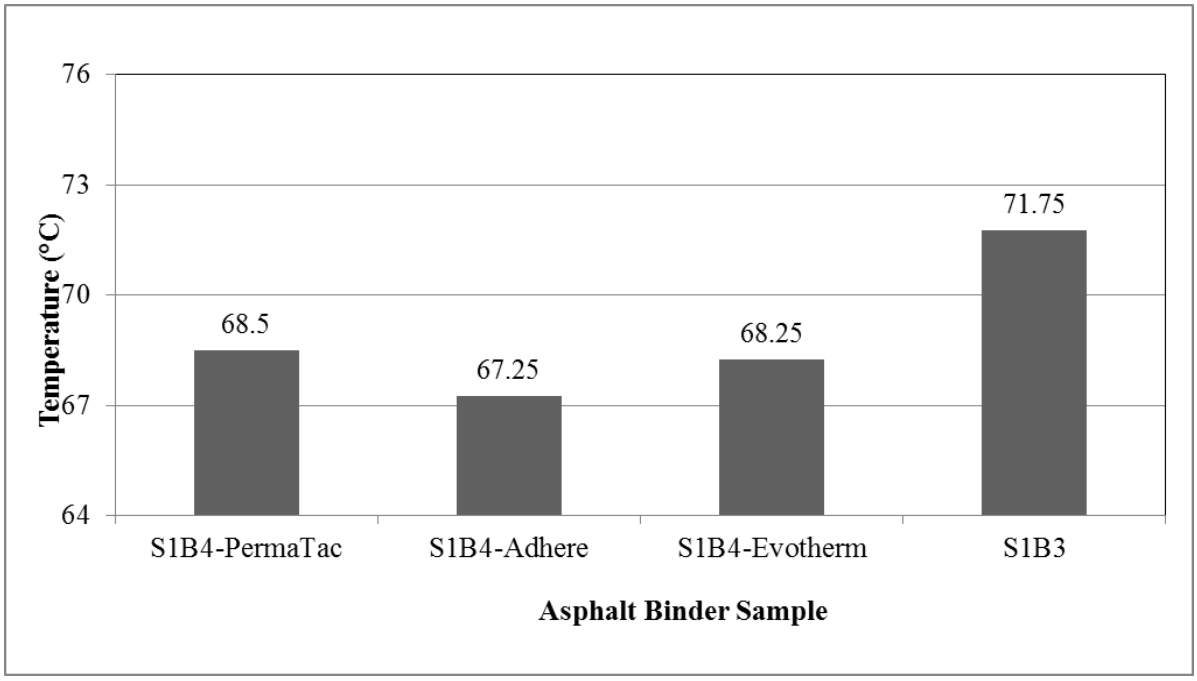

Figure 84. Failure temperature (°C) from DSR test of unaged LAA-modified asphalt binders from S1.

Table 34. Summary of DSR test results of unaged asphalt binders from S2.

Temperature (°C)	G*/sin δ (kPa), S2B1	G*/sinδ (kPa), S2B1	G*/sin δ (kPa), S2B3	G*/sin δ (kPa), S2B3	G*/sin δ (kPa), S2B3	G*/sin δ (kPa), S2B3	G*/sin δ (kPa), S2B8	G*/sin δ (kPa), S2B8
61	2.39	0.07	-	-	-	-	-	-
64	1.623	0.01	-	-	-	-	-	-
67	1.113	0.04	1.877	0.05	-	-	-	-
70	-	-	1.323	0.04	1.773	0.08	-	-
73	-	-	0.939	0.02	1.313	0.06	-	-
76	-	-	-	-	0.989	0.05	1.547	0.09
79	-	-	-	-	-	-	1.203	0.07
82	-	-	-	-	-	-	0.959	0.04

Table 35. Summary of DSR test results of unaged LAA-modified asphalt binders from S1.

Temperature (°C)	G*/sinδ (kPa), S1B4-PermaTac	G*/sinδ (kPa), S1B4-PermaTac	G*/sinδ (kPa), S1B4-Adhere	G*/sinδ (kPa), S1B4-Adhere	G*/sinδ (kPa), S1B4-Evotherm	G*/sinδ (kPa), S1B4-Evotherm	G*/sinδ (kPa), S1B3	G*/sinδ (kPa), S1B3
67	1.17	0.0006	1.015	0.005	1.143	0.0029	1.717	0.0208
70	0.831	0.0006	0.719	0.0071	0.808	0.004	1.213	0.0152
73	0.596	0.0064	0.517	0.0058	0.57	0.0015	0.865	0.0098

Table 36. Summary of DSR test results of unaged LAA-modified asphalt binders from S2.

Temperature (°C)	G*/sinδ (kPa), S2B4-PermaTac	G*/sinδ (kPa), S2B4-PermaTac	G*/sinδ (kPa), S2B4-Adhere	G*/sinδ (kPa), S2B4-Adhere	G*/sinδ (kPa), S2B4-Evotherm	G*/sinδ (kPa), S2B4-Evotherm	G*/sinδ (kPa), S2B3	G*/sinδ (kPa), S2B3
67	1.053	0.0058	0.982	0.033	1.117	0.0058	1.877	0.05
70	0.736	0.0006	0.704	0.025	0.78	0.0006	1.323	0.04
73	0.525	0.0006	0.525	0.0236	0.553	0.0058	0.939	0.02

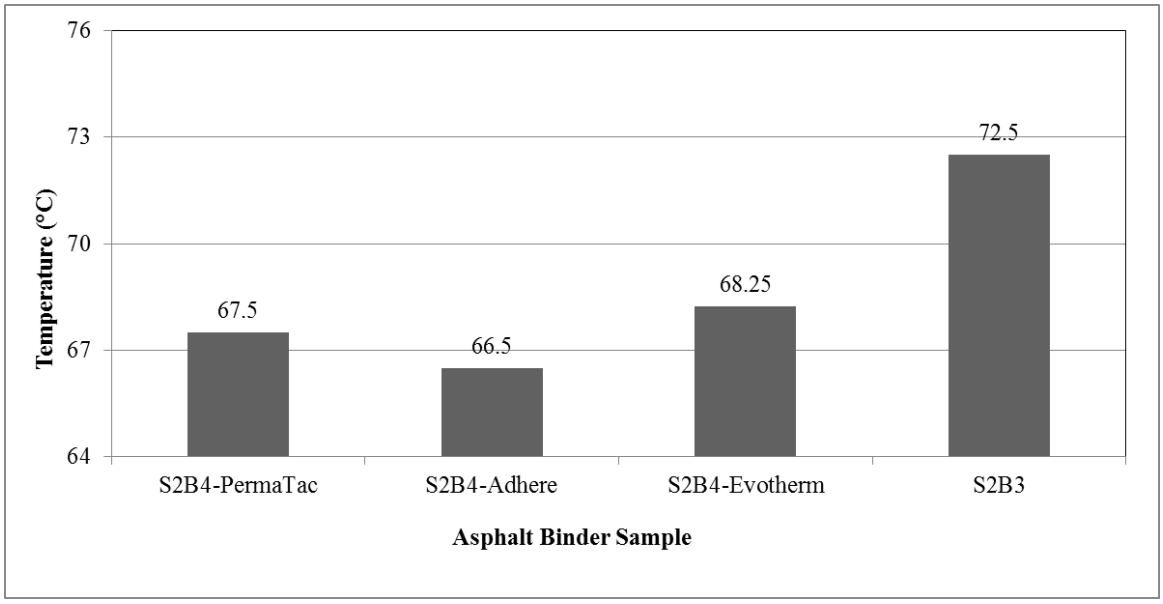

Figure 85. Failure temperature (°C) from DSR test of unaged LAA-modified asphalt binders from S2.

Table 37. Summary of DSR test results of RTFO-aged asphalt binders from S1.

Temperature (°C)	G*/sin δ (kPa), S1B1	G*/sinδ (kPa), S1B1	G*/sin δ (kPa), S1B3	G*/sin δ (kPa), S1B3	G*/sin δ (kPa), S1B7	G*/sin δ (kPa), S1B7	G*/sin δ (kPa), S1B8	G*/sin δ (kPa), S1B8
64	4.517	0.124	-	-	-	-	-	-
67	3.07	0.078	3.867	0.0450	-	-	-	-
70	2.113	0.049	2.697	0.0416	-	-	-	-
73	-	-	1.910	0.02	-	-	7.06	0.044
76	-	-	-	-	3.417	0.167	5.49	0.035
79	-	-	-	-	2.493	0.101	4.267	0.021
82	-	-	-	-	1.823	0.058	-	-

Table 38. Summary of DSR test results of RTFO-aged LAA-modified asphalt binders from S1.

Temperature (°C)	G*/sinδ (kPa), S1B4-PermaTac	G*/sinδ (kPa), S1B4-PermaTac	G*/sinδ (kPa), S1B4-Adhere	G*/sinδ (kPa), S1B4-Adhere	G*/sinδ (kPa), S1B4-Evotherm	G*/sinδ (kPa), S1B4-Evotherm	G*/sinδ (kPa), S1B3	G*/sinδ (kPa), S1B3
67	2.943	0.0681	2.583	0.0451	2.487	0.0306	-	-
70	2.077	0.0681	1.813	0.0503	1.703	0.0153	3.883	0.021
73	1.46	0.0656	1.257	0.0252	1.187	0.0115	2.777	0.015
76	-	-	-	-	-	-	2.0	0.02

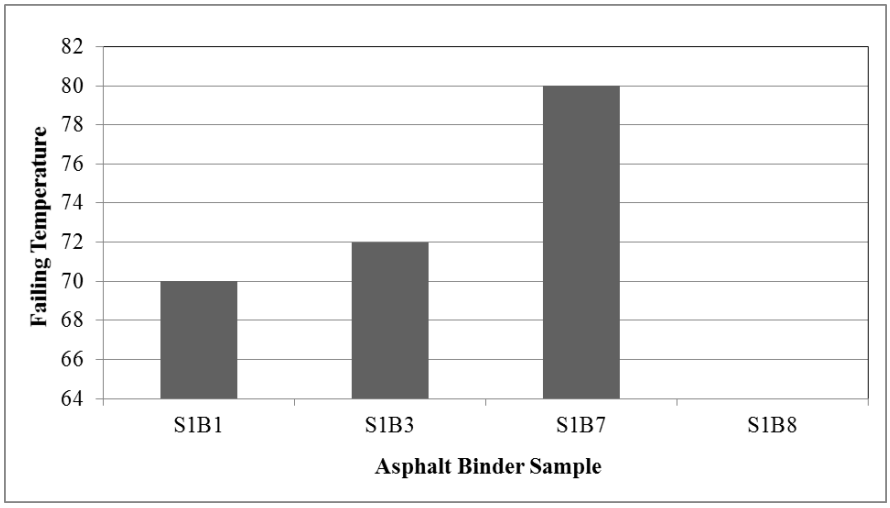

Figure 86. Failure temperature (°C) from DSR test of unaged LAA-modified asphalt binders from S2.

Table 39. Summary of DSR Test Results of RTFO-aged asphalt binders from S2.

Temperature (°C)	G*/sin δ (kPa), S2B1	G*/sinδ (kPa), S2B1	G*/sin δ (kPa), S2B3	G*/sin δ (kPa), S2B3	G*/sin δ (kPa), S2B3	G*/sin δ (kPa), S2B3	G*/sin δ (kPa), S2B8	G*/sin δ (kPa), S2B8
64	3.883	0.1	-	-	-	-	-	-
67	2.59	0.06	-	-	-	-	-	-
70	1.773	0.04	3.427	0.05	3.327	0.04	-	-
73	-	-	2.467	0.03	2.457	0.03	-	-
76	-	-	1.773	0.03	1.81	0.03	3.377	0.02
79	-	-	-	-	-	-	2.643	0.03
82	-	-	-	-	-	-	2.07	0.03

Table 40. Summary of DSR test results of RTFO-aged LAA-modified asphalt binders from S2.

Temperature (°C)	G*/sinδ (kPa), S2B4-PermaTac	G*/sinδ (kPa), S2B4-PermaTac	G*/sinδ (kPa), S2B4-Adhere	G*/sinδ (kPa), S2B4-Adhere	G*/sinδ (kPa), S2B4-Evotherm	G*/sinδ (kPa), S2B4-Evotherm	G*/sinδ (kPa), S2B3	G*/sinδ (kPa), S2B3
67	2.797	0.0321	2.360	0.02	2.087	0.0306	-	-
70	1.953	0.0231	1.657	0.0252	1.443	0.0321	3.427	0.05
73	1.363	0.0153	1.180	0.04	1.038	0.0486	2.467	0.03
76	-	-	-	-	-	-	1.773	0.03

Table 41. Summary of DSR test results of PAV-aged asphalt binders from S1.

Temperature (°C)	G*/sinδ (kPa), S1B1	G*/sinδ (kPa), S1B1	G*/sinδ (kPa), S1B3	G*/sinδ (kPa), S1B3	G*/sinδ (kPa), S1B7	G*/sinδ (kPa), S1B7	G*/sinδ (kPa), S1B8	G*/sinδ (kPa), S1B8
19	5936.670	172.43	5020	52.92	-	-	-	-
22	4323.330	151.44	3646.670	45.09	4546.67	32.15	4326.67	47.26
25	3120.000	42.45	2730.000	60	3193.33	35.12	3235	50.74
28	-	-	-	-	2223.33	40.41	2416.67	23.09

Table 42. Summary of DSR Test Results of PAV-aged Asphalt Binders from S2.

Temperature (°C)	G*/sinδ (kPa), S2B1	G*/sinδ (kPa), S2B1	G*/sinδ (kPa), S2B3	G*/sinδ (kPa), S2B3	G*/sinδ (kPa), S2B3	G*/sinδ (kPa), S2B3	G*/sinδ (kPa), S2B8	G*/sinδ (kPa), S2B8
19	7743.33	60.28	-	-	-	-	-	-
22	5518.33	35.47	4085	196.78	4616.67	35.12	4153.33	105.98
25	3833.33	20.82	3163.33	56.86	3126.67	136.5	2986.67	187.71
28	-	-	2056.67	200.08	2090	52.92	2123.33	132.04

APPENDIX-C: BENDING BEAM RHEOMETER (BBR) TEST DATA

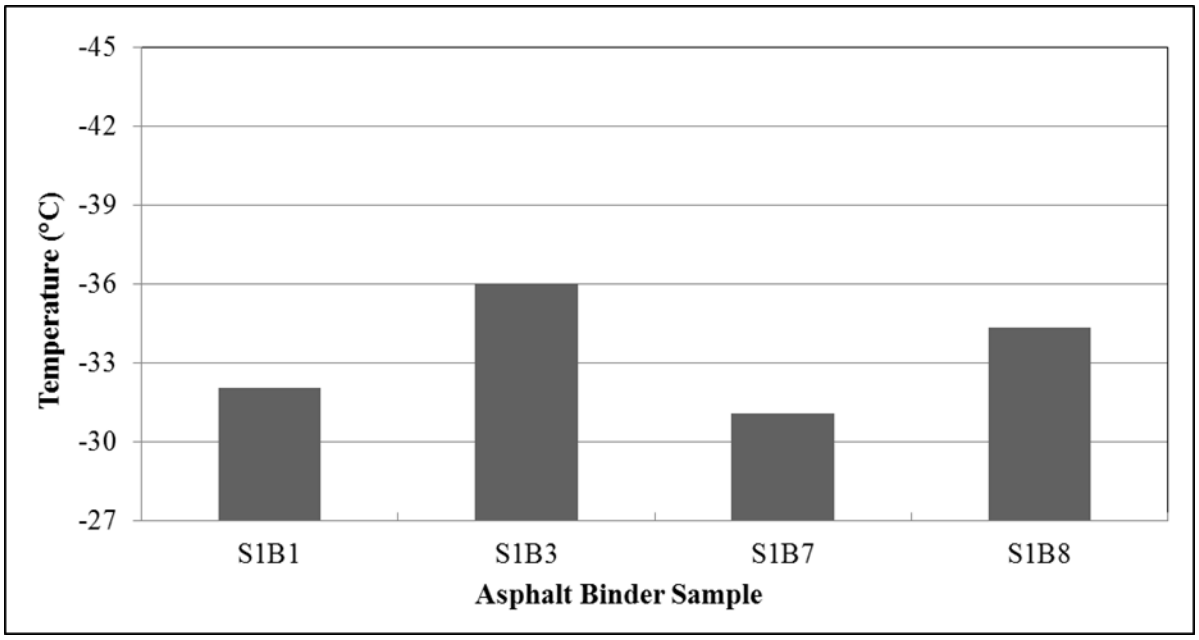

Figure 87. Low PG temperature (°C) of asphalt binders from S1.

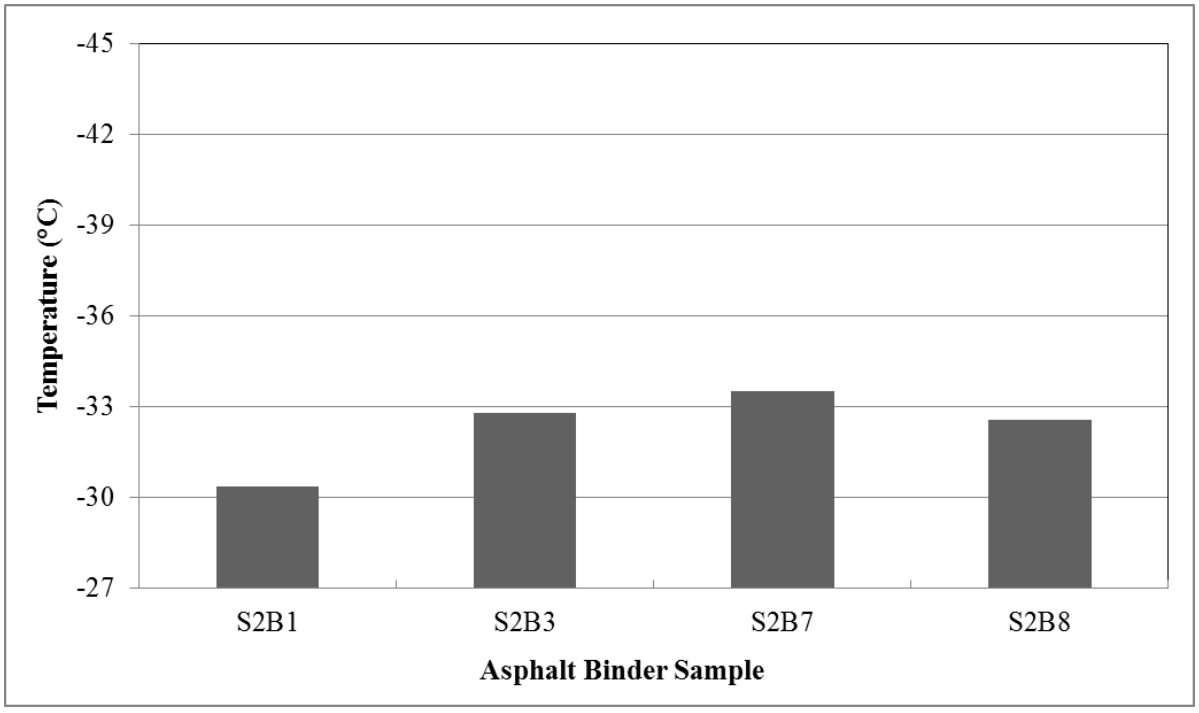

Figure 88. Low PG temperature (°C) of asphalt binders from S2.

APPENDIX-D: ATOMIC FORCE MICROSCOPY (AFM) TEST DATA

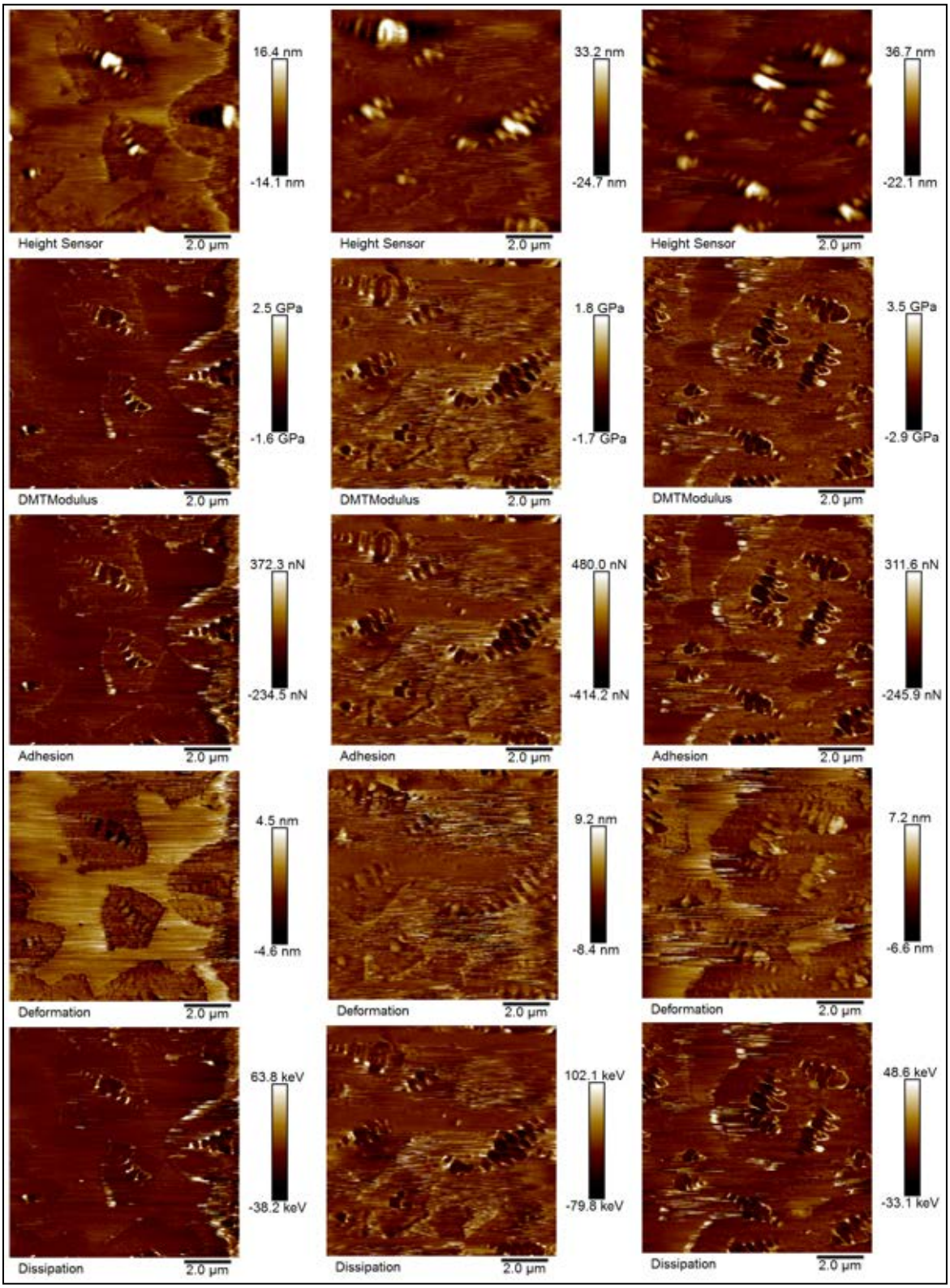

Figure 89. AFM maps of PG 64-22 binder (control) from S1 in dry condition.

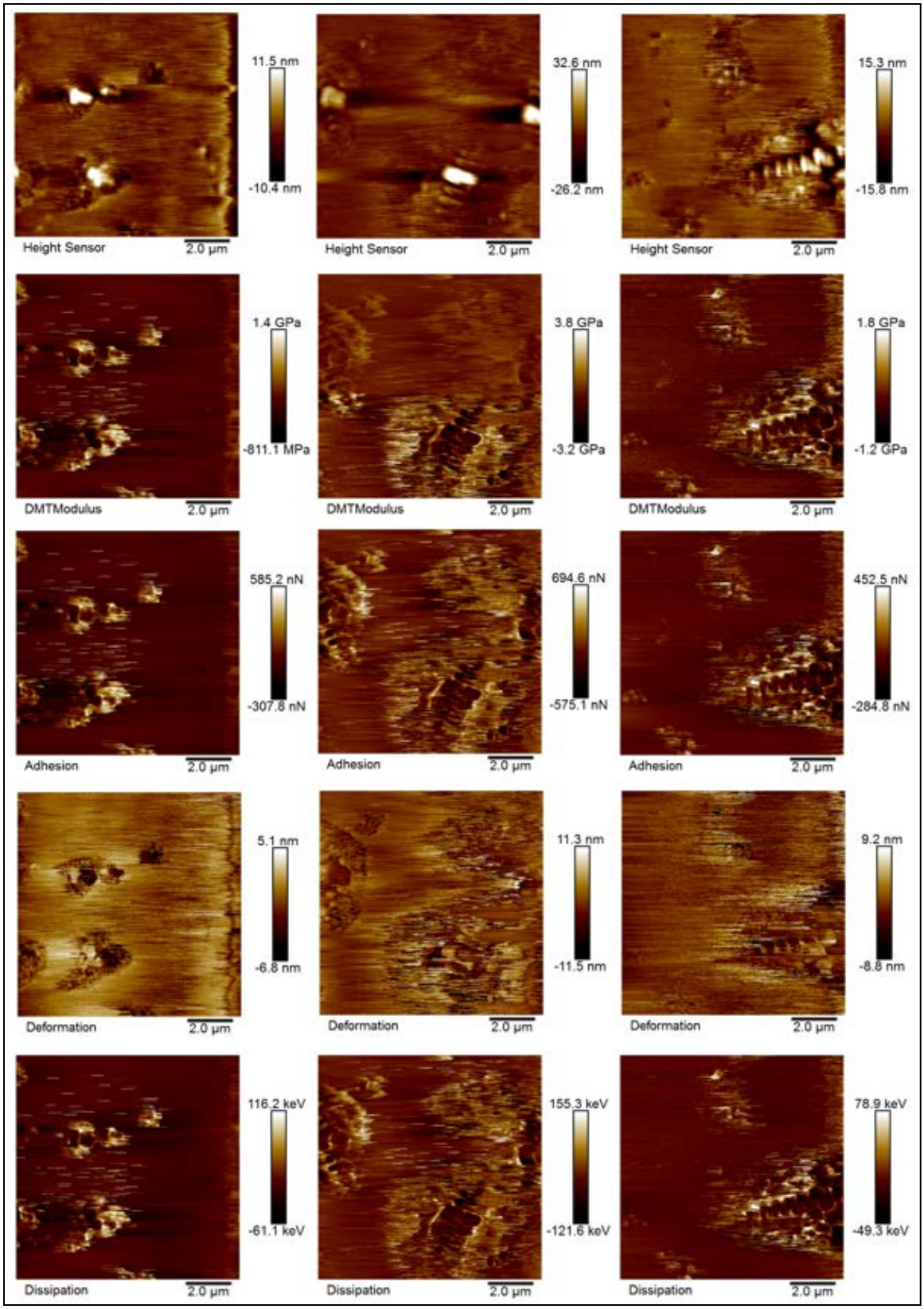

Figure 90. AFM maps of PG 70-22 binder (PPA-modified) from S1 in dry condition.

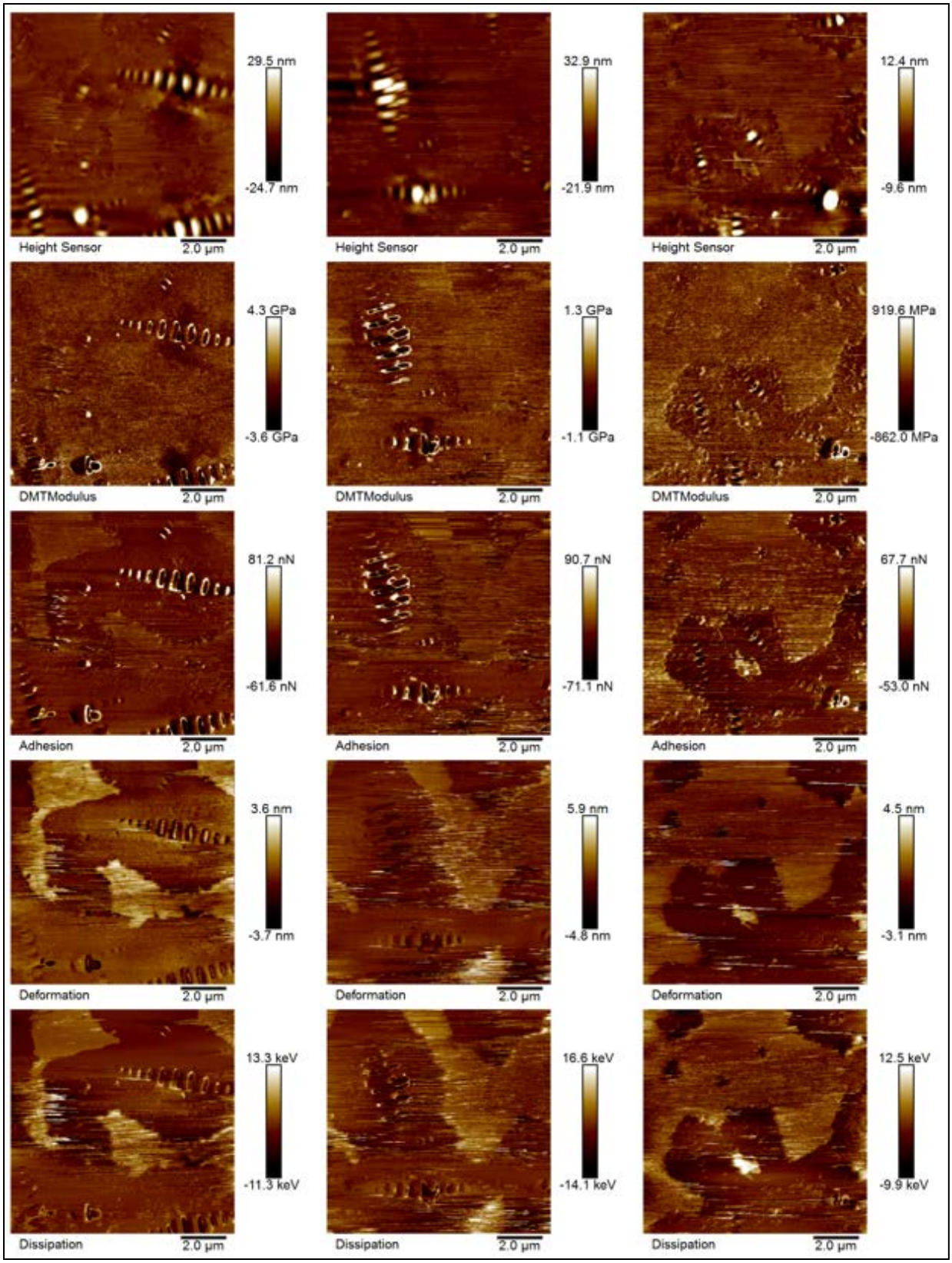

Figure 91. AFM maps of PG 70-22 binder (SBS-modified) from S1 in dry condition.

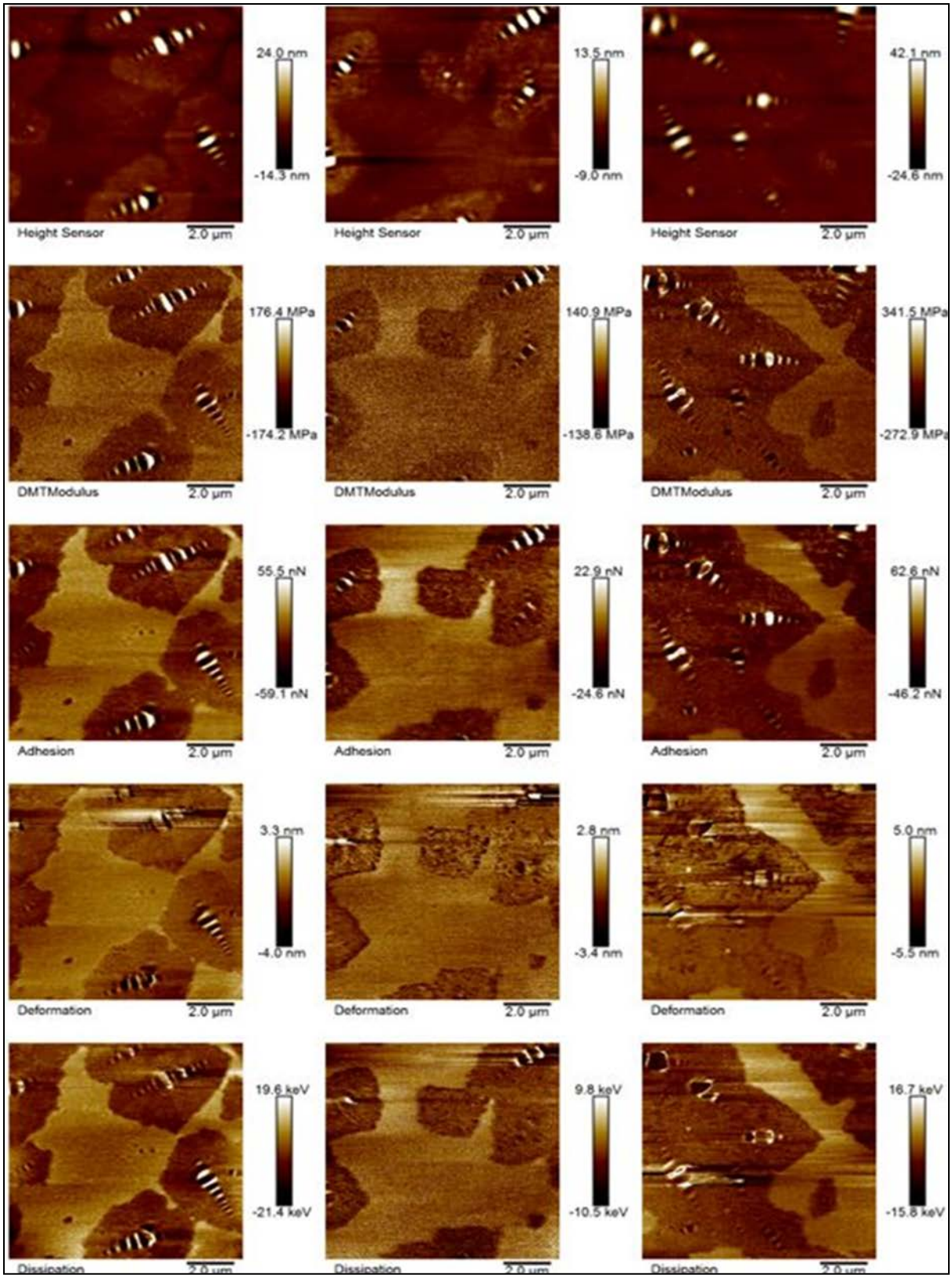

Figure 92. AFM maps of PG 64-22 binder (LAA-modified) from S1 in dry condition.

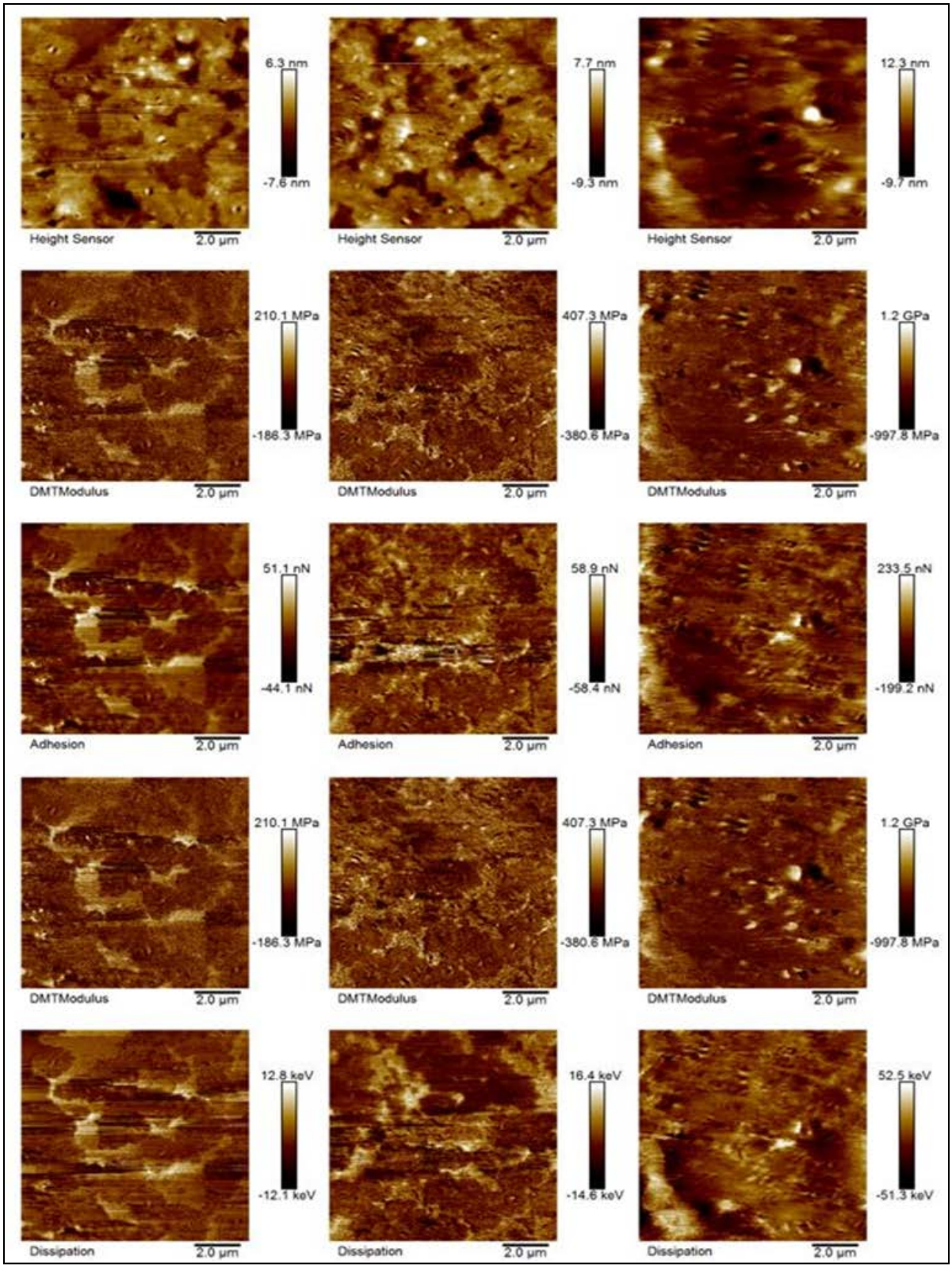

Figure 93. AFM maps of PG 64-22 binder (LAA-modified) from S1 in wet condition.

Table 43. Detailed analysis of AFM tests for morphology or roughness (nm) values of all the tested asphalt binders from S1 and S2.

Binders	Samp. Cond.	Avg. of Entire Spec.	Avg.	Dispersed and Interstitial	Disp. & Interst. Min-Max	Matrix	Matr. Min Max	Avg. of Entire Spec.	Avg.	Dispersed and Interstitial	Disp. & Interst. Min-Max	Matrix	Matr. Min Max
PG 64-22	Dry	6.33	5.45	2.58-9.58	1.72-10.3	0.945-2.05	0.67-2.05	2.36	1.99	1.77-4.5	0.726-4.5	0.390-0.952	0.284-0.952
	Dry	5.71		2.8-9.38		0.67-1.64		1.68		1.46-3.8		0.34-0.65	
	Dry	4.30		1.72-10.3		0.949-1.4		1.94		0.726-4.36		0.284-0.796	
	Wet	1.05	1.57	1.27-3.56	0.817-4.98	0.478-0.75	0.478-1.91	3.20	2.08	2.41-3.77	0.937-4.75	1.61-2.15	0.436-2.15
	Wet	1.07		0.817-2.66		0.653-1.43		1.75		0.937-4.75		0.42-0.726	
	Wet	2.60		1.26-4.98		0.493-1.91		1.28		0.956-4.32		0.436-0.626	
PG 70-22 (PPA)	Dry	2.57	3.98	1.83-4.58	1.69-12.8	0.562-1.62	0.562-4.24	5.21	5.21	3.75-8.22	2.97-8.22	2-2.77	1.56-5
	Dry	5.99		2.46-12.8		1.47-4.24		6.15		5.2-8.22		4.08-5	
	Dry	3.37		1.69-5.56		0.84-1.4		4.27		2.97-7.11		1.56-3.07	
	Wet	1.97	2.14	1.01-2.73	1.01-3.62	0.953-1.31	0.592-1.85	5.16	6.09	3.62-7.9	3.51-10.21	2-3.42	0.856-3.45
	Wet	2.29		1.35-3.62		0.592-1.28		7.42		3.51-8.74		1.78-3.45	
	Wet	2.15		1.18-2.7		0.656-1.85		5.69		3.8-10.21		0.856-3.2	
PG 70-22 (SBS)	Dry	5.30	4.47	3.61-11.8	1.65-11.8	0.727-1.55	0.727-2.36	5.44	4.90	2.34-8.99	1.41-10.6	0.75-1.46	0.386-1.46
	Dry	5.39		2.42-9.6		1.02-2.36		3.39		1.41-6.49		0.386-0.697	
	Dry	2.73		1.65-6.36		0.843-1.28		5.88		2.68-10.6		0.608-1.34	
	Wet	1.60	2.24	0.911-2.37	0.549-4.35	0.386-0.966	0.382-2.11	2.78	2.11	1.72-5.78	1.00-5.78	0.428-0.91	0.277-1.25
	Wet	2.25		0.549-3.69		0.382-0.631		1.44		1.00-2.19		0.277-0.481	
	Wet	2.87		1.64-4.35		0.615-2.11		2.12		1.28-3.47		0.42-1.25	
PG 76-22 (SBS+ PPA)	Dry	5.30	4.60	3.55-12.4	2.78-12.4	0.836-1.34	0.685-1.89	4.88	4.27	3.98-8.05	2.00-8.05	0.336-0.746	0.329-0.914
	Dry	3.70		2.8-8.48		0.946-1.85		4.33		2.00-7.69		0.329-0.696	
	Dry	4.79		2.78-10.5		0.685-1.89		3.59		2.11-6.24		0.411-0.914	
	Wet	1.15	1.66	1.00-1.72	1.00-8.44	0.392-0.68	0.392-3.91	2.84	3.13	2.71-3.54	1.99-7.49	1.25-2.52	1.25-2.52
	Wet	2.31		1.78-8.44		0.82-3.91		3.85		1.99-7.49		1.39-1.83	
	Wet	1.52		1.18-1.89		0.535-1.07		2.70		2.24-3.06		1.35-1.92	
PG 64-22+0.005 AHP	Dry	6.10	4.33	3.86-13.5	1.35-13.5	0.425-0.955	0.316-0.955	3.59	3.32	1.54-9	1.08-12.1	0.355-0.596	0.285-0.596
	Dry	2.76		1.52-5.93		0.342-0.625		3.82		1.08-12.1		0.339-0.551	
	Dry	4.13		1.35-8.25		0.316-0.887		2.56		1.3-7.57		0.285-0.444	
	Wet	2.35	2.35	1.34-3.05	0.938-3.84	0.41-0.97	0.316-1.11	2.35	2.75	1.08-6.52	1.08-7.39	0.294-0.511	0.294-0.903
	Wet	1.76		0.938-2.05		0.316-0.656		2.99		1.22-7.39		0.348-0.571	
	Wet	2.93		1.70-3.84		0.427-1.11		2.91		1.3-6.58		0.435-0.903	
PG 64-22+0.005 PP	Dry	4.16	4.34	2.89-8.08	1.89-10.6	0.572-1.42	0.449-1.42	3.19	3.29	1.26-9.75	1.01-9.75	0.967-1.16	0.298-1.16
	Dry	4.87		3.16-10.6		0.449-0.935		3.20		5.71-8.73		0.298-0.433	
	Dry	3.99		1.89-6.57		0.63-0.995		3.48		1.01-7.86		0.354-0.755	
	Wet	3.05	3.17	1.18-5.66	1.18-8	0.419-0.986	0.419-1.23	2.75	2.23	1.8-3.85	0.635-3.85	0.44-0.654	0.308-0.654
	Wet	2.90		1.4-5.43		0.555-0.984		2.40		0.635-2.61		0.374-0.627	
	Wet	3.55		2.35-8		0.837-1.23		1.53		0.715-2.77		0.308-0.485	
PG 64-22+0.005 E	Dry	3.44	4.24	1.05-6.37	1.05-12.1	0.351-0.843	0.351-1.08	3.49	3.88	1.25-8.1	1.02-13.3	0.354-0.545	0.343-0.675
	Dry	4.99		1.59-12.1		0.671-1.21		4.91		1.02-13.3		0.343-0.675	
	Dry	4.29		4.21-7.82		0.598-1.08		3.23		1.23-8.72		0.383-0.533	
	Wet	3.50	3.02	1.77-5.69	1.20-7.4	0.398-0.903	0.398-0.864	1.75	1.53	0.964-2.05	0.558-2.42	0.405-0.78	0.304-0.78
	Wet	2.87		1.20-5.97		0.477-0.864		1.17		0.558-2.42		0.349-0.481	
	Wet	2.69		1.84-7.45		0.479-0.813		1.67		0.686-1.77		0.304-0.605	

Table 44. Detailed analysis of AFM tests for modulus (MPa) values of all the tested asphalt binders from S1 and S2

Binders	Samp. Cond.	Avg. of Entire Spec.	Avg.	Dispersed and Interstitial	Disp. & Interst. Min-Max	Matrix	Matr. Min Max	Avg. of Entire Spec.	Avg.	Dispersed and Interstitial	Disp. & Interst. Min-Max	Matrix	Matr. Min Max
PG 64-22	Dry	726	536.33	578-842	250-842	232-324	78.9-324	57.8	43.30	49-109	30-114	40.3-50.7	25.8-50.7
	Dry	453		377-645		78.9-322		37.1		37-51.1		29.6-35.5	
	Dry	430		250-787		119-269		35		30-114		25.8-31.4	
	Wet	68.2	271.73	55.6-70.6	55.6-630	53.1-67.8	53.1-339		174.95		42.9-345		39.6-225
	Wet	245		205-442		175-271		299		224-345		195-225	
	Wet	502		203-630		144-339		50.9		42.9-91		39.6-52	
PG 70-22 (PPA)	Dry	241	462.00	152-429	120-1334	55.7-121	55.7-278	946	962.67	863-1124	747-1173	542-880	444-965
	Dry	810		372-1334		84.5-278		941		747-1099		444-843	
	Dry	335		120-516		104-153		1001		921-1173		725-965	
	Wet	160	198.33	69.5-168	69.5-546	57.25-72.6	56.9-122	549	490.67	490-615	195-814	338-494	74.2-494
	Wet	134		72.7-166		56.9-91.4		618		462-814		217-392	
	Wet	301		228-546		76.5-122		305		195-350		74.2-183	
PG 70-22 (SBS)	Dry	952	489.67	950-2028	188-2028	540-723	128-723	693	590.67	455-1085	264-1085	323-473	244-473
	Dry	283		203-433		148-233		414		264-663		244-298	
	Dry	234		188-307		128-200		665		466-1039		275-522	
	Wet	77.8	306.27	64.7-103	64.7-532	44.3-60.6	44.3-353	384	652.33	303-628	303-2005	231-367	231-563
	Wet	384		287-532		256-332		951		515-2005		234-355	
	Wet	457		380-513		298-353		622		543-1263		272-563	
PG 70-22 (SBS+PP)^	Dry	66.9	141.63	35.7-137	35.7-342	19.7-37	19.7-132	221	173.33	218-359	111-359	99.1-130	62.1-130
	Dry	158		134-326		65.9-118		167		111-309		73.2-92.5	
	Dry	200		110-342		68.3-132		132		123-221		62.1-86.6	
	Wet	65.2	75.93	52.7-78	52.7-133	45.5-60.8	45.5-81	303	189.00	281-406	95.1-406	93.1-197	63.7-197
	Wet	84.9		65.4-133		56.9-81		136		95.1-277		63.7-93.6	
	Wet	77.7		67.7-89		45.5-77.8		128		119-174		76.4-90.1	
PG 64-22+ 0.005 AHP	Dry	84.7	60.80	50.2-123	29.8-123	42-49.6	26.4-49.6	127	131.33	96.3-256	96.3-323	79.3-100	79.3-120
	Dry	42.5		34.5-90.2		30.1-36.4		133		98.1-323		85.1-120	
	Dry	55.2		29.8-97.1		26.4-31.8		134		109-287		95.8-115	
	Wet	109	144.97	96.9-122	38.4-359	63.5-79.6	27.9-165	50.1	56.50	36.63-69.4	36.63-129	33.6-38.5	26.2-46.2
	Wet	53.9		38.4-58		27.9-32.6		49.8		46.1-62.5		34-46.2	
	Wet	272		216-359		136-165		69.6		50.5-129		26.2-33	
PG 64-22+ 0.005 PP	Dry	119	85.77	91.2-183	34.5-183	46.3-66.8	24-66.8	247	180.43	214-537	61-537	201-235	50.3-235
	Dry	78.4		64.1-134		25.4-33.6		204		182-366		172-195	
	Dry	59.9		34.5-93.5		24-34.7		90.3		61-235		50.3-57.8	
	Wet	25.7	41.50	20.2-33.4	20.2-81.5	18.1-24.9	18.1-39.2	158	146.07	135-240	61.3-560	77.4-109	19.2-160
	Wet	40.3		35.4-57.5		21.3-31.2		190		177-560		90.9-160	
	Wet	58.5		48.7-81.5		23.9-39.2		90.2		61.3-146		19.2-57.5	
PG 64-22+ 0.005 E	Dry	74.2	99.40	36.9-88.1	36.9-281	31.9-45.4	31.9-101	167	146.00	96.8-366	90-372	93.9-100	76-103
	Dry	130		93.9-281		73.7-101		145		179-372		77.7-96.6	
	Dry	94		83.9-154		65.9-77		126		90-296		76-103	
	Wet	61.5	53.03	48.9-76.3	33.6-76.3	41.6-62.9	23-62.9	55.9	56.40	40-99	36.1-107	25.4-45.3	25.4-51.5
	Wet	48		39.3-69.5		32.4-48.2		41.2		36.1-46.2		32.7-39.1	
	Wet	49.6		33.6-74.4		23-47.6		72.1		50-107		36.8-51.5	

Table 45. Detailed analysis of AFM tests for adhesion force (nN) values of all the tested asphalt binders from S1 and S2.

Binders	Cond.	Avg. of Speci-mens	AVG.	D./I.	D./I. Min-Max	Matrix	Matrix Min Max	Avg. of Speci-mens	AVG.	D./I.		Matrix	Matrix Min Max
	Dry	65.4		59-76	18	13-28	13	6.05		4.37-14.1	2.12	1.93-4.73	1.33
PG	Dry	120	84.67	97-172	-	23-94	-	4	4.61	4.54-6.13	-	2.15-2.9	-
64-	Dry	68.6		18-119	172	16-28	94	3.78		2.12-15.7	15.7	1.33-2.07	4.73
22	Wet	6.99		5.92-11.7	4.29	3.29-5.52	2.1				2.69		2.22
	Wet	21.2	20.16	13.2-26.4	-	12.7-19.4	-	17.1	10.19	8.46-28.6	-	7.08-10	-
	Wet	32.3		4.29-51.8	51.8	2.1-3.74	12.7	3.27		2.69-3.84	28.6	2.22-3.25	10
	Dry	94.4		85.2-167	50.2	12.1-21.7	12.1	194		160-215	160	125-206	113
PG	Dry	167	113.33	123-199	-	26.8-125	-	257	220.67	252-278	-	113-209	-
70-	Dry	78.6		50.2-131	199	12.1-24	125	211		174-244	278	160-191	209
22	Wet	33.6		17.7-45.6	17.7	7.46-13.3	7.46	158		150-190	73.5	47.9-122	33.5
(PPA)	Wet	47.5	53.53	32.5-64.7	-	8.48-30.9	-	116	130.33	107-163	-	42.8-75.6	-
	Wet	79.5		62.9-112	112	10.4-42.2	42.2	117		73.7-167	190	33.5-76.3	122
	Dry	14.5		7.45-23.7	7.45	2.82-11.9	2.82	10.3		3.78-16.2	2.84	1.61-3.02	1.46
PG	Dry	18.4	16.10	9.09-24	-	10.9-14.5	-	6.51	12.67	2.84-8.77	-	1.46-1.94	-
70-	Dry	15.4		9.20-16.8	24	7.09-13.3	14.5	21.2		11.7-37.1	37.1	3.12-8.11	8.11
20	Wet	7.81		6.57-10.2	3.06	2.71-3.88	1.67	6.85		3.18-9.79	3.18	3.09-4.42	1.67
(SBS)	Wet	9.68	8.55	3.86-10.8	-	2.31-3.52	-	10.1	11.48	4.56-19.7	-	1.67-3.44	-
	Wet	8.15		3.06-10.2	10.8	1.67-4.55	4.55	17.5		4.09-18.9	19.7	2.85-7.93	7.93
PG	Dry	27		16.9-64.7	16.9	4.24-14.3	4.24	29		26.2-36.4	12.2	5.89-10.5	2.86
76-	Dry	30.4	30.67	20-53.8	-	6.91-14.1	-	26.3	24.33	13.8-38.5	-	2.98-8.46	-
22	Dry	34.6		17-79	79	6.1-14.2	14.3	17.7		12.2-21.9	38.5	2.86-6.89	10.5
(SBS+	Wet	4.2		2.36-5.48	2.36	1.65-3.19	1.65	59.6		53.7-84.4	14.2	23.9-36.3	4.96
PPA)	Wet	10.4	6.95	6.01-19.7	-	4.13-8.65	-	19	32.83	14.2-34.1	-	4.96-8.68	-
	Wet	6.25		4.83-10.2	19.7	2.98-5.47	8.65	19.9		16.3-28.3	84.4	5.15-13.9	36.3
PG	Dry	14.6		2.97-23.8	2.37	3.06-5.46	1.94	15.8		9.01-39.9	2.92	2.61-3.43	2.5
64-	Dry	7.8	13.13	2.37-21.1	-	1.94-3.26	-	12.9	12.62	2.92-46.9	-	2.34-2.79	-
22+	Dry	17		3.84-35.1	35.1	3.15-5.34	5.46	9.15		4.02-34.6	46.9	2.5-2.82	3.43
0.005	Wet	15		10.1-24	6.58	5.48-8.42	2.5	5.31		4.67-10.5	3.41	2.63-3.48	1.87
AHP	Wet	11.8	27.40	6.58-13	-	2.5-5.94	-	3.74	7.98	3.41-7.17	-	1.87-2.7	-
	Wet	55.4		38.9-60.9	60.9	14.4-32	32	14.9		10.5-29.5	29.5	3.48-5.62	5.62
PG	Dry	16.1		7.26-30.2	6.78	2.72-4.15	2.59	43.8		32.9-117	5.48	29.7-33.9	1.95
64-	Dry	19.9	16.47	21.5-31.7	-	2.59-5.62	-	11	24.10	16.2-32.7	-	1.95-2.64	-
22+	Dry	13.4		6.78-21.6	31.7	4.3-6.29	6.29	17.5		5.48-63.1	63.1	3.09-5.55	33.9
0.005	Wet	4.44		3.84-6.2	3.84	2.11-4.46	2.11	24.4		24.6-33.5	2.92	6.21-8.83	1.32
PP	Wet	17.9	13.45	17.1-29.8	-	4.3-10.9	-	4.1	12.56	2.92-11.5	-	1.32-2.01	-
	Wet	18		16.6-25	29.8	4.03-7.72	10.9	9.19		5.02-20.7	33.5	1.7-3.58	8.83
PG	Dry	14.1		6.78-53.5	4.03	4.12-6.28	2.13	17.2		6.55-49.6	6.55	2.57-6.35	2.57
64-	Dry	11	11.46	4.03-29.7	-	3.07-5.67	-	21.8	18.67	26-68.6	-	5-6.67	-
22+	Dry	9.27		4.3-17	53.5	2.13-3.8	6.28	17		7.6-52.5	68.6	4.87-5.55	6.67
0.005 E	Wet	7.47		3.11-121.7	2.29	2.75-4.97	1.83	12.8		7.68-25.2	3.21	2.46-4.66	1.97
E	Wet	6.39	7.81	2.29-11.6	-	1.83-3.12	-	3.49	12.60	3.21-9.71	-	1.97-3.01	-
	Wet	9.58		3.67-15.4	15.4	2.86-5.45	5.45	21.5		11.7-36.2	36.2	3.95-8.54	8.54

Table 46. Detailed analysis of AFM tests for deformation (nm) values of all the tested asphalt binders from S1 and S2.

Binders	Cond	Avg. of Speci-mens	AVG.	D./I.	D./I. Min-Max	Matrix	Matrix Min Max	Avg. of Speci-mens	AVG.	D./I.	D./I. Min-Max	Matrix	Matrix Min Max
	Dry	1.7		0.816-2.23	0.521	0.38-1.15	0.274	0.399		0.296-0.699	0.206	0.246-0.307	0.145
PG	Dry	2.22	1.73	1.09-3.1	-	0.274-1.33	-	0.321	0.32	0.369-0.50	-	0.184-0.243	-
64-22	Dry	1.27		0.521-1.76	3.1	0.319-1.27	1.33	0.234		0.206-0.37	0.699	0.145-0.199	0.307
	Wet	0.391		0.387-0.799	0.127	0.21-0.416	0.116				0.187		0.195
	Wet	0.17	0.43	0.127-0.378	-	0.116-0.177	-	0.274	0.31	0.207-0.418	-	0.091-0.136	-
	Wet	0.717		0.269-1.02	1.02	0.204-0.565	0.565	0.354		0.187-0.461	0.461	0.195-0.294	0.294
	Dry	1.53		1.13-2.34	1.13	0.598-1.16	0.598	2.46		1.44-3.69	1.44	1.26-1.87	1.01
PG	Dry	2.97	2.25	1.93-3.89	-	0.722-1.75	-	3.75	2.71	2.91-4.58	-	1.38-2.67	-
70-22	Dry	2.26		1.24-3.71	3.89	0.895-1.48	1.75	1.93		1.59-2.53	4.58	1.01-1.8	2.67
(PPA)	Wet	1.15		0.727-0.931	0.56	0.381-0.774	0.667	4.23		3.78-4.84	2.48	0.908-1.74	0.755
	Wet	1.11	1.33	0.56-1.14	-	0.456-0.801	-	4.16	4.34	2.48-4.83	-	1.32-2.61	-
	Wet	1.73		1.14-3.5	3.5	0.667-1.01	1.01	4.63		3.43-6.33	6.33	0.755-3.08	3.08
	Dry	0.933		0.519-1.06	0.369	0.21-0.51	0.21	0.548		0.432-0.630	0.378	0.277-0.374	0.20
PG	Dry	1.27	1.04	0.369-1.48	-	0.337-1.25	-	0.578	0.68	0.378-0.635	-	0.20-0.303	-
70-22	Dry	0.917		0.482-0.846	1.48	0.286-0.575	1.25	0.92		0.688-1.13	1.13	0.255-0.359	0.374
(SBS)	Wet	0.301		0.237-0.408	0.237	0.101-0.174	0.101	0.667		0.396-0.693	0.396	0.235-0.347	0.101
	Wet	0.655	0.57	0.444-0.702	-	0.196-0.325	-	0.714	0.73	0.414-0.875	-	0.176-0.490	-
	Wet	0.751		0.416-1.19	1.19	0.224-0.498	0.498	0.812		0.507-0.926	0.926	0.101-0.374	0.490
	Dry	119		100-161	1.08	20.2-41.4	0.443	0.983		0.721-1.21	0.285	0.231-0.395	0.144
PG	Dry	2.2	2.12	1.62-3.04	-	0.443-1.56	-	0.513	0.64	0.345-0.642	-	0.166-0.311	-
76-22	Dry	2.04		1.08-2.43	3.04	0.181-0.677	1.56	0.421		0.285-0.614	1.21	0.144-0.208	0.395
(SBS+	Wet	0.471		0.219-1.00	0.219	0.169-0.350	0.169	1.84		1.55-2.14	1.07	1.08-1.71	0.462
PPA)	Wet	0.951	0.79	0.611-1.20	-	0.438-0.783	-	1.47	1.48	1.17-2.06	-	0.462-0.948	-
	Wet	0.634		0.364-0.865	1.20	0.275-0.445	0.785	1.14		1.07-1.39	2.14	0.552-0.985	1.17
	Dry	1.32		0.494-1.67	0.273	0.324-0.744	0.252	0.286		0.185-0.513	0.142	0.121-0.139	0.14
PG	Dry	0.795	0.86	0.529-1.88	-	0.406-0.558	-	0.184	0.22	0.142-0.437	-	0.127-0.142	-
64-22+	Dry	0.915		0.273-1.36	1.88	0.252-0.422	0.744	0.198		0.157-0.414	2.14	0.14-0.152	0.152
0.005	Wet	1.23		0.468-1.54	0.468	0.376-0.787	0.176	0.536		0.422-1.12	0.348	0.233-0.313	0.155
AHP	Wet	1.04	1.44	0.652-1.20	-	0.466-0.795	-	0.381	0.44	0.348-0.585	-	0.165-0.238	-
	Wet	1.84		0.709-3.44	3.44	0.176-0.44	0.795	0.398		0.374-0.616	1.12	0.155-0.198	0.313
	Dry	1.18		0.502-1.86	0.502	0.231-0.402	0.231	1.17		1.26-1.77	0.117	0.949-1.19	0.1
PG	Dry	1.38	1.41	0.724-2.2	-	0.619-0.858	-	0.203	0.53	0.117-0.435	-	0.109-0.123	-
64-22+	Dry	1.44		1.23-2.08	2.2	0.808-1.41	1.41	0.211		0.14--0.463	1.77	0.1-0.71	1.19
0.005	Wet	0.658		0.522-0.847	0.522	0.435-0.577	0.323	0.9		0.881-1.17	0.318	0.287-0.351	0.163
PP	Wet	1.03	0.97	0.811-1.49	-	0.371-0.694	-	0.502	0.65	0.318-1.14	-	0.19-0.26	-
	Wet	0.914		0.743-2.08	2.08	0.323-0.41	0.694	0.54		0.495-0.761	1.17	0.163-0.272	0.351
	Dry	1.51		0.583-1.43	0.5	0.563-0.85	0.332	0.343		0.281-0.719	0.281	0.148-0.161	0.148
PG	Dry	1.16	1.45	0.5-2.17	-	0.332-0.781	-	0.553	0.44	0.329-0.956	-	0.269-0.322	-
64-22+	Dry	1.73		0.758-1.82	2.17	0.334-0.985	0.985	0.413		0.307-0.7	0.956	0.258-0.363	0.363
0.005 E	Wet	1.03		0.723-1.27	0.501	0.4-0.738	0.339	0.546		0.508-0.844	0.204	0.205-0.24	0.16
	Wet	0.866	0.99	0.501-1.54	-	0.384-0.588	-	0.301	0.47	0.204-0.663	-	0.173-0.207	-
	Wet	1.11		1.16-1.75	1.75	0.339-0.677	0.738	0.553		0.332-0.546	0.844	0.16-0.227	0.24

Table 47. Detailed analysis of AFM tests for dissipation (eV) values of all the tested asphalt binders from S1 and S2.

Binders	Cond.	Avg. of Speci-men	AVG.	D./I.	D./I. Min-Max	Matrix	Matrix Min Max	Avg. of Speci-men	AVG.	D./I.	D./I. Min-Max	Matrix	Matrix Min Max
PG 64-22	Dry	9383	13996.67	6112-10708	3228 - 28655	2280-4180	2242 - 12333	1426	1527.67	1375-2220	1375 - 2644	642-1163	527 - 1611
	Dry	21854		16736-28655		2564-12333		1498		1420-1859		777-1611	
	Dry	10753		3228-18287		2242-5507		1659		1609-2644		527-1278	
	Wet	2360	3208.33	1661-4449	1052 - 9552	1571-2105	369 - 2105		1859.00		1237 - 2417		1032 - 1619
	Wet	2365		1423-3951		1077-1968		1909		1776-2417		1032-1540	
	Wet	4900		1052-9552		369-1435		1809		1237-1807		1219-1619	
PG 70-22 (PPA)	Dry	19520	22689	10620-36339	6512 - 44779	3770-7848	2644 - 11160	38164	45829.00	30100-43076	30100 - 61753	19777-37084	19777 - 43058
	Dry	34974		32912-44779		5940-11160		56068		48615-61753		27543-43058	
	Dry	13573		6512-22291		2644-3860		43255		36778-50631		22726-37433	
	Wet	5704	8981.33	3112-8907	3112 - 20093	1914-2500	1871 - 4816	30268	26876.00	34889-37623	21131 - 37623	11350-20415	6873 - 20415
	Wet	6829		3343-9482		1871-3313		22832		20963-35086		6873-13244	
	Wet	14411		10964-20093		3075-4816		27528		21131-34846		8265-16827	
PG 70-22 (SBS)	Dry	2946	3247.67	1072-3724	1072 - 4039	333-1807	333 - 2264	1540	1726.33	1220-1828	972 - 3710	132-392	36.2 - 996
	Dry	3860		2620-4039		882-2264		1246		972-1851		36.2-145	
	Dry	2937		2202-3121		1483-2197		2393		1898-3710		204-996	
	Wet	2087	2075.33	1607-3135	917 - 3135	62.4-417	62.4 - 950	1458	2011.33	1346-1877	1114 - 2979	69.2-316	69.2 - 461
	Wet	2043		917-2504		301-689		1876		1114-2530		116-461	
	Wet	2096		1502-2992		150-950		2700		1261-2979		110-429	
PG 76-22 (SBS+ PPA)	Dry	5811	6904.33	3516-12697	3516 - 14402	1847-3540	1446 - 4760	4978	3854.67	3127-5212	1483 - 2866	486-1449	46 - 1695
	Dry	7824		5312-12100		1446-4760		4012		1529-5407		117-1695	
	Dry	7078		5754-14402		1636-2361		2574		1483-2866		46-234	
	Wet	1760	2265.67	1575-2228	1575 - 4129	99.5-539	99.5 - 2250	8496	5434.67	8083-9905	2061 - 9905	3072-6304	1311 - 6304
	Wet	2738		2055-4129		1342-2250		4243		3552-6078		1320-2712	
	Wet	2299		1797-2888		213-666		3565		2061-4093		1311-2442	
PG 64-22+ 0.005 AHP	Dry	4337	4219.67	2239-5580	1817 - 8196	1634-2012	1498 - 2203	2697	2413.33	1562-5479	1562 - 8465	127-742	127 - 1271
	Dry	2926		1817-4755		1498-2153		2413		1889-8465		240-990	
	Dry	5396		2129-8196		1564-2203		2130		1603-6755		517-1116	
	Wet	4407	6962.00	2887-4803	2147 - 14898	1677-2418	1265 - 6283	2040	2154.33	2023-3469	1243 - 4937	1042-1484	104 - 1484
	Wet	3223		2147-3877		1265-2149		1627		1243-1989		104-346	
	Wet	13256		7033-14898		2570-6283		2796		2606-4937		444-947	
PG 64-22+ 0.005 PP	Dry	3681	3986.33	2422-4964	2422 - 6625	1912-2425	1768 - 2740	8881	4540.67	5188-23901	1686 - 23901	4091-4870	113 - 4870
	Dry	4737		3803-6625		1768-2277		1941		1863-4382		113-1049	
	Dry	3541		2540-4388		1801-2740		2800		1686-9795		216-683	
	Wet	2613	15099.33	2256-3504	2256 - 8973	1378-2390	1378 - 2917	5942	3325.67	4126-8011	1391 - 8011	1202-1932	306 - 1932
	Wet	5748		4616-8973		2514-2917		1705		1391-3607		306-972	
	Wet	36937		3584-5596		1927-2439		2330		1789-3885		386-1241	
PG 64-22+ 0.005E	Dry	5770	4917	2447-6782	2184 - 7423	1795-2954	1004 - 3528	2744	2959	1059-6149	1059 - 9923	473-1840	473 - 1908
	Dry	4276		2672-7423		1922-3528		3563		1974-9923		1504-1908	
	Dry	4705		2184-5021		1004-2145		2570		1690-6742		451-1661	
	Wet	3328	3240.67	2154-3043	1457 - 3584	1010-2400	645 - 2463	3137	2605.33	1959-5365	1256 - 5365	961-1718	339 - 1718
	Wet	2652		1457-3139		645-1895		1298		1256-2858		339-833	
	Wet	3742		2229-3584		1748-2463		3381		1994-5175		358-1514	

APPENDIX-E: FOURIER TRANSFORM INFRARED SPECTROSCOPY (FTIR) SPECTRA

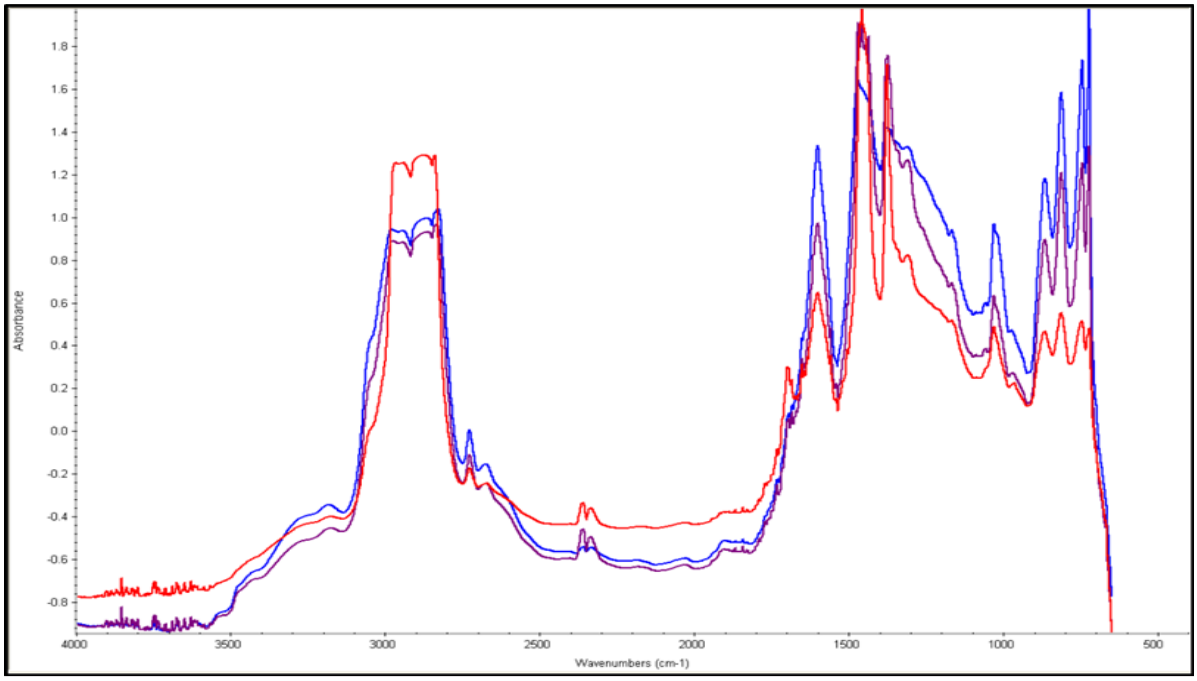

Figure 94. The FTIR spectra S1B1 (Blue-Unaged, Violet-RTFO, and Red-PAV).

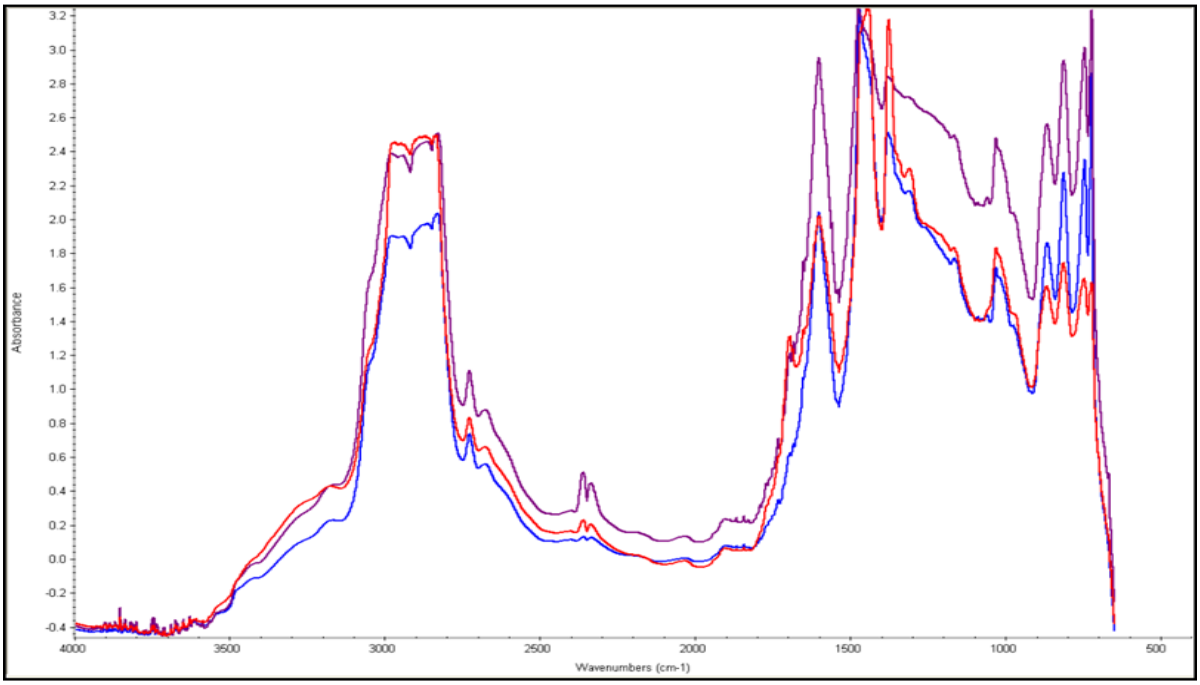

Figure 95. The FTIR spectra S1B3 (Blue-Unaged, Violet-RTFO, and Red-PAV).

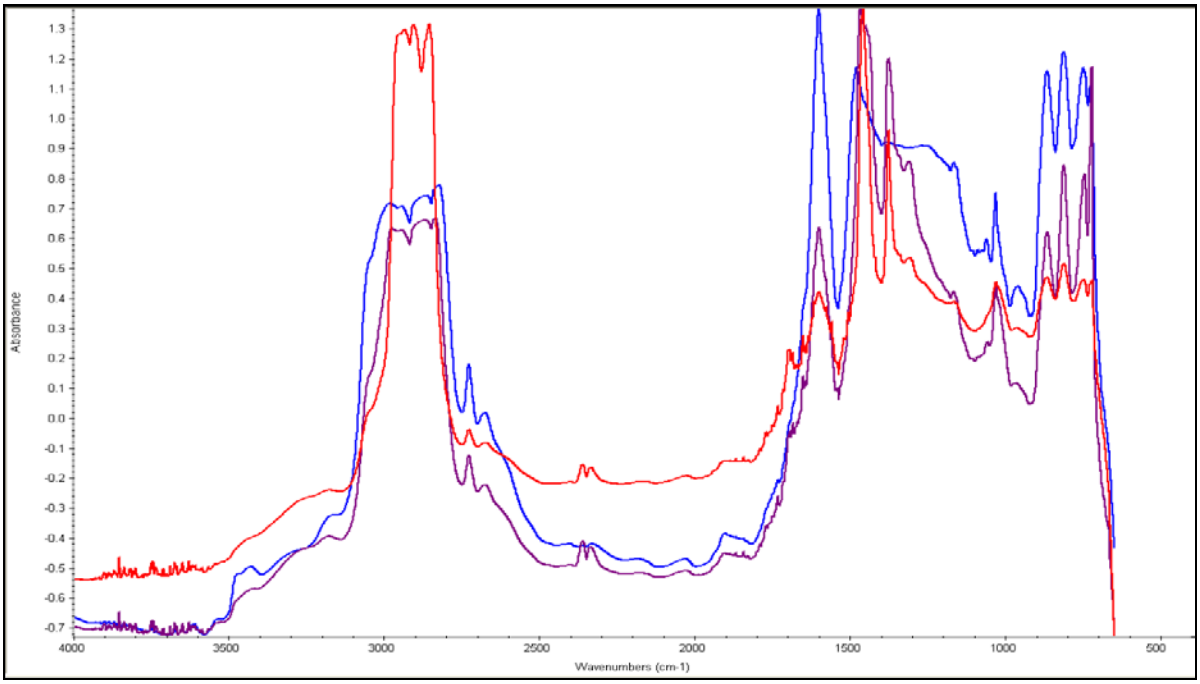

Figure 96. The FTIR spectra S2B1 (Blue-Unaged, Violet-RTFO, and Red-PAV).

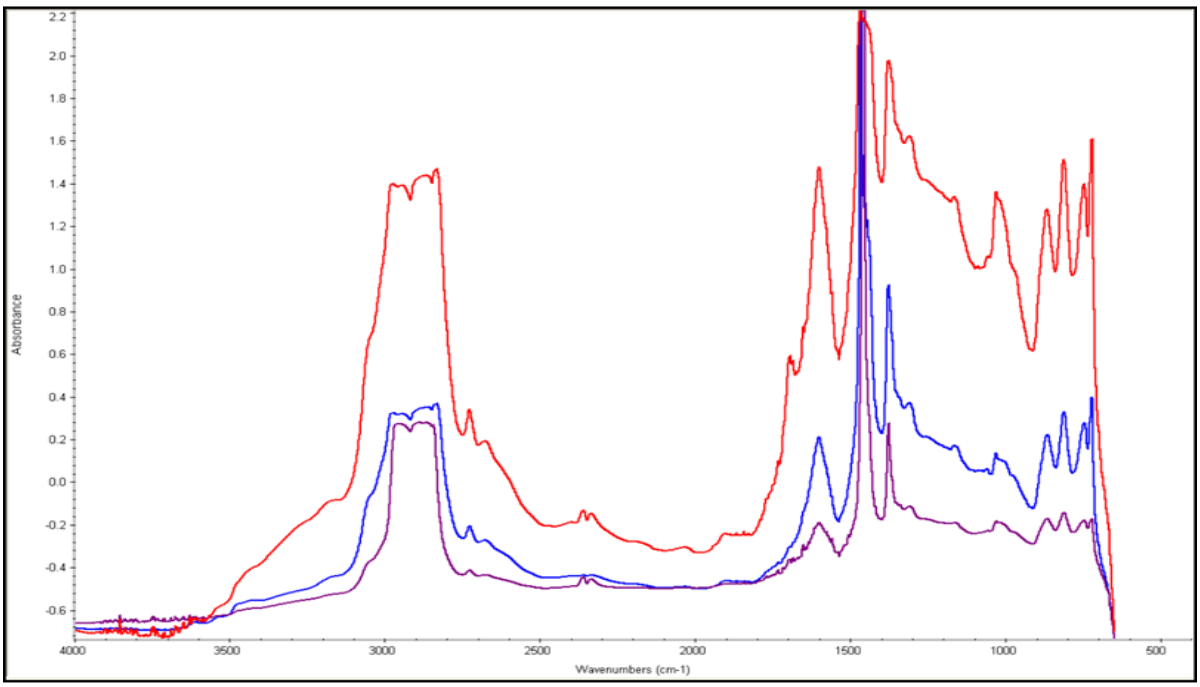

Figure 97. The FTIR spectra S2B3 (Blue -Unaged, Violet-RTFO, Red-PAV).

APPENDIX-F: THEVNMR SPECTRA

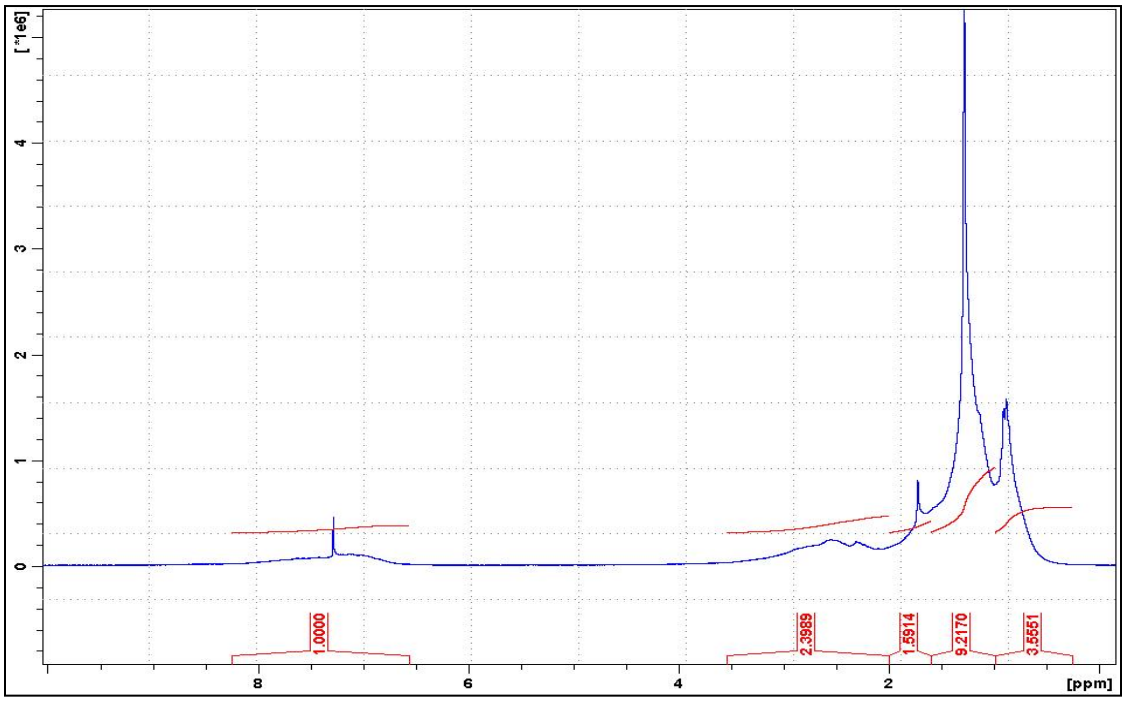

Figure 98. The NMR spectra for S1B1-Unaged-Aromatics.

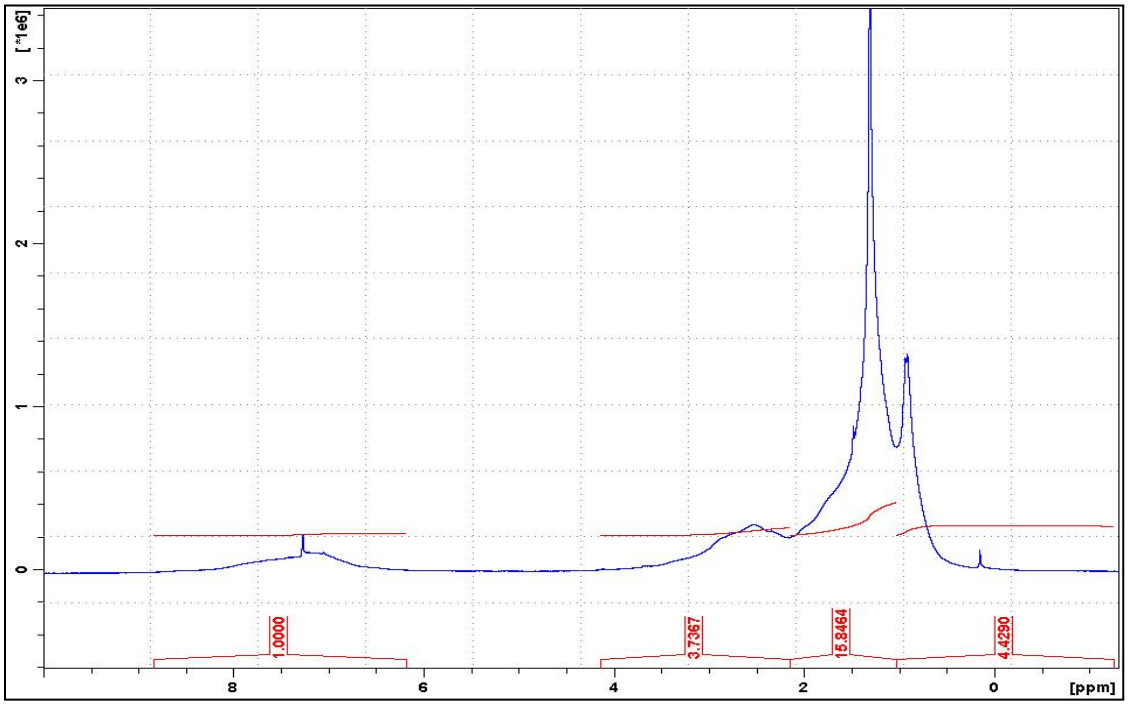

Figure 99. The NMR spectra for S1B1-Unaged-Resins.

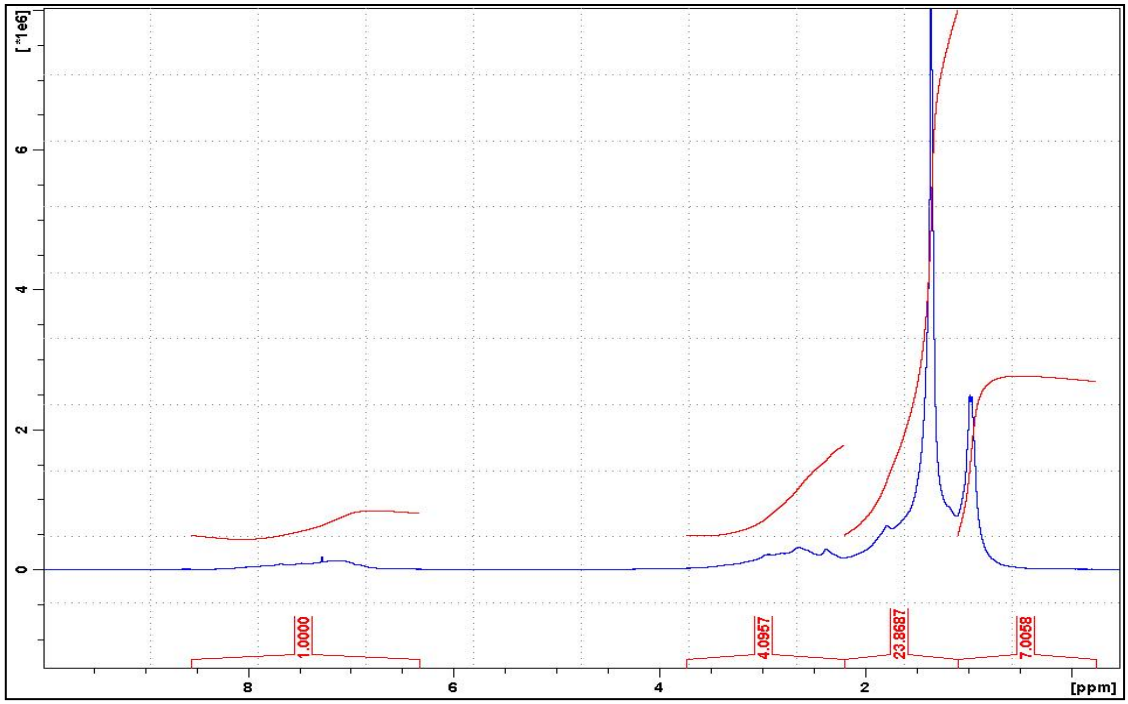

Figure 100. The NMR spectra for S1B3-Unaged-Aromatics.

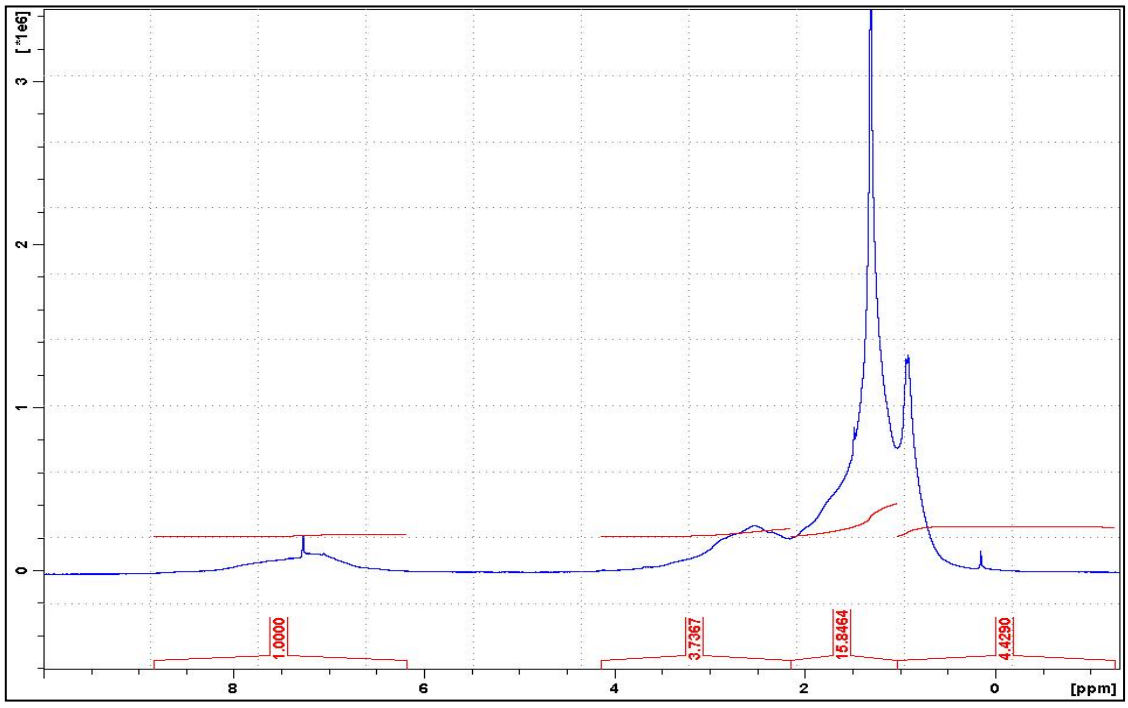

Figure 101. The NMR spectra for S1B3-Unaged-Resins.

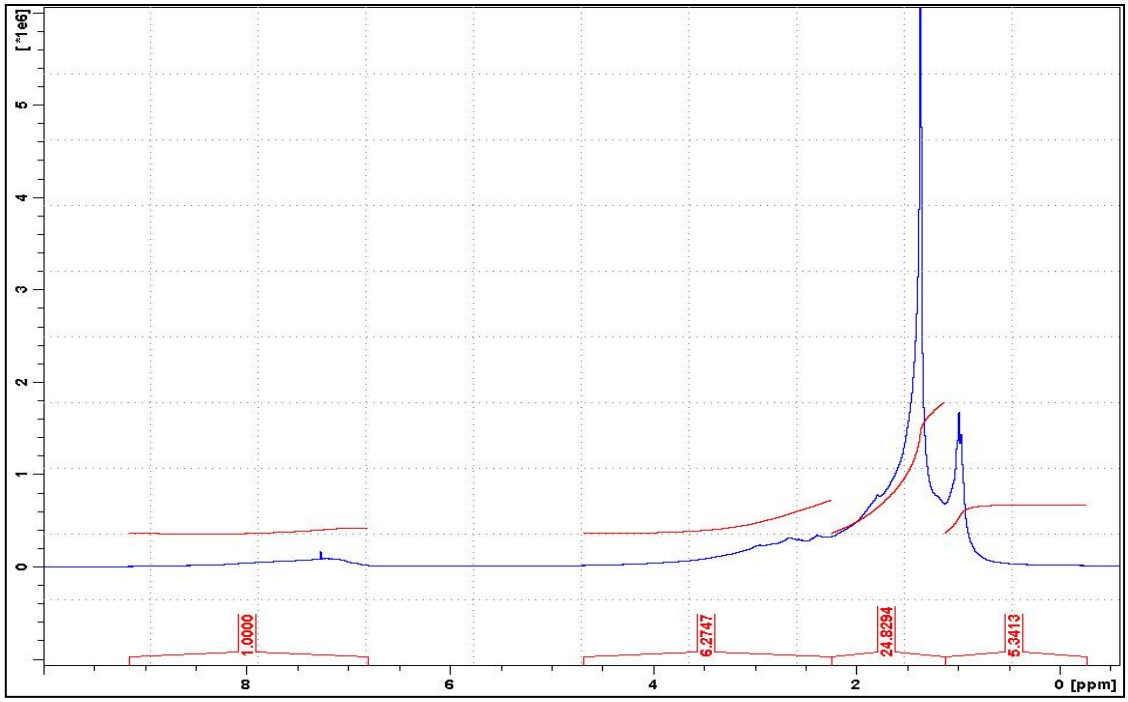

Figure 102. The NMR spectra for S2B1-Unaged-Aromatics.

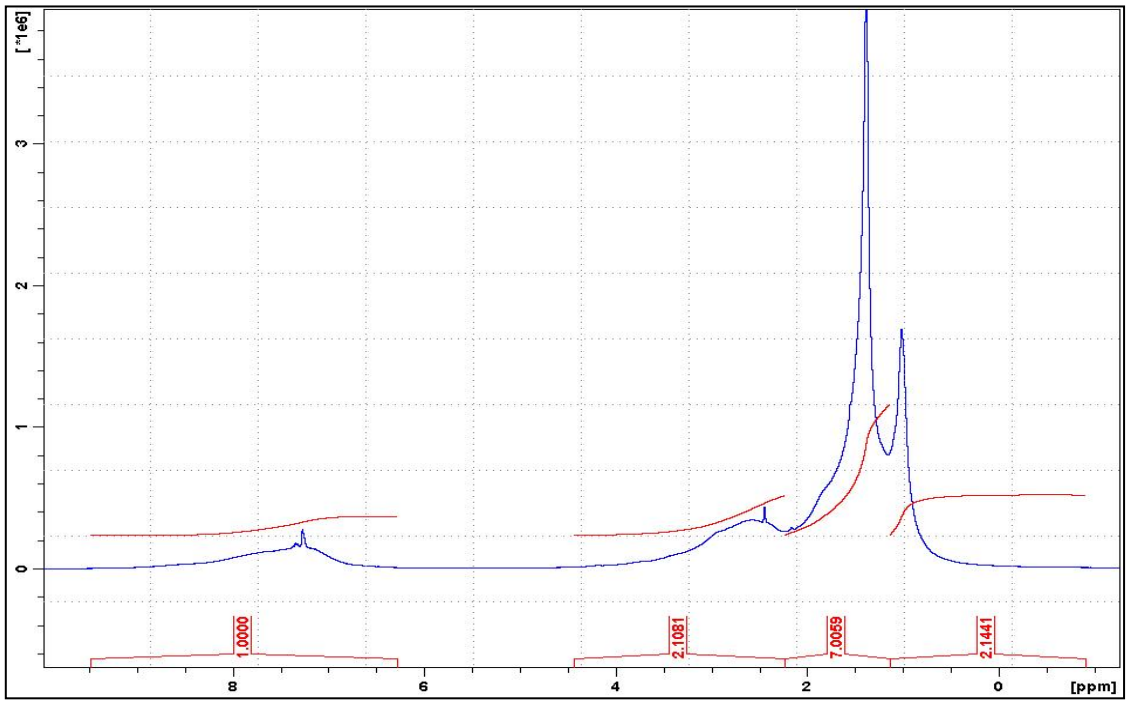

Figure 103. The NMR spectra for S2B1-Unaged-Resins.

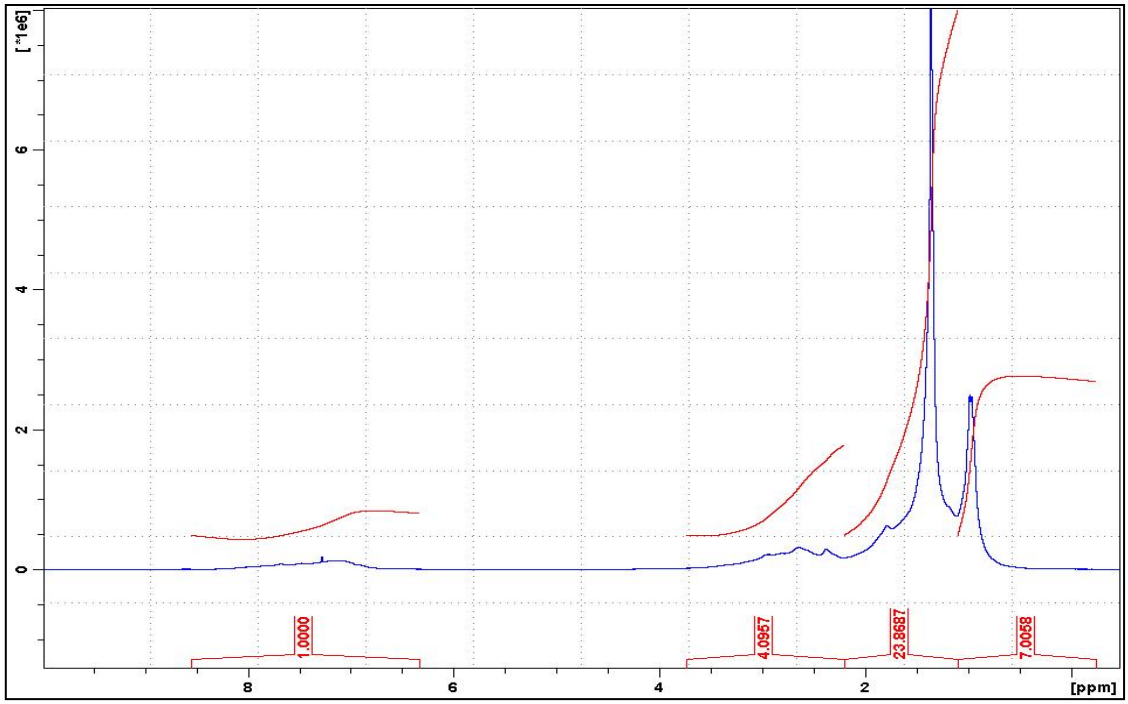

Figure 104. The NMR spectra for S2B3-Unaged-Aromatics.

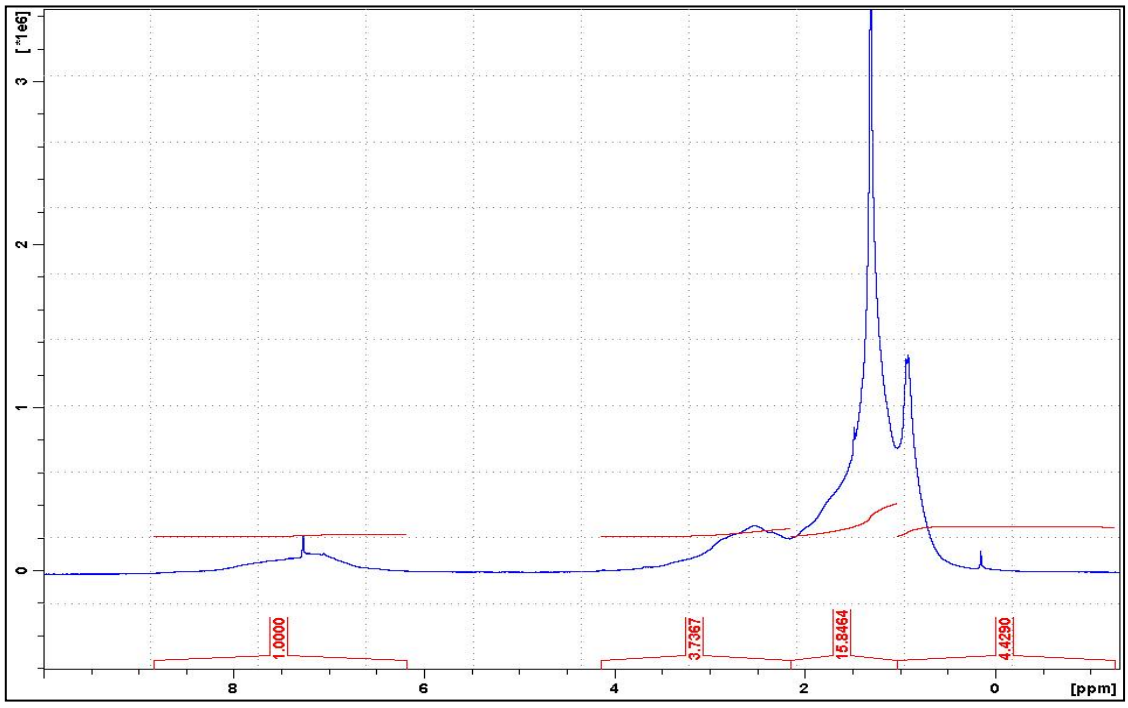

Figure 105. The NMR spectra for S2B3-Unaged-Resins.

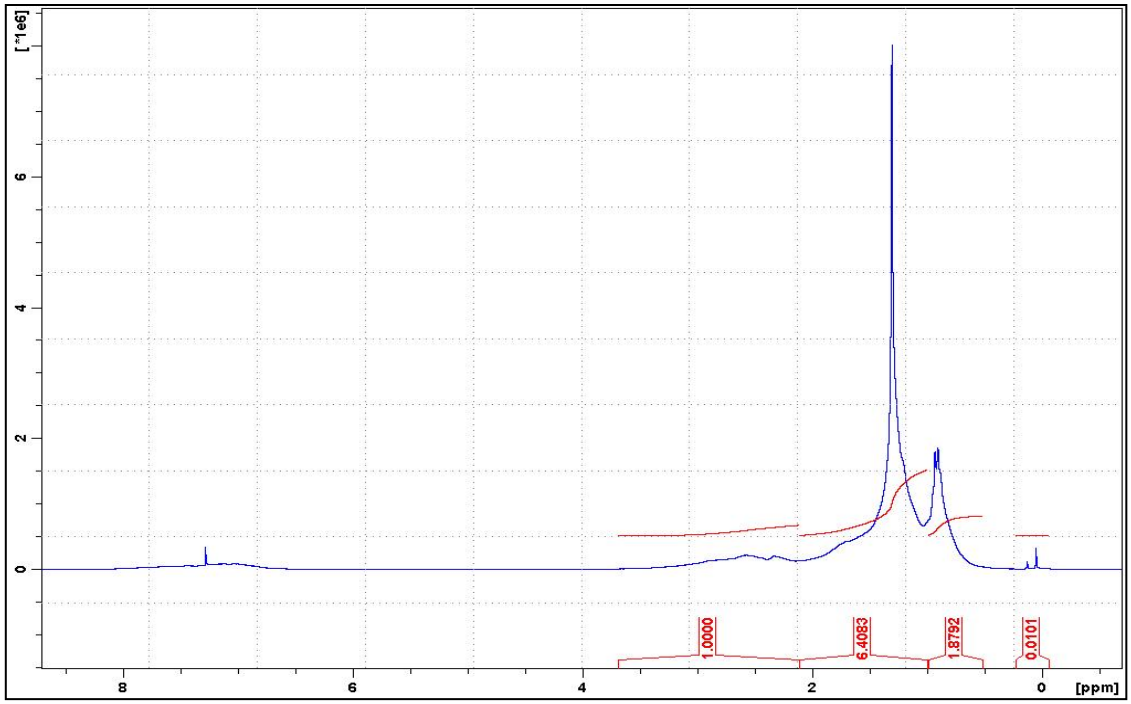

Figure 106. The NMR spectra for S1B1-RTFO-Aromatics.

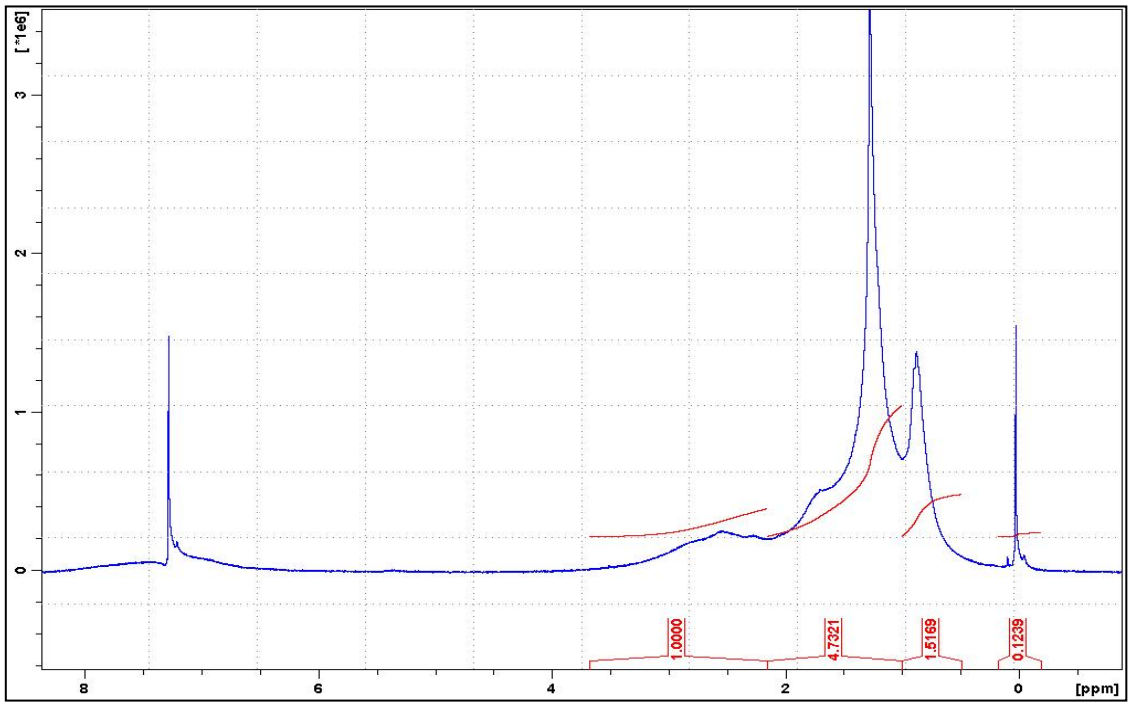

Figure 107. The NMR spectra for S1B1-RTFO-Resins.

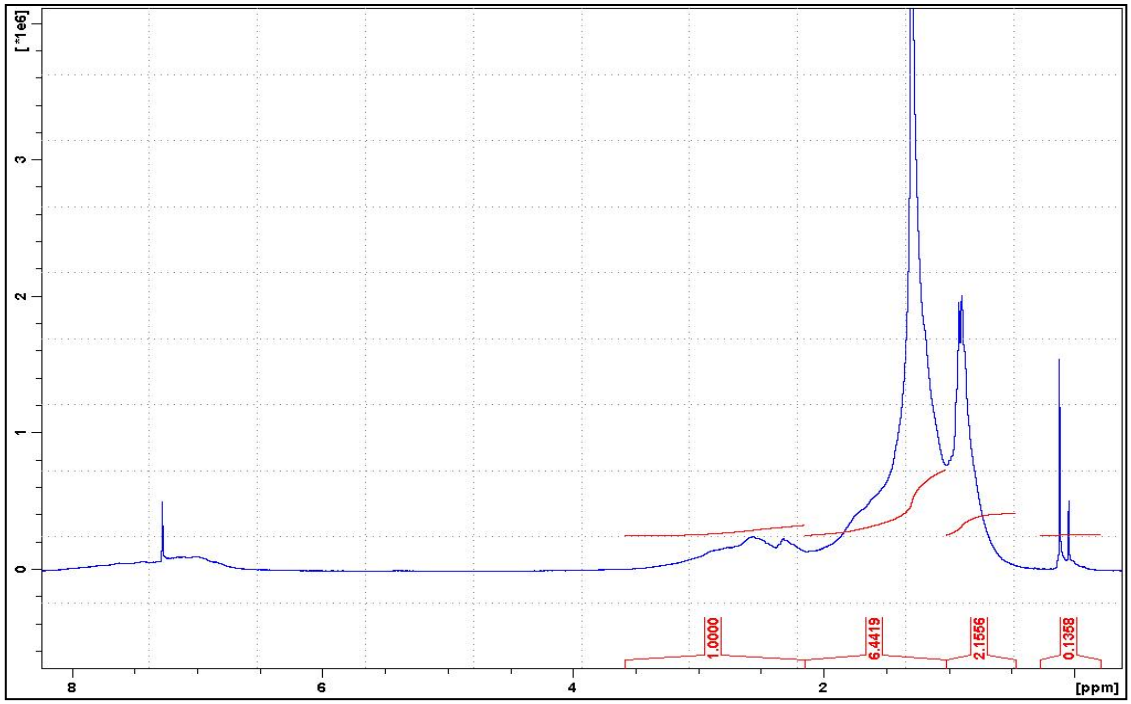

Figure 108. The NMR spectra for S1B2-RTFO-Aromatics.

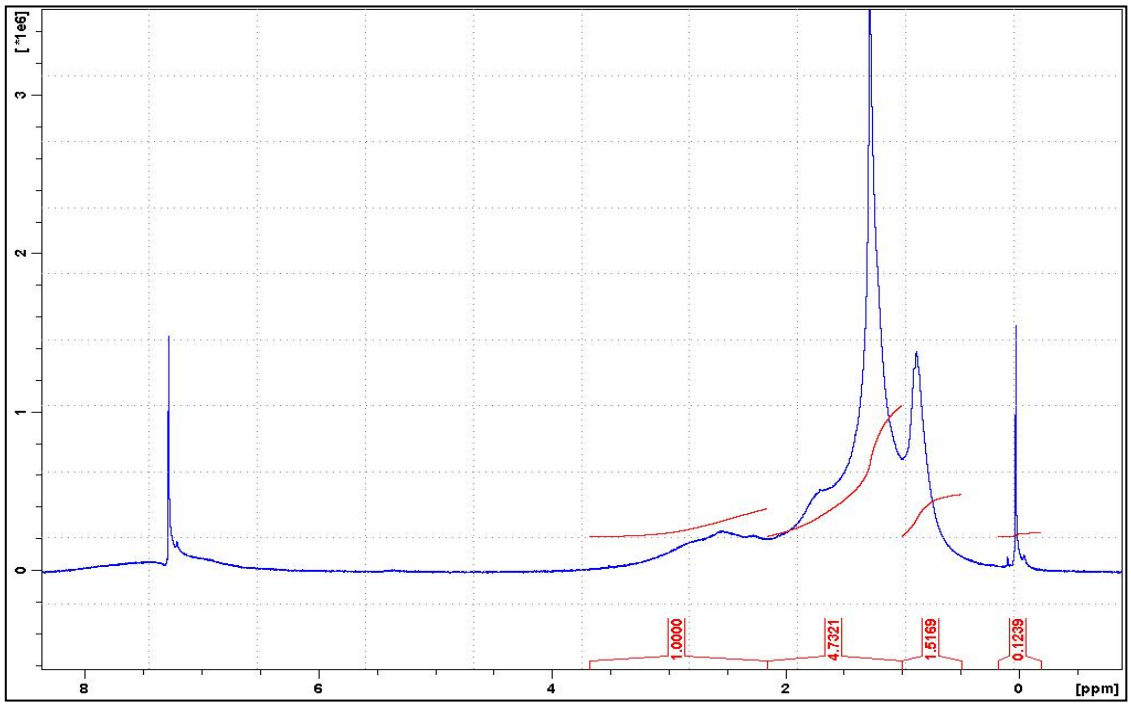

Figure 109. The NMR spectra for S1B3-RTFO-Resins.

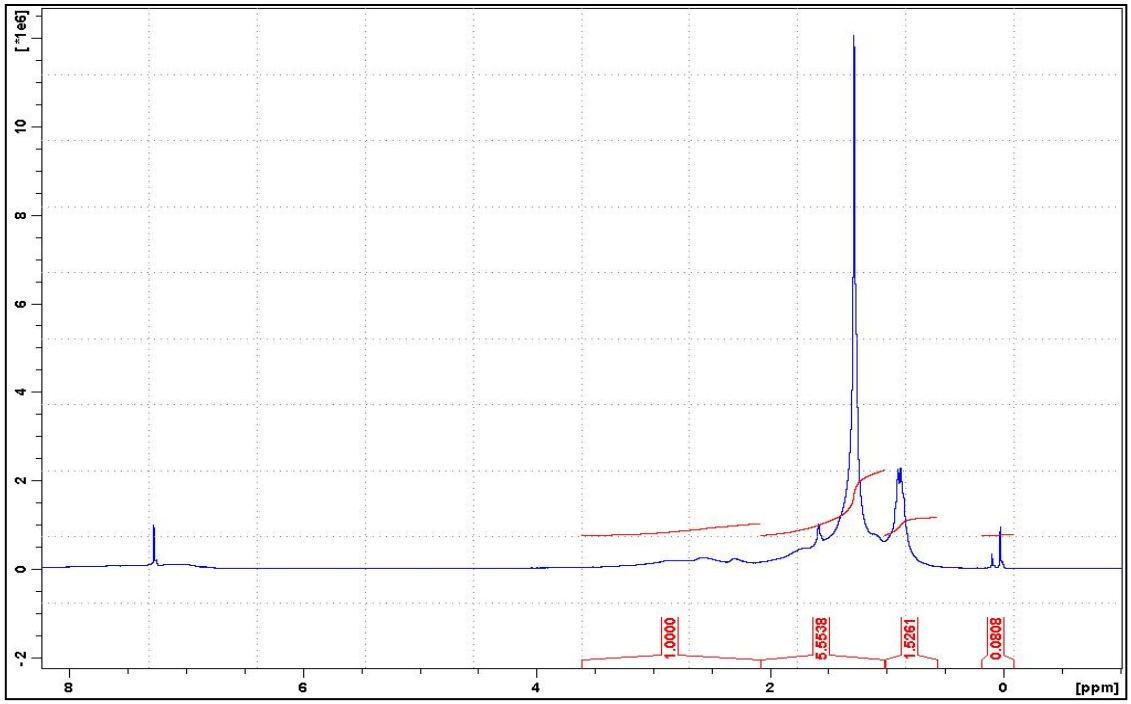

Figure 110. The NMR spectra for S2B1-RTFO-Aromatics.

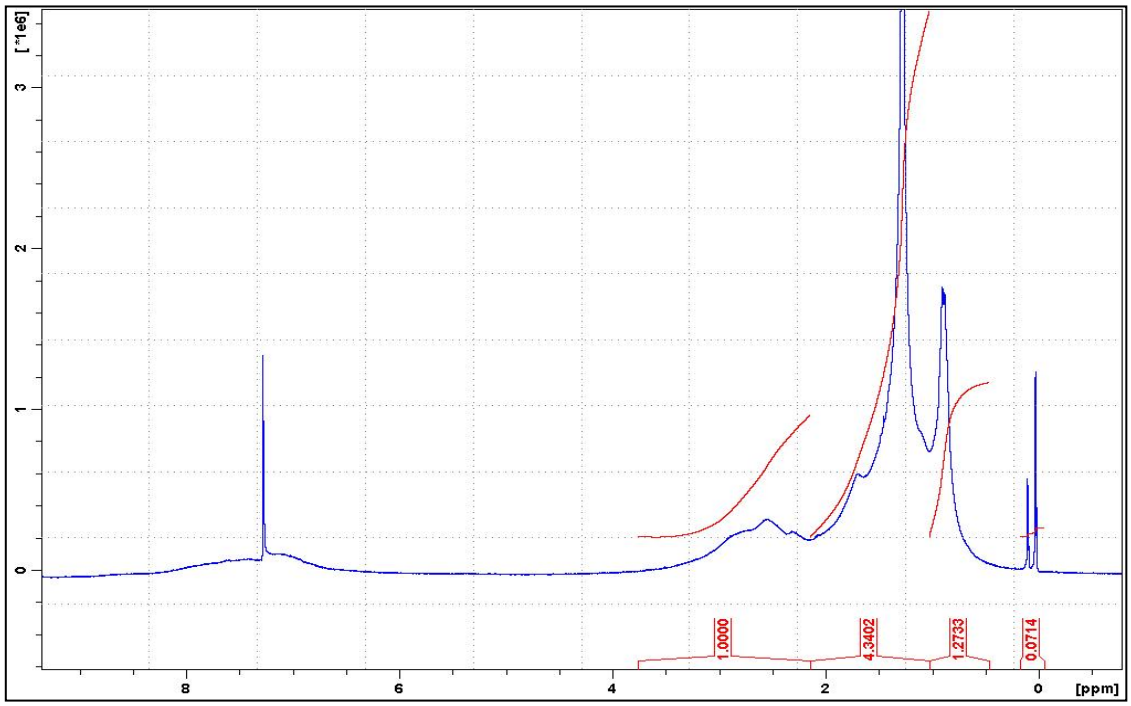

Figure 111. The NMR spectra for S2B1-RTFO-Resins.

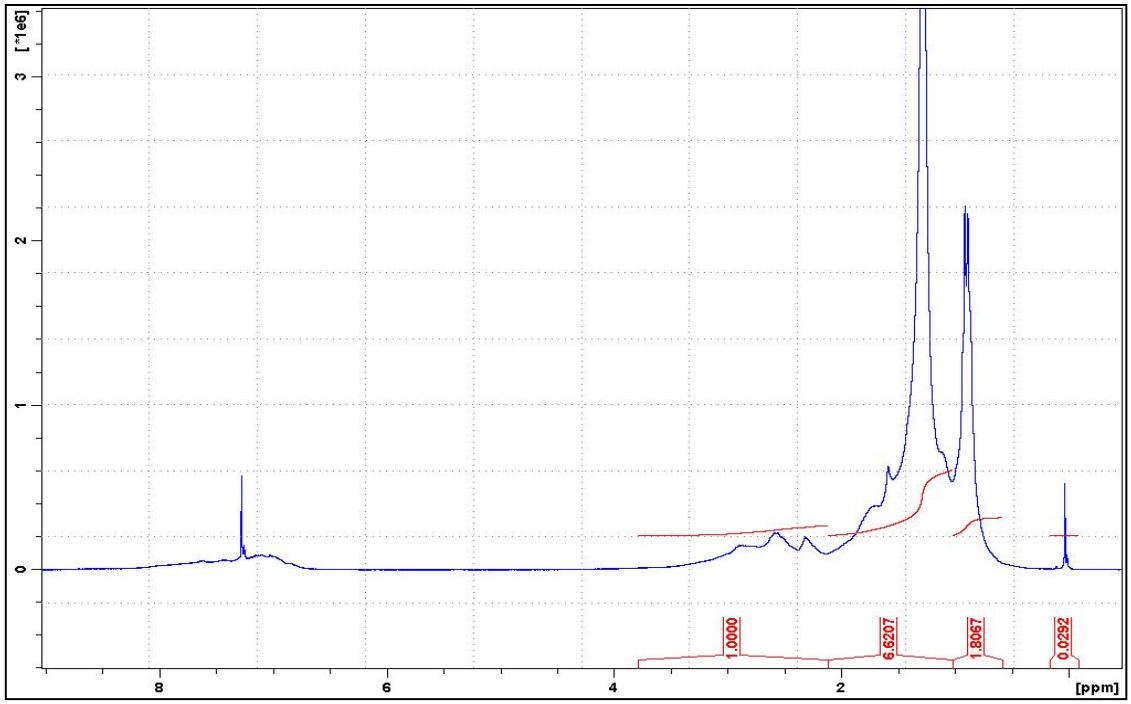

Figure 112. The NMR spectra for S2B2-RTFO-Aromatics.

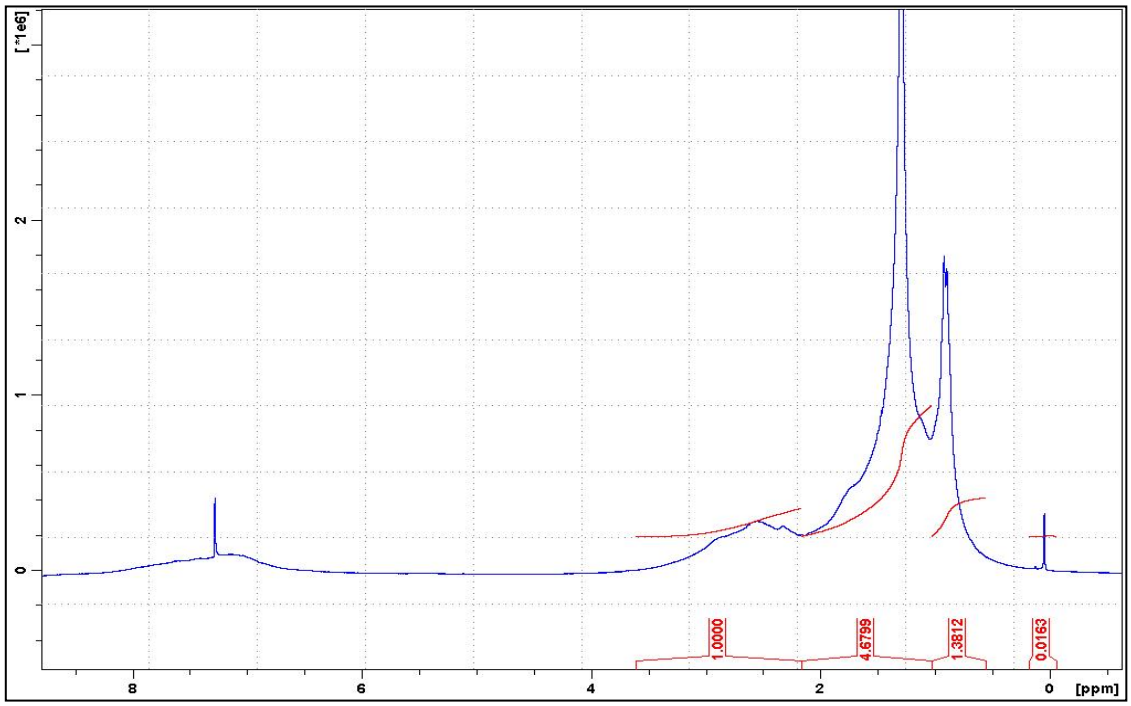

Figure 113. The NMR spectra for S2B6-RTFO-Resins.

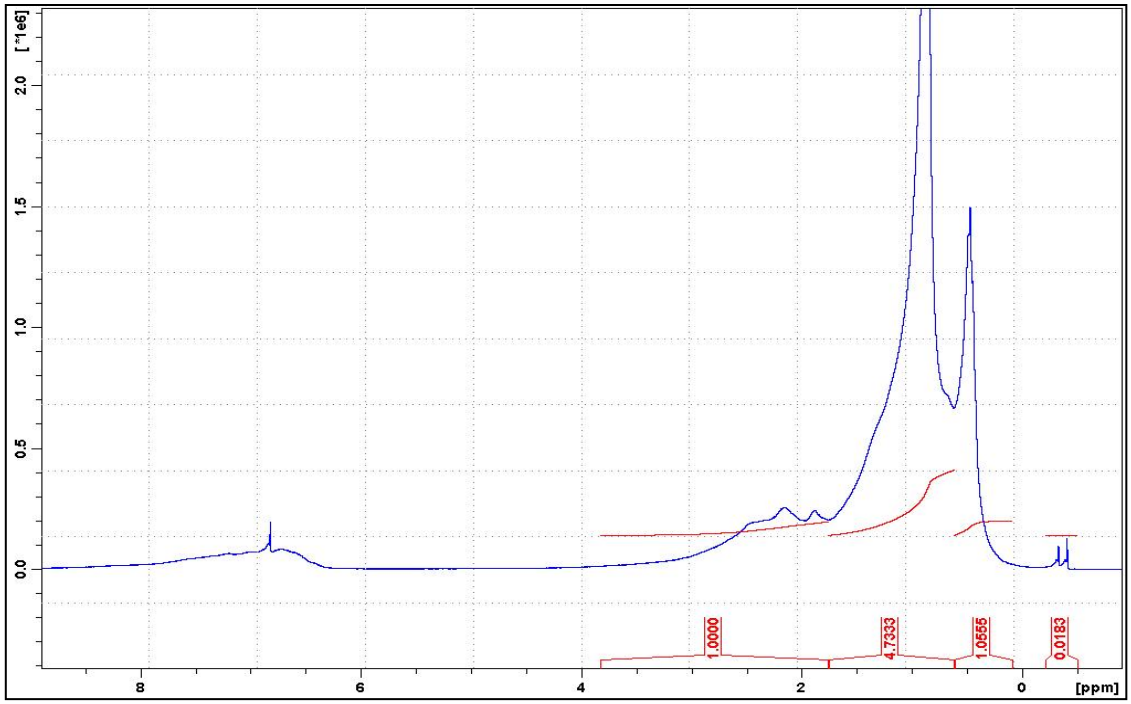

Figure 114. The NMR spectra for S2B3-RTFO-Aromatics.

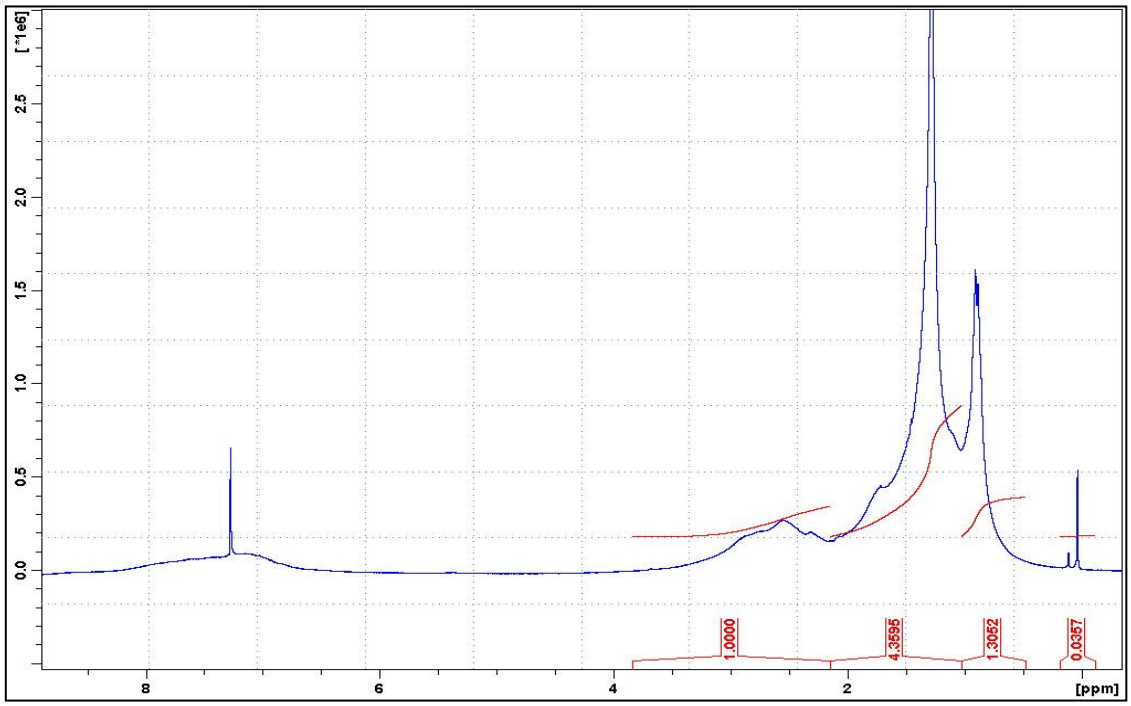

Figure 115. The NMR spectra for S2B3-RTFO-Resins.

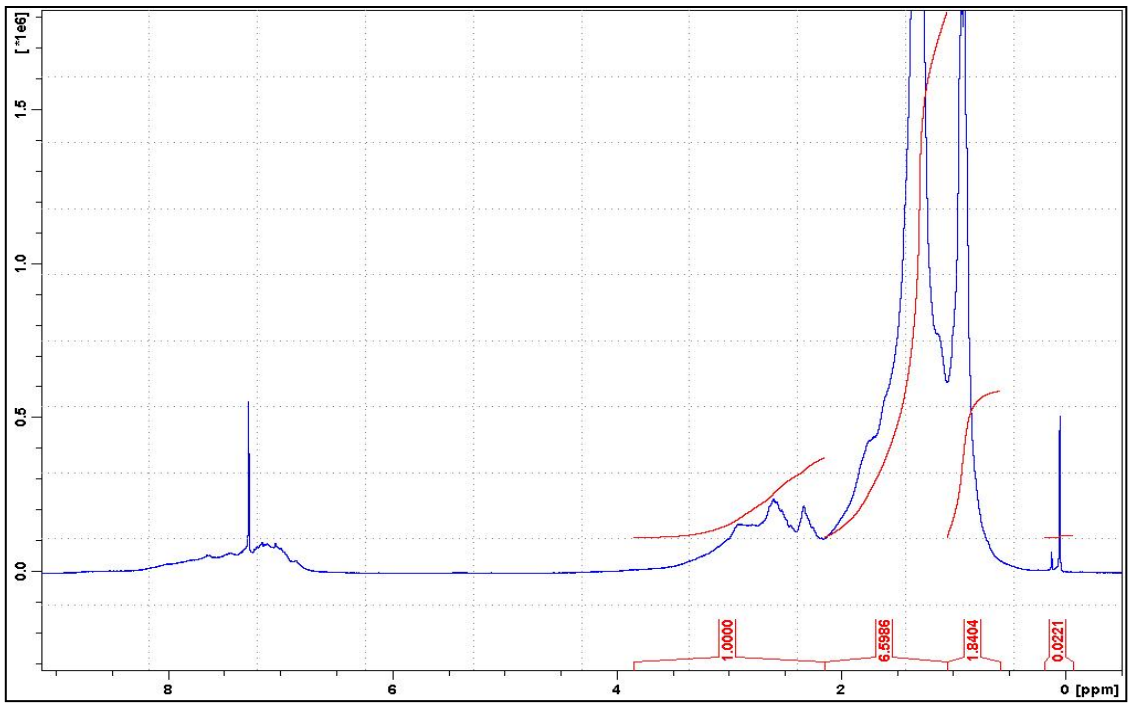

Figure 116. The NMR spectra for S1B1-PAV-Aromatics.

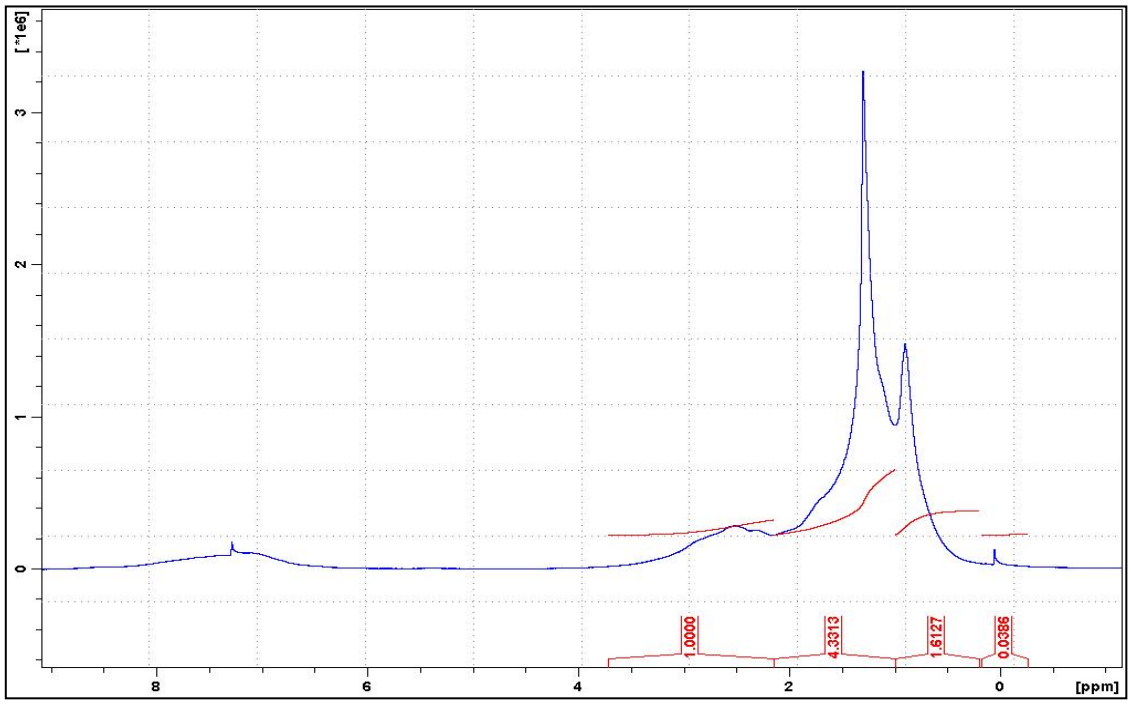

Figure 117. The NMR spectra for S1B1-PAV-Resins.

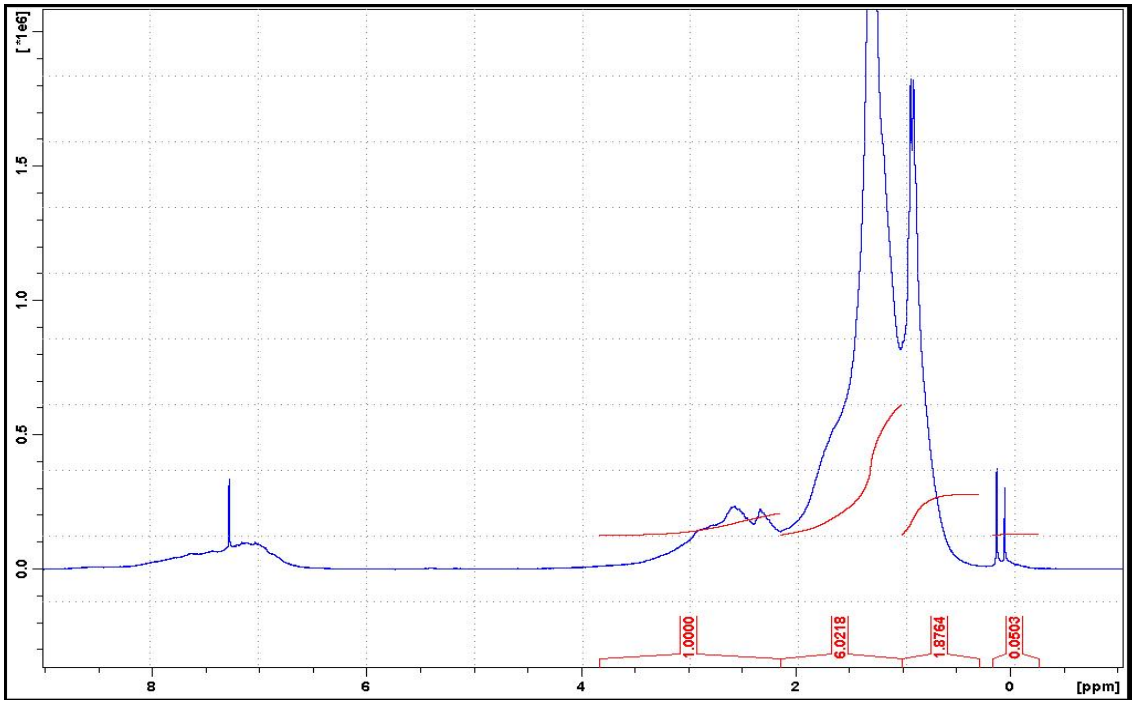

Figure 118. The NMR spectra for S1B3-PAV-Aromatics.

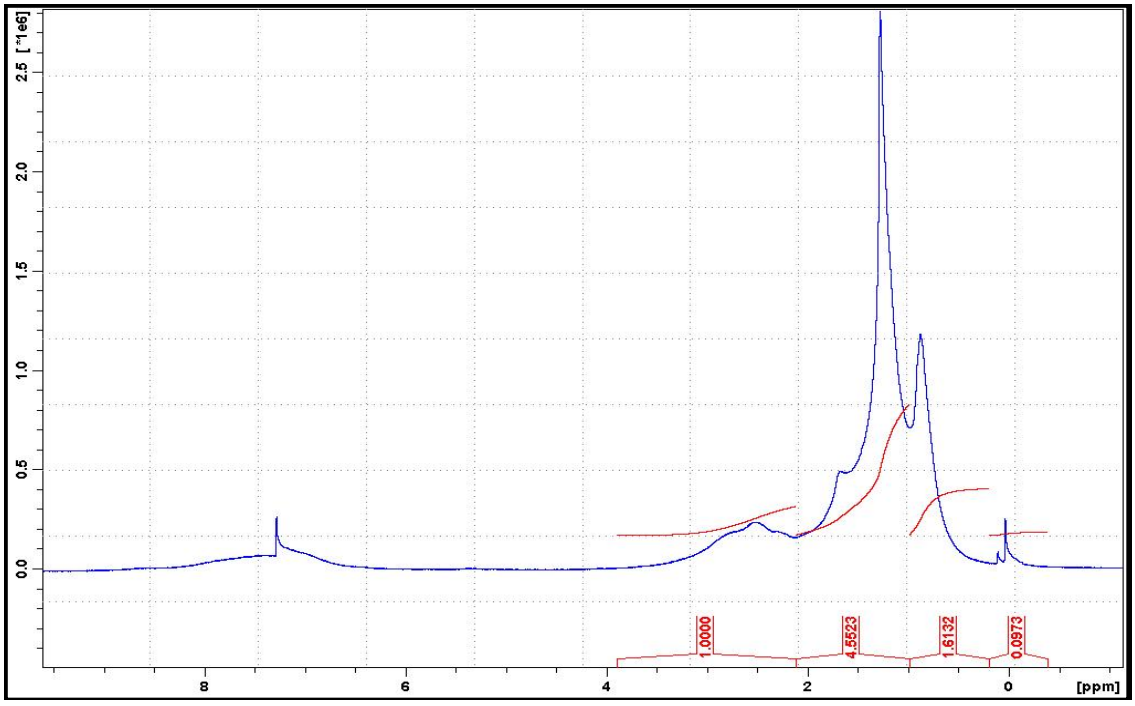

Figure 119. The NMR spectra for S1B3-PAV-Resins.

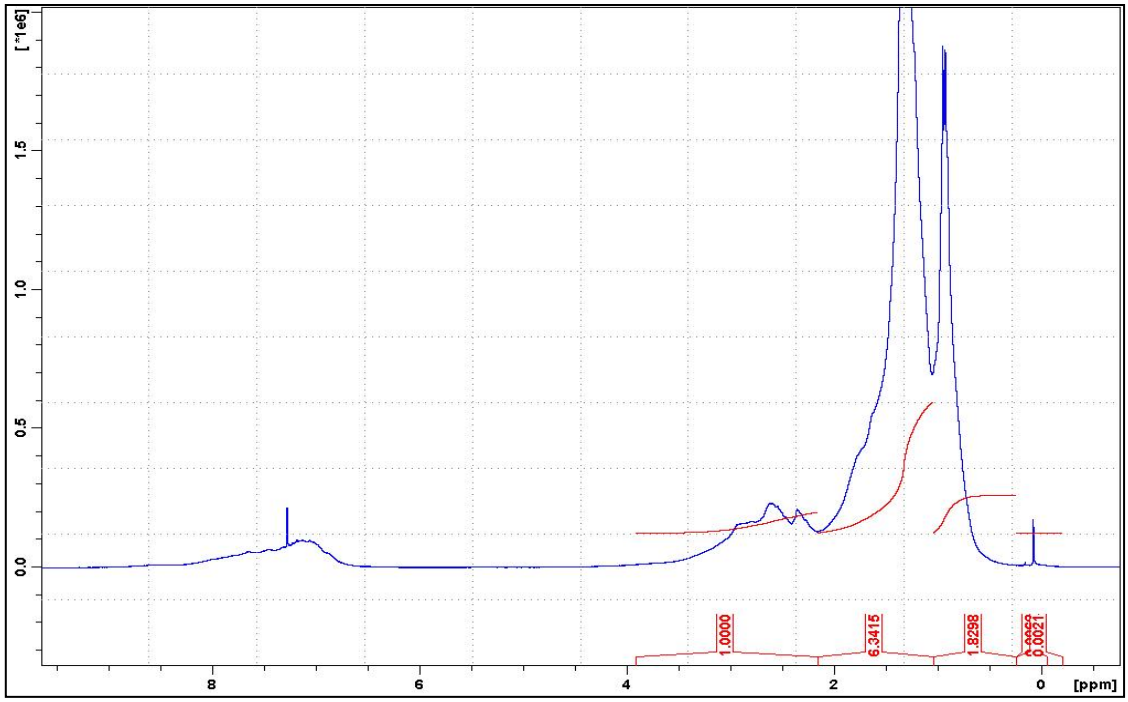

Figure 120. The NMR spectra for S2B1-PAV-Aromatics.

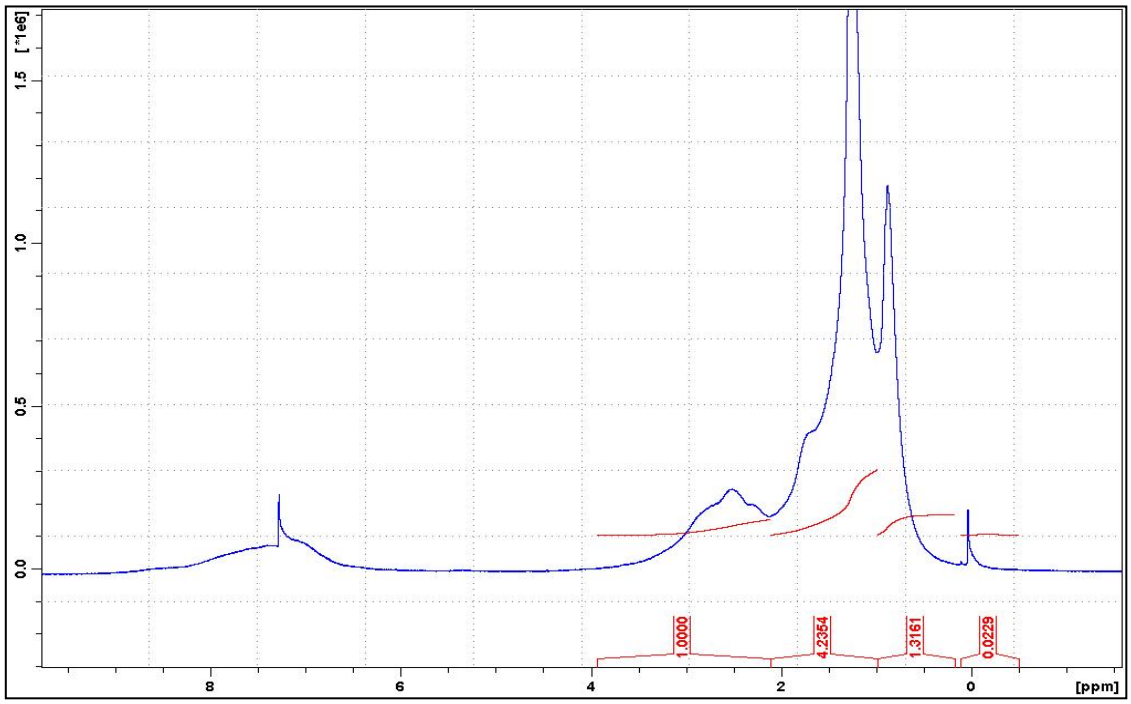

Figure 121. The NMR spectra for S2B1-PAV-Resins.

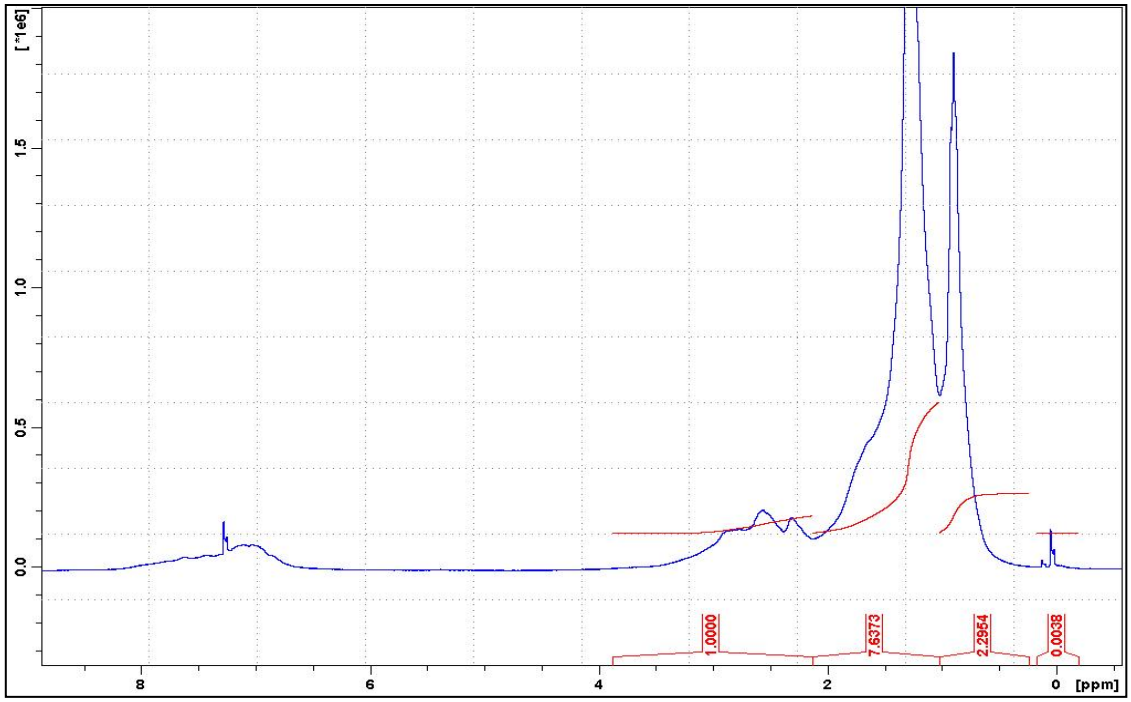

Figure 122. The NMR spectra for S2B3-PAV-Aromatics.

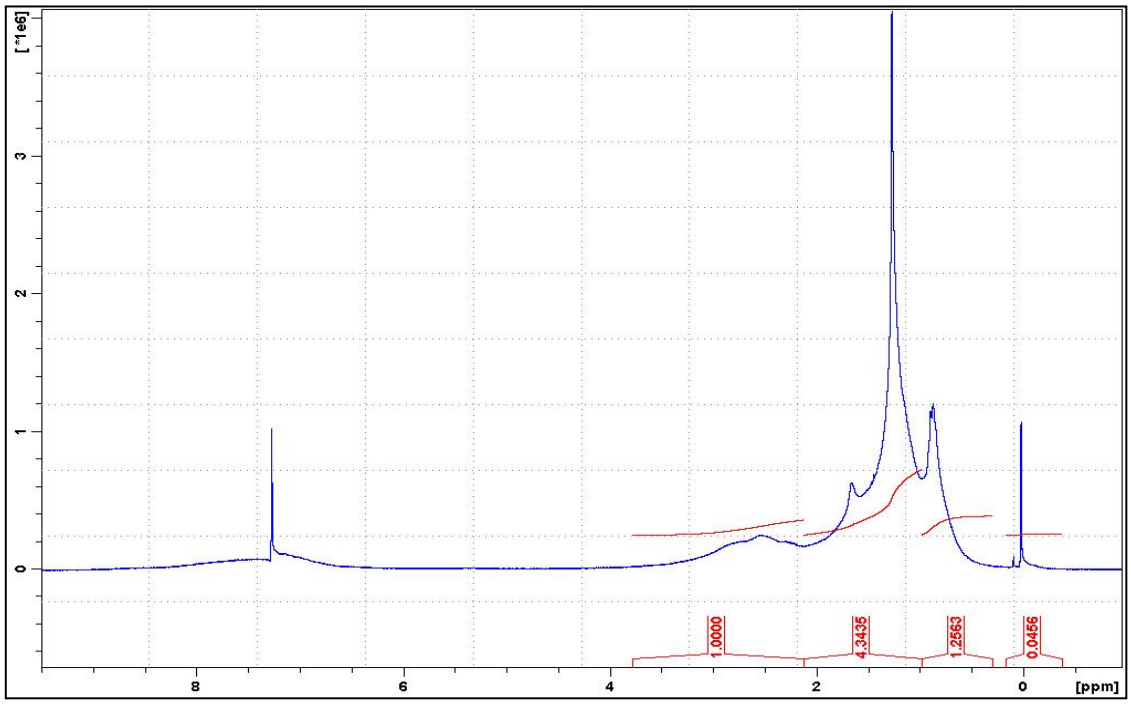

Figure 123. The NMR spectra for S2B3-PAV-Resins.